Self-desiccation and its importance in concrete technology : Proceedings of the second international research seminar in Lund, June 18, 1999.

Persson, Bertil; Fagerlund, Göran

1999

LUND UNIVERSITY
Lund Institute of Technology
Division of Building Materials

Report TVBM-3085

SELF-DESICCATION AND ITS IMPORTANCE IN CONCRETE TECHNOLOGY

B Persson and G Fagerlund, Editors

Proceedings of the Second International Research Seminar in Lund, June 18,1999

ISRN LUTVDG/TVBM—99/3085--SE(1-171)
ISSN 0348-7911 TVBM
ISBN 91-630-8230-6

Lund Institute of Technology
Division of Building Materials
Box 118
SE-221 00 Lund, Sweden

Telephone: 46-46-2227415
Telefax: 46-46-2224427
www.byggnadsmaterial.lth.se

Preface

The first *Research Seminar on Self-Desiccation and its Importance in Concrete Technology* was organised by our department in June 1997. The seminar resulted in a printed report containing 20 papers covering many different aspects of self-desiccation.[1])

Self-desiccation is a consequence of the net volume reduction when cement reacts with water, a phenomenon that was clarified many decades ago by the exceptional concrete scientist Treval C. Powers and his colleagues. This volume reduction creates an almost equivalent air-filled pore volume inside the concrete. This volume reduction and air-volume generation is almost of the same order in normal concrete as in high performance concrete with its low water-binder ratio. In the former, the cement content is low but the degree of hydration is large. In the latter, the reverse is the case.

The effects of the volume reduction, however, are quite different in these two types of concrete. In *normal concrete,* the volume reduction will often occur unnoticed since it will not significantly alter the state of the pore water; the pore structure is too coarse for that. Its only effect is a certain reduction in the degree of saturation of sealed concrete, which of course is a sort of self-desiccation. However, saturation will be easily restored if the concrete stays in contact with water during curing, or if it is put in contact with liquid water after curing.

In *high performance concrete* the volume reduction will cause a significant, more or less permanent, change in the state of the pore water due to the fine-porous structure manifesting itself as an almost horizontal desorption isotherm. This change can be observed as a clear reduction in the RH-level inside the concrete. Therefore, significant mechanical effects occur, such as autogenous shrinkage and internal micro-cracking. The drying effect is maintained for long time also when the concrete is stored in water. Thus, in high performance concrete, the self-desiccation is a long-lasting and significant phenomenon that could either be negative and must therefore be taken into consideration, or that could be utilised for improved concrete performance.

The first Research Seminar gave good insight into the phenomenon of self-desiccation, both the negative effects such as increased shrinkage, and the positive effects such as increased drying rate and enhanced frost resistance. This second seminar will further broaden our knowledge.

Lund, 26 May 1999

Göran Fagerlund

---

1) Persson,B., Fagerlund,G. (Editors). Self-Desiccation and its Importance in Concrete Technology. Lund Institute of Technology, Department of Building Materials, Report TVBM-3075, 1997.

TABLE OF CONTENTS PAGE

Hammer T A and Heese C 7
Early Age Chemical Shrinkage and Autogenous Deformation of Cement Pastes

Miyazawa B and Tazawa E 15
Shrinkage of High-Strength Concrete at Different Ambient Hurnidities

Hedenblad G and Arfvidsson J 25
A Computer Program to Calculate Drying of and Desiccation in Concrete

Weiss W J, Shane J D, Mieses A, Mason T O and Shah S P 31
Aspects of Monitoring Moisture Changes Using Electrical Impedance Spectroscopy

Persson B 49
A Nordtest Method for Verification of Self-Desiccation in Concrete

Toma G, Pigeon M, Marchand J, Bissonnette B and Barcelo L 61
Early Age Autogenous Restrained Shrinkage: Stress Build Up and Relaxation

Justnes H, Sellevold E J, Reyniers B, Van Loo D, Van Gemert A, Verboven F and Van Gemert D 73
Chemical Shrinkage of Cementitious Pastes with Mineral Additives

Persson B 85
Influence of Mix Design on Self-Desiccation in Concrete

Barcelo L, Boivin S, Rigaud S, Acker P, Clavaud B and Boulay C 109
Linear vs Volumetric Autogenous Shrinkage Measurement: Material Behaviour or Experimental Artefact?

Bentz D P 127
Effects of Cement PSD on Porosity Percolation and Self-Desiccation

Persson B 135
Evaluation of Under-Pressure in the Pore Water of Sealed High Performance Concrete, HPC

Radocea A 153
A Model of Self-Desiccation in Concrete

Sato R, Tanaka S, Hayakawa T and Tanimura M 163
Experimental Studies on Reduction of Autogenous Shrinkage and Its Induced Stress in High-Strength Concrete

EARLY AGE CHEMICAL SHRINKAGE AND AUTOGENOUS DEFORMATION OF CEMENT PASTES

Chemical shrinkage and autogenous deformation

T.A.HAMMER
SINTEF Civil and Environmental Engineering, Trondheim, Norway and
C. HEESE
Technical University of Aachen, Germany

Abstract

In the very early age, i.e. the initial phase that is before and during the time of setting, the cement paste changes from a liquid to a solid. The result of the chemical shrinkage on the external deformation, the autogenous deformation, has proven to change considerably in this period: i.e. from shrinkage rate equal to the chemical shrinkage to a rate which is in the magnitude of 1/10 of the chemical shrinkage. The point of time when the autogenous deformation departs the chemical shrinkage development has been investigated. The results suggest that the relation between the chemical shrinkage and the autogenous deformation in the initial phase not only depend on degree of hydration, but also the initial consistency (stiffness) of the paste. Thus, it may not be expected to find any unique relation between the autogenous shrinkage of pastes and equivalent concretes.

1 Introduction and Scope

Provided no external moisture exchange, the chemical shrinkage (CS) due to the hydration is the fundamental driving force resulting in external volume changes, autogenous deformation (AD) and voids as expressed in Fig. 1. The AD may be defined as all the external volume change taking place without any mass change. The CS is the main driving force, but the relation between CS and AD of the concrete is in general influenced by several factors: Any re-absorption of bleed water and/or absorbed water in the aggregates as well as the size of the hydration generated pores and the aggregate restraint.

Measurements have shown that AD may develop shortly after mixing and thus contribute to cracking while the concrete is still plastic, i.e. in the "initial phase" [1]. In order to predict the AD contribution to the crack risk in this phase we want to measure the "linear" AD development (the one-dimensional horizontal component) and the development of the tensile strain capacity of the concrete. Work at NTNU/SINTEF reveals that there is an inconsistent relation between what we consider

as the "true driving force", namely the volumetric AD measured on pastes with rotation, and the measured linear AD of the concrete. Therefore, in order to arrive at a reliable method for the measurement of the linear AD of concrete we started to determine the relations starting with the **CS** of the paste and ending with the "linear" AD of the concrete. The first step is to measure the **CS** on the pastes. The next step is to measure the consequence on the volumetric external contraction, i.e. the volumetric AD of the paste, see Fig 1. The third step is to measure the linear AD of the pastes, i.e. the horizontal component and the settlement. The logical relation should give the results that two times the linear deformation + settlement equals the volumetric deformation. The fourth step is to go from linear measurements on pastes to linear AD of the equivalent concrete. This is discussed in [1] with focus on the third step that proves to cause the main concern, regarding the inconsistency.

The present paper deals with the first step, i.e. the relation between the **CS** and the volumetric AD of pastes. It is based on the thesis of Christian Heese [2].

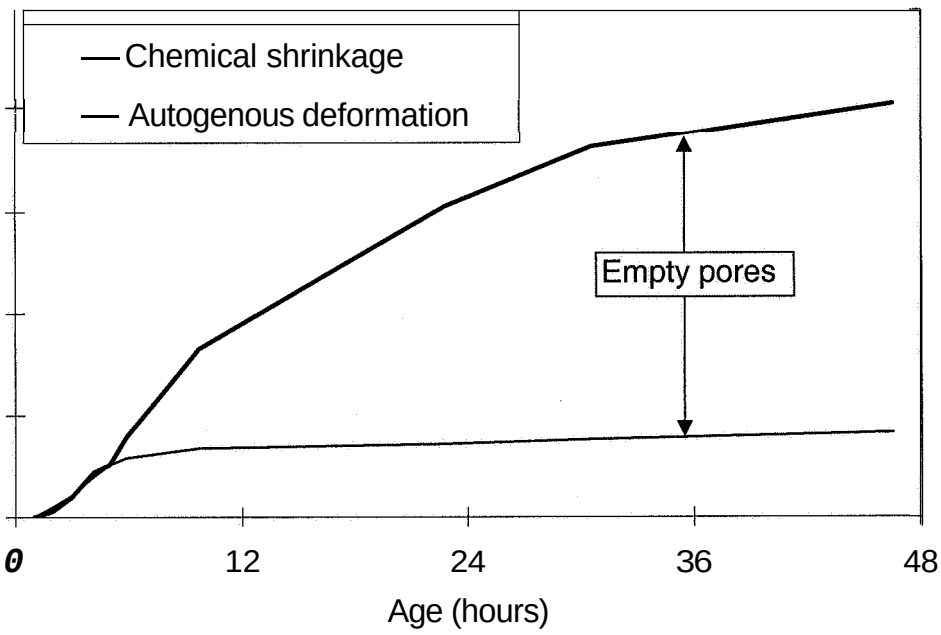

Fig. 1. Principle development of the chemical shrinkage and volumetric autogenous shrinkage of cement paste.

In Fig. 1, it can be seen that the autogenous deformation develops rather similarly to the chemical shrinkage until some point, the diverting; point. Apparently, there is a full "collapse" (liquid behaviour) of the paste in this period.

From the above it follows that the relation between the autogenous shrinkage and the chemical shrinkage changes rather dramatically during the initial phase. Therefore, we have divided the initial phase in two sub-phases: liquid and semi-liuuid, as discussed below.

In the liquid phase, starting from the time of casting, the stiffness of the paste-

mortar-concrete is very low and, thus, the chemical shrinkage results in an identical external volumetric contraction. Consequently, the autogenous deformation equals the chemical shrinkage. The duration of depends on the initial fluidity, material composition and possibly any external weight.

At the start of the semi-liquid phase a sufficiently rigid skeleton, is formed, i.e. with sufficient stiffness, to enable the sample to support its own weight (+ any external weight). The stiffness development in this phase will gradually prevent the external contraction, seen as a flattening out of the AD-curve curve in Fig. 1, and result in empty pore space. At the end of this phase the under-pressure in the pore system will be the dominating driving force for the AD.

For a given mixture, the stiffness development and thus the diverting point depends on the degree of hydration. However, one may assume that the degree of hydration needed to make the sufficient skeleton depends on the particle spacing, i.e. "initial stiffness" of the paste. To test the hypotheses we tested the CH and AD of pastes where we changed the stiffness by different means: w/b, silica fume and inert filler, see Table 1.

Table 1. Paste compositions

w/b	Cement, *) Blaine (m^2/kg)	Silica fume content (% by weight of cement)	Filler (0-125 Tm), green stone/gabbro (% by weight of cement)	Cone penetration (mm)
0.290	370	0	0	34.2
0.310	370	0	0	> 40.0
0.335	370	5	0	34.3
0.360	370	5	0	36.0
0.370	370	5	17.6	32.2
0.400	370	5	0	> 40
0.410	370	5	35.3	33.3
0.360	370	10	0	26.3
0.368	516	0	0	36.9
0.420	516	0	0	> 40
0.355	516	5	0	24.1
0.368	516	5	0	25.0
0.400	516	5	0	33.5
0.406	516	5	17.6	30.1
0.476	516	5	35.3	31.6
0.367	516	10	0	20.1

*) 370 m^2/kg: Cement type “Anl.”, 516 m^2/kg: Cement type “Ind.”

2 Test Methods

2.1 Chemical Shrinkage

The total chemical shrinkage was determined according to the following method [3]: **A** small amount (about 25 cm^3) of paste is filled in an Erlenmeyer flask with a graded pipette on top. The rest of the volume is filled with distilled water. The volume change is recorded as the reduction of the water level in the system [3]. The flasks are placed in a water bath for temperature control. The method has proven to be reliable, and it may be started at a short time after mixing (less than 15 minutes).

The method is based on the assumption that the pores, when created, fills with water. This is true in most cases because the thickness of the paste samples is small (i.e. maximum 10 mm), at least in the first day(s) of age. Thus, the method gives the true chemical shrinkage in the early thermo phase, also.

2.2 Autogenous shrinkage

The autogenous shrinkage was measured according to the buoyancy principle, using a rubber balloon (a condom) filled with paste of which the weight in water is recorded continuously or at fixed intervals [2]. The method may allow bleeding water to lay on the surface. If so, the subsequent absorption will be observed as an extra contraction. In order to avoid the bleeding, the filled condom is usually placed in a tube and placed on rolls to be rotated. The effect of rotation is discussed by Justnes et al [3]. The procedure has proven to give good correlation with the chemical shrinkage method [3]. Thus, the method gives the "true" chemical shrinkage in this phase. Temperature control is taken care of by the continuos immersion in water. In the present case the rotation was performed manually in steps, i.e. 180 ° rotation every 5 minutes until the time of around initial setting.

2.3 Consistency

The consistency was measured on 20 minutes old pastes by the use of a Vicat apparatus with a cone shaped plunger with a maximum diameter of 29 mm and a height of 39 mm. The weight was 56,4 grams. The consistency was expressed as the depth of penetration of the cone (0 – 40 mm) and presented as the mean value of to measurements (i.e. on two separate samples). The difference between the two measurements were in the range of 0 – 0,5 mm.

3 Results

Fig 2 shows a typical result. There was not always a good coincidence between the CS and the AD development in the liquid phase. This is due to some discrepancy in the CS measurements and AD in particular, especially in the time before about 180 minutes. Nevertheless, the diverting point is detectable with fair accuracy as the change in shrinkage rate between the two becomes rather clear. This has been used to determine the diverting point.

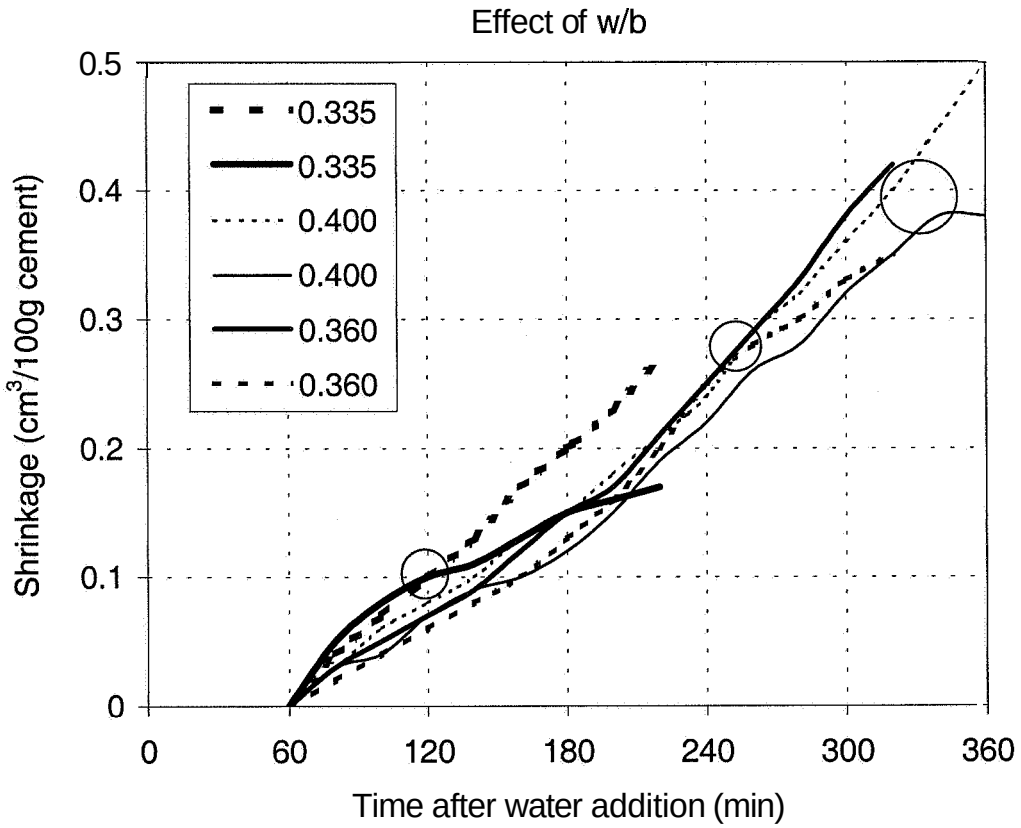

Fig. 2. Chemical shrinkage (dotted lines) and autogenous deformation (solid lines) of pastes with different w/b (all with 5 % silica fume).

Fig 3 shows the relation between the diverting point and the w/c of all the pastes. Apparently, there is no good relation. If any, the diverging point decreases with increasing w/c, which is very surprising. However, when considering the pastes with equal cement type and silica fume content, it can be seen that the diverting point increases with increasing w/c. Consequently, when considering pastes with equal cement type, there must be more than the w/c itself that influences the diverting point.

Fig 4 shows the relation between the diverting point and the consistency of all the paste. As can be seen, the relation is much better than the one in Fig 3, showing that the consistency is an important parameter. Note the rather small difference in DP and consistency of the pastes with w/c in the range of 0.35 to 0.36 and 5 % silica fume (Anl05) and the equivalent pastes with 17.6 and 35.3 % filler (Anl05+filler) in spite of higher w/c; 0.38 – 0.43.

The results suggest that the relation between the CS and the AD in the initial phase not only depends on w/c and cement type, but also the silica fume and aggregate content because it influences the consistency of the paste. Thus, it may not be expected to find any unique relation between the AD of pastes and equivalent concretes (i.e. equal w/(c + s)) in this phase. Another important parameter which strengthen this is the

(super)-plasticising admixtures, which is not investigated here: As the paste is much less water demanding than the equivalent concrete, it is practically impossible to make a sound paste (without filler) with the same amount of (super)-plasticiser as the equivalent concrete.

Furthermore, a consequence of increased initial stiffness is that the total AD in the initial phase is decreased. The AD development in the thermo phase is probably not influenced.

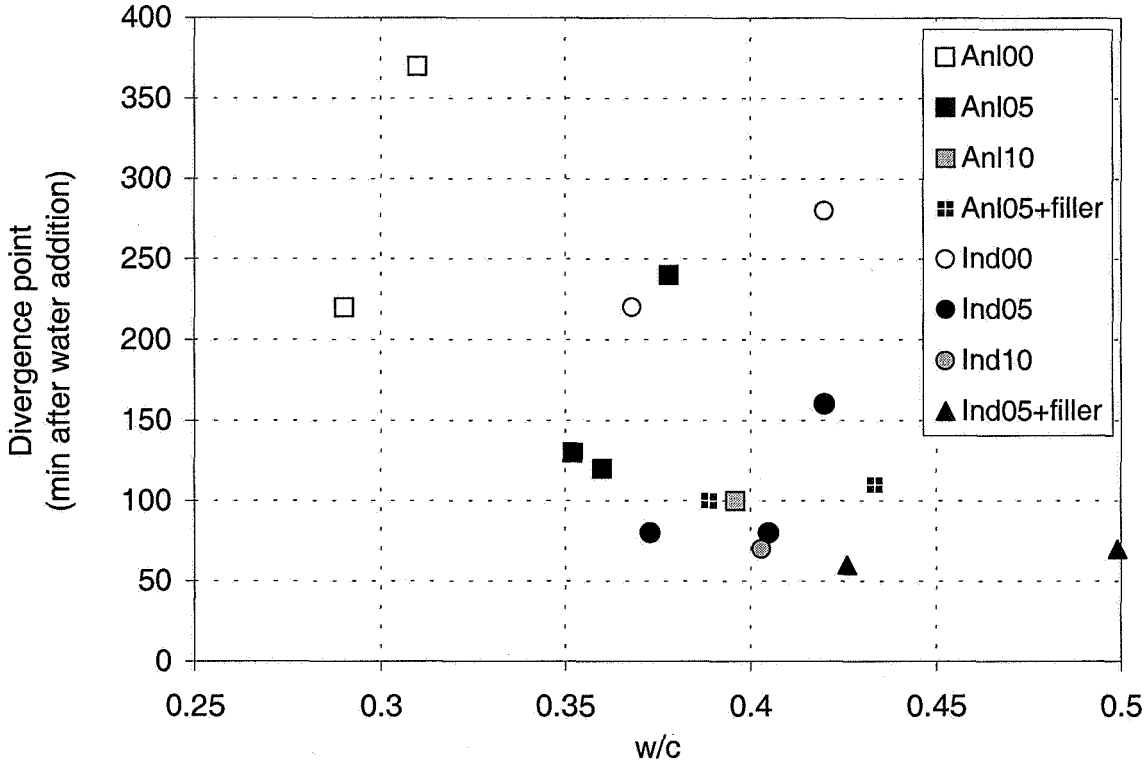

Fig. **3.** Relation between the point of time where the autogenous shrinkage divert from the chemical shrinkage and the water to binder ratio of all the pastes tested

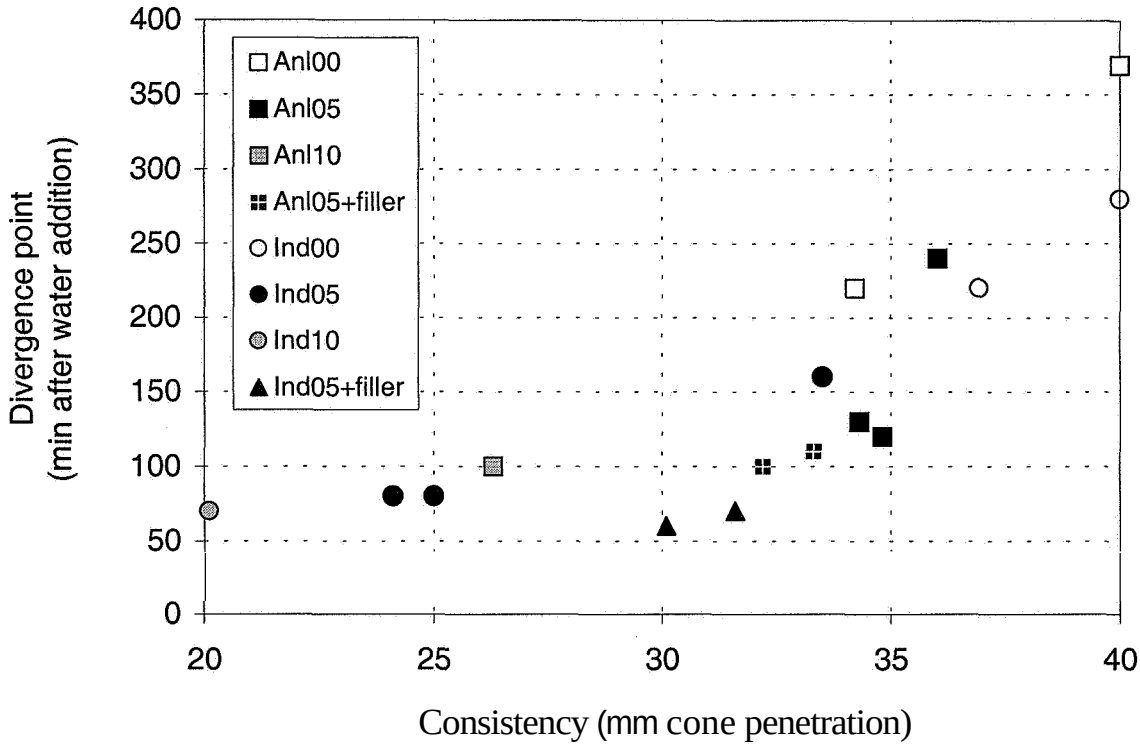

Fig.4. Relation between the point of time where the autogenous shrinkage divert from the chemical shrinkage and the consistency of the paste measured 20 minutes after water addition.

4 References

1. Hammer, T.A. (1998) Test Method for Linear Measurements of Autogenous Shrinkage before setting, Autogenous Shrinkage of Concrete, (ed. E. Tazawa) E & FN Spon, London, pp. 143-154.

2. Heese, C. (1999) The Relationship between Chemical Shrinkage and Autogenous Shrinkage of Cement Paste at Early Ages – Effect of External Load, Consistency and Mix Composition. Diploma work at the Norwegian Institute of Technology, Trondheim, Norway and the Technical University of Achen, Germany.

3. Justnes, H., Reyniers, B. and Sellevold, E.J. (1994) An evaluation of methods for measuring chemical shrinkage of cementitious pastes. Nordic Concrete Research, publication no. 14. 1/94, Norwegian Concrete Association, Oslo 1994, pp. 44 – 61.

SHRINKAGE OF HIGH-STRENGTH CONCRETE AT DIFFERENT AMBIENT HUMIDITIES

S. MIYAZAWA
Department of Civil Engineering, Ashikaga Institute of Technology, Ashikaga, Japan
E. TAZAWA
Department of Civil Engineering, Hiroshima University, Hiroshima, Japan

Abstract
Changes in length and mass of concrete specimens with different water-cement ratio which have been exposed to different ambient humidity are experimentally investigated. The relation between ambient relative humidity and drying shrinkage has been discussed. It has been proved that the balance of internal relative humidity and ambient relative humidity affects shrinkage of concrete under dried conditions and that high-strength concrete may expand at high relative humidity.
Keywords: high-strength concrete, shrinkage, relative humidity, water-cement ratio

1 Introduction

Volume change of concrete, which is not caused by temperature change nor external load, includes autogenous shrinkage, drying shrinkage and carbonation shrinkage. It is important to predict shrinkage of concrete in order to estimate cracking tendency and long term deformation of concrete members. A prediction model for autogenous shrinkage, which is dominant in shrinkage of high-strength concrete, has been proposed by the authors **[1].** **As** for drying shrinkage, some production models such as CEB-FIP model **[2]** and JSCE model ***[3]*** have been proposed, but they may not be applicable to high-strength concrete with 80 N/mm^2 and 55 N/mm^2 respectively. The ultimate purpose of this study is to obtain a prediction model for shrinkage of high-strength concrete including both autogenous shrinkage and drying shrinkage.

2 Experimental procedures

2.1 Materials and mix proportion of concrete

Ordinary Portland cement, river sand (specific gravity: 2.63, absorption: 1.39 %, fineness modulus: 2.68) and gravel (specific gravity: 2.56, absorption: 1.84 %, maximum size: 25 mm) were used. Concretes with water-cement ratio of 0.2, 0.3, 0.4, 0.5 and 0.6 were prepared. A polycarboxylic acid type superplasticizer was used for concretes with water-cement ratio less than 0.40 and an air-entraining agent was used for concretes with water-cement ratio more than 0.50. Mix proportions of the concretes and properties of flesh concrete are shown in Table 1.

2.2 Measurement of length change

Specimens of 100×100×400 mm beam were prepared for measuring autogenous shrinkage and drying shrinkage. Three specimens were prepared for each condition. Autogenous shrinkage test was done in accordance with a JCI test method [4]. For the first 24 hours after casting, the measurements were done with mixtures in a steel mold by dial gauges (Fig 1). In order to eliminate the restraint by the mold, a Teflon plate 1 mm in thickness was put on the bottom of the mold. The measurements were started at the time of initial setting which was determined by Japanese Industrial Standard (JIS A 6204). During the first day, the temperature of the specimens rose due to cement hydration. Therefore, the thermal expansion strain was excluded from the measured strain on the assumption that the thermal expansion coefficient of the concretes was $10\times10^{-6}/℃$. After the specimens were demolded at the age of 24 hours, the specimens were sealed with aluminum tape in order to prevent from evaporation. And length change of the specimens was measured with contact chips attached on the surface of the specimens, where the gauge length was 300 mm. The maximum change in mass of the sealed specimen was no more than 0.02% during the test periods (it is specified to be less than 0.05 % in the JCI method), therefore the influence of moisture movement to or from the specimens can be ignored.

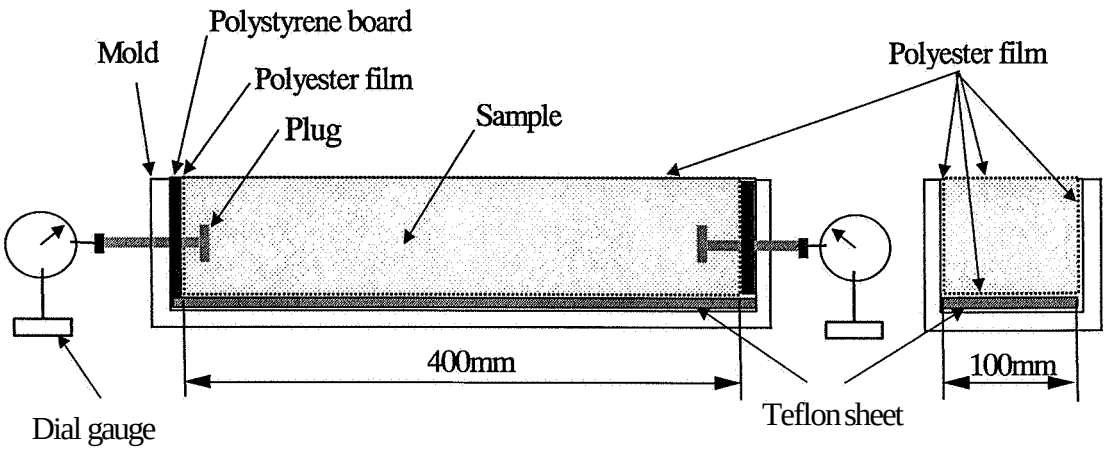

Fig. 1 Measurement of autogenous shrinkage of concrete during first 24 hours

Table 1 Mix proportion and properties of flesh concrete

w/c	s/a (%)	Mass content (kg/m^3)				Admixture (c×%)	Slump(cm) (Slump flow)	Air (%)
		W	C	S	G			
0.20	30	160	800	439	998	2.3	20.0 (55×55)	3.0
0.30	33	160	533	539	1066	0.8	21.5 (53×44)	3.2
0.40	34	160	400	611	1104	0.8	21.5	4.4
0.50	37	162	324	667	1106	0.04	16.0	2.3
0.60	39	163	272	719	1095	0.036	5.0	6.9

For drying shrinkage test, the specimens were sealed immediately after demolding and were cured under sealed condition until the age of 7 days. The aluminum tape was removed at the age of 7 days. Then, the specimens were exposed to different ambient relative humidities of 40%, 60%, 80% and 90%. Changes in length and mass of the specimens were measured at specified ages.

3 Results and discussions

Observed length change of the specimens is shown in Figs. 2, 3 and 4. Shrinkage of sealed specimen, that is autogenous shrinkage, increases with decreasing water-cement ratio. For the specimen with 0.5 water-cement ratio, shrinkage is increased by exposure to any relative humidity ranging form 40% to 90%, and shrinkage increases with decreasing relative humidity. For the specimen with 0.2 water-cement ratio, on the other hand, expansion is observed at 90% relative humidity after 7 days of sealed curing, and volume change is hardly observed at 80% relative humidity. For the specimen with 0.3 water-cement ratio, volume change is hardly observed at 90 % relative humidity.

Change in mass of the specimens with increasing age is shown in Figs. 5, 6 and 7. For the specimen with 0.5 water-cement ratio, the mass of the specimens decreases at relative humidity ranging form 40% to 80%, although change in mass is hardly observed at 90 % relative humidity. For the specimen with 0.2 w/c, on the other hand, increase in mass is observed at 80% and 90% relative humidity. For the specimen with 0.3 water-cement ratio, increase in mass is observed at 90 % relative humidity.

Vapor pressure in small pores is generally less than the saturated vapor pressure at the same temperature, and it decreases as the size of pore becomes smaller and as the moisture content of the porous body becomes lower. For high-strength concrete with low water-cement ratio, pore size in hydrates is very small and the amount of capillary water is very little due to consumption of water by cement hydration, so the vapor

pressure in pores is thought to be significantly low. Therefore, moisture movement from the environment into concrete with low water-cement ratio occurs when the concrete is exposed to humid environment. In concrete with low water-cement ratio, carbonation may occur only in the exterior part of a specimen, therefore it can be thought that the increase in mass is not caused by carbonation but by moisture movement into the specimens.

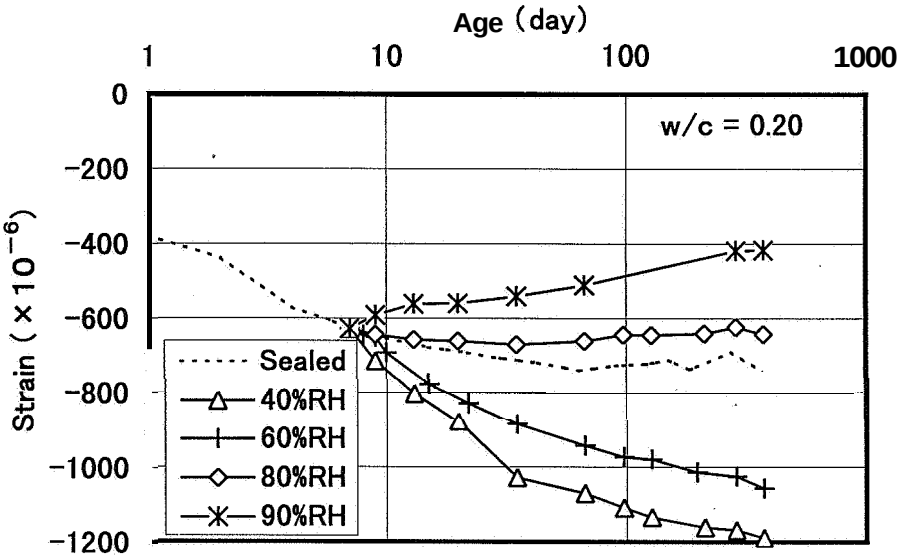

Fig. 2 Influence of relative humidity on length change (w/c = 0.20)

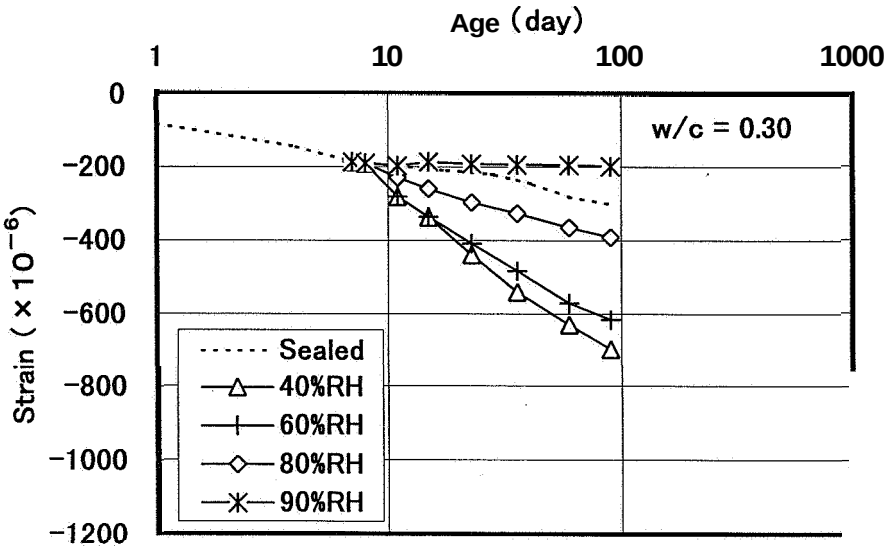

Fig. 3 Influence of relative humidity on length change (w/c = 0.30)

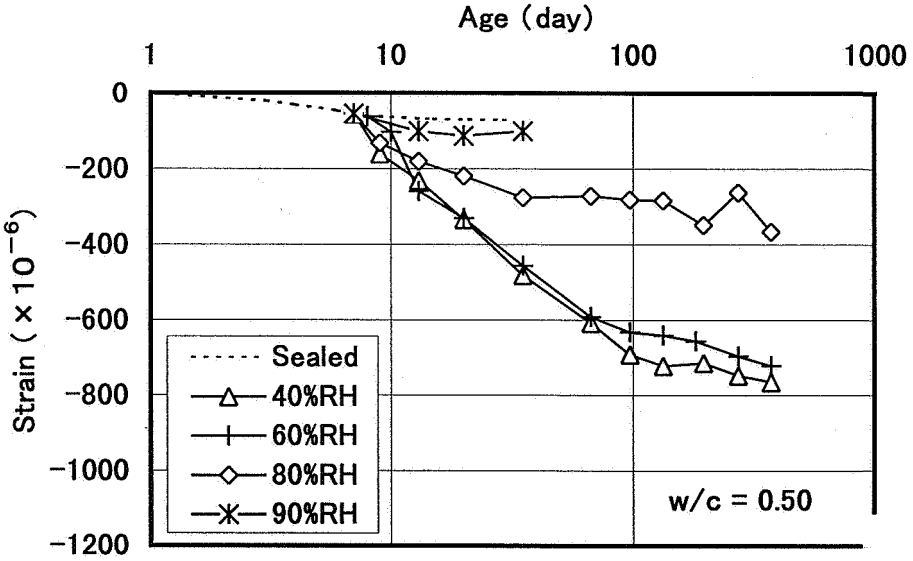

Fig. 4 Influence of relative humidity on length change (wlc = 0.50)

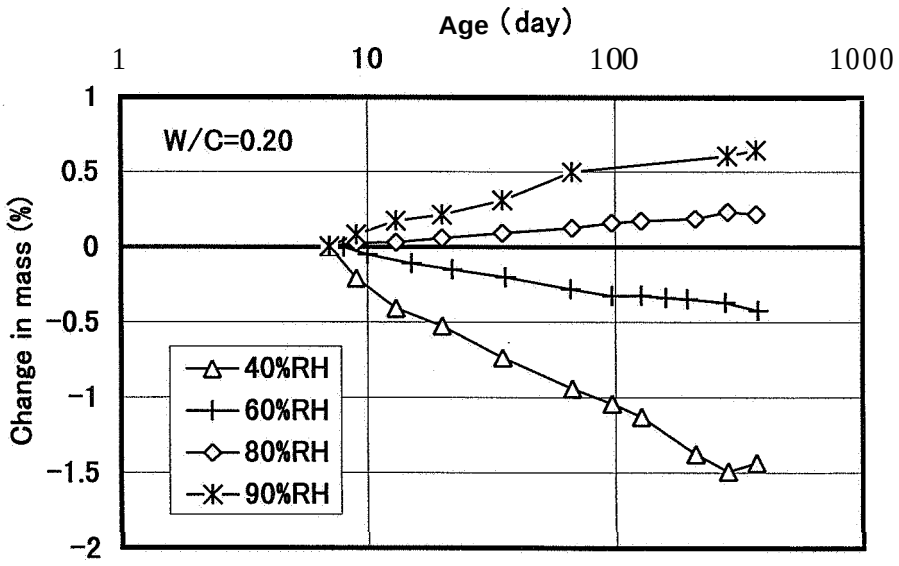

Fig. 5 Influence of relative humidity on mass change (w/c = 0.20)

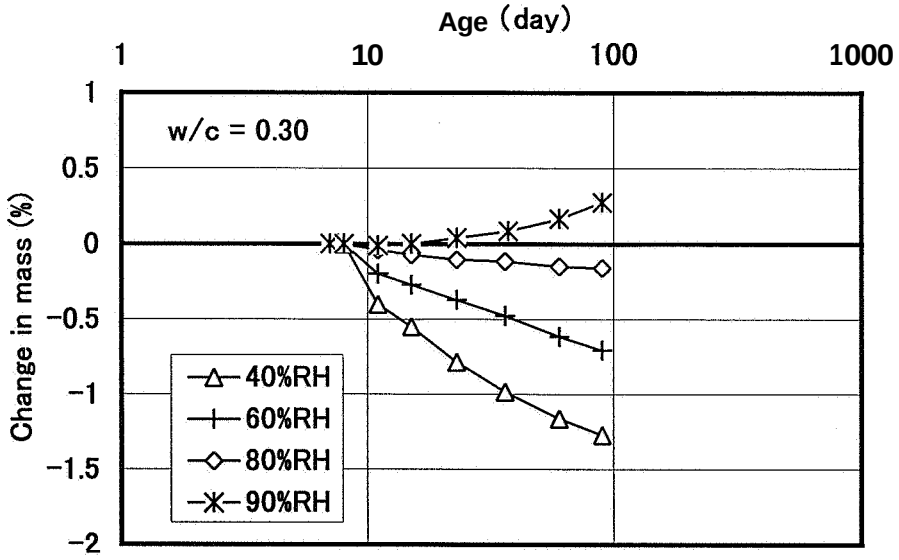

Fig.6 Influence of relative humidity on mass change (w/c = 0.30)

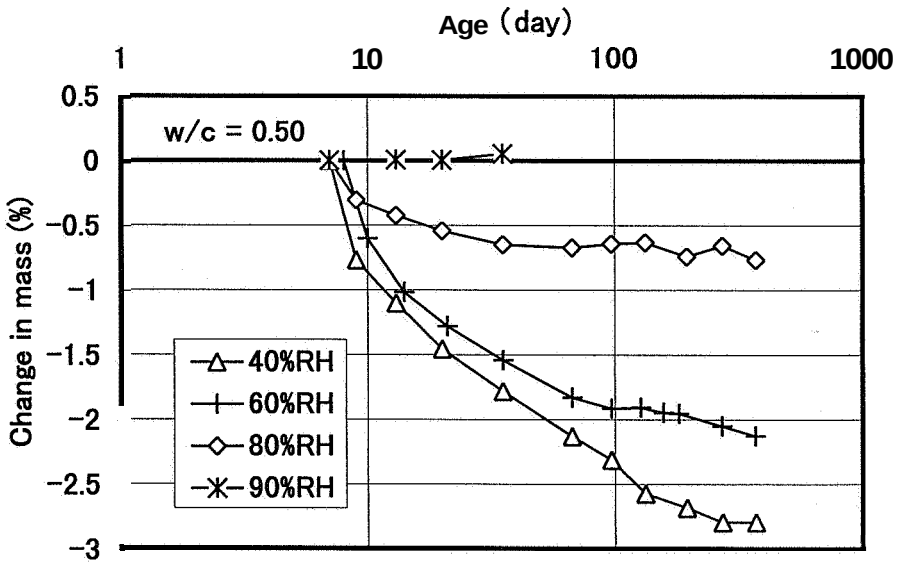

Fig.7 Influence of relative humidity on mass change (w/c = 0.50)

Relation between drying shrinkage and change in mass is shown in Figs. 8, 9 and 10. Drying shrinkage in these figures are determined by subtracting autogenous shrinkage strain from the total strain, where autogenous shrinkage of dried specimen is assumed to be the same as that of sealed specimen. It can be seen that expansion is observed in high-strength concrete with 0.2 and 0.3 water-cement ratio when the mass of the specimens increases due to moisture movement into the specimen.

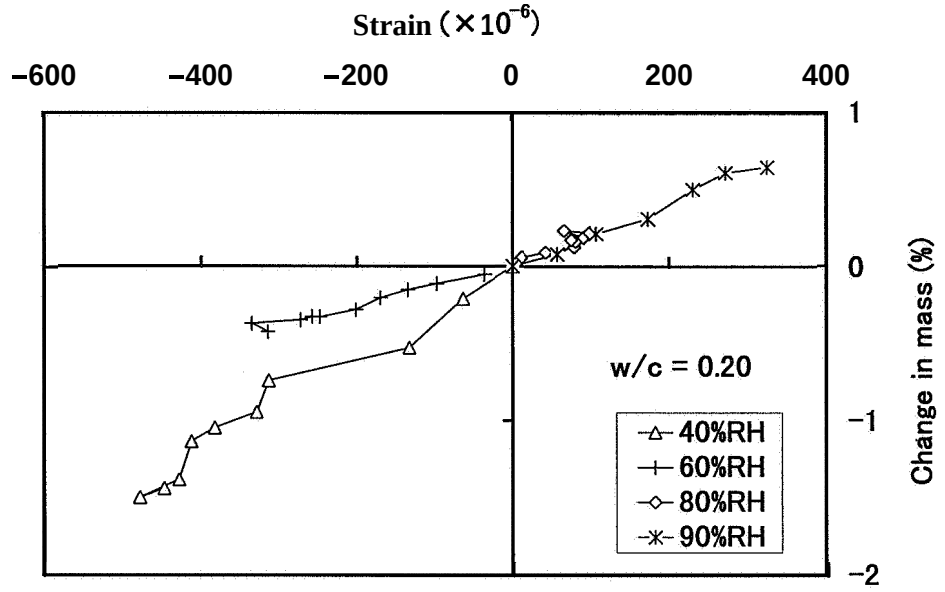

Fig.8 Relation between drying shrinkage and mass change (w/c = 0.20)

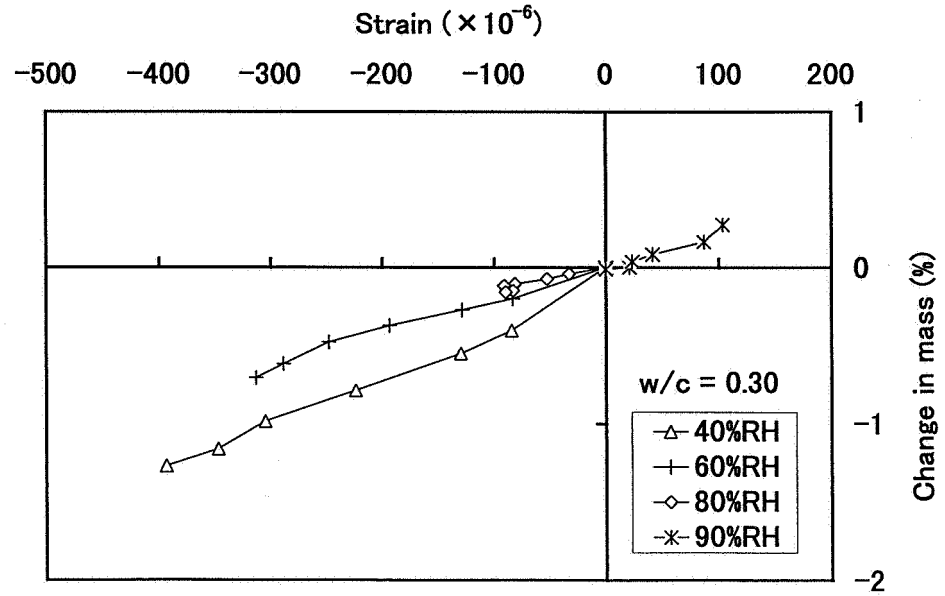

Fig.9 Relation between drying shrinkage and mass change (w/c = 0.30)

Relation between ambient relative humidity and drying shrinkage is shown in Fig. 11. In any case, shrinkage decreases with increasing ambient relative humidity and expansion can be recorded when ambient relative humidity is more than a certain value that is dependent on water-cement ratio. The value of the specific ambient relative humidity (P_0) at which neither drying shrinkage nor expansion is not recorded can be

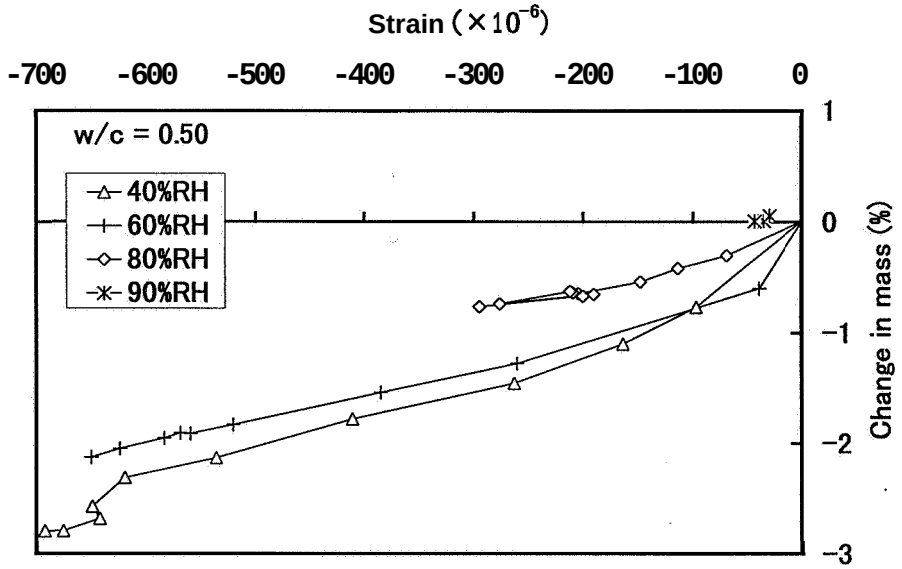

Fig.10 Relation between drying shrinkage and mass change (w/c = 0.50)

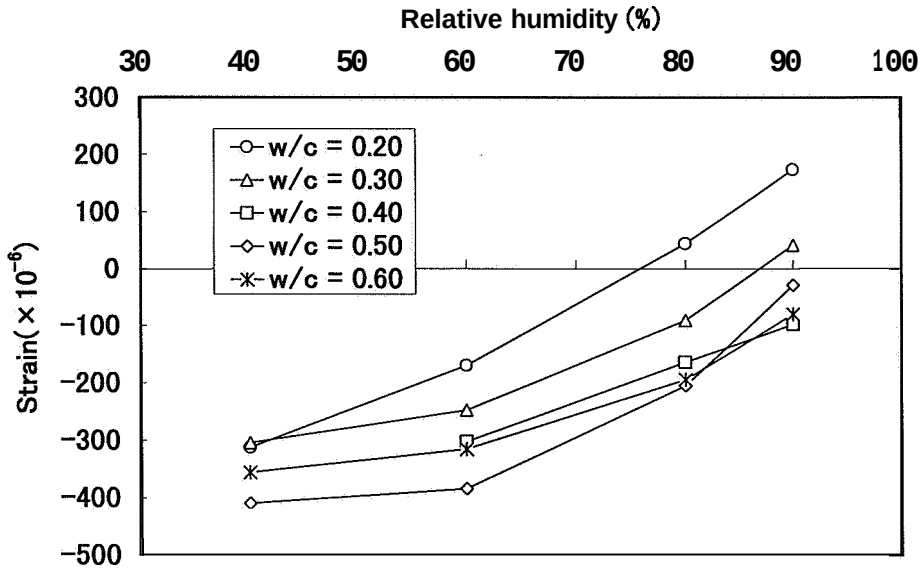

Fig.11 Relation between relative humidity and drying shrinakge at different relative humidity (age: 35 days, duration of sealed curing: 7days)

determined from this figure. As shown in Figs. 12, the value of ρ_0 decreases with decreasing water-cement ratio. The internal relative humidity of concrete calculated from eq. (1) proposed by Persson is also shown in Fig. 12. He proposed a prediction model for internal relative humidity of sealed concrete as follows [5].

$$\phi(w/c, t) = 1.08 \cdot (1+0.00003 \cdot t) \cdot (w/c)^{0.16 \cdot (1+0.0017 \cdot t)} \quad (1)$$

where, ϕ denotes the internal relative humidity of concrete, t denotes age and w/c denotes water-cement ratio.

The internal relative humidity has been also predicted by French Chapter of RILEM (AFREM) *[6]*from eq (2). Calculated values from eq (2) are shown in Fig. 13.

$$\phi(f_{c28}) = 72\exp(-0.046 f_{c28}) + 75 \quad (2)$$

where, f_{c28} denotes the compressive strength of concrete at 28 days.

It has been suggested that internal relative humidity of high-strength concrete decreases with increasing degree of hydration due to self-desiccation. It can be seen from Fig. 12 that the value of P, is about the same as the internal relative humidity. It can be said that drying shrinkage is governed by the difference between internal humidity and external humidity. Ambient relative humidity lower than ρ_0 leads to shrinkage and that higher than P, leads to expansion. This concept has been also proposed by AFREM [6].

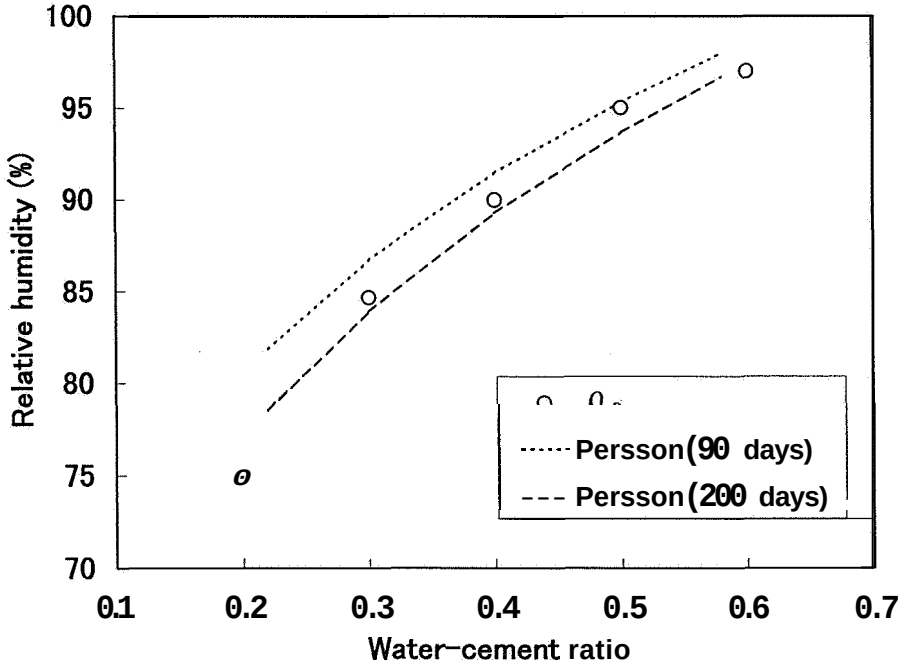

Fig.12 Relation between water-cement ratio and relative humidity

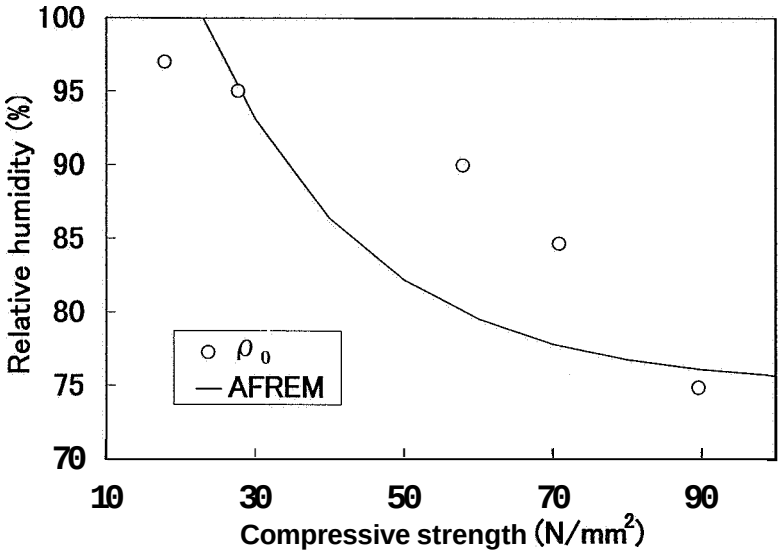

Fig. 13 Relation between compressive strength and relative humidity

4 Conclusions

Influence of ambient humidity on shrinkage of high-strength concrete is quite different from ordinary concrete. Decreases in mass and length of specimen are expected in concrete when the internal relative humidity is higher than the ambient relative humidity. Increases in mass and length are expected in high-strength concrete when the internal relative humidity is lower than the ambient relative humidity.

5 References

1. Tazawa, E. and Miyazawa, S. (1997) Influence of cement composition on autogenous shrinkage of concrete, Proceedings of the *10th* International Congress on the Chemistry of Cement, 2ii071.
2. CEB-FIP (1990) model code CEB-FIP 1990.
3. Japan Society of Civil Engineers (1996) Standard Specification for Design and Construction of Concrete Structures (in Japanese).
4. Tazawa, E. (Editor) (1999) Test method for autogenous shrinkage and autogenous expansion of cement paste, mortar and concrete, Autogenous shrinkage of Concrete, E & FN SPON, pp.56-59.
5. Persson, B. (1997) Moisture in concrete subjected to different kinds of curing, Materials and Structures, Vol.30, pp.533-544.
6. Le Roy, R., De Larrard, F. and Pons, G. (1996) The AFREM code type model for creep and shrinkage of high-performance concrete, Proceedings of the 4th International Symposium on Utilization of High-strength1 High-performance Concrete, pp.387-396.

A COMPUTER PROGRAM TO CALCULATE DRYING OF AND DESICCATION IN CONCRETE

G. HEDENBLAD and J. ARFVIDSSON
Building Materials and Building Physics,
Lund Institute of Technology, Lund, Sweden

Abstract
A computer program, TorkaS 1.0, to calculate drying of and desiccation in concrete is presented in the paper. In the paper the background to the development of the program, a brief description of the theoretical structure and a description of how to use TorkaS 1.0 are described.
Keywords: Moisture, concrete, drying, self-desiccation.

1 Introduction

A good indoor climate requires competence and experience on the part of both the customer and the executor at the erection or rebuilding of a building. The demands concern many different areas, e.g. sound, light, moisture, thermal comfort and air but also the physical design of the building. The demands of the customer and the demands for competence have to be satisfied throughout the building process. Keen competition, costs for building loans and the desire to take possession of the building have made the rate of production much more rapid. The drying of construction water normally takes such a long time that it often is a critical activity in the schedule of the building. By choosing the design of the structure, concrete quality, method of production etc., the drying time can be influenced, that is, prolonged or shortened. If a preliminary moisture design is worked out during the planning phase, the drying time of the construction water can be estimated, and then there is a chance to achieve a more economic design for the concrete construction.

The computer program TorkaS 1.0 is the latest chain in a long process. At the Building Materials and Building Physics, Lund Institute of Technology we have worked with moisture issues since its foundation in 1964. In 1973 the results of some drying experiments with concrete were published /1/. In 1977 Nilsson /2/ published the well-known (in Sweden) Table for predicting the drying times to 90% relative humidity (RH).

From 1981, work in the different departments has been co-ordinated by the Moisture Research Group of the Institute. From 1985 the Swedish Council for Building Research has financially supported the Computational Group at the Division of Building Physics, and the Division is a member of the Moisture Research Group. During this period there has been an

informal co-operation between Building Materials and Building Physics. This made it natural to co-operate on the development of a computer program for predicting the drying of concrete. The development of TorkaS 1.0 has received financial support from the Swedish Building Industry Development Found (SBUF).

2 Redistribution of moisture after the floor covering is laid − depth of measurement

Drying of a concrete slab or wall begins at the surface, while the moisture content in the middle of the construction remains high. When a more or less impervious floor covering is laid on the surface, the moisture in the concrete below the impervious floor covering is redistributed and equalized. The moisture level at a certain "equivalent depth" from the surface is exactly equal to the moisture level, which will be achieved at the surface after the floor covering is laid. In principle, this equivalent depth depends on the impermeability of the flooring material. The most dangerous case occurs when the flooring material is completely impervious. This case is dealt with below.

Drying from both sides of a construction: Equivalent depth ≈ 0.2 H.

Drying from one side only: Equivalent depth ≈ 0.4 H.

H is the thickness of the slab (wall).

Drying from both sides of a construction applies, for instance, to intermediate floors and partitions. The drying from this type of constructions normally continues from the other side of the construction even after an impervious covering is laid on one side. This means that the redistributed higher moisture level persists only for a "limited" time.

Drying from one side only of a construction applies to a concrete slab on the ground, but also to concrete floors cast on impervious permanent formwork (e.g. decking). The value of 0.4 H is probably on the safe side. In slabs on the ground, underlain by expanded plastics, some drying can nevertheless take place downwards. In a floor on the ground underlain by mineral wool, drying takes place downwards due to a temperature difference across the insulation if this is dry. In spite of this, no differentiation is made in the equivalent depth, and the value 0.4 H is used irrespective of the properties of the insulation material.

3 Some notes on the theoretical structure of TorkaS 1.0

An important starting point for the model of the drying of concrete is the moisture transport properties of mature concrete, which were presented in /3/. Even if these moisture transport properties are valid for mature concrete, they can be related in principal to the capillary porosity. They can then be related to the water cement ratio (w/c) and to the degree of hydration. The degree of hydration is a function of w/c, temperature, RH, type of cement and time. From these relations it is possible to calculate the moisture transport properties of concrete after the construction. Some other important parts are the development of the degree of hydration and the sorption isotherm. In TorkaS 1.0, the latest published research on the degree of hydration /4/ has been used. The calculations are made according to the finite difference method and are described in /5/. The program has been developed for the Swedish cement, Slite Std, which is an ordinary Portland cement (OPC).

4 The interface of the program

The first input page is shown in Fig. 1. The texts on the input and result pages are here translated from Swedish to English. The requested input data are climate (place in Sweden), type of construction, time of the casting, time when the house is tight (roof on), time when controlled drying starts, time when the drying is ended. **A** calendar is included in the page and the date from the calendar can be transported to the time of the casting etc. The program also asks for the thickness of the construction, w/c and the cement content (kg/m^3 concrete).

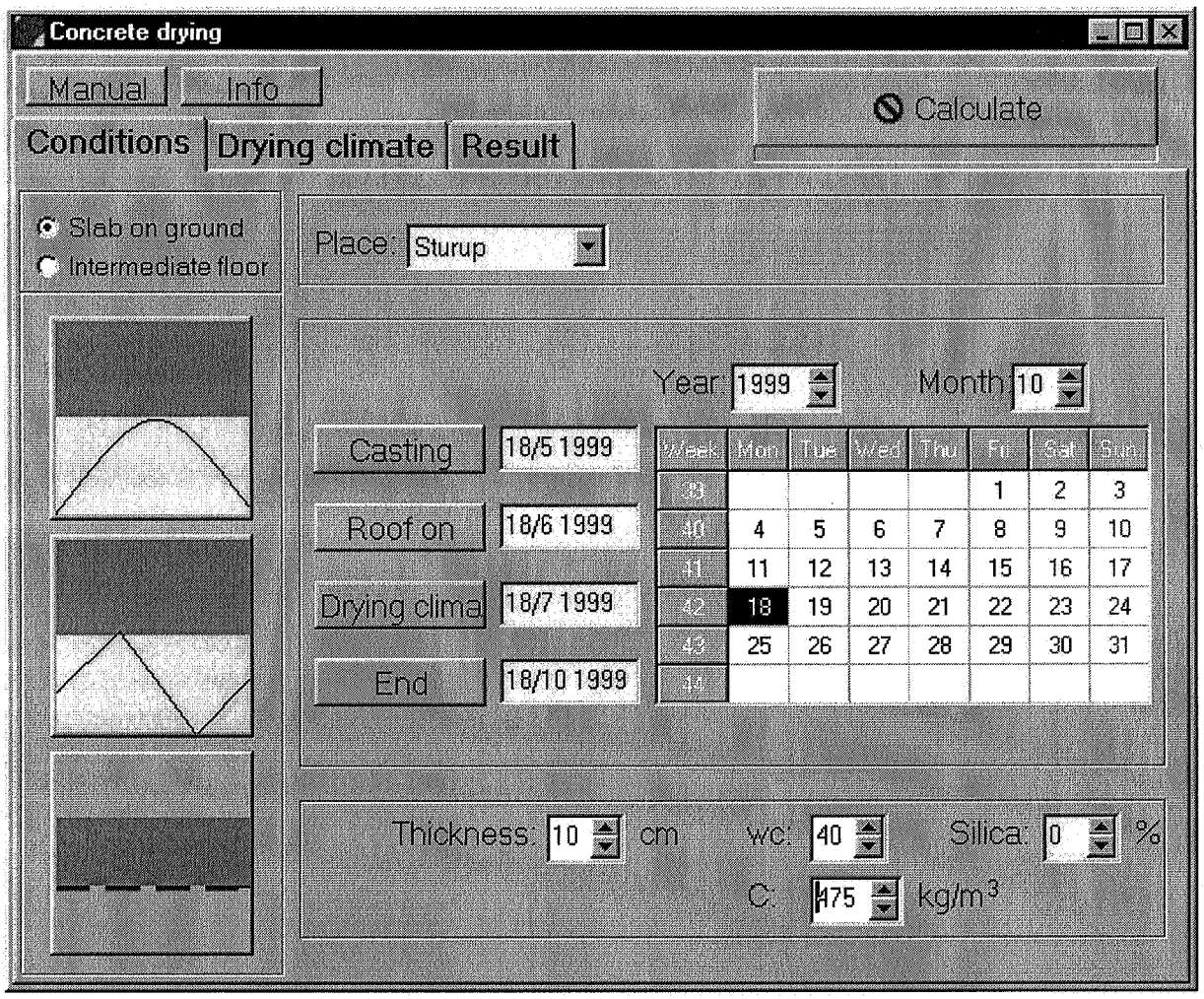

Fig. 1. First input page of the program TorkaS 1.0.

There are two types of construction, namely, slab on the ground and intermediate floor. For slabs on the ground there are three different types of layer beneath the concrete; mineral wool, expanded polystyrene and an impermeable layer. For intermediate floors there are also three different construction types; homogenous concrete slab drying from both sides, concrete slab cast on a concrete formwork and impermeable formwork (e.g. steel sheeting).

For slabs on the ground with mineral wool beneath the concrete, it is supposed that the thickness of the insulation is 10 cm. With this thickness of the insulation and with normal ground-areas of one-family houses, in most cases drying can take place downwards. The calculations are based on the assumption that the moisture permeability of the mineral wool is

$10 \cdot 10^{-6}$ m^2Is. The relative humidity of the ground is set to 100%. If the mineral is wet, from rain etc., it is probable that no drying can take place downwards. In this case it is more correct to calculate this as slab on the ground with impermeable layer.

For slabs on the ground with expanded polystyrene (EPS), it is supposed that some drying can take place downwards. The calculations are based on the assumption that the moisture permeability of the EPS is $1 \cdot 10^{-6}$ m^2/s and RH in the ground is 100%. For slabs on the ground with extruded polystyrene (XPS), it is supposed that this material is so impermeable that no drying can take place downwards and can be calculated as slabs on the ground with impermeable layer.

For a conventional intermediate floor the top surface of the concrete can be exposed to rain etc. Both the top and bottom surface of the concrete is supposed to have the same RH and temperature. The drying take place on both sides of the concrete.
For an intermediate floor cast on a concrete formwork, we have the same conditions except that in the calculations the total thickness, including the concrete formwork, is used. In TorkaS 1.0 the thickness of the formwork is set to 5 cm. For an intermediate floor with impermeable formwork, drying takes place on one side only. The second input page is shown in Fig. 2.

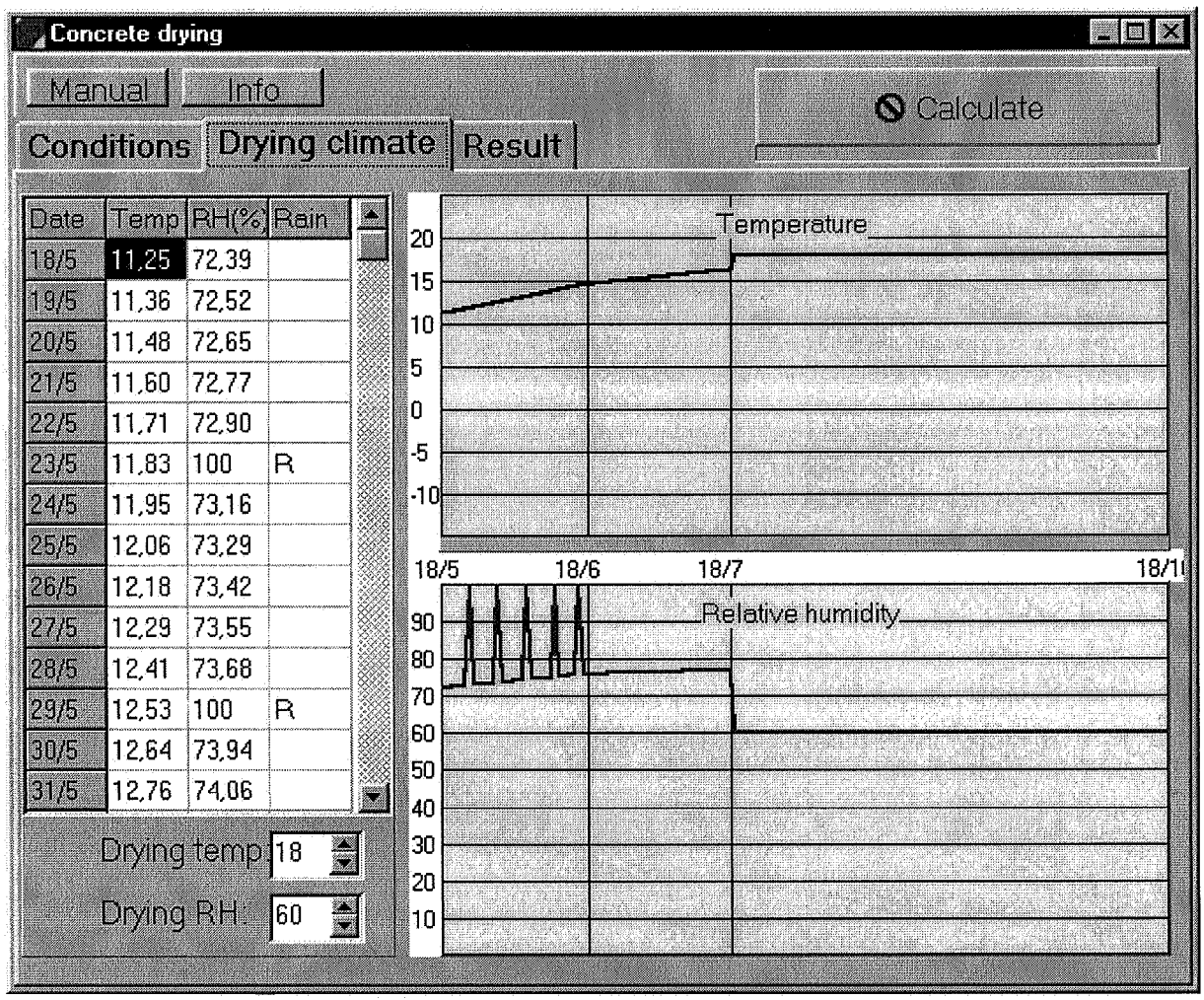

Fig. 2. Second input page of the program TorkaS 1.0.

Under the second input page "climate" it is possible to choose temperature, relative humidity and rain (R) and also membrane curing (M) during the period from the casting to the start of the drying. Depending on the location in Sweden, which is selected on the first input page, different values of temperature and RH and also days with rain are automatically calculated and shown in the table. But one can easily change the values in the table to values which are more valid for the actual building, e.g. higher or lower temperature or RH or more or fewer days with rain. From the start of the drying to the end of the drying period one selects the drying temperature and the drying relative humidity, which are constant during the drying period. The third (result) page is shown in Fig. 3.

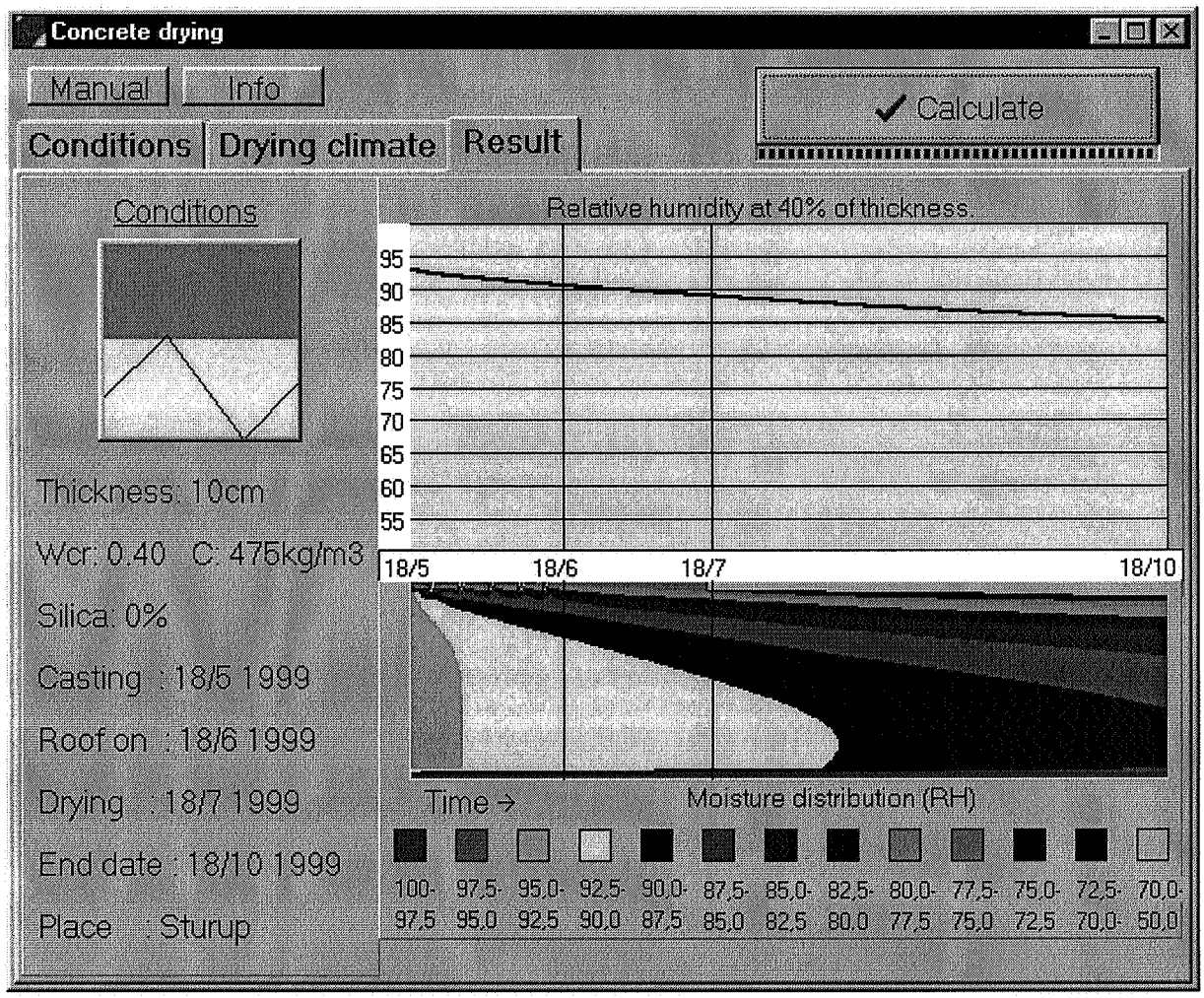

Fig. 3. Third (result) page of the program TorkaS 1.0.

The results of the calculations are shown both as RH at the equivalent depth as a function of time and as the distribution of RH in the concrete as a function of time. The upper diagram shows the RH at the equivalent depth.

TorkaS 1.0 can also be used to calculate the self-desiccation of concrete, the user just sets M (membrane curing) in the column for rain in the table in the second input page. One can at the same time select an appropriate curing temperature.

Comparisons between measured drying times, both in the laboratory and in the field, and drying times calculated with TorkaS 1.0 have been made and are presented in /6/. About 50 comparisons are made and in most cases the differences between calculated and measured RH are small.

5. Limitations of the program

Thickness of the concrete construction: 10 – 30 cm.
w/c: 0.35 – 0.80.
Maximum drying temperature: 30°C.

6. References

1. Ahlgren, L. (1973). *Moisture in concretefloors with impermeableflooring* (in Swedish). *Byggmastaren* no. 6, p 17.
2. Nilsson, L-0. (1977). *Moisture problems in concretefloors* (in Swedish). Division of Building Materials, Lund Institute of Technology, Lund, Sweden. Report TVBM-3002.
3. Hedenblad, G. (1993). *Moisture Permeability of Mature Concrete, Cement Mortar and Cement Paste.* Division of Building Materials, Lund Institute of Technology, Lund, Sweden. Report TVBM-1014.
4. Norling Mjornell, K. (1997). *Moisture Conditions in High Performance Concrete – mathematical modelling and measurements.* Department of Building Materials, Chalmers University of Technology, Goteborg, Sweden. Report P-97.6.
5. Arfvidsson, J. (1998). *Moisture Transport in Porous Media. Modelling based on Kirchhoff potentials*. Department of Building Technology, Building Physics, Lund Institute of Technology, Lund, Sweden. Report TVBH-1010.
6. Hedenblad, G. (1998). *Comparison between measured RH and with TorkaS 1.0 calculated RH* (in Swedish). Division of Building Materials, Lund Institute of Technology, Lund Sweden. Report TVBM-7133.

ASPECTS OF MONITORING MOISTURE CHANGES USING ELECTRICAL IMPEDANCE SPECTROSCOPY

Monitoring Moisture Using Electrical Impedance

W. J. WEISS, J. D. SHANE, A. MIESES, T. O. MASON, and S. P. SHAH
Center for Advanced Cement-Based Materials, Northwestern University
2145 Sheridan Road, Suite A130, Evanston, IL 60208-4400

Abstract

Concrete may be susceptible to early-age cracking if volumetric changes are prevented. Previous researchers illustrated that the potential for cracking can be amplified in low water-to-cement ratio (w/c) concrete mixtures due to a combination of reduced stress relaxation (creep), increased stiffness (elastic modulus), increased brittleness, and increased early-age shrinkage. Although the majority of research has focused on the behavior of thin specimens (assumed uniform moisture throughout the cross-section), it is of practical importance to understand how moisture and shrinkage gradients influence the behavior of thicker concrete sections. These moisture profiles induce differential shrinkage rates throughout the depth resulting in curling displacements and stress gradients. This paper describes the use of electrical impedance spectroscopy as a method for assessing moisture profile development based on the simple assumption that the electrical properties of concrete can be related to moisture properties. Measured electrical resistance is correlated to relative humidity using geometrically similar calibration specimens stored at known relative hurnidities. In addition to correlating relative humidity with electrical resistance, the electrical response of the calibration specimens was investigated to understand how changes in the moisture condition influence the electrical response. This research illustrates the need for frequency scanning to ensure that bulk electrical properties are measured. In addition, frequency scanning may have additional benefits since characteristic features develop during drying that may provide additional insight into water-loss mechanisms and microstructural features.

Keywords: Electrical Properties, Humidity Profiling, Impedance, Moisture Distribution, Self-Desiccation

1. Introduction

Previous research has shown that as concrete dries a non-linear moisture gradient develops [1]. Moisture profiles cause differential shrinkage which may result in excessive curling and cracking, especially in slabs, pavements, and floors [2]. The shrinkage characteristics of low water-to-cement ratio (w/c) concrete differ fiom conventional concrete however. In low w/c mixtures a significant portion of the overall 'drying' can be caused by self-desiccation (internal drying) as opposed to water lost to the environment (external drying) [3]. While moisture loss to the surrounding environment is a diffusion based problem that is highly dependent on section thickness [4], autogenous shrinkage is generally assumed to be independent of specimen size. However, recent research has suggested that autogenous shrinkage/water loss may not occur uniformly throughout the cross section [5]. Since low w/c concrete has a more uniform moisture distribution (i.e., less severe moisture profiles), these mixtures may be useful in reducing curling displacements, provided cracking can be prevented.

2. Research Motivation

Self-desiccating concrete may be a useful method to reduce shrinkage curling, improve aggressive ion penetration resistance, improve freeze-thaw resistance [6], reduce reinforcement corrosion, and reduce moisture related problems that arise in some floor covering applications [7]. However, research is still required to develop methods for combating the harmful effects associated with self-desiccation which increase the potential for early-age shrinkage cracking [8,9] and may result in strength reduction over time [10]. This paper presents results from an ongoing investigation aimed at using electrical properties as a method to characterize the moisture distribution in cement-based materials. Specifically, this research investigated three model paste systems with different water-to-cement ratios (w/c's). Electrical properties were monitored on a variety of specimens to understand how changes in moisture influence the electrical response. In addition, the electrical response was measured as a function of depth to understand how moisture profiles develop in different mixtures. The measured electrical properties were then correlated with the humidity profiles that develop in concrete.

3. A Review of Electrical Profile Measurements in Concrete

Several studies have been focused on using electrical properties as a method to assess the moisture profiles that are induced in concrete due to drying and wetting. Schieβl and co-workers [11,12] have proposed the use of a multi-ring electrode configuration to characterize the electrical resistivity profiles that develop in cement-based materials as they dry. In addition, McCarter and co-workers [13,14,15,16,17] have conducted a wide range of experiments using electrode pairs spaced at different distances fiom the drying surface to assess the drying and wetting depth in concrete using normalized conductivity and resistivity. Yuasa et al. [18] compiled a review of similar techniques that have been developed in Japan to assess moisture content. In addition, the authors [19] have attempted to correlate the measured electrical resistance to physical drying properties by considering aging and relative humidity effects using calibration specimens.

4. Experimental Program

4.1 Mix Constituents

In this work, a series of paste mixtures were prepared to investigate the influence of water-to-cement ratio (wlc) and drying on the characteristic moisture profile and electrical response. Three paste mixtures were used in this study with water-to-cement ratios (w/c) of 0.3, 0.4, and 0.5. The mixtures were cast using a commercially available Type I ordinary portland cement with a chemical composition of 54% C_2S, 19% C_3S, 10% C_3A, 7% C_4AF, and a Blaine fineness of 368 m^2/kg.

4.2 Specimen Geometry

Three different specimen geometries were cast as shown in Figure 1. The first specimen geometry (75 mm depth, 75 mm width, and 150 mm length) was intended to investigate the development of moisture and electrical impedance gradients as a function of drying time and depth from the drying surface. These specimens were exposed to one-sided drying in a constant 40% RH, 30°C environment. Nine electrode pairs were placed at different depths from the drying surface (6.25, 9.5, 12.5, 19, 25, 31, 38, 50, 70 mm) to monitor changes in electrical response at different depths. The second specimen geometry used in this investigation was intended to permit accelerated drying (equilibration) in environments of different relative humidity to provide a calibration for the larger specimen. Therefore, the calibration specimens were chosen to be relatively thin, 75 mm width, 12.5 mm depth, and 50 mm length. In both geometries unpolished stainless steel rods were used as the electrodes. The 2.4 mm diameter rods were spaced 12.5 mm apart and placed in the acrylic forms before casting. It should be noted that the holes in the acrylic were slightly oversized and filled with a rubberized sealant to permit shrinkage movements while minimizing restraint. In addition, twenty calibration specimens (25 mm dia. x 75 mm) for each mixture were cast for the determination of the depth dependent evaporable and non-evaporable water of the sample with time.

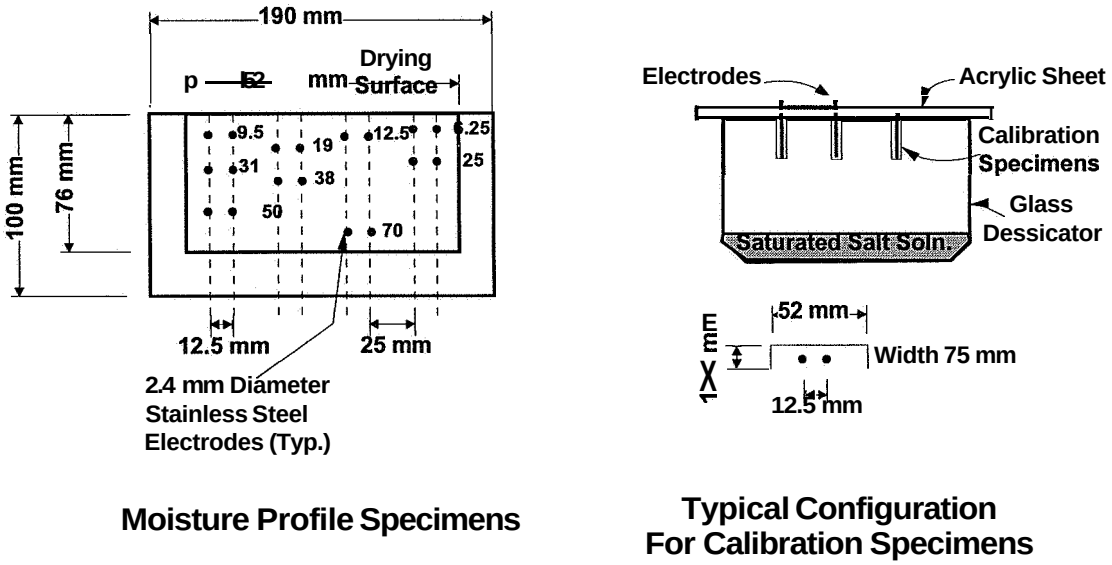

Figure 1: Specimen Geometry

4.3 Sample Preparation

The casting procedure was identical for all the mixtures investigated. The mix constituents were weighed, combined in a rotary mixer, and mixed for 20 minutes at low speed while frequently scraping the sides of the mixer to ensure a uniform mix composition. After mixing, the cement paste was placed in the acrylic forms, rodded, and vibrated for a short time (<15 sec) before the surface was finished with a steel trowel. After casting, the forms were covered with thin plastic sheets to minimize moisture loss and covered with wet burlap and plastic sheeting for 24 hours. After curing for 24 hours, the calibration specimens were demolded, weighed, and placed in their respective environmental chambers.

As shown in Figure 1, two calibration specimens from each mixture were stored over salt solutions of known relative humidity. The different salt solutions used in this investigation were Sodium Bromide (NaBr) - 60% RH, Sodium Chloride (NaCl) - 75% RH, and Zinc Sulfate Heptahydrate ($ZnSO_4 \cdot 7H_2O$) - 90% RH. One set of calibration specimens were sealed between acrylic plates to prevent moisture loss, while the 50% RH specimens were stored in an environmental chamber as were the 40% RH specimens, cylindrical specimens, and moisture profile specimens. In some cases, samples were stored over pure water to obtain a 100% RH environment. The electrodes of each specimen were permitted to protrude through the top of the glass desiccator to facilitate age-dependent measurement without disturbing the samples.

5. Experimental Procedures

Frequency scanning electrical impedance measurements provide a method for assessing the bulk and electrode behavior of cement-based systems [20,21,22]. Impedance was measured by applying a small (1V) sinusoidal voltage at a known frequency to induce a current flow. The magnitude of the current and phase angle were measured. This process was repeated over a wide range of frequencies (typically mHz to MHz) to facilitate the separation of mechanisms with different relaxation frequencies. The phase angle and current can be rearranged into real, imaginary, and total impedance components, which can be represented graphically as shown in Figure 2. Section 6 provides a description of the most prominent characteristics of the impedance spectra in addition to illustrating how this data can be used to interpret cement-based systems.

In this study, impedance measurements were conducted using a Solartron 1260 impedance/gain-phase analyzer that was interfaced to a personal computer for automated data collection. Readings were taken over a frequency range of 1 Hz to 10^7 HZ with ten measurements per decade. Measurements were taken at 1, 3, 7, 17, 28, 49, and 98 days. In addition to the non-destructive electrical measurements, a destructive procedure was used to assess the evaporable and non-evaporable water contents. This method involved splitting the cylindrical specimens at 12.5 mm intervals along the length, crushing the sample, and oven-drying of a cement paste sample. Evaporable water was computed based on the water lost when dried at 105°C for 18 hours, while the non-evaporable water was determined based on the water lost when an oven-dried paste is ignited to 1000°C.

6. Electrical Impedance Spectra Characteristics

Figure 2 provides a graphical representation of a typical electrical impedance response for a cement-based system. In the Nyquist plot (Fig. 2a) the imaginary impedance is plotted against the real impedance. The curve that results can be nominally considered as two arcs, a bulk response arc (smaller - left) and an electrode arc (larger - right). While the larger arc contains low frequency measurements corresponding to the interfacial electrode effects, the small arc consists of higher frequencies and corresponds to the bulk material effect. Christensen et al. [22] suggested that the most useful parameter for describing the cementitous system is the intersection point between the two arcs. Since this point occurs at the minimum imaginary impedance, it is composed primarily of the real impedance of the system as shown in Figure 2b. For this reason, the point of minimum imaginary impedance is commonly referred to as the bulk resistance (R_b). Since impedance measurements will be taken over a wide range of frequencies, IS can resolve the electrical response to obtain a 'true' bulk resistance in cemetitous systems regardless of mixture composition [21,22,23].

In addition to measuring the bulk resistance, other characteristic features of these curves can be used to describe the cementitous system. Both the electrode and bulk arcs are frequently represented using parallel electrical circuits combining a resistor and a capacitor while another feature is commonly referred to as the offset resistance (R_O). While it has been suggested that the offset resistance may be an experimental artifact [24], Christensen et al. [25] proposed that this high-frequency behavior (R_O) may be attributed to the presence of a secondary arc corresponding with features of the conduction path. In addition, if the bulk response is fitted with a semi-circular arc, the center is observed to fall below the horizontal axis. The degree to which the circle is depressed is frequently referred to by computing the depression angle of a circle in which the diameter passes through a point on the circumference with no imaginary impedance. While this section has provided a brief overview of important IS properties, the reader is referred to a recent review by Christensen et al. [22] for further information on applications and interpretation of IS in cementitous systems.

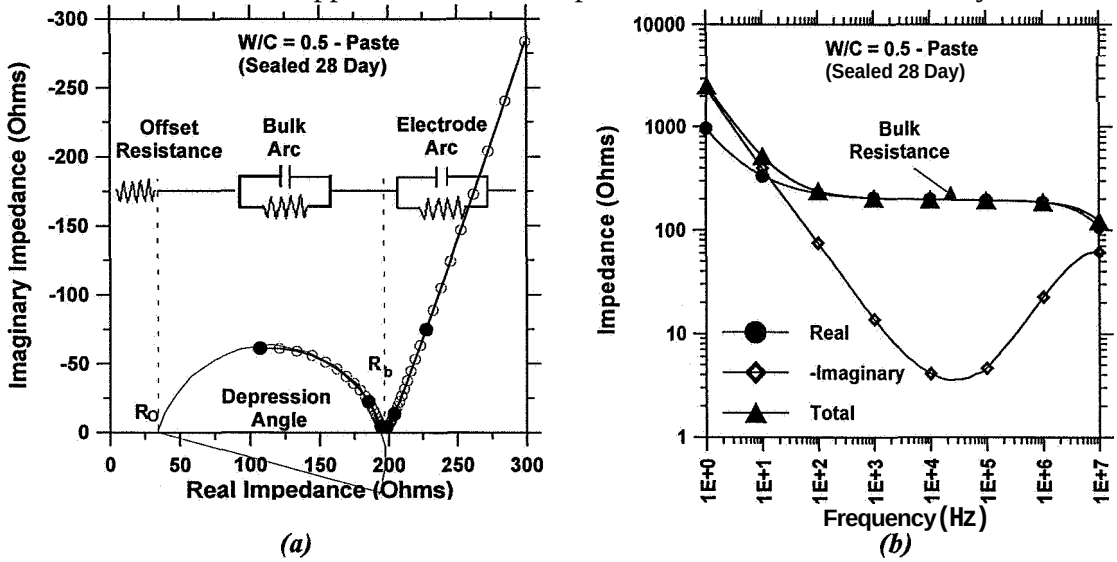

Figure 2: Typical Alternating Current Electrical Impedance Measurements in a Cementitous System (W/C=0.5, 28 Days, Sealed): (a) Nyquist and (b) Bode Plots

7. Features of the Electrical Response - Calibration Specimens

7.1 Influence Of Aging

Two characteristic mixtures (w/c=0.5 and 0.3) were selected to illustrate the influence of aging (hydration) and self-desiccation (internal drying) on the measured bulk resistance. Figure 3 illustrates the experimentally measured electrical bulk resistance and relative proportions of internal water measured on sealed specimens at different ages. The lower w/c paste has a higher measured bulk resistance and lower evaporable and non-evaporable water contents. The increase in bulk resistance that occurs with decreasing w/c is primarily attributed to the lower relative volume of the most conductive component (water or pore fluid) in the system. Changes in the combined water occur most rapidly at early-ages since it is commonly assumed that the hydration reaction is relatively logarithmic with time. The substantial changes in the electrical bulk resistance that occur at early-ages may result for a variety of reasons including rapid consumption of the water by the hydration reaction [26], changes in pore fluid composition [27], and filling of pore space essentially creating a more tortuous, discontinuous path [28]. It is interesting to note that the lower w/c mixture demonstrates a more distinguishable increase in bulk resistance over time. These trends are similar to the data presented by Scuderi et al. [29] for different w/c mixtures in which hydration was investigated at early ages.

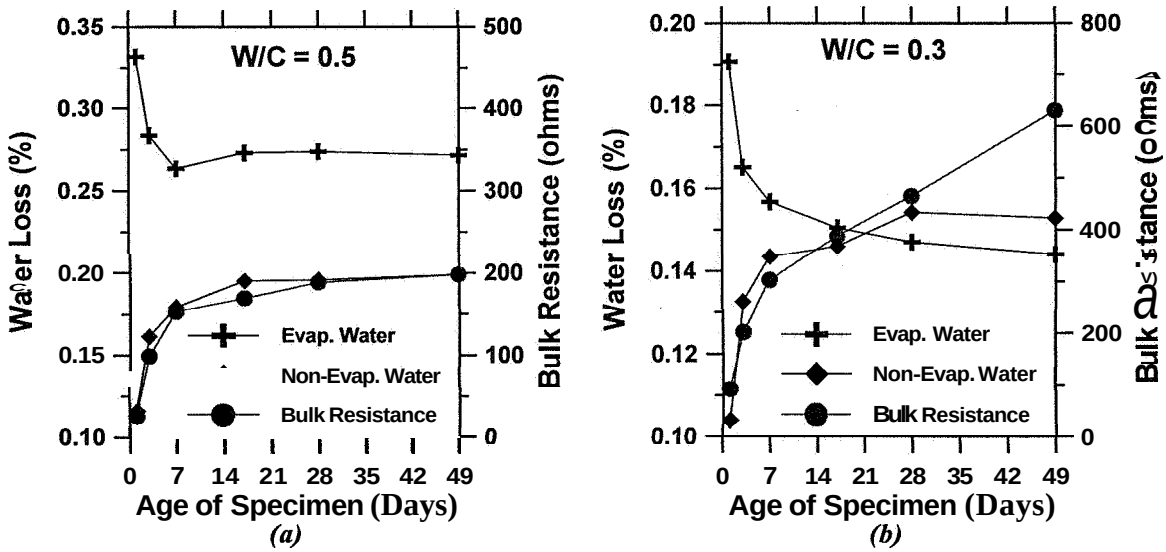

Figure 3: Influence of Aging on the Hydration Reaction, Water, and Electrical Resistance of a Normal (w/c = 0.5) and Self-Desiccating Paste (w/c = 0.3)

It can be noted that time dependent change in the bulk resistance corresponds reasonably well with the changes in evaporable or non-evaporable water in the w/c = 0.5 mixture. Conceptually this is reasonable since it can be reasoned that primary path of electrical conduction (path of least resistance) is most likely a combination of the connected or disconnected capillary pore water solution (water filled pores). As the cement paste hydrates, water is consumed by the hydration reaction effectively reducing the relative volume of water available for conduction while the volume of the less conductive hydration products is increased. Conceptually, these time dependent changes in the volume proportions of the mix constituents can be

illustrated using the descriptive model proposed by Powers and Brownyard [26] as shown in Figure 4a. It can be seen that over time water reacts with cement to form a volume of gel and an abundance of capillary water is present in the high w/c mixtures. The influence of hydration on the volume proportions differs in low w/c mixtures however. It can also be shown that when a low w/c mixture is considered in a sealed system (no external drying or wetting) there is an abundance of cement in comparison with water. As a result, water in the fluid filled pores begins to react with the surrounding cement resulting in self-desiccation. Low w/c mixtures, even after complete hydration, will have a portion of the cement that remains unreacted in addition to air filled pores that develop due to self-desiccation. It can be observed that the time dependent development of bulk resistance does not correlate directly with the measured changes in non-evaporable water in the low w/c mixture. This may be explained in part by self-desiccation (internal drying) which causes an additional air phase (high resistivity) to develop, thereby making the conduction path more discontinuous (Fig 4).

If we consider a conceptual model for electrical conduction similar to that suggested by MacPhee et al. [28] and McCarter et al. [14] (Fig. 4b), it can be reasoned that the electrical conduction could occur along five main paths through a paste phase. First, the least resistive path would correspond to the connected capillary porosity (pore fluid). Over time, as the degree of hydration increases, the continuous phase begins to become more discontinuous and tortuous (disconnected porosity). This maze of hydration products and fluid-filled porosity results in an increase in resistivity. The final two phases, unhydrated cement paste and air voids, are highly resistive and as such probably do not contribute significantly to the electrical conduction other than reducing the volume of conducting material. It should also be noted that in the low w/c paste, the self-desiccation of the paste contributes to a further reduction in the available capillary and gel water while the more resistive component, air, is increased.

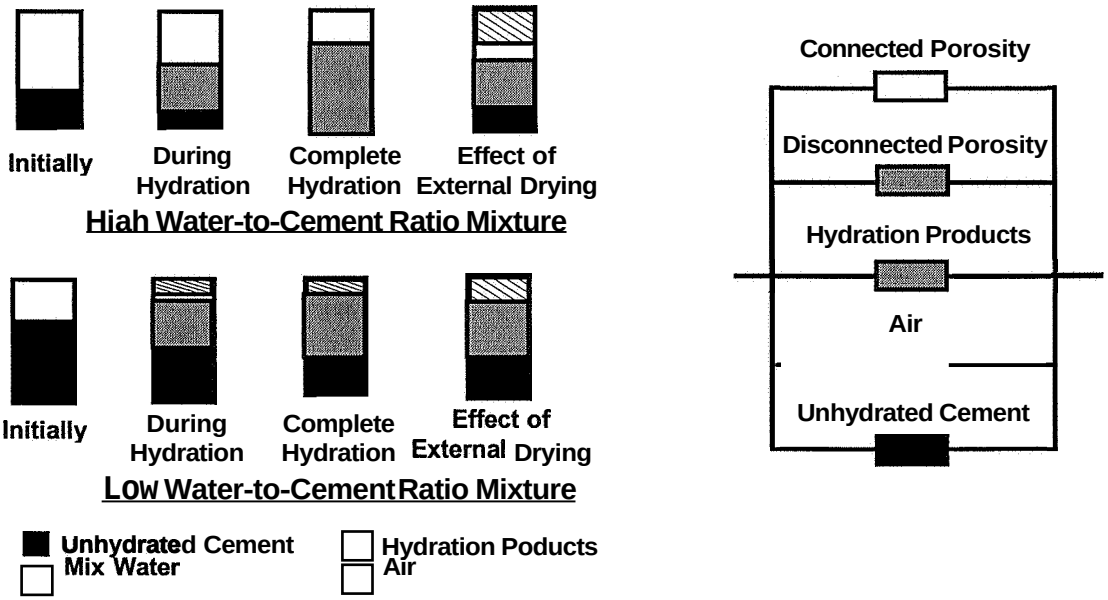

Figure 4: Conceptual View of the Hydrated Products and Electrical Conduction Through Different Phases of the Cement Paste

Frequently, the 'bulk feature arc' appears to be composed of overlapping arcs corresponding to different conduction paths. Scuderi et al. [29] observed that a secondary feature became visible in low w/c mixtures at certain early-ages, however only one arc was discernable at later ages. McCarter [30] observed a secondary arc near the electrode in systems containing fly ash and MacPhee et al. [28] observed the existence of secondary feature arcs in pressed cement pastes. In addition, Chen and Chung et al. [31] observed a secondary arc feature in fiber reinforced composites. More recently, Hwang et al. [32] and Ford et al. [33] suggested that this arc may be attributed to imperfect contact effects at the electrode/cement interface. Implications of the results obtained in these simulations and their connection with the measured impedance behavior will be discussed in the following sections.

7.2 Influence Of Drying

While it is commonly accepted that dry concrete is more electrically resistive than moist concrete [2, 34], this work attempted to correlate the increase in resistance with the environmental conditions. In addition, this work began to describe how the features of the electrical response are altered by drying. Figure 5 illustrates time dependent Nyquist plots for a w/c=0.5 calibration specimen stored in a severe drying environment (40% RH). Although the specimen is relatively thin, it may take 2 months to equilibrate with the surrounding environment. It can be seen that as the specimen dries it becomes more resistive. This is most likely attributed to the decrease in the conductive fluid-filled pores as previous described in Figure 4. In addition to increased resistance, it should be noted that the frequency at which the bulk resistance occurs is reduced due to hydration and further reduced due to drying. When the specimen was measured at an age of one day, the bulk feature arc was barely distinguishable as noted by others at early ages [29]. When measurements were taken at an age of three days the bulk arc is clearly visible and relatively circular. As the specimen continued to hydrate and dry, the arc developed more completely, however the angle of depression increased. At an age of 28 days, the bulk arc is relatively flat with a distinguishable difference in curvature from one side of the arc to the other. This suggests that two (or more) distinct feature arcs may be present. As the specimen dries further a second arc is definitely distinguishable at high frequencies and the electrode arc begins to disappear.

A less-than semi-circular bulk arc may develop in the drying specimens for several reasons including a combination of true bulk material behavior, preferential drying along the electrode, layered drying/properties surrounding the electrode, drying of the pores along the electrode, or cracking at the electrode. Previous arguments suggest that different conduction paths could provide a partial explanation for this secondary feature [27]. It is believed that the non-semi-circular arcs observed in this study is not caused by preferential drying at the electrodes since the surface of the specimen which was penetrated by the electrode was sealed in all the specimens with a combination of a rubberized silicon and acrylic sheeting. The sealed end conditions would also eliminate the idea of a layered interface developing around the electrode since there would be no mechanism for differential drying along the specimen between the electrodes. It is also conceivable that small cracks develop at the

interface due to shrinkage, however no visible cracking was observed. Another possible explanation could explain the occurrence of additional features is the development of air 'gaps' between the electrode and 'cement-paste' caused by drying (Fig. 6). This would be similar to the case described by Hwang et al. [32] in cerium oxide where the electrodes would not have perfect contact with the bulk material due to surface imperfections. Figure 6 illustrates that in a saturated system the water would occupy the pores along the electrodelcement paste interface, however as the specimen dries in both the phase and at the electrode/bulk interface, the contact area between the electrode and bulk cement could be reduced. Ford et al. [33] observed that the secondary feature would decrease for cement paste as the electrode surfaces were rewet or treated with silver paint. Figure 6b illustrates the relationship between the 'bulk-resistance' of an arc that is fitted to the arc at low values of real impedance ($R_{B\text{-}FIT}$) and the bulk resistance measured at the point of low imaginary impedance ($R_{B\text{-}IMIN}$). It can be seen that for the majority of the calibration specimens, the fit and minimum imaginary impedance bulk resistance values are relatively similar (i.e. ratio ~1.0), however for dry systems the bulk resistance measured at the lowest imaginary impedance exceeds the fit value considerably, especially for the higher wlc mixtures. Unfortunately, due to specimen geometry, the DC resistance can not be measured directly and the electrode surfaces can not be rewet without the danger of saturating the entire specimen. While further studies are planned to isolate the cause of the difference between the fit and observed bulk arc, for the remainder of this work the point of minimum imaginary impedance will be used since it is assumed that any differences that develop due to contact effects between the electrode and bulk would be similar between calibration and profile specimens.

Figure 7 compares the measured bulk resistance of the three water-to-cement ratio mixtures investigated in this study over a range of different relative humidities. First, it should be noted that the vertical axis is plotted using a logarithmic axis due to the wide difference in the measured bulk resistance suggesting the high sensitivity of an electrical impedance based technique. The change in bulk resistance covers approximately five orders of magnitude for the high wlc mixture, however it is only three for the lower wlc mixture. This suggests that the sensitivity of the measurement technique may be reduced as the w/c is decreased.

The general shape of the relationship between bulk resistance and the change in relative humidity (100%-$RH_{ENVIRONMENT}$) can be separated into two distinct regions. The first region exists between a 0 and 40% change in relative humidity (i.e., low drying) while the second region illustrates a more substantial change as the relative humidity is reduced by ~ 40% or more. Non-linearity observed in Roper's [35] shrinkage versus water weight loss curves implies that different mechanisms occur as differing levels of drying are applied. As the specimen begins to dry (i.e., between ~ 90% and saturated) the water loss primarily occurs from the largest capillary pores. As the humidity isdecreased further, the water in the smaller capillary and larger gel pores begins to leave the system. This sharp division in slopes may be correlated to either the breakdown of water in capillary and large gel pores or the initiation of Van der Walls forces overcoming the disjoining pressure (typically assumed to occur around 50% RH) drawing the particles closer together [36].

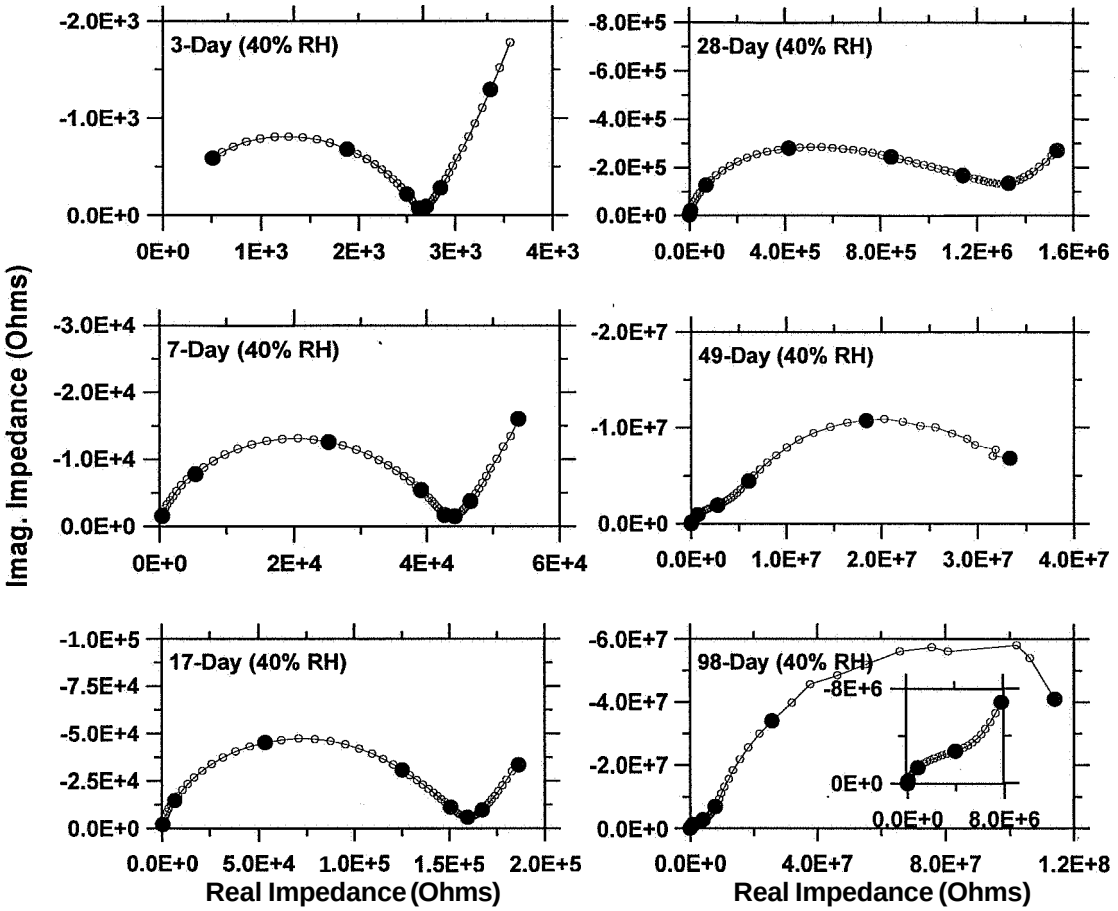

Figure 5: The Measured Nyquist Response for Paste as Drying Occurs for a w/c = 0.5 Mixture in a 40% Environment (Note: Solid Circles Correspond with Decade Frequencies While Open Circles Correspond to Individual Measurements)

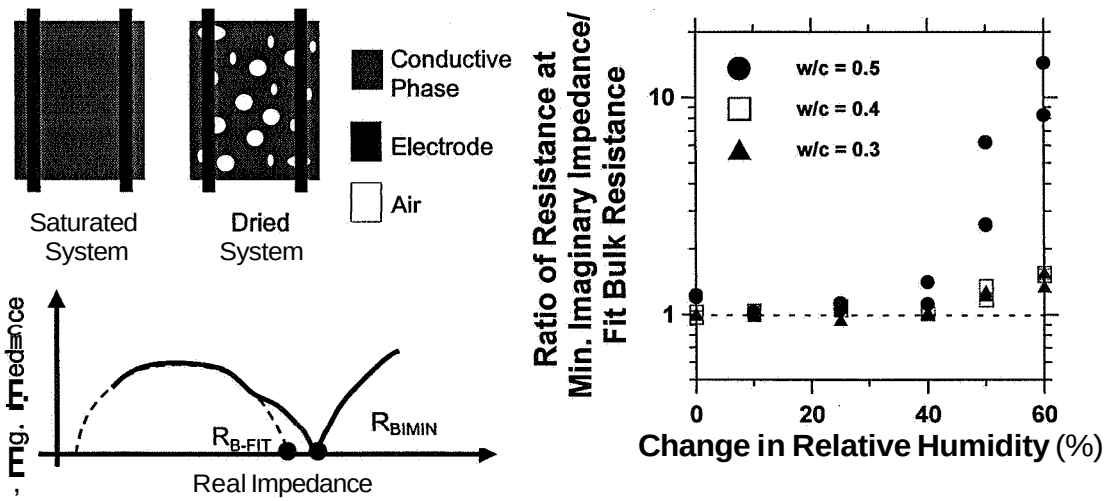

Figure 6: Difference Between the Measured Bulk Resistance and Resistance Computed by Fitting a Semi-Circle to the Lower Real Impedance Values

The wlc = 0.3 mixture exhibited the lowest difference in measured bulk resistance in the high relative humidity region. However, it is important to note that a change in relative humidity of approximately 25-30% could be expected in a sealed paste with this composition [37]. The bulk resistance of the sealed specimens was higher than the response of either the 90% RH samples and comparable to the specimens stored at 75% RH. It should be noted that the relatively low difference in the measured electrical properties of low w/c mixtures at high relative humidity might be masked by the additional water supplied to the system that causes continued hydration. Further research is required before any conclusions can be drawn.

Considering the aged specimens (97 days of drying), the resistance of the specimens stored at a high relative humidity increased as the w/c of the paste decreased. It should be noted that this trend reverses as the relative humidity is decreased (i.e., the specimen dries) and the higher wlc mixtures become more resistive. This is consistent with the argument presented in Figure 4. As the w/c is increased for a sealed specimen, the bulk resistance decreases due to the increase in the volume of conducting capillary pore fluid and decrease in volume of the resistive cement grains. As these specimens dry, the removal of the water has a more substantial effect on the higher wlc mixtures since a higher volume of water is lost and a greater volume of non-conductive medium, air, is introduced.

In addition to substantial changes in the bulk resistance, it should be noted that the fi-equency measured at the 'cusp' between the electrode arc and bulk arc shifts substantially throughout the test. This implies that while a measurement monitored at one frequency may illustrate measurable differences, it is likely that different features of the system are being monitored. It should be noted that the frequency listed for the w/c = 0.5 mixture was only the highest fi-equency measured, since the bulk arc did not approach the real axis.

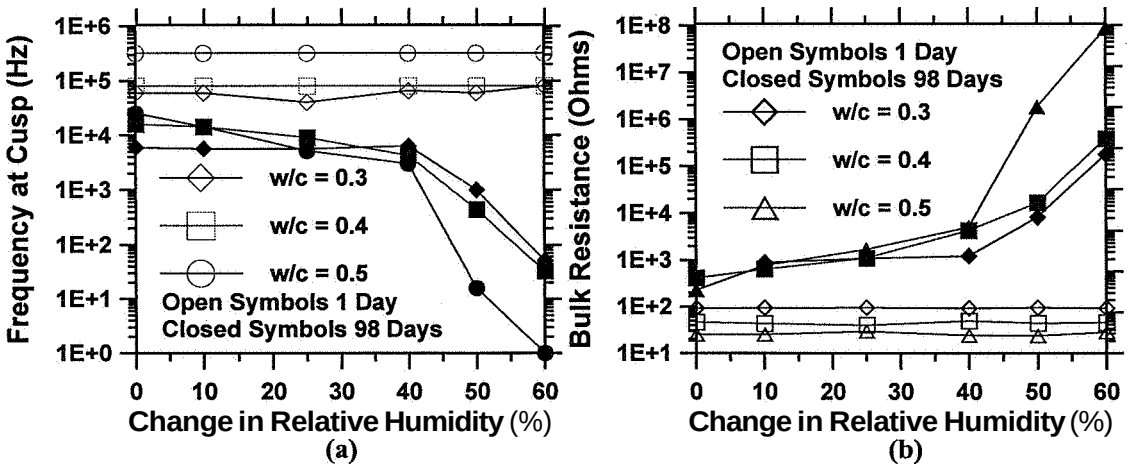

Figure 7: Influence of Drying on (a) the Frequency at Which the Bulk Resistance Occurs and (b) the Measured Bulk Resistance

If a semi-circular arc is fitted to the bulk response using three points (a point with a slightly higher frequency than the bulk resistance, a point at the peak of the arc, and a

point approximately midway between), some general trends in the depression angle can be observed. Figure 8 illustrates the normalized response (impedance divided by the bulk resistance) for two material compositions. It can be seen that as the age of a sealed specimen increases, the offset resistance appears to decrease and the depression angle increases slightly, consistent with frequently observed trends. However if the specimen is dried, a similar or reduced offset resistance is obtained with a larger depression angle. In addition, the high frequency 'tail' is clearly not represented by the semi-circle. If the same analysis is applied to the low w/c paste it can be observed that a negative bulk resistance would be required which physically does not make sense. This appears to provide further evidence that the bulk arc may be a combination of several overlapping conduction paths.

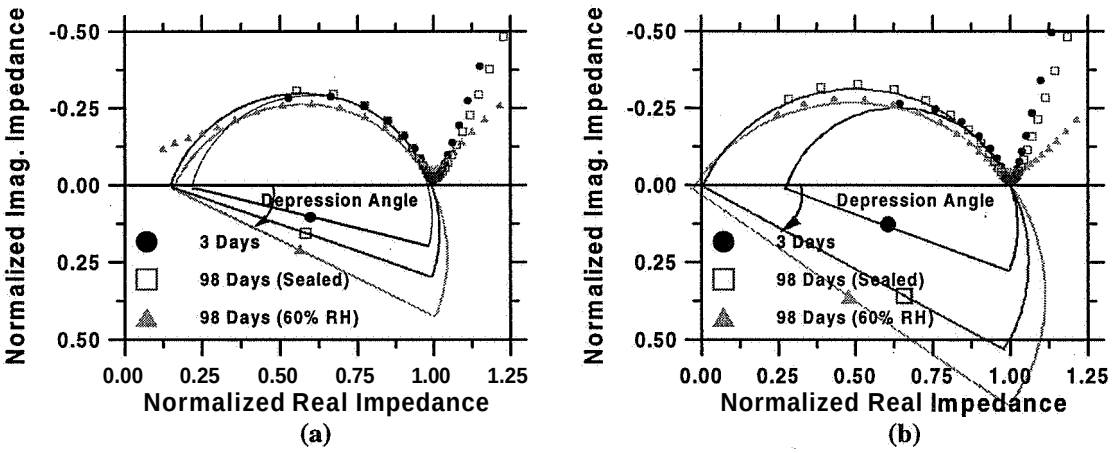

Figure 8: Influence of Aging and Drying on the Bulk Response and Depression Angle: (a) w/c = 0.5 and (b) w/c = 0.3

8. Moisture Profiles

The final section of this work will describe the behavior of the thicker specimens exposed to one-sided drying. Figure 9 illustrates a comparison of the normalized measured bulk resistance ($R_b/R_{b1\text{-}Day}$) for the three mixtures studied in this investigation at different ages. It can be seen that the general behavior of the three mixtures is relatively similar. The changes in normalized bulk resistance are greatest for the highest w/c and lowest for the low w/c mixture. It should be noted that this does not imply that the lowest w/c mixture has the smallest change in RH however, since the high w/c measurements appear to be more sensitive to changes in moisture content. The readings change most drastically near the surface, due to more rapid drying. This is confirmed in measurements of evaporable water which demonstrate the most dramatic change in the top section of the cylindrical specimen, and a lesser change in evaporable water in the section split section when compared with the sealed case. Sections taken from below the top 25 mm of the cylinder were nearly identical to the measurements in the sealed specimens. The changes near the core of the specimen occur for two reasons, increasing R_b due to hydration and self-desiccation in some mixtures. Further work is required to appropriately separate these effects. This is consistent with the previous observations [11,13].

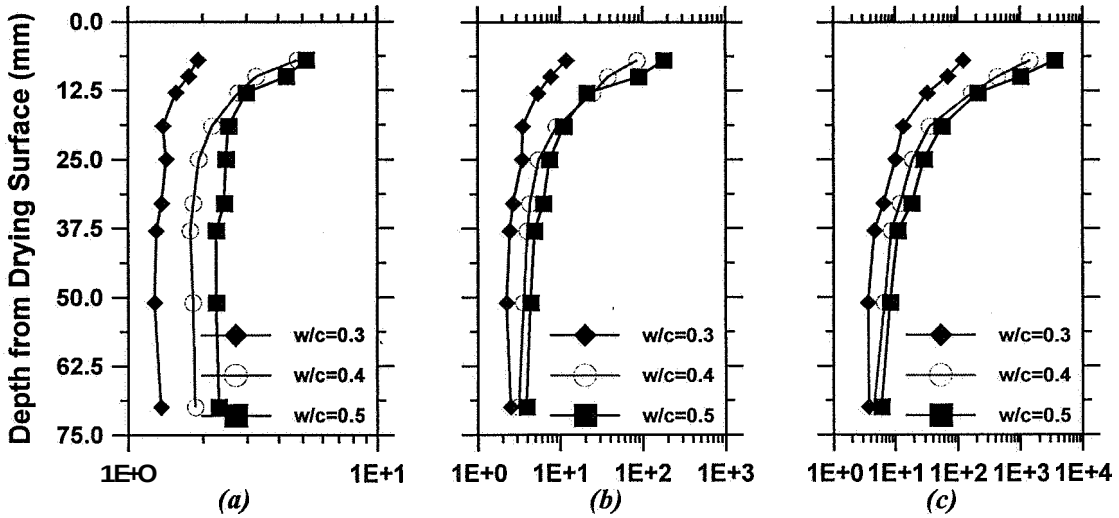

Figure 9: Normalized Bulk Resistance Profiles for the Mixes Studied in this Investigation (a) 3 Days, (b) 28 Days, and (c) 98 Days

Figure 10 illustrates that a correlation can be made between the measured bulk resistance and a relative humidity profile using a correlation function of the form

$$R, = 10^{\left(C_0 + C_1\Delta_{RH} + C_2\Delta_{RH}^2 + C_3\Delta_{RH}^3\right)} \quad (1)$$

where C_0 through C_3 are coefficients that can be computed with a regression analysis from the data presented in Figure 8a and Δ_{RH} is the change in relative humidity. Table 1 provides a summary of the coefficients. It should be noted that as previously mentioned the bulk resistance measurements for the lowest w/c mixture becomes relatively consistent at higher relative humidities.

Table 1. Measured Coefficients for Equation 1

Mixture	C_0	C_1	C_2	C_3
w/c = 0.3	2.533E+00	6.939E-02	-3.218E-03	4.700E-05
w/c = 0.4	2.415E+00	5.284E-02	-1.818E-03	3.017E-05
w/c = 0.5	2.425E+00	4.618E-02	-1.748E-03	4.265E-05

The mixture with the highest wlc has the largest profile since the core of the specimen appears to remain relatively saturated. The w/c = 0.4 mixture illustrates a slightly drier profile and reduced humidity (95%) at the core which may be attributed to some self-desiccation. The w/c = 0.3 mixture is relatively similar, albeit drier, until the point of at which self-desiccation appears to dominate the behavior at the core specimen. The dashed line corresponds with the relative humidity predicted for the sealed specimen (–79%). Again it should be noted that the low w/c mixture exhibited less pronounced differences in bulk resistance at the higher relative humidities, therefore further work will be aimed at investigating these mixtures.

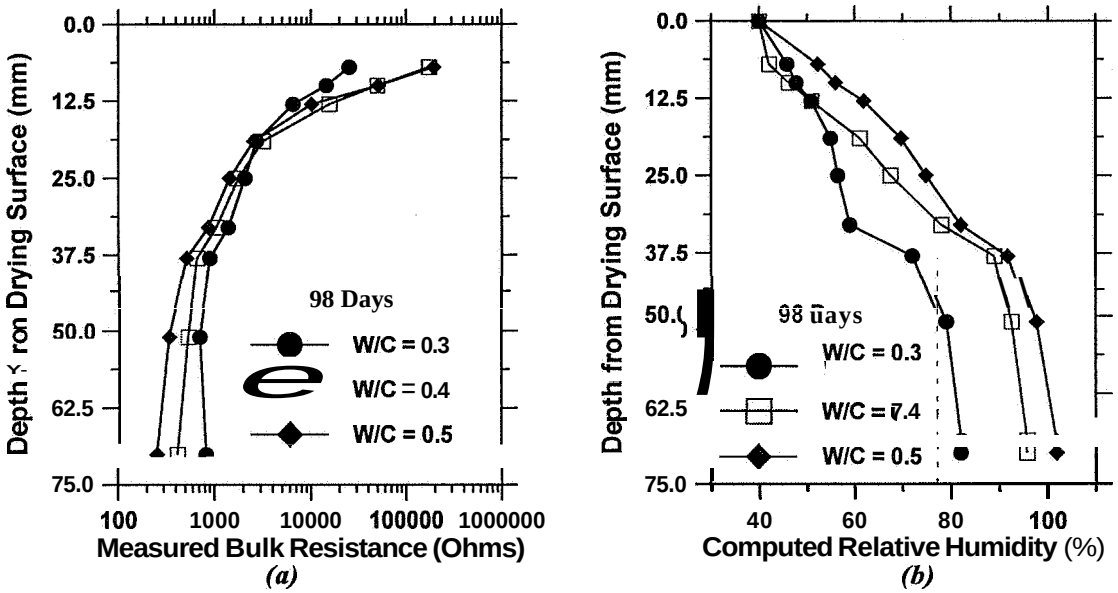

Figure 10: Influence of Water to Cement Ratio on the Measured Electrical Impedance Profile and Its Correlation with A Relative Humidity Profile

9. Future Directions and Concluding Remarks

Electrical impedance spectroscopy is a powerful non-destructive technique that has been previously shown to be sensitive to hydration, wetting and drying, and mix composition. The work presented in this study has illustrated differences in the electrical impedance response as the specimen is dried to different levels of severity. This paper has illustrated the following.

- Changes in measured bulk resistance caused by drying are less sensitive in lower w/c mixtures. This may be attributed to a higher relative volume of unreacted cement and a lower relative volume of a more conducted pore fluid solution.

- Experimental evidence is presented for a sealed system to show that the evaporable/non-evaporable water and bulk resistance are proportional in high wlc pastes. These changes are most rapid during the first days of hydration and appear to follow a logarithmic development curve. As the w/c is decreased the relationship between the evaporable water and bulk resistance is non-linear which presumably occurs as a result of self-desiccation.

- It can be seen that drying and hydration reduce the frequency at which the bulk resistance is measured. This shift can be quite drastic (> 6 orders of magnitude) illustrating the need for a technique which sweeps through the frequencies to ensure the bulk resistance is accurately measured.

- Experimental evidence illustrates that the 'bulk' arc may actually a combination of various conduction paths. As the matrix dries, the conducting properties of these paths are altered giving rise to increased resistance and changes in the features of the bulk arc.

- It is possible to approximate a relative humidity profile by combining the electrical bulk resistance of the calibration specimens with the bulk resistance profile of a similar specimen.

Although further work is required to combine aging, drying, and self-desiccation effects, the preliminary research presented in this paper illustrates that by combining electrical impedance profiles measurements with a calibrated electrical response a relative humidity profile can be determined.

Acknowledgements
The authors gratefully acknowledge support of the National Science Foundation (NSF) Center for Science and Technology of Advanced Cement-Based Materials and Grace Construction Products and Division of W. R. Grace and Co.-Conn. In addition, the third author gratefully acknowledges support received through the NSF Grant 'Interdisciplinary Team Research in Civil Engineering, NSF-#EC9531302' which funded her through the NSF-Northwestern Research Experience for Undergraduates (REU) program.

References

1. Carlson, R. W., "Drying Shrinkage of Large Concrete Members," Proceedings of the American Concrete Institute, Jan.-Feb., 1937, Vol. 33, p. 327-340
2. Neville, A. M, "Properties of Concrete," Fourth Edition, © 1996
3. Aitcin, P.-C., "Autogenous Shrinkage Measurement," Autoshrink '98, Proceedings of the International Workshop on Autogenous Shrinkage of Concrete, June 1998, Hiroshima, japan, Ed. E. Tazawa, pp. 245-256
4. Bazant, Z. P., and Najjar, L. J., "Nonlinear Water Diffusion In Nonsaturated Concrete," RILEM Journal of Materials and Structures, Vol. 5, No. 25, pp. 3-20
5. Tazawa, E., and Miyazawa, S., "Effect of Self-Desiccation on Volume Change and Flexural Strength of Cement Paste and Mortar," Self-Desiccation and Its Importance on Concrete Technology, Proceeding of an International Research Seminar Held in Lund, Sweeden, June 10, 1997, Eds. Persson, B., and Fagerlund, G., pp. 8-14
6. Fagerlund, G., "Effect of Self-Desiccation on the Internal Frost Resistance of Concrete", Self-Desiccation and Its Importance on Concrete Technology, Proceeding of an International Research Seminar Held in Lund, Sweeden, June 10, 1997, eds. Persson, B., and Fagerlund, G., pp. 227-238
7. Persson, B.S.M., "Self-Desiccating High-Strength Concrete Slabs," High Strength Concrete, Proceedings of the Utilization of High Strength Concrete Conference, Lillehammer, Norway, June 1993, ed. I. Holand, E. Sellevold, pp. 882-889
8. Wiegrink, K., Marinkunte, S., Shah, S.P., "Shrinkage Cracking of High-Strength Concrete, ACI Materials Journal, Vol. 93, No. 5, pp. 409-415
9. Weiss, W. J., Schiessl, A., Yang, W., and Shah, S. P., "Shrinkage Cracking Potential, Permeability and Strength for HPC: Influence of W/C, Silica Fume, Latex, and Shrinkage Reducing Admixtures," International Symposium on High

Performance and Reactive Powder Concretes, August 1998, Sherbrooke Canada, Eds. Aitcin, P.-C., and Delagrave, Y., pp. 349-364

10. Tazawa, E., and Miyazawa, S., "Autogenous Shrinkage of Cement Paste with Condensed Silica Fume," Proceedings of the Fourth CANMET/ACI International Conference on Fly Ash, Silica Fume, Slag, and Natural Pozzolans, in Concrete, ACI
11. Schiessl, P., Breit, W., and Raupach, M., "Investigations into the Effect of Coatings on Water Distribution in Concrete Using Multi-Ring Electrodes," SP-151-6, Concrete in Aggressive Environments, Ed. R. E. Weyers, pp. 119-133
12. Schiessl, P., and Breit, W, "Monitoring of the Effectiveness of Surface Protection Systems after Repair Measures Using Multi-Ring-Electrodes," International Symposium Non-Destructive Testing in Civil Engineering (NDT-CE), October 1995, pp. 1251-1258
13. McCarter, W. J., "Monitoring the Influence of Water and Ionic Ingress on Cover – Zone Concrete Subjected to Repeated Absorption," ASTM Cement, Concrete, and Aggregates, Vol. 18, No. 1, June 1996, pp. 53-63
14. McCarter, W. J., Emerson, M., and Ezirim, H., "Properties of Concrete in the Cover Zone: Developments in Monitoring Techniques," Magazine of Concrete Research, Vol. 47, No. 172, 1995, pp. 243-251
15. McCarter, W. J., and Watson, D., "Wetting and Drying of Cover-Zone Concrete," Proceedings of the Institution of Civil Engineers, Structures, and Building, Vol. 112 May, 1997, pp. 227-236
16. McCarter, W. J., Ezirim, H., and Emerson, M., "Properties of Concrete in the Cover Zone: Water Penetration, Sorptivity, and Ionic Ingress," Magazine of Concrete Research, 1996, Vol. 48, No. 176, Sept. 149-156
17. McCarter, W. J., "AC Impedance Profiling Within Cover Zone Concrete: Influence of Water and Ionic Ingress," Advances in Cement Research, Vol. 10, No. 2, April, 1998, pp. 57-66
18. Yuasa, N., Kasai, Y., and Matsui, I., "Method for Measuring Moisture Content in Concrete Using Small Stainless Steel Electrodes," SP 179, Recent Advances in Concrete Technology, Proceedings of the Fourth CANMET/ACI/JCI International Conference, Tokushima, Japan, Ed. V. M. Malhotra1998, pp. 499-516
19. Scheiβl, A., Weiss, W. J., Shane, J. D., Berke, N. S., Mason, T. O., Shah, S. P., "Assessing the Moisture Profile of Drying Concrete Using Impedance Spectroscopy," Submitted for publication
20. McCarter, W. J., Brousseau, R., "The A.C. Response of Hardened Cement Paste," Cement and Concrete Research, Vol. 20., No. 6, 1990 pp. 891-900
21. Gu, P., Xie, P., Beaudoin, J. J., "Some Aspects of AC Impedance Spectroscopy in Cement Research," ASTM Cement, Concrete, and Aggregates, Vol. 17, No. 2, Dec., 1995, pp. 113-118
22. Christensen, B. J., Coverdale, R. T., Olson, R.A., Ford, S. J., Garboczi, E. J., Jennings, H. M., and Mason, T. O., "Impedance Spectroscopy of Hydrating Cement-Based Materials: Measurement, Interpretation, and Application," Journal of the American Ceramic Society, Vol. 77, No. 11, Nov. 1994, pp. 2789-2804

23. McCarter, W. J., "A Parametric Study on the Impedance Characteristics of Cement-Aggregate Systems During Early Hydration," Cement and Concrete Research, Vol. 24, No. 6, 1994, pp. 1097-1110

24. Xie, P., Gu, P., and Beaudoin, J.J., "Contact Capacitance Effect in Measurement of A.C. Impedance Spectra for Hydrating Cement Systems," Journal of Material Science, Vol. 31, 1996, pp. 144-149

25. Christensen, B. J., Mason, T. O., and Jennings, H. M., " Influence of Silica Fume on the Early Hydration of Portland Cements Using Impedance Spectroscopy," Journal of the American Ceramic Society, Vol. 75, No. 4, 1992, pp.939-945

26. Powers, T. C., and Brownyard, T. L., "Studies of the Physical Properites of hardened Portland Cement Paste," Bulletin 22 of the Research Laboratories of the Portland Cement Association, Chicago, Illinois, March, 1948

27. Coverdale, R. T., Christensen, B. J., Jennings, H. M., Mason, T. O., Bentz, D. P., and Garboczi, E. J., Interpretation of the Impedance Spectroscopy of Cement Paste Via Computer Modelling, Part I Bulk Conductivity and Offset Resistance," Journal of Materials Science Letters, Vol. 30, 1995, pp. 712-719

28. MacPhee, D. E., Sinclair, D. C., Stubbs, S. L., "Electrical Characterization of Pore Reduced Cement By Impedance Spectroscopy," Journal of Material Science Letters, Vol. 15, 1996, pp. 1566-1568

29. Scuderi, C. A., Mason, T. O., and Jennings, H. M., "Impedance Spectra of Hydrating Cement Pastes," Journal of Materials Science, Vol. 26, 1991, pp. 349-353

30. McCarter, W. J., "A Parametric Study of the Impedance Characteristics of Cement-Aggregate Systems During Early Hydration," Cement and Concrete Research, Vol. 24, No. 6, 1994, pp. 1097-1110

31. Chen, P.-W., and Chung, D. D. L., Composites B 27, Vol. 11, 1996

32. Hwang, J.-H., Kirkpatrick, K. S., Mason, T. O., Garboczi, E. J., "Experimental Limations in Impedance Spectroscopy: Part IV. Electrode Contact Effects," Solid State Ionics, 98, 1997, pp. 93-104

33. Ford, S. J., Shane, J. D., and Mason, T. O., "Assignment of Features in Impedance Spectra of the Cement-Pastelsteel Interface," Cement and Concrete Research, Vol. 28, No. 12, 1998, pp. 1737-1751

34. Whittington, H. W., McCarter, J., and Forde, M. C., "The conduction of Electricity Through Concrete," Magazine of Concrete Research, Vol. 33, No. 114, March 1981, pp. 48-60

35. Roper, H., "Dimensional Change and Water sorption Studies of Cement Paste," The Structure of Portland Cement Paste and Concrete, Highway Research Board Special Report 90, 1966, pp. 74-83

36. Mindess, S. and Young, J. F., Concrete, Prentice-Hall, Inc., Englewood Cliffs, New Jersey , © 1981

37. Mjornel, K. N., "Moisture Conditions in High Performance Concrete; Mathematical Modeling and Measurements," Ph.D. Thesis, Chalmers University of Technology, Goteborg, Sweeden, 1997

A NORDTEST METHOD FOR VERIFICATION OF SELF-DESICCATION IN CONCRETE

B. PERSSON
Lund Institute of Technology, Division of Building Materials, Lund University, P.O. Box 118, 221 00 Lund, Sweden

Abstract

This article outlines a preliminary NORDTEST method for verification of self-desiccation in concrete. The method signifies measurements of the internal relative humidity, RH, on pieces of concrete at one month's age. The measured RH then is compared with the requirements according to the owner. The new NORDTEST method for self-desiccation permits requirements to be made on the self-desiccation of HPC in accordance with present demands on strength. During the development of the test method experimental studies were carried out on nine concretes with w/c varying between 0.32 and 0.50. Half of the concretes contained five per cent silica fume. The experiments showed a significant effect of cement type, silica fume and w/c on the self-desiccation in concrete. The test method was also verified in the field, both when manufacturing the concrete and on site. The method was developed after a corporation between the Technical University of Denmark and Lund University. The experimental studies were performed at Division of Building Materials, Lund Institute of Technology, Lund 1995-1999.

Keywords: Concrete, High Performance Concrete, Hydration, Relative Humidity, Self-desiccation, Silica fume, Strength.

1 Introduction and objective

Ever since the self-desiccating effect of High Performance Concrete, HPC, can into practical use in Sweden nine year ago, no damages on the building sites as regarding moisture and fungus have been reported [1,2]. Still there has been a demand from the owner or the contractor to control the quality of the concrete in a standard procedure as related to self-desiccation. Owner and contractors wants to have a confirmation on the self-desiccating ability of the concrete. They also wishes to know if the concrete fully meat with the demands in practical use. A request of self-desiccation often is connected to a time limit, i.e. the production of the building. Until now requirement on concrete most often are dealing with strength (for example at 1 month' age) or with durability (for example minimum 5% air-entrainment). When composing self-

desiccating concrete the manufacture often compares the self-desiccating ability with a strength level of the concrete. This coupling of the mix design to strength often hinders the development of new compositions, i.e. use of alternative materials and methods when producing self-desiccating concrete like lightweight aggregate and air-entrainment. The "strength method also leads to unnecessary high strength level for example in dwelling houses, often more than three times as high strength as required. The w/c is namely the leading parameter for achieving self-desiccation, not the strength. It was the objective of this work to develop and in practise use a method for testing the self-desiccation of concrete at 1 month' age.

2 Method

2.1 Requirement

The following requirement were existed when the method was developed:

1. A rapid and safe method of collecting the concrete for the specimens
2. An affective moisture insulation of the concrete during the curing period
3. Moisture measurement during realistic conditions

2.2 Procedure

It was practical to use the type of specimens that were used for strength tests in the manufacture of concrete. It was not feasible to use a cube since its upper face was difficult to insulate as regards moisture losses. Instead Standard cylinders were used in the methods cast in steel cylinders (100 x 200 mm). In this way all the moisture of the specimen was kept in the specimen directly from casting. After demoulding the cylinder specimens was stored three by three in thick plastic pipes at 20 ± 2 °C for one month. The plastic pipe with its content of concrete cylinders was weighed before and the one-month storage in order to control possible moisture losses. The cylinders were tested for strength after one month. Parallel to the strength tests fragments of concrete were collected from the inner face of the cylinders and put in glass pipes, Figure 1.

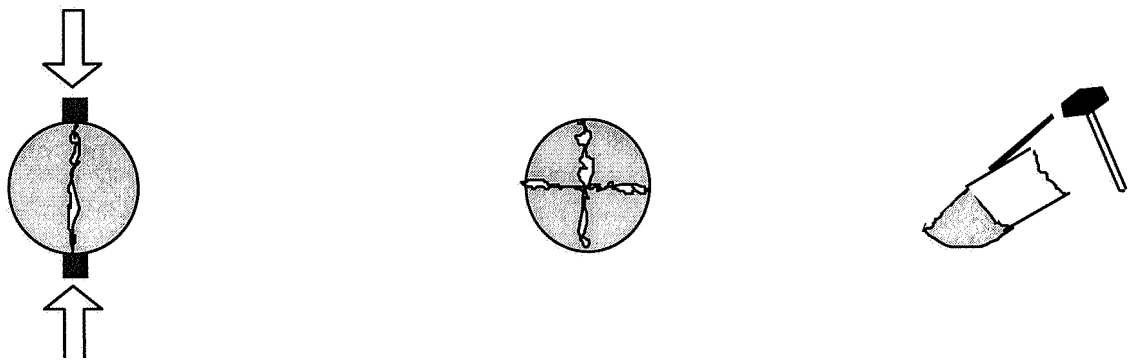

Fig. 1. Fragments of concrete were collected parallel to the strength tests from the inner face of the cylinders and put in glass pipes. Rubber plugs tightened the pipes.

Rubber plugs rapidly tightened the pipes. The glass pipes in turn were stored for one day at 20 ± 2 "C. During the measurement of moisture the device was entered into the pipe and tightened towards the inner face of the pipe by an expanding rubber ring, Figure 2. The measurement of RH was carried out for one day at 20 ± 0.5 "C. To achieve the temperature demand the measurement was performed in a climate chamber. The concrete mix number, possible losses of weight during curing, strength and RH was noted in a protocol as shown in Table 1.

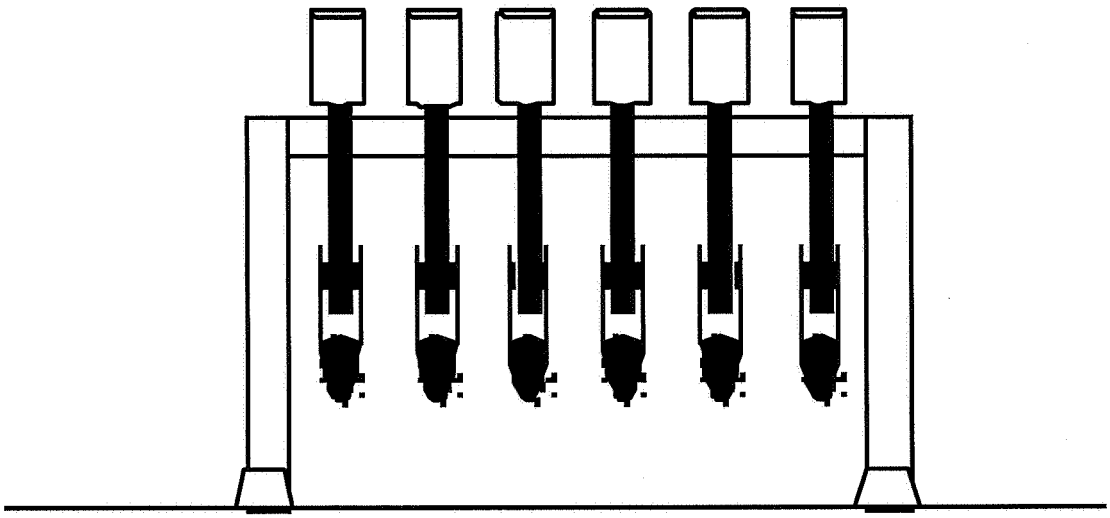

Fig. 2. During the measurement of moisture the device was entered into the pipe and tightened towards the inner face of the pipe by an expanding rubber ring,

Table 1. A form for the NORDTEST method for self-desiccation of concrete.

Mix number			
Date of casting			
Weight at demoulding (g)			
Testing date			
Weight at testing (g)			
Moisture losses (g):			
Compressive strength (MPa)		Displayed value	Calibrated value
Specimen 1			
Specimen 2			
Specimen 3			
Average strength			
Relative humidity, RH (%):	Device number	Displayed value	Calibrated value
Specimen 1			
Specimen 2			
Specimen 3			
Average RH (%)			

3 Application in laboratory

3.1 Effect of w/c, age and silica fume

First of all it was important to check how the method functioned in a laboratory primarily as concerned sources of errors and accuracy [3]. Composition and main characteristics of the concretes tested in the laboratory are given in table 2. The concrete had a high content of air in order to increase the workability and diminish the density. A high content of air did not affect the self-desiccation of the concrete [4]. At an early stage of the development of the testing method it became clear that the temperature during curing and especially during the measurement of RH was of great importance. The temperatures at testing in the laboratory therefore were kept at 18, 20.5 och 23 "C. Figure 3 shows RH at one month's age when testing in the laboratory.

Table 2. Composition and characteristics of concretes in laboratory tests (kglm^3) [3].

Material/Concrete	32L	32N	32N S	38L	38N	38N S	50L	50N	50N S
Quartzite sandstone 12-16	669	686	725	532	535	549	407	417	434
Quartzite sandstone 8-12	137	141	149	258	259	266	320	329	343
Natural sand 0-8 mm	704	722	763	747	750	771	830	852	887
Natural sand 0 mm (filler)	107	110	93	43	43	44	32	33	34
Cement (Appendix 1)	395	405	428	343	345	354	274	281	293
Granulated silica fume, s	-	-	21	-	-	18	-	-	15
Air-entrainment (fir oil, g)	43	44	50	34	35	35	26	26	27
Superplasticiser (melamine)	3.4	2.5	3.6	1.7	1.7	1.8	0.9	0.9	1.0
Water-reducing agent	1.7	1.8	1.9	0.9	0.9	0.9	1.0	1.1	1.1
Total water incl. moisture	127	131	137	131	131	135	136	138	144
Water-cement ratio, w/c	0.32	0.32	0.32	0.38	0.38	0.38	0.50	0.50	0.50
Air content (% by volume)	12.5	10.5	6.0	13.0	13.0	10.5	15.5	13.5	11.0
Aggregate content	0.75	0.75	0.75	0.76	0.76	0.76	0.80	0.80	0.80
Slump (mm)	90	100	80	140	170	150	200	180	180
Density - fresh state (kg/m^3)	2145	2200	2330	2090	2100	2175	2000	2050	2150
28-day cylinder density[1]):	2280	2330	2370	2280	2260	2290	2060	2150	2200
curing at 18 "C (kg/m^3) [2)]	2290	2330	2350	2300	2260	2280	2040	2150	2210
curing at 20.5 "C (kg/m^3) [2)]	2290	2320	2390	2290	2270	2310	2100	2180	2190
curing at 23 "C (kg/m^3) [2)]	2270	2340	2380	2260	2250	2290	2040	2130	2210
Air-content loss, AA (%)[3)]	6.5	6.0	2	9.0	7.5	5.5	3.0	5.0	2.5
Air-content - cured (%)[4)]	7.5	6.0	5.5	5.5	7.0	6.5	14.0	10.0	10.0
28-day cylinder strength[1]):	47	51	71	51	38	51	20	27	33
curing at 18 "C (MPa) [2)]	47.0	53.0	72.0	56.5	41.0	54.5	20.5	26.5	32.5
curingat20.5 °C (MPa) [2)]	49.5	51.0	74.0	52.0	39.5	52.0	21.9	30.0	33.0
curing at 23 °C (MPa) [2)]	45.0	48.0	67.0	44.0	34.5	46.0	18.5	24.0	33.0
Strength decline (MPa/°C)	0.5	1	1.1	2.5	1.3	1.7	0.5	0.6	0

[1)] average of 9 cylinders, [2)] average of 3 cylinders, [3)] $100\cdot[(\rho_{28d}/\rho_{fresh})-1]$ %, [4)] A_{fresh}-$\Delta A+1.5\%$, L = low-alkali cement, N = normal-alkali cement, NS = normal-alkali cement and 5% silica fume, 32 = w/c (%).

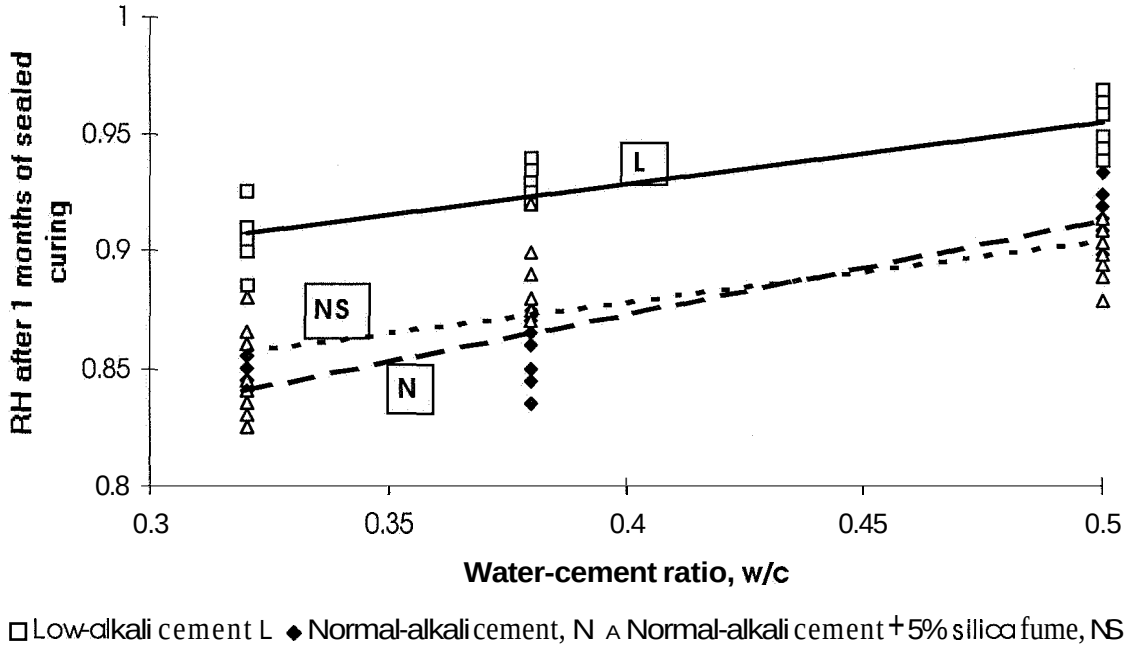

Fig. *3*. RH at one month's age of the concretes that were tested in the laboratory. L= low-alkali cement, N = normal-alkali cement, S = *5%* silica fume.

2.2 Conclusions of the laboratory tests

The following conclusions were drawn from the laboratory tests [3]:

- Curing may be performed at *20 ± 2* °C with no significant effect on self-desiccation
- The measurement of moisture must be performed at *20 ± 0.5* °C the achieve the required accuracy of RH ± *2%*
- Concrete with normal-alkali Portland cement (Slite Standard) obtained about *5%* lower RH after one month than concrete with low-alkali Portland cement (Degerhamn anlaggning) did
- Silica fume concrete (with low-alkali Portland cement and *5%* silica fume) obtained about *5%* lower RH after one month than concrete without silica fume did
- Silica fume concrete (with normal-alkali Portland cement and *5%* silica fume) obtained the same RH after one month as concrete without silica fume did.

4 Field tests

4.1 General

The new NORDTEST method was used at a building site in Malmö and at a concrete manufacture in Trelleborg, Sweden. Standard cylinders were fabricated on the building site, Figure 4 [6]. The same procedure was performed at the factory in Trelleborg, i.e. sample of concrete was taken directly from the transport of concrete, Figure *5*. The selection of testing sample coincided well with a normal concrete production, partly on the factory for concrete, partly from the building site directly. Table *3* shows the mix composition of the tested concrete in the field [6].

Fig. 4. Standard cylinders were fabricated on the building site [6].

4.2 Procedure

The following procedure applied after the sampling:

1. After curing one day in a steel mould the cylinders were placed in thick plastic pipes. The ends of the pipe was tightened by plugs with rubber rings, Figure 6.
2. The cylinders were stored at 20 ± 2 °C for one months until testing of moisture.
3. The plastic pipes with content were weighed before after the curing period
4. At 28 days' age the cylinders were tested for strength. Fragment were taken from each compressive test and placed in glass tubes, Figure 1. The tubes were tightened by rubber plugs and stored in 20 ± 2 "C for one day
5. One days the strength testing the a dew point meter was entered into the tube and tightened with an expanding rubber ring towards the glass, Figure 2
6. The dew point meter was measured for another day and the value on the display calibrated according to ASTM E 104-85, [7].

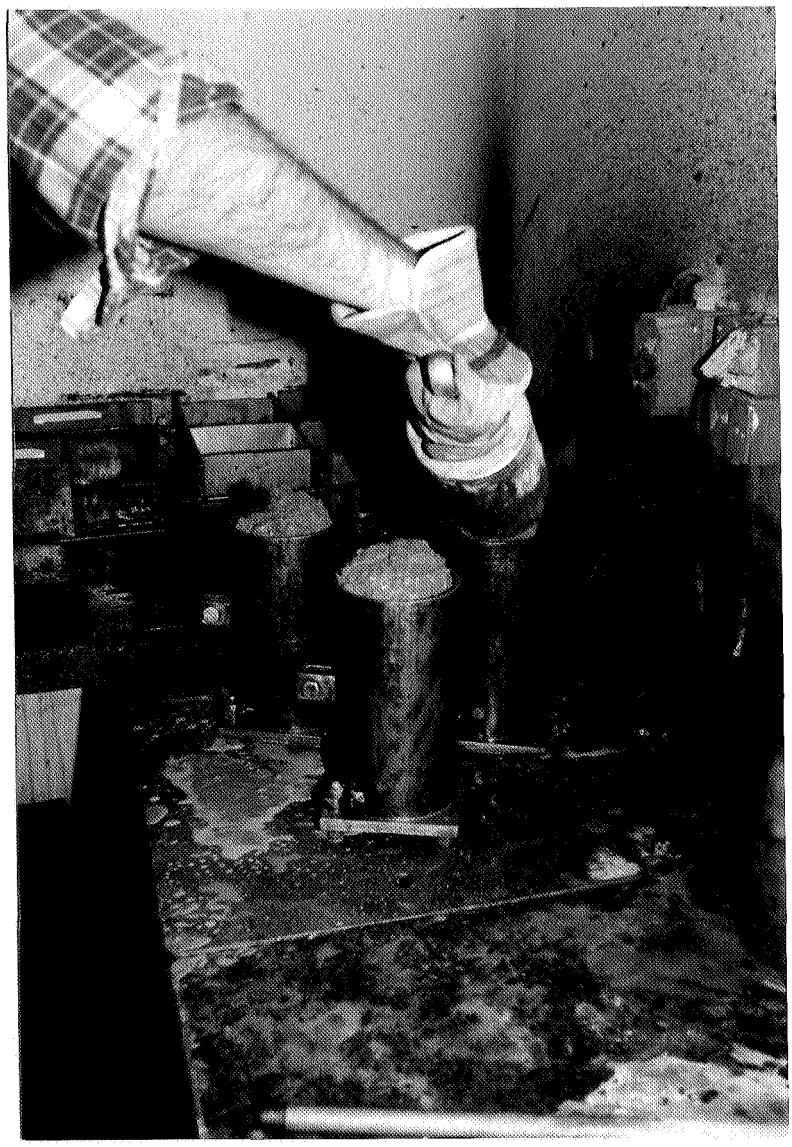

Fig. 5. Standard cylinders were fabricated at the concrete factory, i.e. sample of concrete was taken directly from the transport of concrete [6].

4.3 Results

Results of the NORDTEST method is given in Table 3 and Figure 7. Figure 7 shows RH and strength at 1 month's age versus w/c. The results reflect both the accuracy (± 2% R) and the variations in the production of concrete. The temperature during the measurement was held 20 ± 0.5 "C. The value on the display of the dew point meter was read after 1 day. Calibration was performed according to ASTM E 104-85 [7].

4.4 Discussion

Figure 8 shows RH estimated according to equation (1) versus RH measured at the field tests [6]. The equation was obtained at the laboratory tests illustrated above [3].

$$Ø = [A \cdot \ln(t) + B] \cdot (w/c) + C \cdot \ln(t) + D \qquad (1)$$

Table 3. Mix composition and characteristics of concrete tested in the field (kg/m^3) [6].

Material	38K	38S	40G	44L	68R	70GV
Coarse aggregate 16-25 mm				804		927
Coarse aggregate 11-18 mm	928	716	920		753	
Gravel 0-8 mm	881	886	718	999	1153	1028
Glass filler	60	99	62		35	17
Cement Slite standard	456	518	552	419	289	269
Superplasticiser (polycarboxylic ether)')	2.72	2.18				
Air-entrainment (fir oil)[2)]	0.91			0.6		
Water including all moisture	174	199	219	184	197	188
Coarse aggregate content	0.50	0.42	0.54	0.45	0.39	0.47
Density	2500	2420	2471	2405	2429	2429
Air content (%)	2.6	1.2	1.1	5.6	1.4	2.6
Water-cement ratio, w/c	0.38	0.38	0.40	0.44	0.68	0.70
Mixing time (s)	246	300	121	192	158	113
Slump (cm)	14	> 28	10.5	12	-	14.5
Slump flow (cm)		56x63				
Flow time until 50 cm diameter		4.5 s				
Workability	Good	Good	Good	Good	Good	Good
Strength 28 days (factory, 20 "C, MPa)	54	58	43	38		31
Strength 28 days (site, 20 "C, MPa)	45	61	46	37		30
RH, 28 days (factory, 20 "C, % RH)	86	86.5	87	92		97
RH, 28 d (site, 20 "C, % RH)	85.5	86	87	90		97

Notations: 1) dry content 42%; 2) dry content 10%

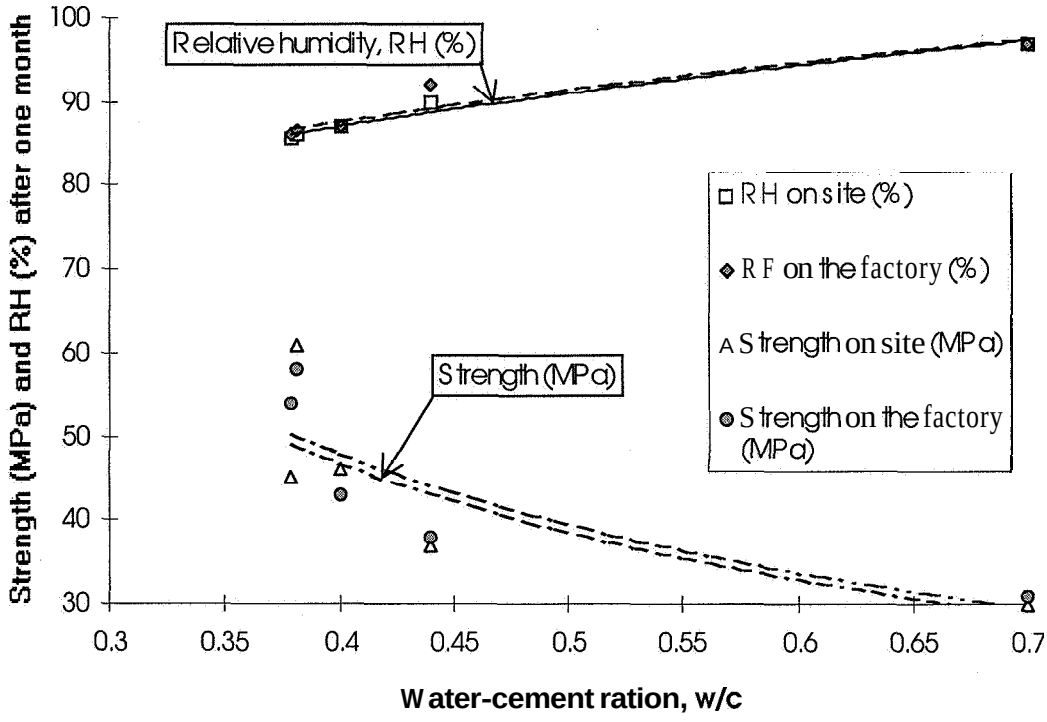

Fig. 7. RH and strength at 1 month's age versus w/c [3].

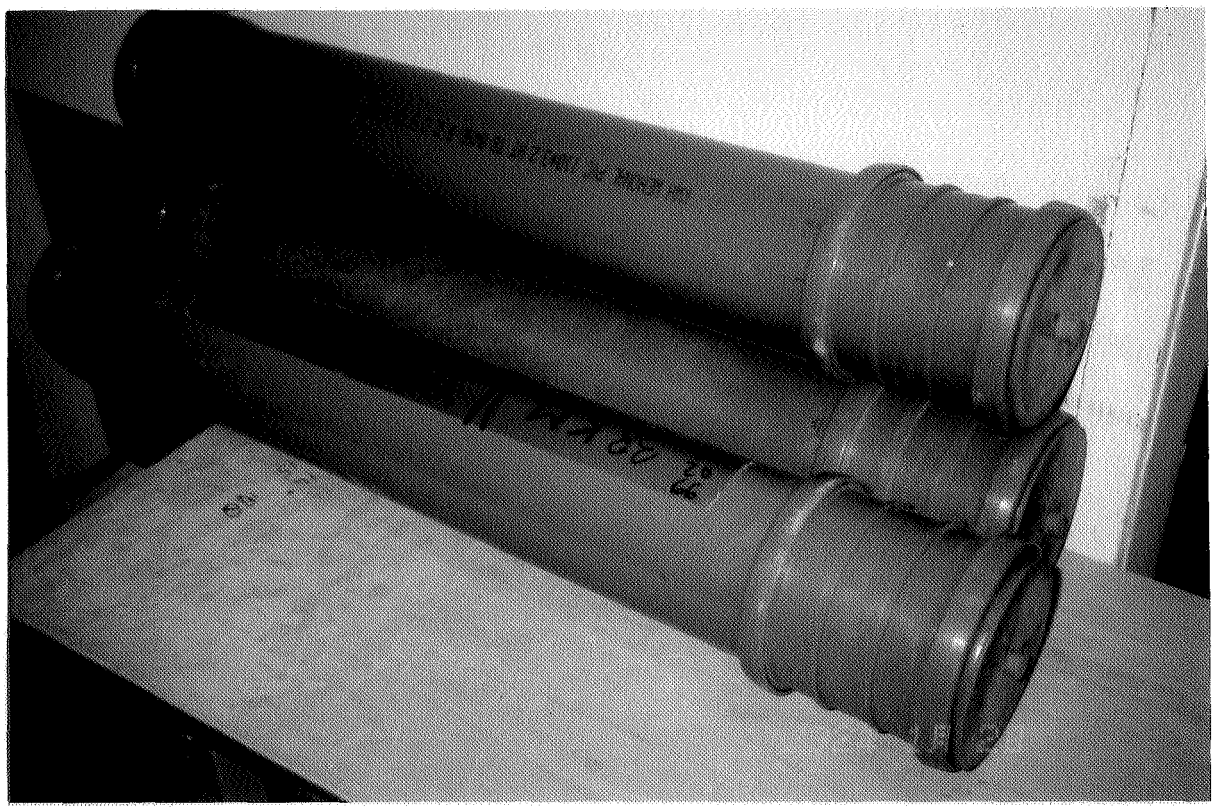

Fig. 6. The cylinders in thick plastic pipes tightened by plugs with rubber rings [6].

ln(t)	denotes the natural logarithm of the concrete age (month)
A, B, C, D	denotes constants given in table 4
R^2	denotes an accuracy parameter in equation (2)
Y_i	denotes the measured value
Y_m	denotes the measured average value

$$R^2 = 1 - \frac{\sum (Y_i - Y_m)^2}{(\sum Y_i^2) - \frac{(\sum Y_i)^2}{n}} \qquad (2)$$

Table 4. Constants in equation (1) [3].

Cement type, silica fume/constants	A	B	C	D	R^2
Low-alkali cement	0.0378	0.185	-0.042	0.83	0.63
Normal-alkali cement	0.0588	0.219	-0.059	0.79	0.75
Normal-alkali cement + 5% silica fume	0.0351	0.223	-0.051	0.78	0.49

Figure 8 shows that the concrete producers (in spite of small variation of the results within an accuracy of ± 2% RH) was able to verify that the concrete after one months obtain the same RH during self-desiccation in the field like in the factory. The quality of the concrete was proved to be high since the variation in RH of the same type of concrete was small. This type of documentation was of great importance both for economical reasons and for the construction time of the project.

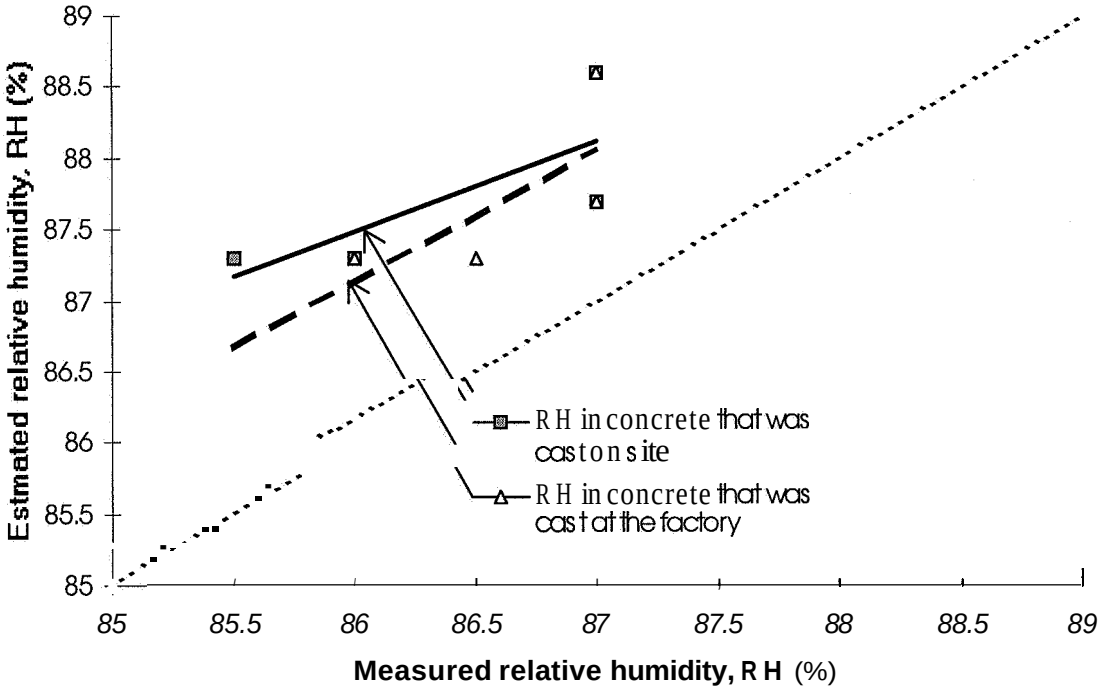

Fig. 8. RH estimated according to equation (1) versus RH measured in field tests [6].

The concrete producer furthermore was able to verify in what way changes in the mix composition affected the self-desiccation in the concrete [6]. The new NORDTEST method also permits the owner to define requirement as related to the self-desiccating quality of the concrete owing to a standard procedure.

Estimation of self-desiccation in HPC may be performed according to a newly developed computer program [8]. Required data are w/c, age and type and amount of silica fume. silikastoft. The program also estimates strength (split tensile and compressive), the elastic modulus, Poissons's ratio, creep and shrinkage and the creep coefficient of High-Performance Concrete.

5 Summary and Conelusions

In this article a new NORDTEST method for self-desiccation in concrete is described. The methods signifies the relative humidity, RH, in concrete at one month's age after a specified sealed curing. RH is measured on control cylinders parallel to the production of the concrete. RH measured during self-desiccation is compared with RH as required by the owner or the contractor. The new Nordic method allows for demands as related to RH in the concrete besides the normal strength specification and air-entrainment. The following conclusions were drawn:

1) The method showed significant differences in RH of concretes with varying w/c.
2) The method was successfully applied on a building site in Malmö and in a concrete factory in Trelleborg

3) Variations in the results reflected both the accuracy in measurement (± 2% RH) and possible variations in the concrete production
4) With the new method concrete producers and contractors may verify the quality of the concrete as related to self-desiccation
5) Concrete producers may verify in what way changes in the mix composition affect RH during self-desiccation.
6) The owner may use the method in the specification of a project how to define self-desiccation in a standard procedure.

6 Acknowledgement

Financial support from NORDTEST OY, Helsinki, Finland the Swedish Association of Ready Mixers, Sweden and Cementa Ltd, Danderyd, Sweden is gratefully acknowledged. I am also most grateful to Professor Göran Fagerlund at Division of Building Materials for his critical review.

References

1. L.-0. Nilsson (1998). *Is HPC the Solution on the Moisture Problems?* Magazine of Building Research. Stockholm. 2/98, 40-41
2. G. Fagerlund; B. Persson (1990). *HPC without Moisture.* Cementa 3/90, 18-19
3. B. Persson (1999). *Effect of Cement Type, Silica Fume, Water-cement Ratio, Age and Moderate Shift in Temperature on Self-desiccation in Concrete.* NCR 111999. Edited by the Nordic Concrete Federation. Oslo, 97-116.
4. G. Jonsson (1998). *Rapid-drying Concrete without Superplasticiser.* Master Thesis. Report TVBM-5036. Div. Building Materials. Lund Institute of Techn.. 199 pp.
5. G. Hedenblad; M Janz (1994). *Effect of Alkali on the Measured Moisture in Concrete.* Report TVBM-3057. Div. Building Materials. Lund University., 5-12.
6. B. Persson (1998). *Compatibility between Different Kinds of Flooring on Concrete.* Report U98.11. Div. Building Materials. Lund Institute of Technology, 22 pp.
7. ASTM E 104-85 (1985). *Standard Practice for Maintaining Constant Relative Humidity by Means of Aqueous Solutions.* The ASTM. Philadelphia, 33-34,637.
8. Bertil Persson; Mikael Lundahl (1999). *Computer Program CREEP for Estimation of Mechanical Properties of HPC.* Report U99.06 + CD-room. Div. Building Materials. Lund Institute of Technology, 2 pp.

EARLY AGE AUTOGENEOUS RESTRAINED SHRINKAGE: STRESS BUILD UP AND RELAXATION

Stress build up and relaxation

G. TOMA[1], M. PIGEON', J. MARCHAND[1], B. BISSONNETTE[1], AND L. BARCELO[2]
[1]CRIB- Université Laval, Ste-Foy, Québec, Canada
[2]Lafarge, Laboratoire central de recherche, Lyon, France

Abstract
Restrained autogenous shrinkage can cause cracking of concrete at early age. A special experimental device was built up at Laval University to study the behavior of restrained concrete from casting up to seven days. In the same time an unrestrained specimen was used to measure free shrinkage of concrete. At the end of the test information about shrinkage, creep, stress, and elastic modulus are obtained. The influence of w/c ratio was investigated.
Keywords: autogenous shrinkage, early age, restrained shrinkage apparatus, w/c ratio

1. Introduction

According to many recent reports [1], [2], [3], early age cracking is nowadays one of the most significant problems facing the concrete community. If this type of cracking is (apparently) more and more common, it is generally considered to be due (or at least related) to the use of high performance concretes, since self-desiccation increases as the water-binder ratio decreases. Many authors [4], [5], [6] consider that self desiccation under restrained conditions is one of the main causes of early age cracking, although other effects such as thermal shrinkage and lack of proper curing are also probably involved in most cases. To understand how early age autogenous (i.e. self desiccation induced) restrained shrinkage can cause craclung, it is necessary not only to develop a better knowledge of the parameters which govern the intensity of the shrinkage due to this phenomenon, but also to analyze how concretes react under such conditions, and particularly how relaxation can influence the stress build-up. Various devices [7], [8], [9] have been developed in recent years to study the influence of relaxation at early ages. This paper describes how such a device was used to study the influence of the water-cement ratio on the cracking tendency of normal Portland cement concrete at early ages.

2. EXPERIMENTAL

2.1 Materials, mixture characteristics, and specimens cast

Three normal Portland cement mixtures were prepared for this series of experiments: one with a water-cement ratio of 0,25, one with 0,35, and one with 0,45. Such values were considered to cover fairly well the range of water-cement ratios for which self desiccation is known to have significant effects. The characteristics of the cement and aggregates used for these mixtures are presented in Tables 1 and 2. The coarse and fine aggregates were saturated when they were incorporated into the mixtures. The maximum size of the coarse aggregate was fixed at 10 mm, i.e. one fifth of the smallest dimension of the mould in the restrained shrinkage test equipment.

Table 1. Chemical and mineralogical compositions

Chemical analysis (%)		Bogue composition (%)		Physical properties
Silicon dioxide (SiO_2)	20,47	C_3S	57	Blaine
Aluminium oxide (Al_2O_3)	3,96	C_2S	16	2600 cm^2/g
Ferric oxide (Fe_2O_3)	2,97	C_3A	5	
Calcium oxide (CaO)	62,08	C_4AF	9	Spec. density
Magnesium oxide (MgO)	2,84			3,15 g/cm^3
Sulfur trioxide (SO_3)	3,39			
Potassium oxide (K_2O)	0,84			
Sodium oxide (Na_2O)	0,87			
Titanium dioxide (TiO_2)	0,17			
Manganese oxide (MnO)	0,06			
Phosphorous oxide (P_2O_3)	0,20			
Loss on ignition	2,49			

Table 2. Grading of the aggregates

Coarse aggregates		Fine aggregates	
Sieve size (mm)	Percentage passed	Sieve size (mm)	Percentage passed
12,70	100	4,76	97
9,51	99,1	2,38	93
8,00	96,1	1,19	83
4,76	11,6	0,59	50
2,38	2,4	0,30	17
1,19	1,7	0,15	4
		0,07	1

Table 3. Composition and properties of fresh concrete

Composition					Properties of concrete		
w/c	cement (kg/m3)	fine agg. (kg/m3)	coarse agg. (kg/m3)	SP (%ES)	slump (mm)	density (kg/m3)	Air content (%)
0,45	390	823	1050	0,43	90	2440	2,5
0,35	450	848	995	0,68	150	2453	3,2
0,25	520	830	1010	2,44	195	2502	3.6

Table 3 presents the composition and fresh concrete properties of the mixtures. These mixtures were designed to have approximately the same paste content (30%). The amount of cement in each case corresponds relatively well to that found in typical concretes with such water-cement ratios. The only admixture that was used was a sulphonate-based superplasticizer. The dosage was selected in order to obtain an adequate slump for a sufficient period of time after the first contact between cement and water.

For each mixture, in addition to the two specimens required for the measurements under free and restrained autogenous shrinkage, 36 cylinders of 100 x 200 mm were cast to determine the strength in tension and in compression as a function of time. These cylinders were kept sealed until testing.

2.2 Restrained shrinkage equipment

The special equipment that was used for the tests has been described in detail in a previous publication [10]. It consists of a set up to measure the free autogenous shrinkage from time t=0, together with a more sophisticated one with a movable head to determine the increase in load due to autogenous shrinkage also from time t=O (Figure 1). In both cases, the specimens are cast directly into the mould (which has a 50 x 50 mm section and an active length of approximately 1000 mm) after mixing, and are then sealed using a special film. In the equipment with a movable head, the specimen is allowed to shrink (or swell) freely until it reaches a predetermined strain, at which time a sufficient force is applied to pull (or push) it back to its original position. It is then left again to shrink (or swell) while the force that was applied is maintained constant until the predetermined strain is once more reached, at which point the force is increased in order to pull (or push) it back to its original position. Such a procedure allows the determination of the stress build up in the specimen as a function of time. It also allows the determination of the creep deformation (and thus of the stress relaxation) in the restrained shrinkage specimen by subtracting (at any given point in time) the cumulative sum of the strains in the restrained shrinkage specimen from the free shrinkage in the companion specimen (see Figure 2).

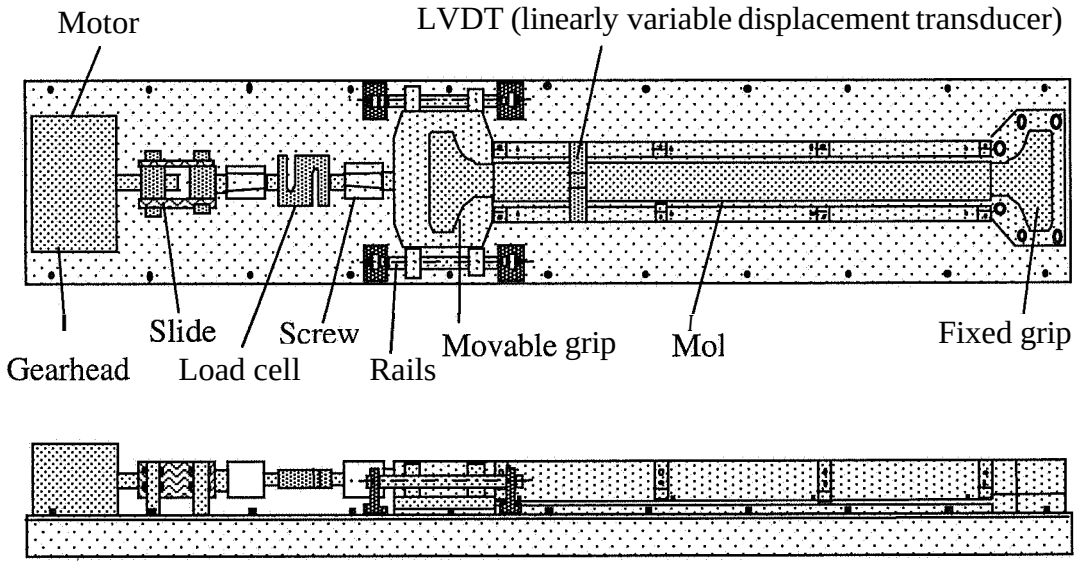

Figure 1. Restrained shrinkage apparatus

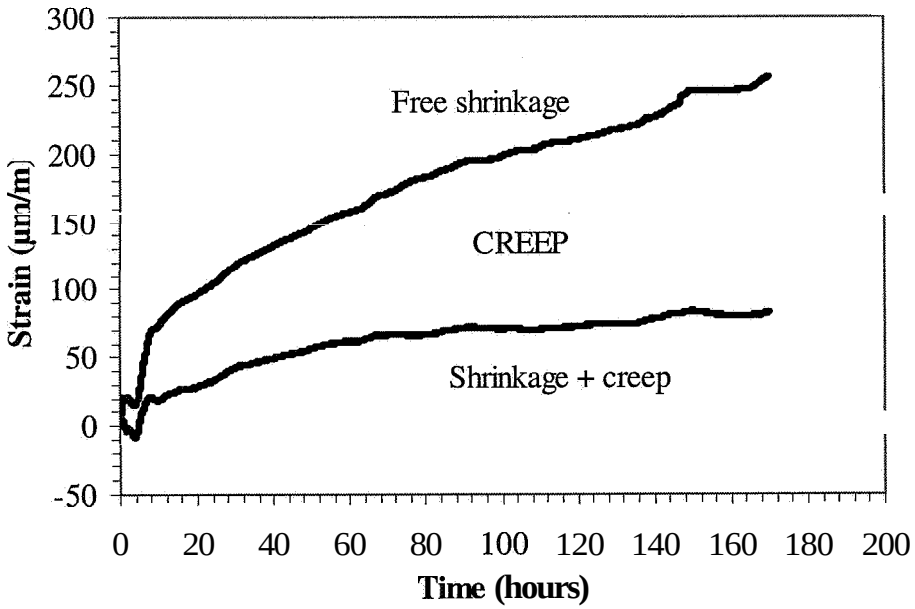

Figure 2. Cumulative curve of strains versus free shrinkage

To better understand how the creep component is obtained, one simply has to consider what would happen for a purely elastic material with no creep or relaxation capacity. In such a case, the stresses in the restrained specimen would be purely elastic and the cumulative sum of the strains would be equal to free shrinkage (considering that shrinkage deformations and elastic deformations do not influence one another, i.e. that

the principle of superposition of stresses and strains applies). If the cumulative sum of the strains is not equal to free shrinkage, it is because, as it shrinks, the specimen that is restrained creeps under the load applied to restrain it. Therefore, as just mentioned, the creep deformation in the restrained shrinkage specimen is equal to the difference between the cumulative sum of the strains measured in the restrained shrinkage specimen and the free shrinkage in the companion specimen.

2.3 Test results

The results obtained for the three mixtures tested are presented in Figure 3 (free autogenous shrinkage versus time), Figure 4 (stress versus time), and Figure 5 (creep versus time). Figure 6 shows the plot of the deformations versus time in the restrained shrinkage apparatus for one of the mixtures tested (0,35). Figure 7 shows for all three mixtures the stress relaxation as a function of time. Such curves are simply obtained by subtracting from the theoretical elastic stress (calculated using the free shrinkage results and the elastic modulus values) that measured in the restrained shrinkage apparatus. The value of the elastic modulus (see Figure 8) can be obtained each time an additional force is applied to bring back the specimen to its original position. The values of the tensile and compressive strengths determined on sealed cylinders are given in Figures 9 and 10 respectively. These values were measured at 12 hours, 1 day, 2 days, 7 days, and 28 days.

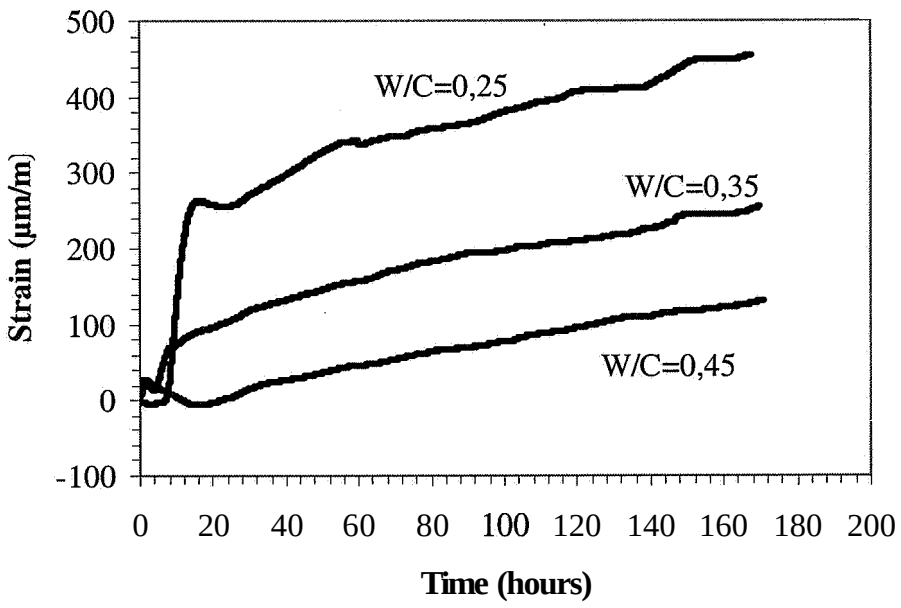

Figure 3. Free autogenous shrinkage

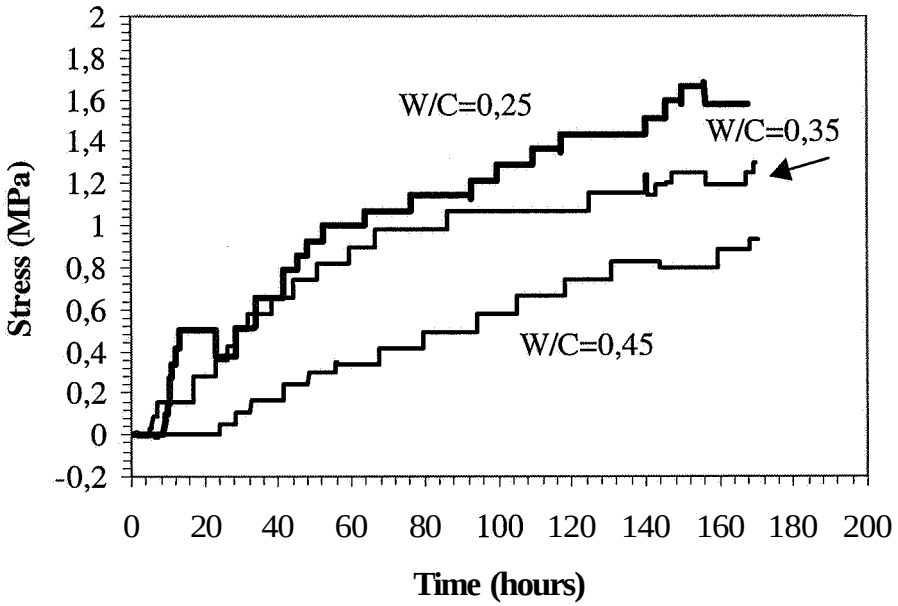

Figure 4. Stress

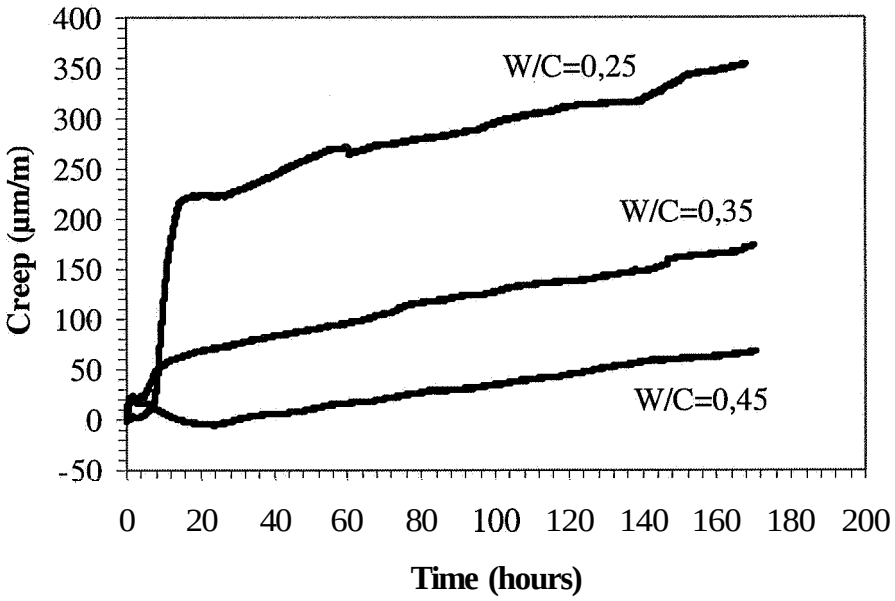

Figure 5. Creep

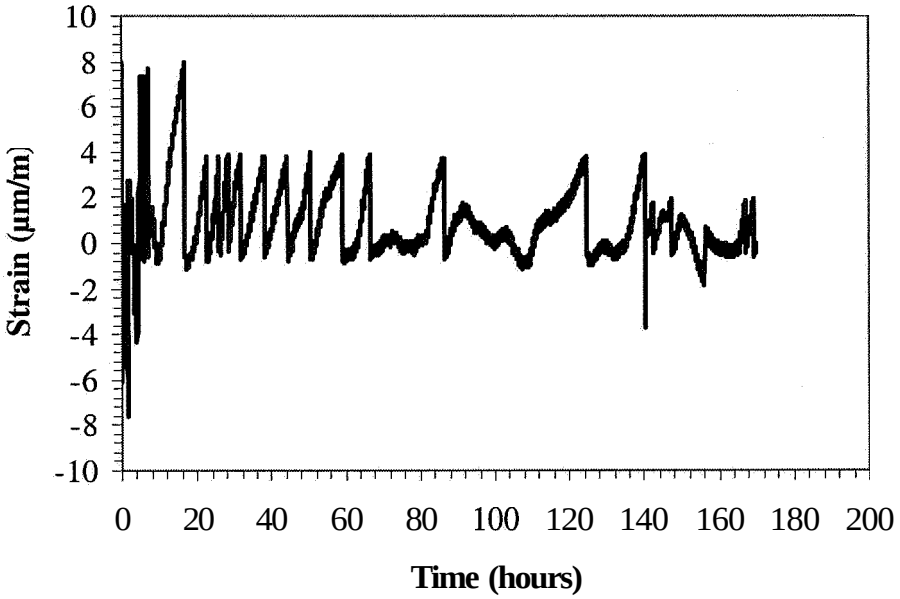

Figure 6. Restrained shrinkage W/C = 0,35

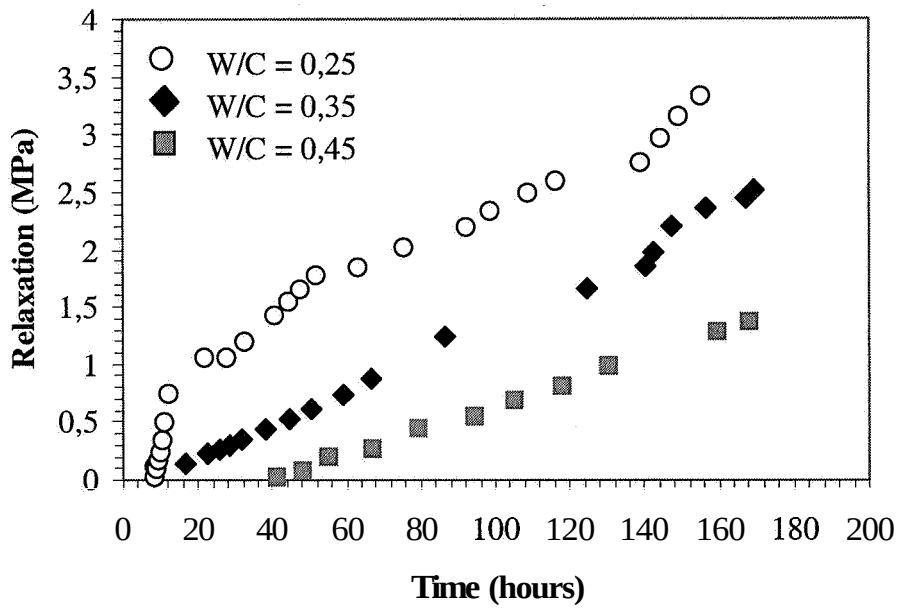

Figure 7. Relaxation

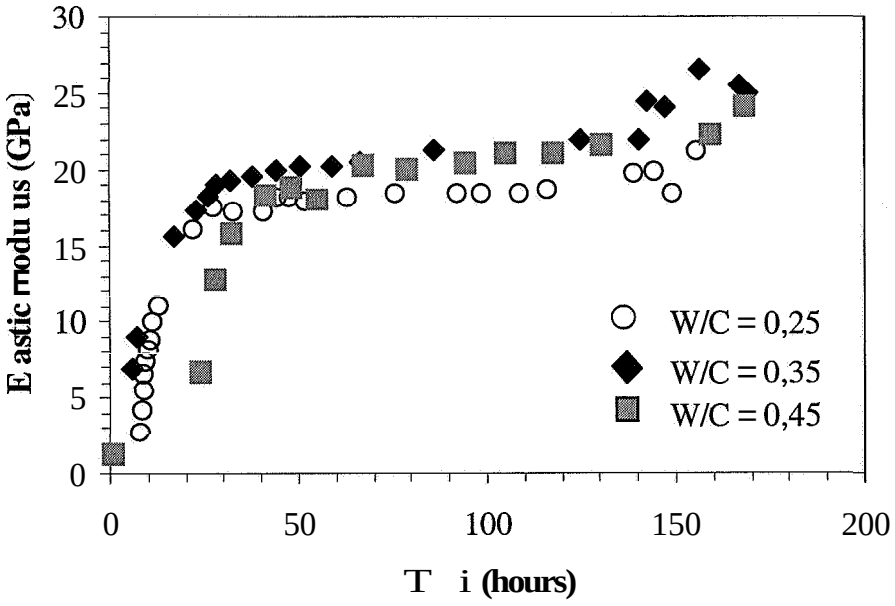

Figure 8. Elastic modulus

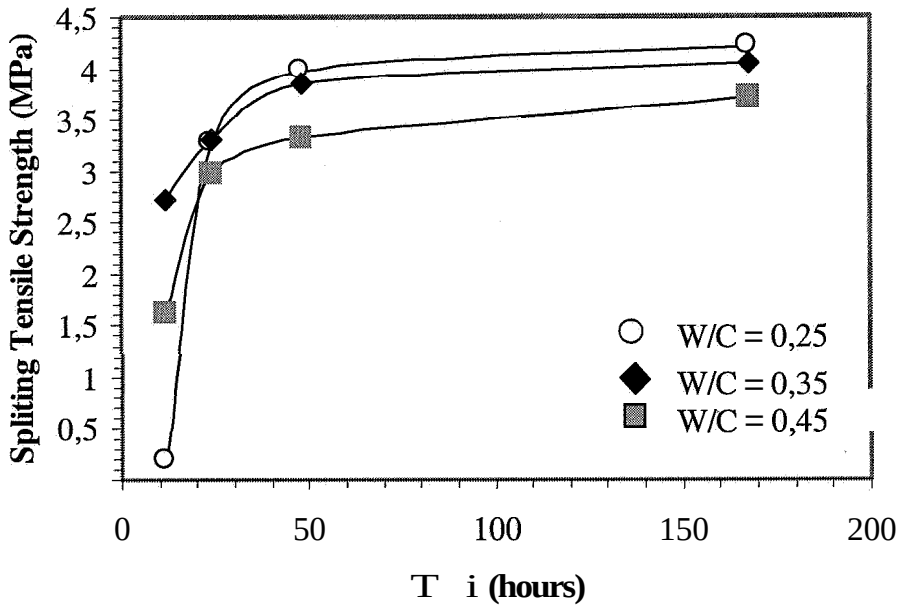

Figure 9. Tensile strength

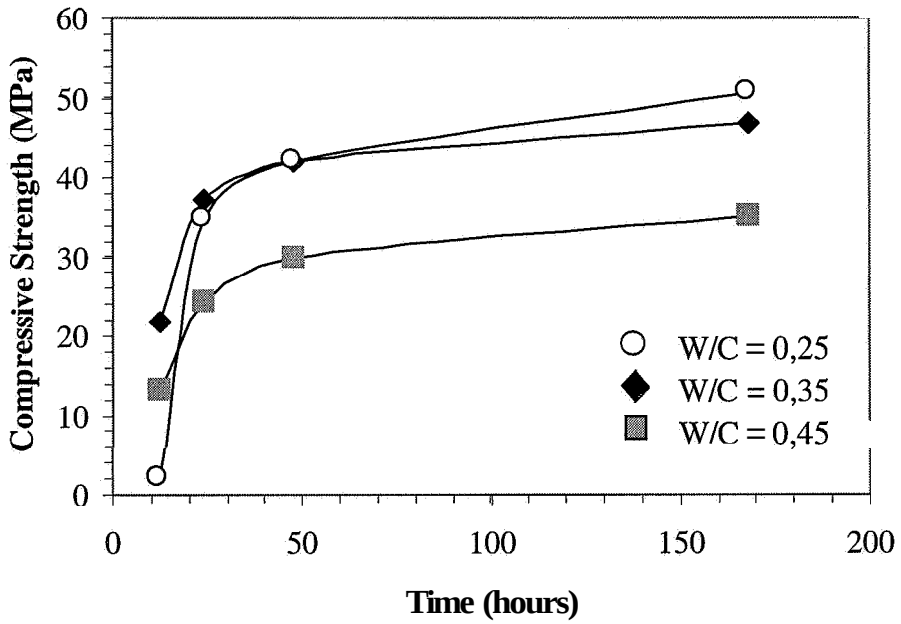

Figure 10. Compressive strength

3. Discussion

As expected, the free autogenous shrinkage (Figure 3) increases as the water-cement ratio decreases. In mixtures with a low water-cement ratio, the process of hydration reduces more quickly the percentage of free water in the capillary pores and self-desiccation thus has a more pronounced influence. The results show however that it is mostly during the first 24-h period that the difference between the three mixtures is apparent. At 24 h, the free shrinkage is approximately 0 for the 0,45 mixture, 100 µm/m for 0,35 and close to 300 µm/m for 0,25. After the first 24-h period, the curves are quite parallel.

From the data in Figure 3, one would expect that the stress induced by the autogenous restrained shrinkage would be much higher for the 0,25 mixture. However, the results in Figure 4 indicate that this is not the case. Although, at 24 h, the 0,45 mixture has almost no stress, at 7 d, its tensile stress is close to 1 MPa, while that of the 0,25 mixture is about 1,6 MPa. This can only be explained, of course, by creep (or more properly, relaxation), which fact can be verified from Figure 5.

The stress relaxation can be calculated, as previously mentioned, on the basis of the stress that would be generated if there was no creep. As can be seen in Figure 7, the relaxation phenomenon is not very high for the 0,45 mixture (although it does represent 1,4 MPa at 7 d), but more significant for the 0,35 (2,5 MPa at 7 d) and, particularly, for the 0,25 mixture (3,3 MPa at 7 d). It should be pointed out, however, that the calculation of the intensity of the stress relaxation rests on a number of hypotheses. First, it has to be assumed that the restrained shrinkage has not damaged the material and that the elastic modulus is that which would be determined on a non restrained specimen. Second, the principle of superposition of strains and stresses must always be

accepted. Notwithstanding the hypotheses on which the calculations rest, it is clear that relaxation is an extremely important phenomenon, and that analysing the risk of early age cracking solely on the results of autogenous shrinkage measurements is not a satisfactory procedure. The results further indicate that the tensile stress that can be generated by self desiccation in normal concretes, such as that with a water-cement ratio of 0,45, are quite significant, and not very different from that generated in lower water-cement ratio mixtures. In this series of experiments, the tensile stress generated under restrained shrinkage at 7 d represents 23% of the failure load (as determined from the results of Brazilian tests on accompanying cylinders) at a water-cement ratio of 0,45, 29% at 0,35, and 36% at 0,25. The corresponding free autogenous shrinkage values are respectively 120 μm/m, 240 μm/m, and 440 μm/m.

There is very little data in the technical literature on the direct measurement of tensile stress at early ages due to autogenous shrinkage from time t=0. In an experiment similar to those described in this paper, van Breugel and de Vries [11] found a tensile stress of more than 2 MPa at 7 d for a 0,4 water-binder ratio mixture containing slag. This mixture failed after 12 days at a stress of 3,3 MPa. A second mixture with a water-binder ratio of 0,37 was observed to fail after less than 48 hours at a stress of 3,5 MPa. There thus exists a wide range of possible performances in this regard, and it is important to analyse in depth the influence of all composition parameters in order to determine the composition of the mixtures which will be less likely to fail, taking into account both the level of stress generated and the failure stress. The level of stress generated, as the results described show, is closely linked to the relaxation capacity of the mixture. This property should thus be investigated in depth and analysed, in order to design mixtures where, as much as possible, the stress will be generated at a time when the relaxation capacity is the highest, including during the first 24 h period when creep is combined with, as is clear from the data presented, plastic deformation.

4. Conclusion

The level of tensile stress generated by self-desiccation in restrained normal Portland cement concrete specimens increases as the water-cement ratio decreases. This level was observed to be 36% of ultimate for a ratio of 0,25, 29% for 0,35, and still quite significant at 23% for 0,45. It was also observed that stress relaxation has a very significant influence on this phenomenon. Calculations indicate for instance that the stress measured in the 0,25 water-cement ratio concrete was 32% of that which would be observed in a purely elastic material, i.e. with no relaxation capacity (1,6 MPa versus a theoretical elastic stress of 4,9 MPa). From a comparison with data published recently by other investigators, it appears that the relaxation capacity of concrete varies quite significantly with the composition of the mixture. This indicates that optimisation of mixtures to reduce the risk of early age cracking due to self-desiccation is possible, but much more testing will be required before this can be done. It should be remembered, in addition, that early age cracking could be due to a number of causes, including thermal effects. It is probable that, in many cases if not in most cases, early age cracking is not solely due to self-desiccation induced shrinkage.

5. Acknowledgements

This project was funded partly by the Natural Sciences and Engineering Research Council of Canada (NSERC), through its grant to the Network of Centers of Excellence on High Performance Concrete (Concrete Canada), and by the Fonds pour la Formation de Chercheurs et l'Aide à la Recherche (FCAR) of the Québec government. The authors wish to thank Anik Delagrave from Laval University who reviewed the manuscript.

6. References

1. Justness H., Van Gemert A., Verboven F. and Sellevold E. J. (1996) Total and external chemical shrinkage of low w/c ratio cement pastes. *Advances in Cement Research*, 8, No.31, pp. 121-126
2. Tazawa E., Miyazawa S. (1996) Influence of autogenous shrinkage on cracking in high-strength concrete. *4th International Symposium on the Utilisation of High Strength and High Performance Concrete*, Paris, France, pp. 321-330
3. Le Roy R. and De Larrard F. (1993) Creep and shrinkage of high-performance concrete: the LCPC experience. *5th International Rilem Symposium on Creep and Shrinkage of Concrete*, E&FN SPON, London pp. 499-504
4. Paillère M., Buil M. and Serrano J.J. (1989) Effect of fiber addition on the autogenous shrinkage of silica fume concrete. *ACI Materials Journal* V86, No.2, pp. 139-144
5. Tazawa E., Miyazawa S. (1998) Effect of constituents and curing condition on autogenous shrinkage of concrete. *Proceedings of the International Workshop on Autogenous Shrinkage of Concrete*, Hiroshima, Japan, pp. 257-268
6. Kovler K and Bentur A. (1998) Shrinkage and creep of steel fiber reinforced concrete under restraint. paper presented at the *Spring Convention, ACI*, Houston Texas, U.S.A.
7. Bloom R. Bentur A. (1995) Free and restrained shrinkage of normal and high-strength concretes. *ACI Materials Journal* V92, No. 2, pp. 211-217
8. Kovler K. (1994) Testing system for determining the mechanical behaviour of early age concrete under restrained and free uniaxial shrinkage. *Materials and Structures* V27, no.170, pp. 324-330
9. Springenschmid R., Breitenbiichner R. and Mangold M. (1994) Development of the cracking frame and the temperature-stress testing machine. *Thermal cracking in Concrete at Early Age, Proceedings of the International Symposium of the Rilem*, E&FN SPON, Miinic, pp. 137-144
10. Pigeon M., Marchand J., Bissonnette B., Prince J.C. and Toma G. (1999) Equipment for the analysis of the behaviour of concrete under restrained shrinkage at early ages. paper submitted to publication
11. Van Breugel K. and De Vries J. (1998) Mixture optimisation of low water/cement ratio high strength concretes in view of reduction of autogenous shrinkage. *International Symposium on High-Performance and Reactive Powder Concretes*, Sherbrooke, Canada, vol.1, pp. 365-375

CHEMICAL SHRINKAGE OF CEMENTITIOUS PASTES WITH MINERAL ADDITIVES

Harald Justnes, Dr. Ing., Chief Scientist, SINTEF Civil and Environmental Engineering, Cement and Concrete, N-7465 Trondheim, NORWAY

Erik J. Sellevold, Ph.D., Professor, Department of Structural Engineering,
The Norwegian University of Science and Technology, N-7034 Trondheim, NORWAY

Bert Reyniers, M. Sc., Dirk Van Loo, M. Sc., Arne Van Gemert, M. Sc.
Frank Verboven, M. Sc. and Dionys Van Gemert, Ph.D., Prof.,
Katholieke Universiteit te Leuven, Faculteit Toegepaste Wetenschappen,
Departement Burgerlijke Bouwkunde, B-3001 Heverlee, BELGIUM

Abstract
In order to overcome the increased cracking tendency of high performance concrete applied in practice (e.g. bridge decks), a better understanding of the fundamental process in the equivalent binder must be obtained.

The influence of mineral additives on total and external chemical shrinkage has been studied, excluding platicising admixtures in the present paper. Pozzolanic silica fume has been compared with inert calcium carbonate of equivalent surface area, both relative to reference without additive. The additives were tested in combination with a number of different Portland cements.

The fineness of the cements dominated the initial rate of chemical shrinkage (i.e. hydration rate) and the "flattening out level" (i.e. fraction of external chemical shrinkage corresponding to the time the time where a self-supporting skeleton is formed) seems to be quite independent of fineness. The induction period prior to setting is shown not to be "dormant", but rather quite active in terms of volume changes the first hour.

The influence of mineral additives on chemical shrinkage was dependent of cement type; sometimes accelerating and sometimes equal to the reference. The external chemical shrinkage levels also varied with cement type, as the effect of mineral additives varied from increasing the level to being the same relative to the reference.

Key words: Chemical shrinkage, mineral additives, silica fume, calcium carbonate

1. INTRODUCTION

Practical experience has shown that high performance concrete is sensitive to cracking at early ages (from placing to a few hours after finishing), even when great care is taken to avoid evaporation from the surface that initiates plastic shrinkage 11, 2/. The main reason for this early shrinkage is considered to be early volume change producing stresses under restraint conditions, couple with low stress/strain capacity of the concrete at this stage. The present study is part of a larger work, and focuses on early volume change in cement paste containing silica fume. Silica fume is compared with calcium carbonate to differentiate between chemical and physical effects, and the comparison is done for a number of Portland cements.

The total chemical shrinkage during the hydration of cement is caused by the smaller volume of products (e.g. CSH gel and CH) compared with the reactants (e.g. alite and water). As a rule of thumb, the total chemical shrinkage at 100 % hydration is about 6.25 ml/100 g cement (i.e. 25 % of the chemical bound water corresponding to a w_n of 0.25) /3/. The total chemical shrinkage equals the external chemical shrinkage until the network of hydration products bridging the unreacted cement grains is strong enough to resist the contracting forces. At this point (5-9 h depending on cement composition, fineness, w/c etc.), the external chemical shrinkage rate slows down drastically and the shrinkage vs. time curve flattens out. Thereafter, the second manifestation of total chemical shrinkage; the formation of internal contraction pores, is dominating. The relationship between the two is considered important in the cracking problem. Both quantities are measured in parallel in the present work.

The terminology in the present paper is total chemical shrinkage, which is the sum of external chemical shrinkage and the volume of empty contraction Pores at all stages. In literature, there is a terminology confusion: Total chemical shrinkage may be named chemical shrinkage, water absorption, volume contraction, or Le Chatelier shrinkage after the first scientist who examined the shrinkage of cement paste. External chemical shrinkage is also named external volume change, bulk shrinkage and autogenous shrinkage.

The methods for measuring total chemical shrinkage all have in common that the sample has to be kept water saturated and that the water needed to replace the volume decrease is measured, while the common methods for measurement of external chemical shrinkage are characterised by sealed curing of the cement paste. There are mainly three techniques for measuring chemical shrinkage; 1) dilatometry, 2) gravimetry and 3) pycnometry.

Dilatometry is based on direct measurements of length or volume change.

The most common dilatometry technique for total chemical shrinkage measurement is to put the paste in a recipient (e.g. glass tube), filling the rest of the recipient with water and plugging the recipient with a stopper with a water filled pipette stuck through. Reading the fall of the water level in the pipette versus time gives the total volume change. Knudsen and Geiker /4/ have pioneered a variety of applications for this method since the 1980's. This method is used in the present paper.

A dilatometry technique for external shrinkage measurement has been utilised by measuring the uniaxial length change of a flexible, sealed tube by inductive sensors /5/.

Gravimetry is based on indirect measurement of volume change by recording reduced buoyancy under water by weighing (i.e. the law of Archimedes). If the weight change of a container filled with paste and excess water having at least one flexible wall is recorded, the total chemical shrinkage is measured /6/. If the weight change of a sealed elastic bag filled with paste only is registered, the external chemical shrinkage is measured. The latter method is used in the present paper.

Pycnometry is only applicable for total chemical shrinkage measurements, and is carried out by filling a pycnometer with paste and topping it with water. Water is added to refill

the pycnometer at different ages, and the weight increase relates to the total volume change.

2. EXPERIMENTAL

2.1 Chemicals

The cements were all Portland cements produced by Norcem A/S, Norway, over a period of time. The cement characteristics are given in Table 1. The water was distilled before use.

Silica fume slurry (delivered by Elkem Materials, Fiskaa plant, Kristiansand, Norway) was composed of 93.0 % SiO_2, 2.1 % Fe_2O_3, 1.2 % MgO, 1.0 % CaO, 1.0 % C, 0.56 % K_2O, 0.42 % SO_3, 0.30 % Na_2O, 0.29 % Al_2O_3 and 0.11 % H_2O. The BET specific surface area was 22 m^2/kg.

Precipitated calcium carbonate, $CaCO_3$, laboratory grade (>96 % pure) was delivered by KEBO Lab A/S, Trondheim, Norway. The specific surface was measured to 18 m^2/g by nitrogen adsorption (BET).

2.2 Methods

2.2.1 Mixing procedure

Cement and water was mixed in a Hobart mixer of 5 litre capacity. Mixing times were 2 min at gear 1 and 1 min at gear 2. The bowl with paste was put on a vibrating table to remove most of the entrained air. The starting time of the experiments was the first contact between cement and water (time = 0), and the first measurements started at 1 h.

2.2.2 Total chemical shrinkage

Cement paste was put into three Erlenmeyer flasks for parallel experiments. The weights of the empty and filled recipients were measured in order to determine the amount of paste. The recipients were then carefully filled with distilled water at room temperature in a manner to avoid turbulence. A silicon rubber stopper was used to plug each recipient, taking care not to enclose any air bubbles. A pipette was filled with water and stuck through a hole in the stopper. A graded pipette of 0.2, 0.5 or 1 ml was chosen depending on the expected volume change. The recipients were put in a water bath at 20±1°C. Every hour until 48 h, the position of the meniscus in the pipettes was read. The decrease of the water column in ml is directly the total chemical shrinkage (as a drop of liquid paraffin on top prevented evaporation), which were expressed as ml/100 g cement after a calculation of the mean value from the three parallel measurements. The method relies on the assumption that all contraction pores are filled with water.

2.2.3 External chemical shrinkage

Three elastic rubber bags (i.e. condoms) were filled with cement slurry while the condoms were inserted in a 100 mm plastic tube of 50 mm inner diameter. Each condom was closed by twisting the upper part and tying it with a thin copper wire, and sealed by spraying silicon glue into the open end. The excess end part was cut off and the total mass determined.

The filled and sealed condoms in their tubes were kept in a water bath of 20±1°C after the tubes had been turned perpendicularly to their axes in order to let all air bubbles escape. The tubes were kept on an ordinary rotating table modified to function under water (i.e. a chain transfer between the motor and the rollers placed under water). During the first 10 h, the condom was weighed every hour under water. According to Archimedes principle, an external shrinkage will lead to a reduction in buoyancy, which will be registered as a weight increase. Each condom was weighed in a basket under water hanging on a scale in a separate water bath with no stirring to avoid turbulence. The transfer between the bath for rotation and the bath for weighing took place under water at all times by placing the tube in a water filled glass under water in one bath and taking it out of the glass under water in the second bath. This was done to avoid trapping of any air bubbles in the transfer process.

After the last weighing under water at 48 h, the condoms were wiped dry and weighed in air. Finally, the condom, including copper wire and silicon glue, were stripped off and weighed in order to calculate the net weight of the cement slurry after subtracting the weight of the tube. The external shrinkage is presented as the mean value of three parallel measurements and given in ml/100 g cement or vol%. In the present study, many of the samples with mineral additives were not rotated since no bleeding occurred. In such a case the tube in the preceding procedure was excluded and the condoms carefully weighed as such.

3. RESULTS AND DISCUSSION

The total chemical shrinkage as a function of time of P30 cement without and with 10% replacement of silica fume and calcium carbonate at water to solid ratio (w/s) 0.50 is shown in Fig 1 until 48 h. In the same figure the results for ***G*** cement without and with 10 % silica fume replacement are plotted as well. The chemical shrinkage of the P30 mix with calcium carbonate seems to be accelerated just after assumed setting (around 5 h) relative to the reference. P30 with silica fume seems to follow the reference but ends up at a slightly lower chemical shrinkage level compared with the reference. The curves for G cement without and with 10% silica fume are virtually identical, but lower than the curve for P30, reflecting the lower surface area of the G cement. The acceleration of P30 by calcium carbonate is a well-known filler effect /7/ for some cements. The mechanism may be that calcium carbonate serve as nucleation points for calcium hydroxide growth supplied by cement hydration. Alternatively there is an active interaction between calcium carbonate and C_3A forming carboaluminates/8/.

Table 1 Cement characteristics

Cement	P30	P30c	P30k	HS65	G
Oxides:					
CaO (C)	63.16	63.44	63.61	64.32	64.82
SiO_2 (S)	20.28	20.92	20.84	22.13	22.0
Al_2O_3 (A)	4.89	4.60	5.04	4.05	3.53
Fe_2O_3 (F)	3.61	3.54	3.30	3.39	4.78
MgO (M)	2.21	1.80	-	1.03	1.42
SO_3 ($\bar{S}$)	2.98	3.06	2.70	3.07	1.75
Alkalis	1.13	0.94	1.06	0.51	0.60
Blaine (m^2/kg)	309	358	361	418	303
Minerals (Bogue)					
C_3S	57	55	54	53	61
C_2S	16	19	19	24	17
C_3A	6.9	6.2	7.8	5.0	1.3
C_4AF	11.0	10.8	10.0	10.3	14.6
$C\bar{S}$	5.1	5.2	4.6	5.2	3.0

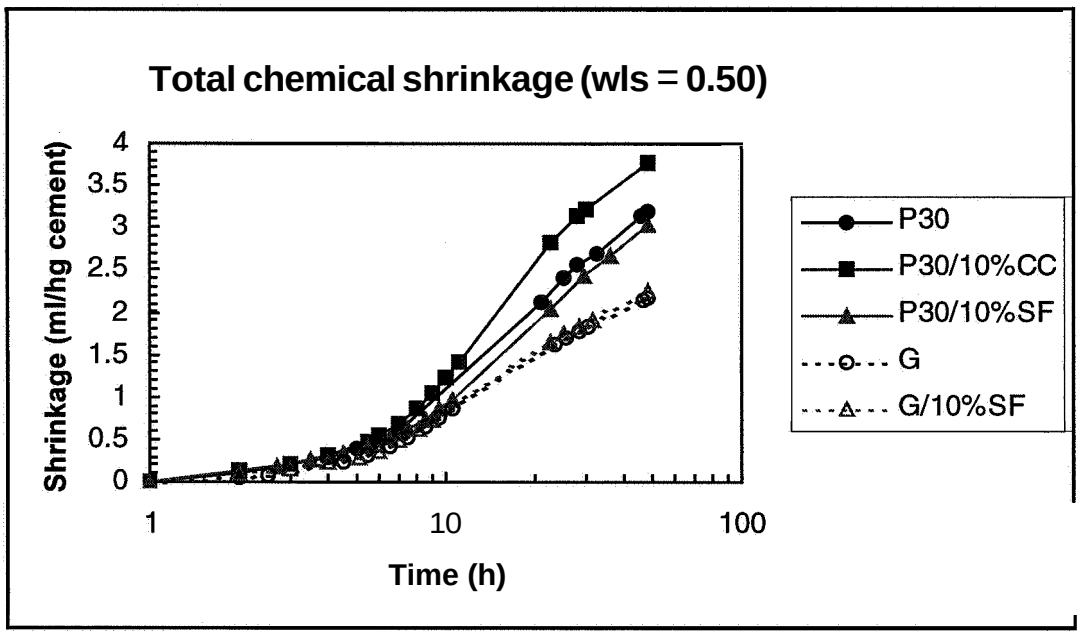

Fig 1 Total chemical shrinkage versus time curves for P30 and G cement without and with 10 % replacement of calcium carbonate and silica fume and wls = 0.50.

The total and external chemical shrinkage versus time for G cement without and with 10% replacement of calcium carbonate and silica fume are shown in Figs 2 and 3 for w/s = 0.40. The total chemical shrinkage curves are virtually identical for calcium carbonate and silica fume replacements until 288 h (reference only measured to 46 h while silica

fume mix was measured until 672). The neat G cement showed about 0.5 ml less total chemical shrinkage per 100 g cement than the mixes with mineral replacements at 46 h, which must reflect a lower degree of hydration for the neat G cement paste. The external chemical shrinkage versus time curves in Fig **3** are virtually identical in the plastic stage until a strong enough network is formed to resist the contraction forces. Apparently the mix with silica fume replacement requires a somewhat higher degree of hydration than the mix with calcium carbonate replacement to form sufficiently strength.

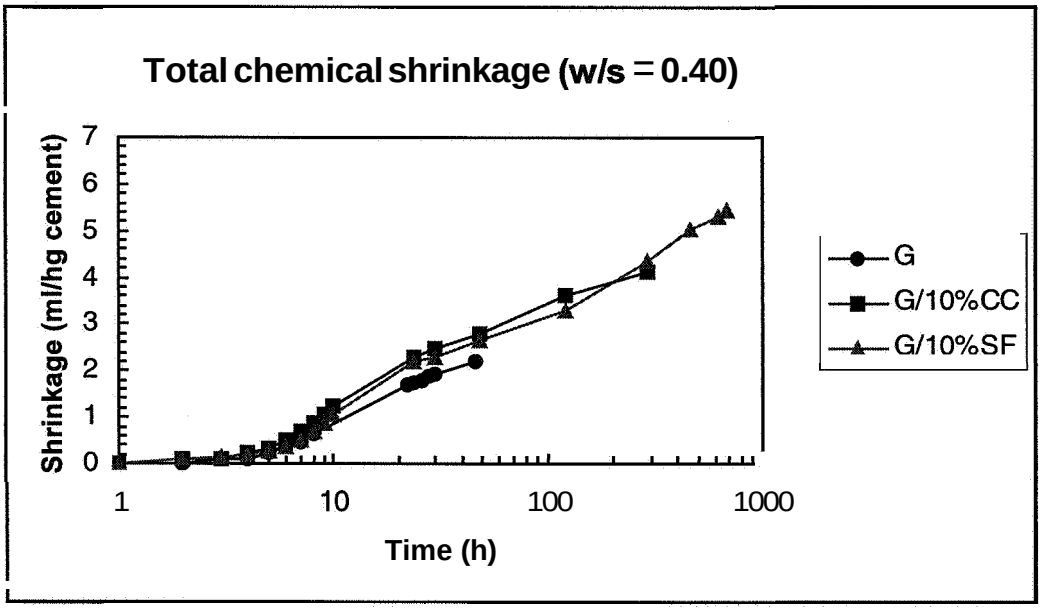

Fig 2 Total chemical shrinkage versus time curves for G cement without (until 46 h) and with 10% replacement of calcium carbonate (until 288 h) and silica fume (until 672 h) for w/s = 0.40.

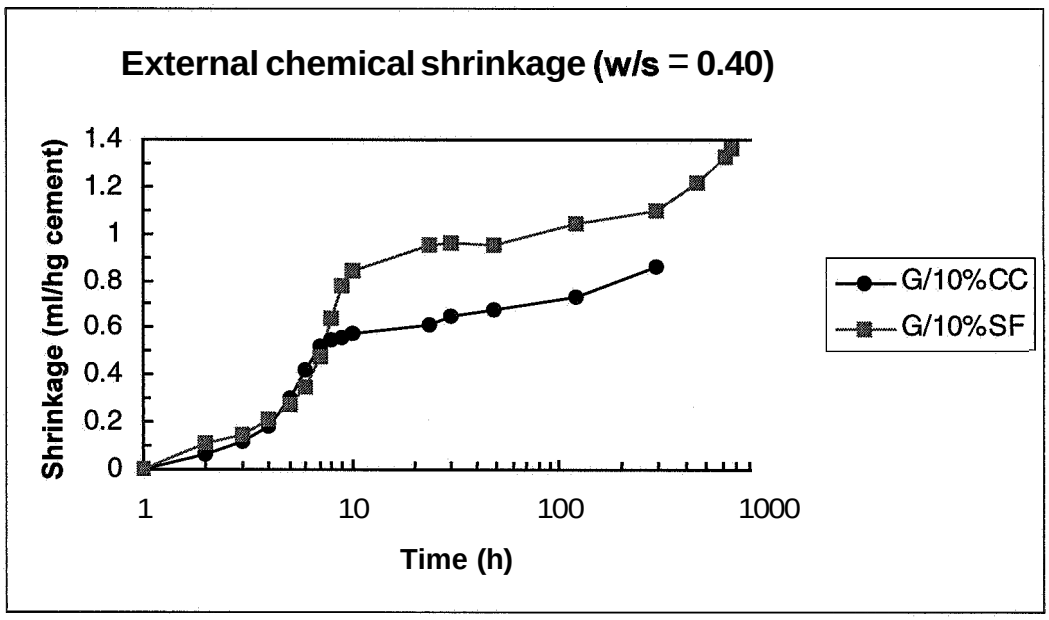

Fig **3** External chemical shrinkage versus time curves for G cement with 10% replacement of calcium carbonate (until 288 h) and silica fume (until 672 h) for w/s = 0.40. Samples were not rotated.

Note that the samples in Fig. 3 were not rotated. The next data-set document that rotation is not necessary when 10 % cement is replaced with such fine minerals at w/s = 0.40. Fig 4 and 5 shows the total and external chemical shrinkage curves, respectively, of P30k cement without and with 10% replacement of calcium carbonate and silica fume. The total chemical shrinkage of the silica fume mix seems to be a little accelerated up to 10 h compared to the calcium carbonate mix, but there after they are close to identical. The mixes with mineral replacements have a higher chemical shrinkage than the neat cement paste (about 0.6 ml/100 g cement at 48 h).

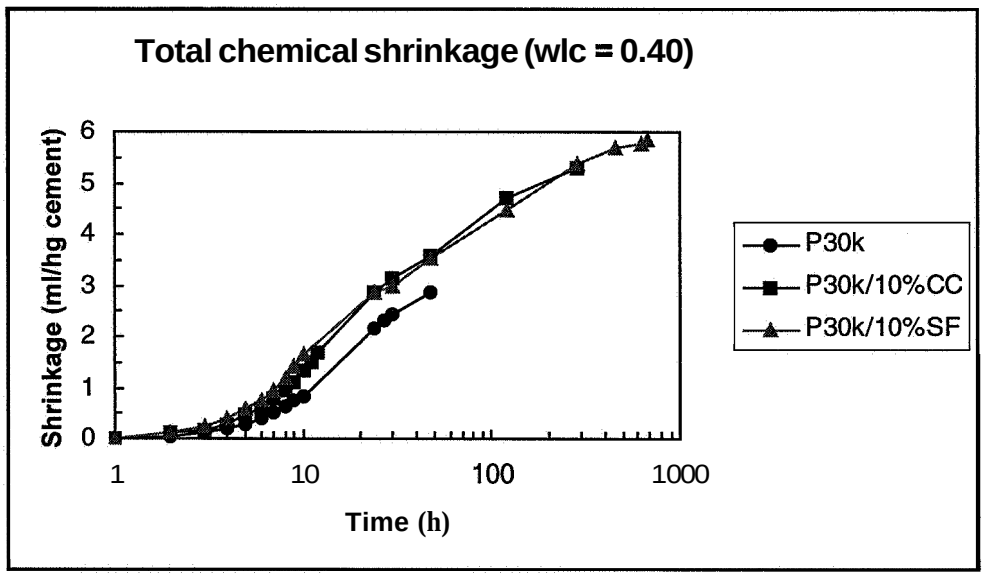

Fig 4 Total chemical shrinkage versus time curves for P30k cement without (until 48 h) and with 10% replacement of calcium carbonate (until 288 h) and silica fume (until 672 h) for w/s = 0.40.

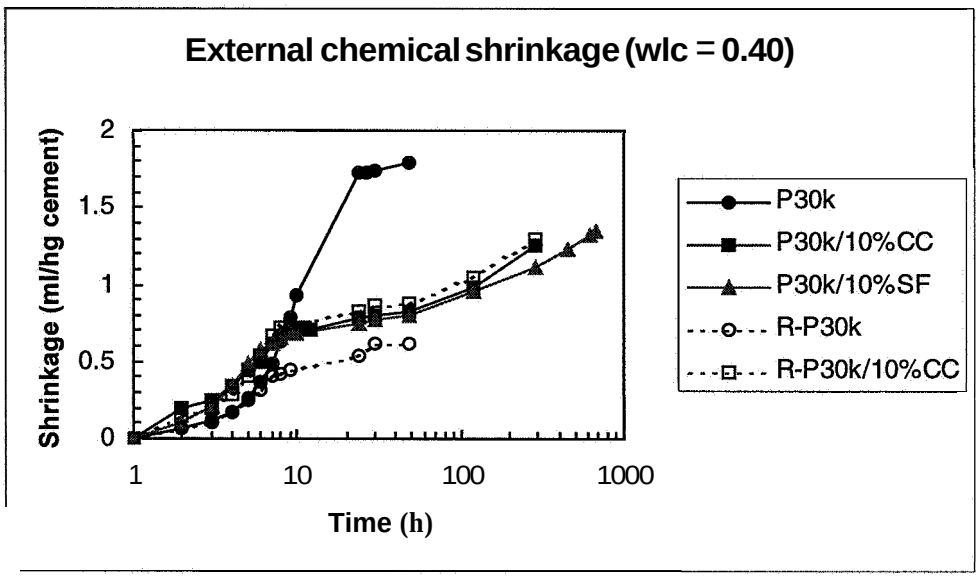

Fig 5 External chemical shrinkage versus time curves for P30k cement without (until 48 h) with 10% replacement of calcium carbonate (until 288 h) and silica fume (until 672 h) for w/s = 0.40. The legend R- means that the sample was rotated.

The neat P30k cement paste and the mix with 10% calcium carbonate replacement were measured both static and rotated, as shown in Fig. 5. The much higher external shrinkage for the static neat cement paste compared with the rotated one after setting is a result of "bleeding water" (i.e. separation of mix) formed in the liquid state and a delayed suction of it into the hardened sample when the contraction pores are formed as previously described /9, 10/. Note that the two curves are identical when the samples are in their plastic state prior to setting. The close to identical curves for the static and rotated sample of the P30k cement with 10% calcium carbonate replacement indicates that separation is not a problem for such a low w/s and fine powder replacement.

Fig. 5 also shows that the external chemical shrinkage of mixes with 10% replacement by calcium carbonate and silica fume are about equal until 120 h, and there after the "creep" (i.e. the continuing increase in external chemical shrinkage after the knee-point) are higher (about 0.2 ml/100 g cement) for the calcium carbonate until 288 h (last data point). The mixes with mineral replacements have a higher "flattening out" level for the external chemical shrinkage than the neat cement paste, indicating that a higher amount of hydration is necessary to obtain the required strength to resist the contraction forces.

The total and external chemical shrinkage versus time, respectively, for P30c cement without and with 10% replacement of calcium carbonate and silica fume are shown in Fig 6 and 7 for w/s = 0.40. The total chemical shrinkage for the mixes with mineral replacement was about equal and higher than the corresponding neat paste until 7 h, but the silica fume mix had a higher total chemical shrinkage than the carbonate mix, which again had a higher shrinkage than the reference, from this point. The external chemical shrinkage curves for the 3 mixes in Fig 7 are about equal (neat paste rotated to avoid bleeding). The shrinkage curve for static and rotated neat P30c paste deviates more than usual in the plastic stage when using continuous rotation, which could be attributed to this sample being rotated by hand (i.e. turned manually every 15 minutes).

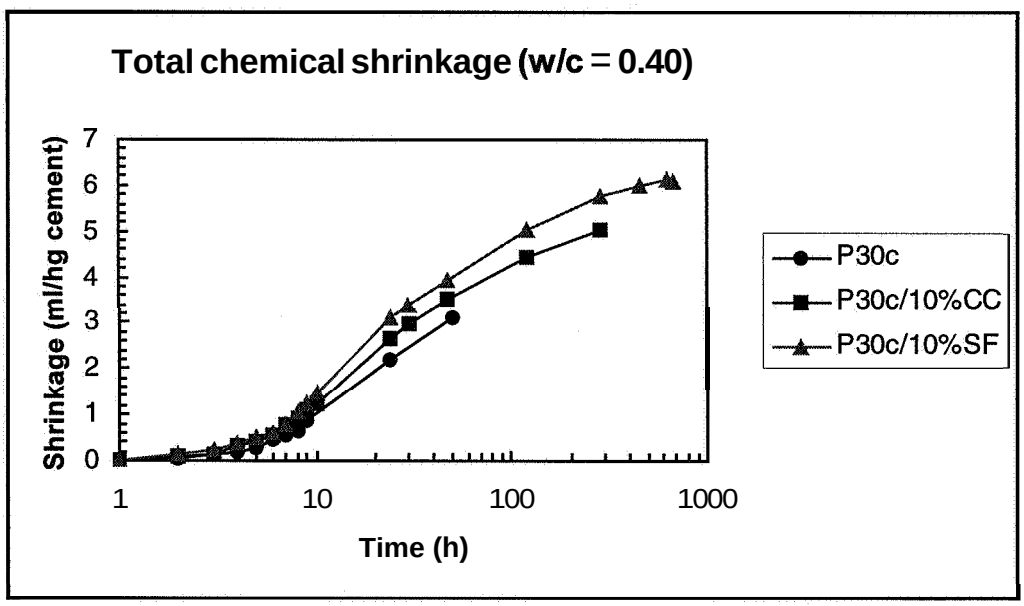

Fig 6 Total chemical shrinkage versus time curves for P30c cement without (until 50 h) and with 10% replacement of calcium carbonate (until 288 h) and silica fume (until 672 h) for wls = 0.40.

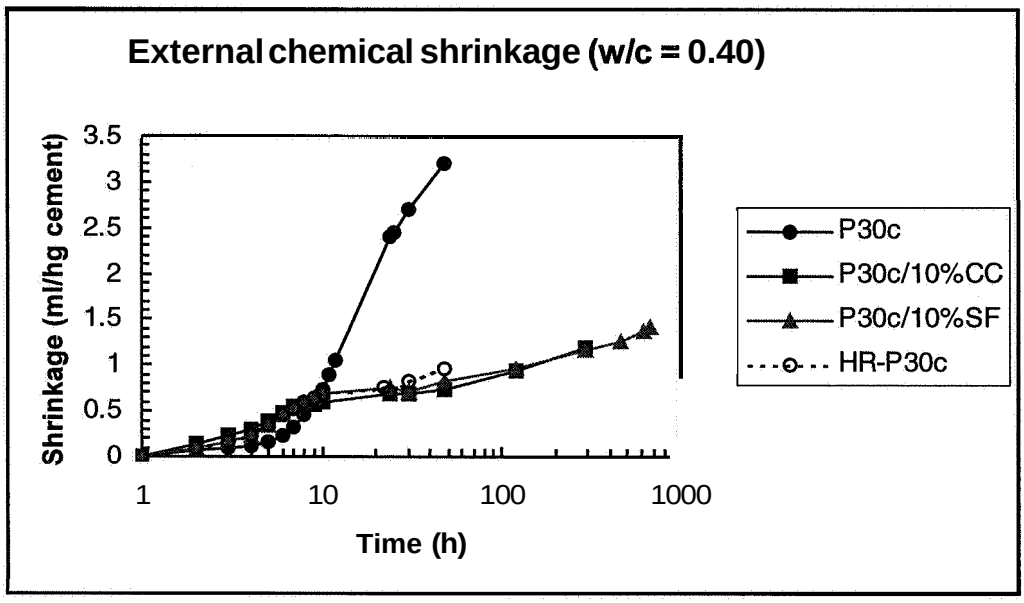

Fig 7 External chemical shrinkage versus time curves for P30c cement without (until 48 h) with 10% replacement of calcium carbonate (until 288 h) and silica fume (until 672 h) for w/s = 0.40. The legend HR- means that the sample was rotated by hand.

The last data set is a high strength type Portland cement (HS65). The total and external chemical shrinkage curves are shown in Fig 8 and 9, respectively, for HS65 cement without and with 10% replacement of calcium carbonate and silica fume for w/s = 0.40. The total chemical shrinkage versus time curves in Fig 8 show that the two pastes with mineral replacements behave close to identical and are accelerated compared to the reference. The same features can be seen from the external chemical shrinkage curves in Fig. 9 as well for the plastic state prior to setting. After the knee point, the two mineral substituted mixes only deviate marginally with slightly higher values for the calcium carbonate mix. The flattening out levels for the mineral mixes are, however, substantially higher (about 0.35 ml/100 g cement) than the neat cement paste. This indicates that much more hydration has to take place before the mineral substituted pastes achieve sufficient strength to resist the contraction forces created by the continuing chemical shrinkage.

General speaking, the substitution of cement with a non-pozzolanic (e.g. calcium carbonate), or pozzolanic mineral (e.g. silica fume) with minor reaction the first 15 h, should lead to a higher degree of hydration to form a hydration net-work strong enough to resist the forces created by the contraction pores after setting. This situation should apply if the mineral particles are dispersed around the cement grains and prevent them from direct interaction with each other. If the fine minerals used here (average particle diameters 0.15-0.2 pm) are rather filled in the cavities formed by the packing of the irregular cement grains (average diameter in the order of 10 pm), this should lead to displacement of water and also for this reason move the cement grains further apart. Among the cements tested (not measured for G), the flattening out levels are higher for the mineral substituted pastes for HS65 and P30k compared with the neat pastes, while the levels are equal for the three mixes for the P30c cement. The higher level for the silica fume substituted G-cement compared with the calcium carbonate mix in Fig. 3 is difficult to explain since the opposite should be expected if

a certain reactivity was acknowledged for the silica fume. **A** non-reactivity for both additives could still lead to equal levels of external shrinkage higher than the reference, since the pore refinement by the smaller particles will create menisci leading to stronger forces when the initial contraction pores are formed.

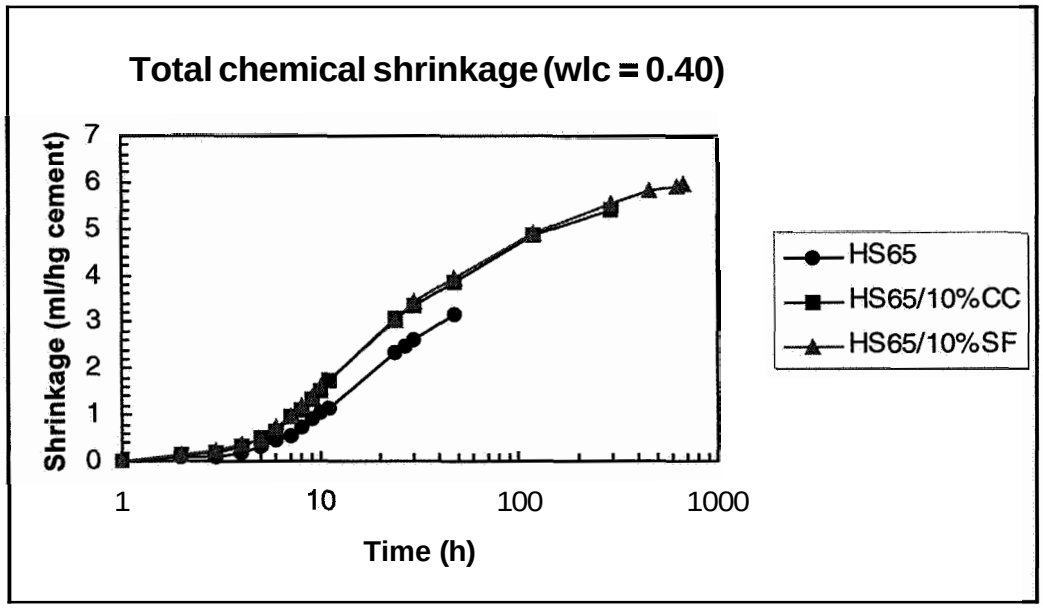

Fig 8 Total chemical shrinkage versus time curves for HS65 cement without (until 48 h) and with 10% replacement of calcium carbonate (until 288 h) and silica fume (until 672 h) for w/s = 0.40.

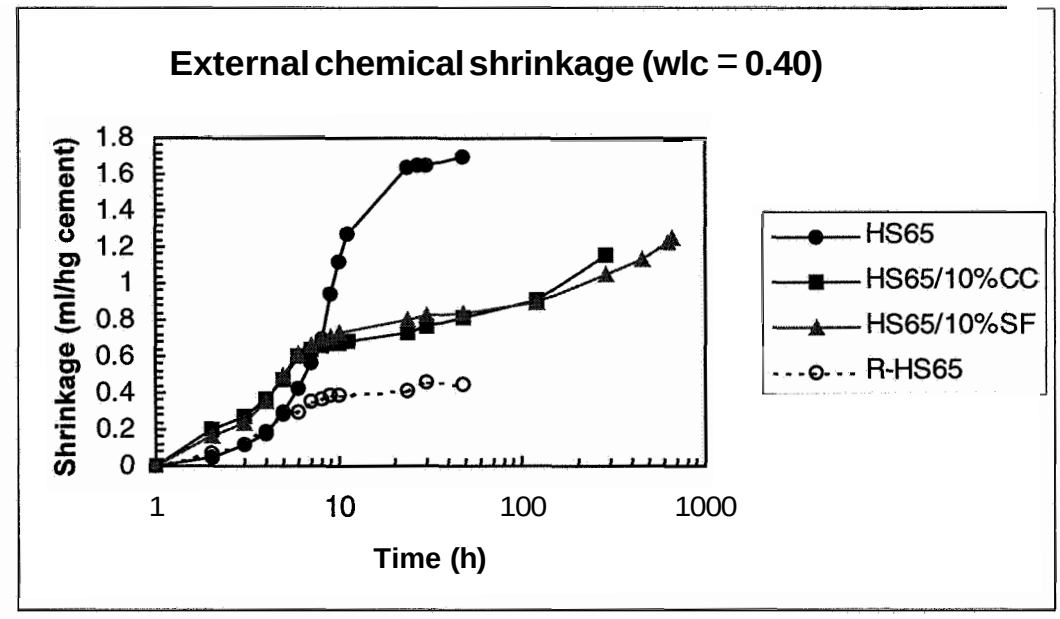

Fig 9 External chemical shrinkage versus time curves for HS65 cement without (until 48 h) with 10% replacement of calcium carbonate (until 288 h) and silica fume (until 672 h) for w/s = 0.40. The legend R- means that the sample was rotated.

Justnes et al /11/ crudely estimated the total chemical shrinkage of the pozzolanic reaction between silica fume and lime to be 8.8 ml/100 g reacted silica as compared with 6.3 ml/100 g portland cement. Justnes et al /11/ found also that the total chemical shrinkage of portland cement replaced with the pozzolans showed that the early shrinkage rate increased probably due to the filler effect supplying nucleation points for hydration products. The chemical shrinkage of the pozzolanic reaction itself was confirmed in the cement blend since a substantial higher total chemical shrinkage persisted over time.

Sellevold et al /12/ showed for pastes of w/s= 0.6 with addition of 12 % silica fume and calcium carbonate of similar surface, that the chemical bound water (W, in g/g ign. cem.) was equal for the two additions, but higher than the reference until 28 days.

Justnes et al /13/ also tested the influence of different cements on chemical shrinkage and found that the early reactivity depends largely on fineness, and the contents of the most reactive phases; C_3A, C_3S, alkalis and sulphates, confirming some of the results obtained in the present paper.

5. CONCLUSIONS

Total and external chemical shrinkage initiates upon the contact between cement and water. Thus, the period prior to setting is not "dormant" in terms of volume changes. The two quantities are identical until a solid skeleton is formed (6-10 hours). Further hydration results in empty pores (self-desiccation) and greatly reduced external chemical shrinkage.

The early total chemical shrinkage of different cements depends largely on fineness, and the contents of the most reactive phases; C_3A, C_3S, alkalis and sulphates. The influence of mineral additives on chemical shrinkage was dependent of cement type; sometimes accelerating and sometimes equal to the reference.

The external chemical shrinkage levels also varied with cement type, as the effect of mineral additives varying from increasing the level to being the same relative to the reference. A higher level for pastes with fine mineral additives can be explained by pore refinement and menisci formed by initial contraction pores leading to stronger forces. Thus, more hydration is required to create stronger network to resist them.

6. REFERENCES

/1/ Sellevold E.J., Bjøntegaard, Ø., Justnes, H. and Dahl, P.A. "High Performance Concrete: Early Volume Change and Cracking Tendency" Proceedings of the International RILEM Symposium "Thermal Cracking in Concrete at Early Ages", Munich, October 10-12th, 1994, pp. 229-236, Editor R Springenschmid, Pub. E&FN Spon, London, UK, ISBN: 0 419 18710 3

/2/ Kompen, R. "High Performance Concrete: Field Observations of Cracking Tendency at Early Age" Proceedings of the International RILEM Symposium "Thermal Cracking in Concrete at Early Ages", Munich, October 10-12th, 1994, pp. 229-236, Editor R Springenschmid, Pub. E&FN Spon, London, UK, ISBN: 0 419 18710 3

/3/ Powers, T.C.: "Structure and Physical Properties of Hardened Portland Cement Paste", J. Am. Ceramic. Soc., Vol. 41, No. 1,1958, pp 1-6.

/4/ Knudsen, T. & Geiker, M.: "Chemical Shrinkage as an Indicator of the Stage of Hardening", Proceedings of the International RILEM Conference on Concrete of Early Ages, Vol. I, Session V: "Methods of Indicating the Stage of Hardening", Ecole National des Pouts et Chaussees, Paris, April 6-8,1982, pp 163-167.

/5/ Jensen, O.M.: "Autogen Deformation og RF-ændring - selvudtørring og selvudtørringssvind", Dr. Thesis TR 284193 (ISSN 0907-7073), The Technical University of Denmark, Department of Civil Engineering, Building Materials Laboratory, May 1993, 117 pp (in Danish).

/6/ Paulini, P.: "Reaction Mechanisms of Concrete Admixtures", Cement and Concrete Research, Vol. 20, 1990, pp. 910-918.

/7/ S. Jiang and H. Van Damme: "Influence of Fillers on Textural and Mechanical Properties of C3S Paste", in "Nuclear Magnetic Resonance Spectroscopy of Cement-based Materials" edited by P. Colombet, A.-R. Grimmer, H. Zanni and P. Sozzani, Springer Verlag, Berlin, 1998, pp. 379-385.

/8/ Y. Ohba, A. Nakamura, J.K. Lee, E. Sakai, M. Daimon: "Influence of $CaCO_3$ on the Hydration of Various Types of Calcium Aluminates with Anhydrite". Proceedings of 10th International Congress on the Chemistry of Cement, Gothenburg, Sweden, 2-6 June, 1997, paper 2ii022, 8 pp.

/9/ Justnes, H., Van Gemert, A., Verboven, A. and Sellevold, E.J.: "Total and External Chemical Shrinkage of Low W/C-ratio Cement Pastes", Advances in Cement Research, Vol. 8, No. 31, 1996, pp. 121-126.

/10/ Justnes, H., Van Gemert, A., Verboven, F., Sellevold, E.J., Van Gemert, D.: "Influence of Measuring Method on Bleeding and Chemical Shrinkage Values of Cement Pastes", Proceedings of 10th International Congress on the Chemistry of Cement, Gothenburg, Sweden, 2-6 June, 1997, paper 2ii069, 8 pp.

/11/ Justnes, H., B. Ardoullie, E. Hendrix, E.J. Sellevold, D. van Gemert: "The Chemical Shrinkage of Pozzolanic Reaction Products", Proceedings of the 6th International Conference on Fly Ash, Silica Fume, Slag and Natural Pozzolana in Concrete, Bangkok, Thailand, May 31-June 5,1998, ACI SP 179-11, pp. 191-205.

/12/ Sellevold, E.J., Bager, D.H., Klitgaard Jensen, E. and Knudsen, T. "Silica Fume Cement Pastes: Hydration and Pore Structure", Proceedings of the Nordic Research Seminar "Condensed Silica Fume in Concrete", 10th December 1981, Report BML 82.610, NTH, 1982-02-15, pp. 19

/13/ Justnes, H., Sellevold, E.J., Reyniers, B., Van Loo, D, Van Gemert, A., Verboven, F., Van Gemert, D.: "The Influence of Cement Characteristics on Chemical Shrinkage", Proceedings of the International Workshop on Autogeneous Shrinkage of Concrete, Hiroshima, Japan, June 13-14, 1998, pp. 67-76.

INFLUENCE OF MIX DESIGN ON SELF-DESICCATION IN CONCRETE

B. PERSSON
Div. Building Materials, Lund University, Box 118, 221 00 Lund, Sweden

Abstract

This article outlines an experimental and numerical study on the influence of the mix composition on self-desiccation of concrete. For this purpose 81 sealed cylinders made of 9 concretes with w/c varying between 0.32 and 0.50, based on two types of Portland Cement, were manufactured. Five per cent silica fume was used in one third of the concretes as calculated on the basis of the cement content. The measurement was done at 1 and 6 months' age. The results indicated high influence of w/c, age and cement type on self-desiccation. Silica fume in the concrete influenced the self-desiccation only when combined with low-alkali cement. The study was performed at Lund Institute of Technology 1997-1998.

Keywords: Alkali-effect, Compressive strength, High Performance Concrete, Internal relative humidity, Self-desiccation, Silica fume.

1 Background, aim and general scheme of the study

1.1 Background

The chemical shrinkage that takes place during hydration of water to cement is the fundamental cause of self-desiccation [1]. The specific volume of the hydrated water in the gel of concrete is reduced by about 26% compared with the specific volume of water in the capillary pores [2]. Especially at low w/c < 0.38 the influence of self-desiccation becomes more pronounced due to the decreased size of the capillary pores [3]. Self-desiccation influences the properties of the young concrete as well as the long-term behaviour of the concrete, i.e. deformations, stability and durability. Due to self-desiccation concrete with low w/c deforms even with sealed curing, free of imposed stresses (autogenous shrinkage) [4,5]. Furthermore low-w/c concrete with silica fume exhibits a very low long-term increase of the compressive strength due to self-desiccation, which may influence the long-term stability and durability [6]. Favourable parameters related to self-desiccation are low internal relative humidity close to the reinforcement bars, which may decrease the rate of corrosion [7]. Frost resistance and scaling of materials and structures is clearly improved due to self-desiccation since an air-filled volume is created due to the chemical shrinkage, as mentioned above [8-10]. A

low amount of built-in moisture during construction time is another favourable property of low-w/c concretes caused by self-desiccation [11-13].

1.2 Aim of the study

The main aim of the study was to ascertain the influence of cement type, w/c, silica fume and age on the measurement of internal relative humidity, RH, due to self-desiccation in concretes with w/c varying between 0.32 and 0.50. The influence of age on the RH at self-desiccation properties was secured by studying concrete at 1 and 6 months' age. The influence of cement type was ascertained by studies on low- and normal-alkali cement. Half of the number of specimens was made with normal-alkali cement blended with 5% silica fume as calculated on the basis of the cement content. Another aim was to observe the influence of cement type, silica fume and temperature on the compressive strength of concrete with sealed curing.

1.3 General scheme of the work

Nine different types of concrete were examined. After sealed curing the concrete strength was tested at 1 month's age. RH was measured on fragments of crushed concrete at 18, 20.5 and 23 "C temperature at 1 and 6 months' age. The density of the concrete was studied in the fresh state and after sealed curing for 28 days.

2 Material, specimens, experimental method and inaccuracy

2.1 Materials and studied concretes

Low-alkali and normal-alkali cement was used. Table 1 gives the chemical composition of the cements [14]. Properties of the aggregate are given in Table 2 [15]. Nine types of concrete were studied, 9 cylinders of each quality, in all 81 cylinders. The w/c varied between 0.32 and 0.50. The mixed design of the concrete was based on theoretical optimisation of the grading curve in the fresh concrete [16]. First of all the dry material was mixed for ½ minute. Then the water with air-entrainment was added and mixed for another ½ minute. Finally the plasticisers were added and mixed for 3 minutes. The concretes had good rheological properties. Workability, density and air-content of the concretes were studied in the fresh state. The slump of the concretes varied between 80 and 180 mm. In the fresh state it was possible to mix, transport and cast HPC with existing methods. The 28-day 100-mm cylinder compressive strength exceeded 20 MPa (comparable with 25 MPa 150-mm cube strength). Table 3 shows the mix design of the concretes and the main properties in the fresh and the cured state.

2.2. Specimens and curing conditions

Density, compressive strength and self-desiccation after sealed curing of the concretes were studied for cylinders 200 mm long and 100 mm in diameter. The mixing of the material took place at 22 "C. Directly after mixing, one third of the moulds with concrete were stored at constant temperatures in a climate chamber, one third at 18.5 "C, one third at 20.5 "C and one third at 23 "C. After demoulding at one day's age the specimens were immediately sealed from moisture by insulation with 3 mm plastic tubes and replaced in the climate chamber where the initial curing took place. The weight of the cylinders was established before and after the 28-day studies.

Table 1. Composition of the cements [14]

Component/Cement type	Low-alkali cement (%)	Normal-alkali cement (%)
CaO	65	62
SiO_2	21.6	20
	3.5	4.4
	4.4	2.3
MgO	0.78	3.5
K_2O	0.58	1.4
Na_2O	0.05	0.2
SO_3	2.07	3.7
CO_2	0.14	1.9
Ignition losses	0.47	2.4
C_2S	21	14
C_3S	57	57
C_3A	1.7	8
C_4AF	13	7
Blaine fineness	305 m^2/kg_3	364 m^2/kg,
Density	3210 kg/m^3	3120 kg/m

Table 2. Properties of aggregate and silica fume [15]

Type of aggregate/property	Elastic modulus	Compressive strength	Split tensile strength	Ignition losses
Quartzite sandstone	60 GPa	332 MPa	15 MPa	0.3%
Natural sand				0.8%
Silica fume (fineness: 17.5 m^2/g)				2.3%

2.3 Experimental methods

The cylinder with the plastic pipe was weighed. Then all concrete cylinders were weighed and measured separately. The plastic pipe was weighed separately in order to detect any increase in weight due to moisture uptake. The cylinder was placed centric in a hydraulic press device and the loading applied at 1 MPa/s. Fragments (minimum 5 mm in size) from the concrete used in the compressive testing were filled in glass tubes 200 mm long and 22 mm in diameter. The temperature of the fragments was adjusted to the measurement for 1 day. The internal relative humidity, RH, was measured by a dew-point meter for 22 h. The probe of the dew-point meter was entered into the glass tube and tightened against the glass with an expanding rubber ring.

2.4 Sources of inaccuracy

The following sources of error were observed during the study:

1. Variations in w/c of the concrete due to the moisture content in the sand and the gravel.
2. Moisture losses during the handling and curing of the cylinders.
3. Calibration faults regarding the hydraulic press device and the dew-point meters.

Table 3. Mix design (kg/m^3 dry material) and properties of the studied concretes [16]

Material/Concrete	32L	32N	32NS	38L	38N	38NS	50L	50N	50NS
Quartzitesandstone12-16	669	686	725	532	535	549	407	417	434
Quartzite sandstone 8-12	137	141	149	258	259	266	320	329	343
Natural sand 0-8 mm	704	722	763	747	750	771	830	852	887
Natural sand 0 mm (filler)	107	110	93	43	43	44	32	33	34
Cement (Appendix 1)	395	405	428	343	345	354	274	281	293
Granulated silica fume, s	-	-	21	-		18	-	-	15
Air-entrainment (fir oil, g)	43	44	50	34	35	35	26	26	27
Superplasticiser(melamine)	3.4	3.5	3.6	1.7	1.7	1.8	0.9	0.9	1.0
Water-reducing agent	1.7	1.8	1.9	0.9	0.9	0.9	1.0	1.1	1.1
Total water incl. moisture	127	131	137	131	131	135	136	138	144
Water-cement ratio, w/c	0.32	0.32	0.32	0.38	0.38	0.38	0.50	0.50	0.50
Air content (% by volume)	12.5	10.5	6.0	13.0	13.0	10.5	15.5	13.5	11.0
Aggregate content	0.75	0.75	0.75	0.76	0.76	0.76	0.80	0.80	0.80
Aggregate to cement ratio	4.2	4.2	4.2	4.6	4.6	4.6	5.8	5.8	5.8
Slump (mm)	90	100	80	140	170	150	200	180	180
Density-freshstate(kg/rn^3)	2145	2200	2330	2090	2100	2175	2000	2050	2150
28-day cylinder density[1)]:	2280	2330	2370	2280	2260	2290	2060	2150	2200
curing at 18 °C (kg/m^3) [2)]	2290	2330	2350	2300	2260	2280	2040	2150	2210
curing at 20.5 "C (kg/m^3) [2)]	2290	2320	2390	2290	2270	2310	2100	2180	2190
curingat23 °C (kg/m^3) [2)]	2270	2340	2380	2260	2250	2290	2040	2130	2210
Air-content loss, AA (%)[3)]	6.5	6.0	2	9.0	7.5	5.5	3.0	5.0	2.5
Air-content - cured (%)[4)]	7.5	6.0	5.5	5.5	7.0	6.5	14.0	10.0	10.0
28-day cylinder strength[1)]:	47	51	71	51	38	51	20	27	33
curing at 18 °C (MPa) [2)]	47.0	53.0	72.0	56.5	41.0	54.5	20.5	26.5	32.5
curing at 20.5 °C (MPa) [2)]	49.5	51.0	74.0	52.0	39.5	52.0	21.9	30.0	33.0
curing at 23 "C (MPa) [2)]	45.0	48.0	67.0	44.0	34.5	46.0	18.5	24.0	33.0
Strength decline (MPa/°C)	0.5	1	1.1	2.5	1.3	1.7	0.5	0.6	0

[1)] average of 9 cylinders, [2)] average of 3 cylinders, [3)] $100\cdot[(\rho_{28d}/\rho_{fresh})-1]$ %, [4)] A_{fresh}-$\Delta A+1.5\%$, L = low-alkali cement, N = normal-alkali cement, NS = normal-alkali cement and 5% silica fume, 32 = w/c (%)

3 One-month self-desiccation and strength

3.1 Density and compressive strength

Table *3* provides the density and compressive strength after curing for 28 days. The fall in air-content was estimated from the difference in density between the fresh and the cured state of the concrete. The losses of air content in the concrete were quite large, Table 3. However, the high amount of air-entrainment was required in order to maintain good workability at the low w/c (low mixing water content) shown in Table 3. Otherwise much larger cement content would have been required. The air-entrainment replaced a good part of the water during the casting. The compressive strength decreased slightly with a moderate increase of the curing temperature, especially at w/c= 0.38, i.e. between 0.5 and 2.5 MPa/°C. Figure 1 shows the air content in the concretes in the fresh state and after curing and the estimated losses of air content.

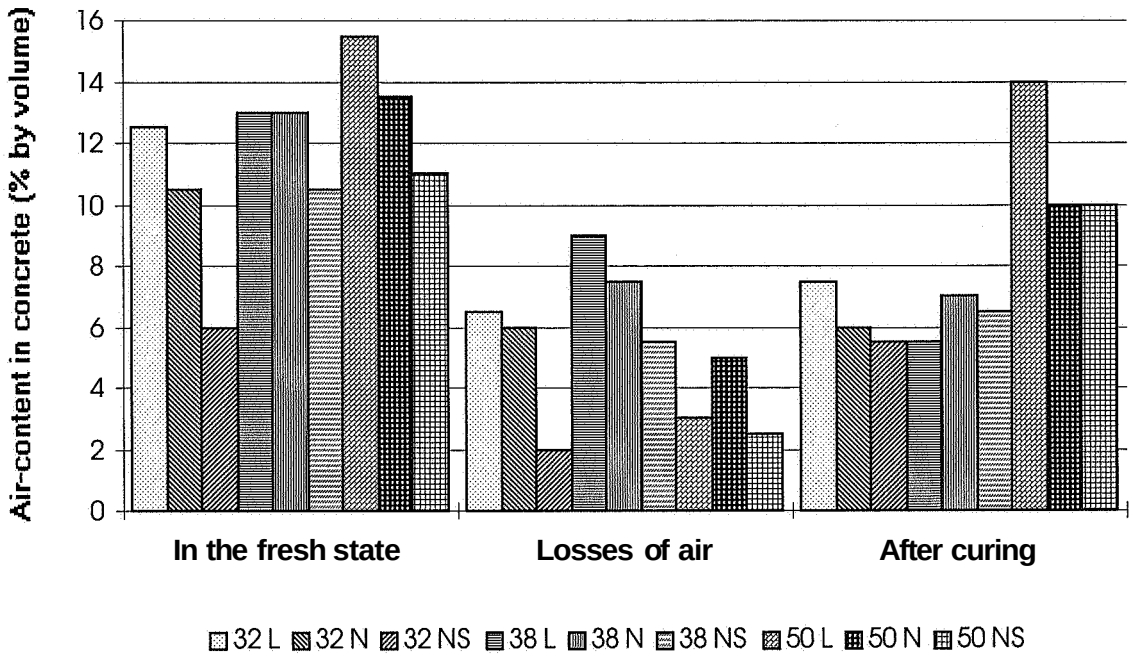

Fig. 1. Air content in the concretes in the fresh state and after curing. Estimated losses of air content. L= low-alkali, N = normal-alkali, S = 5% silica fume, 32= w/c (%).

Figure 2 gives the strength versus w/c and type of the concretes. Besides an increase with lower w/c, a substantial increase of strength was observed for silica fume concretes. At early ages the efficiency factor of silica fume is quite large, perhaps as high as 7 at 28 days' age, but then decreasing. After 7 years no influence of silica fume on the strength was observed [17].

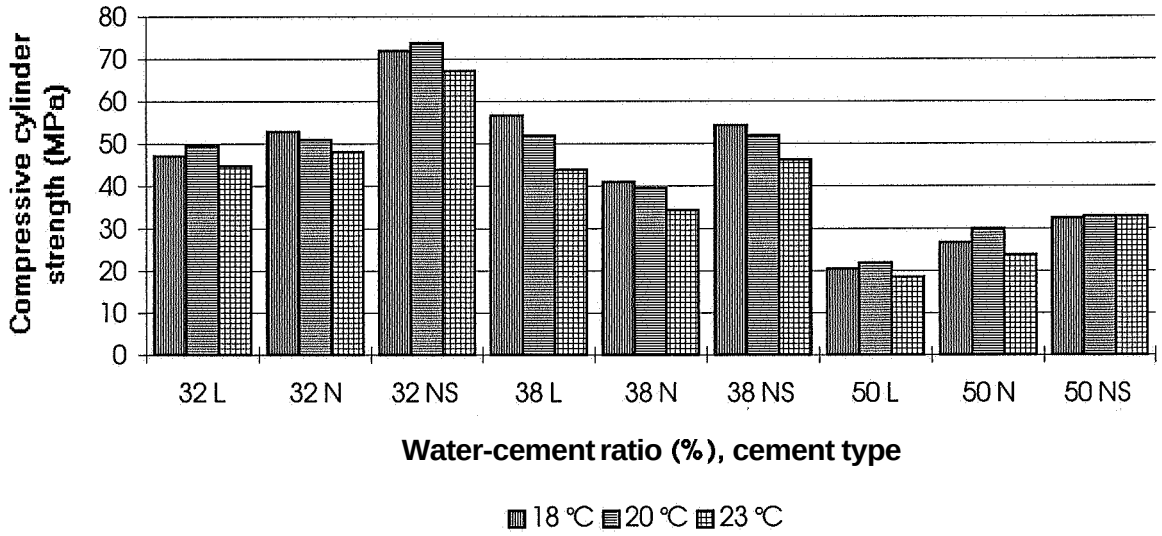

Figure 2. Strength versus w/c and type of the concretes. L= low-alkali cement, N = normal-alkali cement, NS = N+ 5% silica fume, 32= w/c (%).

3.2 Internal Relative Humidity, RH, in concrete dependent on the curing temperature

Figures 3-5 show the difference in RH between curing at 20.5 "C and 23 "C compared with 18.5 "C (ASTM-calibration [18]). Figure 6 shows that small average influence of curing at 20.5 "C was observed. At 23 "C RH was on average 0.5% lower than RH with curing at 18.5 "C, i.e. the influence of a moderate temperature change on RH was small (hardly detectable). Table 4 gives the standard deviation and the average difference in RH of the measurements. The maximum standard deviation was 1.6% (curing at 18.5 "C) and the maximum average standard deviation 0.7% (independent of curing temperature and measured at 20.5 "C).

Table 4. RH-difference dependent on curing temperature (%, ASTM-calibration [18])

Curing at	18.5 °C		20.5 °C		23 °C		18-23 °C	
Measurement at	20.5 °C	23 °C	20.5 °C	23 °C	20.5 °C	23 °C	20.5 °C	23 °C
Average	1.1	-0.6	-0.6	-1	0.1	0.1	0.2	-0.5
Standard deviation	1.6	1.6	1.2	1.4	1.1	1.2	0.7	0.6

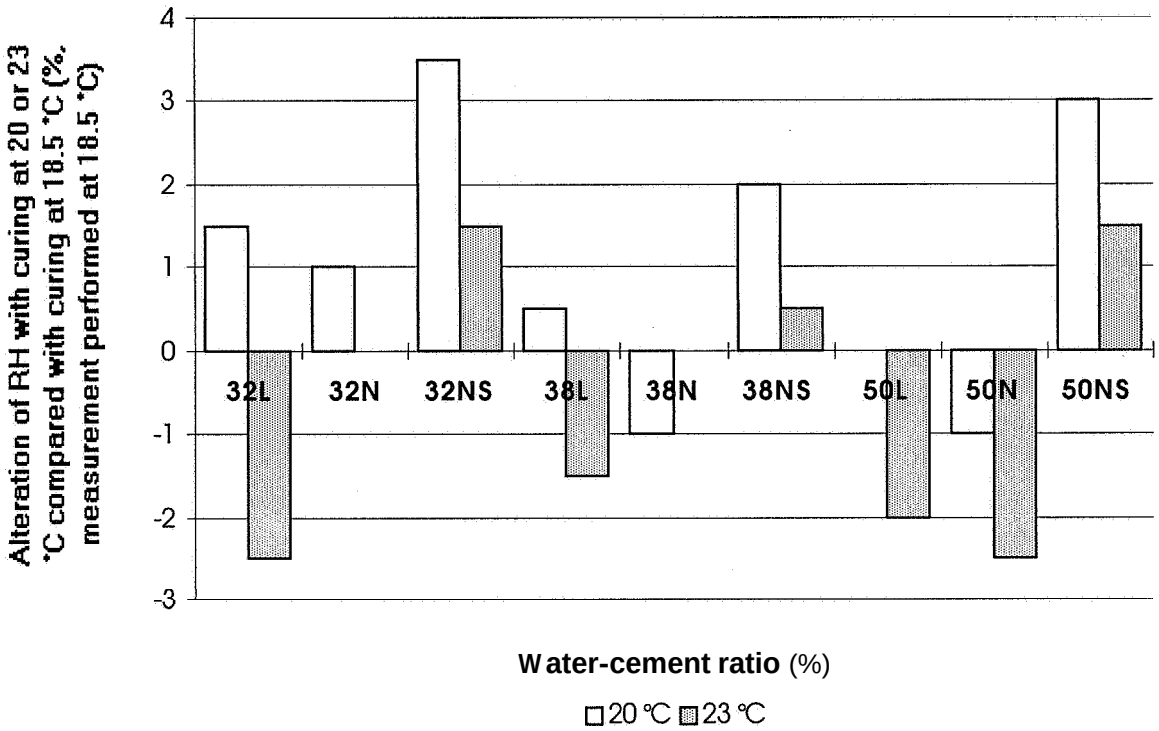

Fig. 3. Alteration of RH with curing at 20.5 "C and 23 "C compared with curing at 18.5 "C (measurement performed at 18.5 "C). L= low-alkali, N = normal-alkali, S = 5% silica fume, 32= w/c (%).

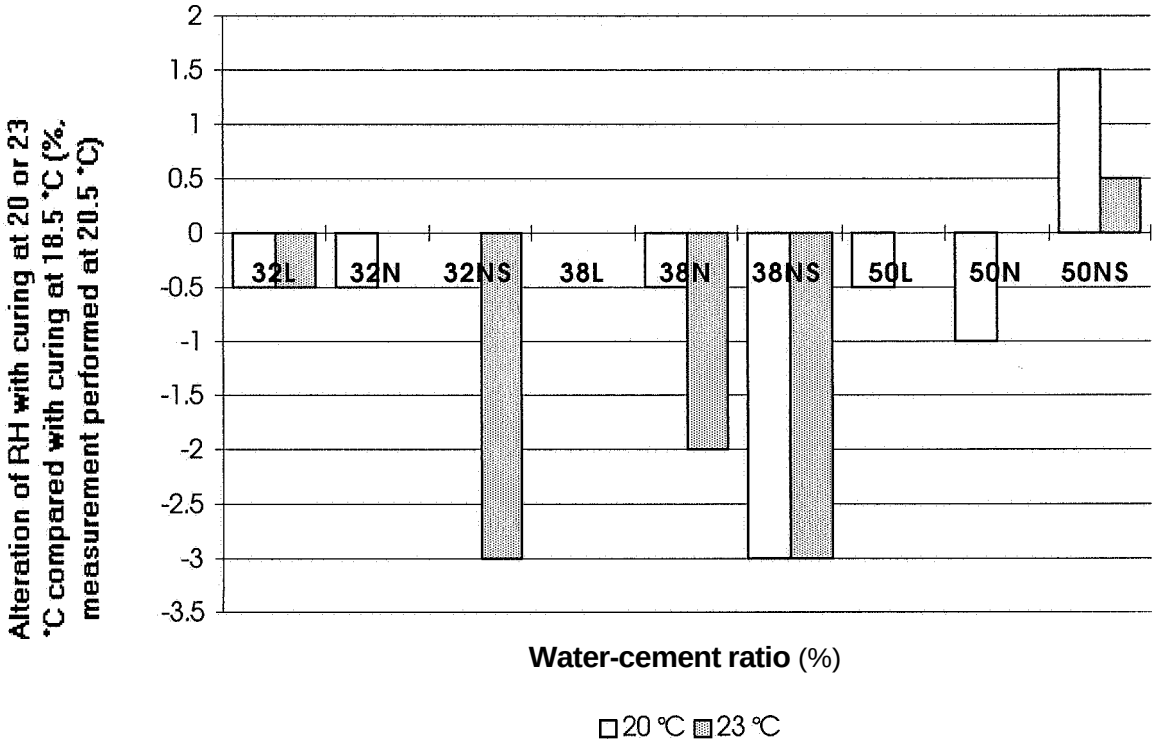

Fig. 4. Alteration of RH with curing at 20.5 "C and 23 "C compared with curing at 18.5 "C (measurement performed at 20.5 "C). L= low-alkali, N = normal-alkali, S = 5% silica fume, 32= w/c (%).

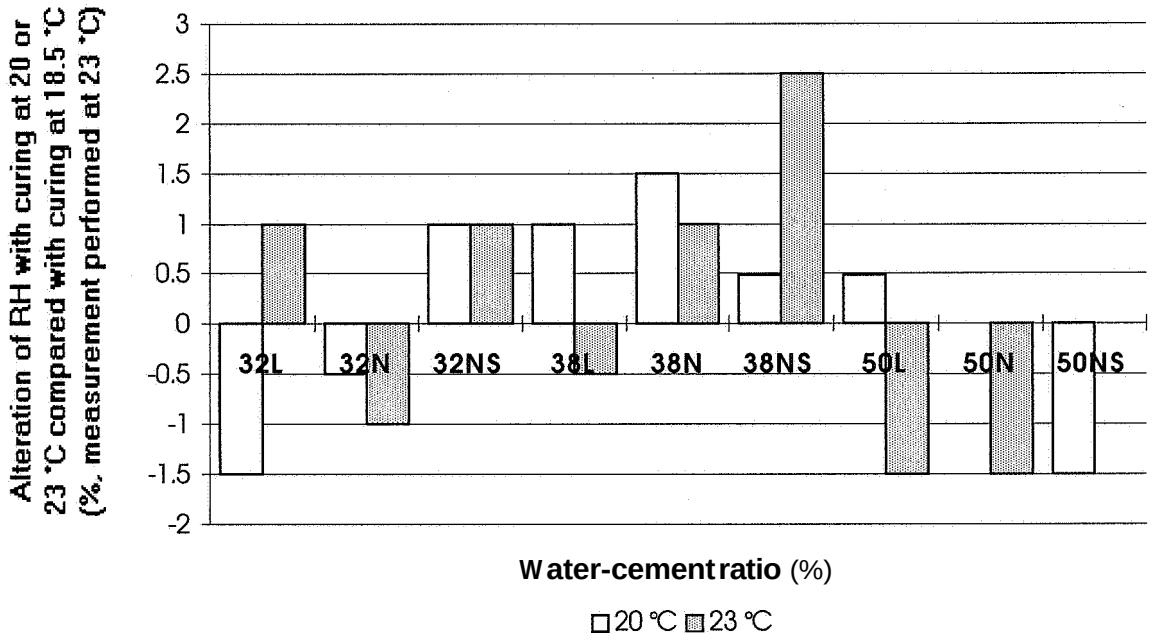

Fig. 5. Alteration of RH with curing at 20.5 "C and 23 "C compared with curing at 18.5 "C (measurement performed at 23 "C). L= low-alkali, N = normal-alkali, S = 5% silica fume, 32= w/c (%).

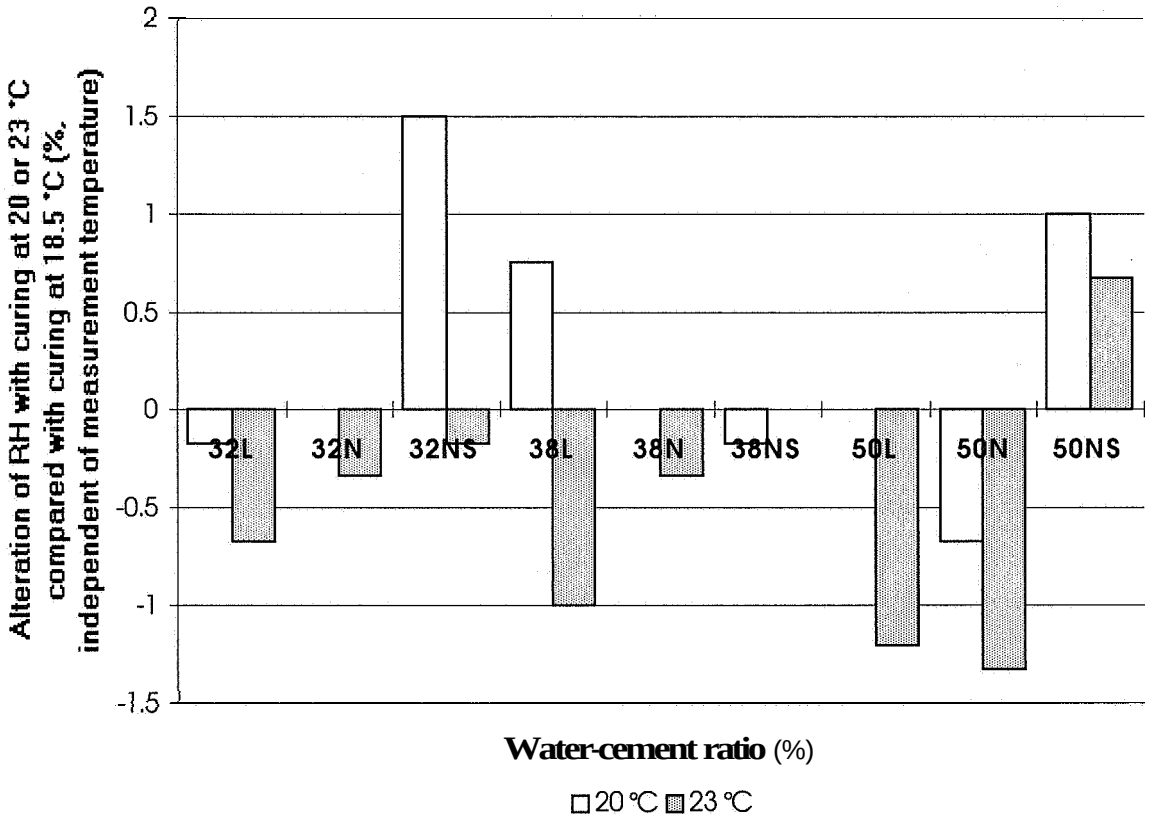

Fig. 6. Alteration of RH with curing at 20.5 "C and 23 "C compared with curing at 18.5 "C (independent of temperature of measurement).

3.3 Influence of temperature on self-desiccation

Figures 7-9 show the difference in RH between measurement at 20.5 "C and 23 "C compared with 18.5 "C. Figure 10 shows that the observed average influence of measurement at 20.5 "C was –0.1% RH. At 23 "C RH was on average -0.6% lower than when it was performed at 18.5 "C. The influence of moderate temperature change at measurement on RH was thus hardly detectable. Table 2 gives the standard deviation and the average difference in RH. The maximum standard deviation was 2.2% (curing at 23 "C) and the maximum average standard deviation 1.5% (independent of measurement temperature of the concrete cured at 23 "C).

Table 5. Difference in RH dependent on measurement temperature (%, ASTM [18])

Measurement at	18.5 "C		20.5 "C		23 "C		18-23 "C	
Curing at	20.5 "C	23 "C	20.5 "C	23 °C	20.5 "C	23 "C	20.5 "C	23 "C
Average	0.6	-1.3	-0.9	-0.3	.04	-0.2	-0.1	-0.6
Standard deviation	1.6	1.8	2	2.2	1.2	1.1	1	1.5

3.4 Influence of cement type and silica fume on self-desiccation

Figure 11 shows the influence of cement type and silica fume on RH compared with RH in concrete based on low-alkali cement when w/c was held constant, i.e. Figure 11 shows the decline of RH. Part of the decline in RH due to the cement type (which varied

between 4 and 8% at 28 days' age) was dependent on the so-called alkali-effect [19]. However, when silica fume was added to the concrete the pozzolanic reaction slightly reduced the alkali-effect. Perhaps variations in RH versus w/c were due to the available amount of pore solution for the probe to react properly.

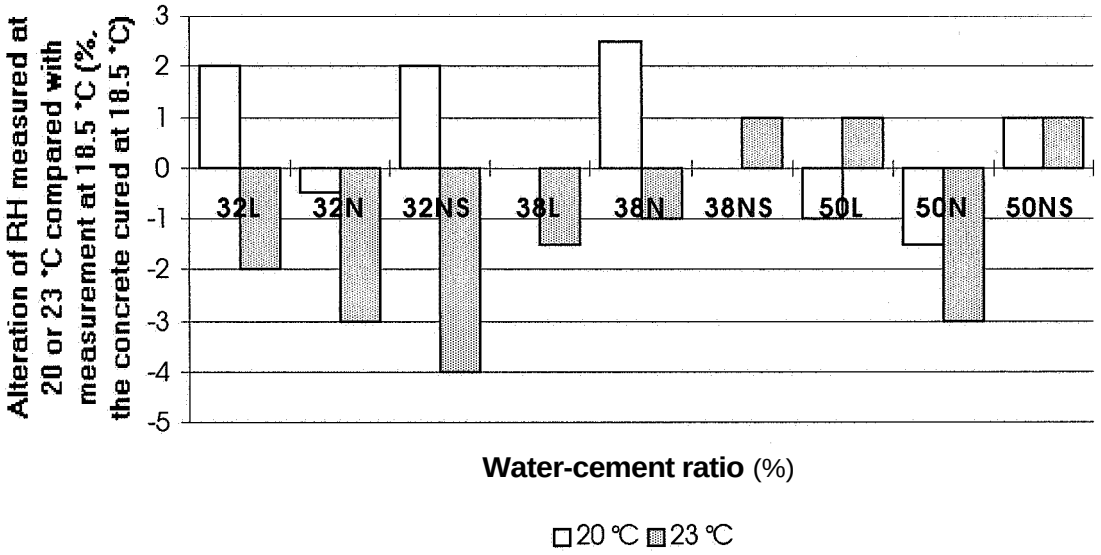

Fig. 7. Alteration of RH with measurement at 20.5 "C and 23 "C compared with measurement at 18.5 "C (curing at 18.5 "C). L= low-alkali, N = normal-alkali, S = 5% silica fume, 32= w/c (%).

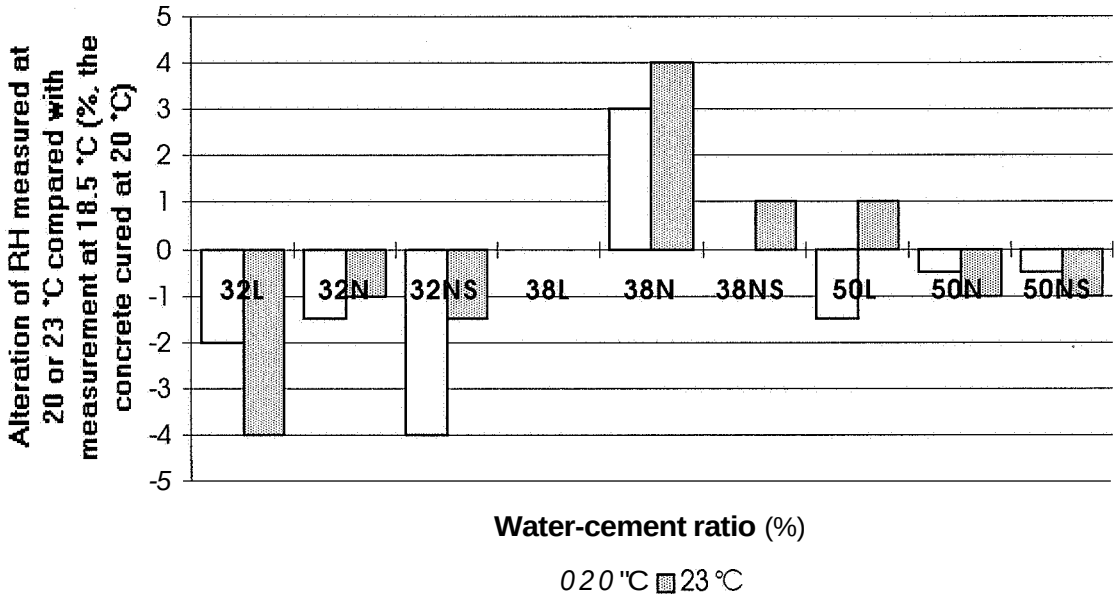

Fig. 8. Alteration of RH with measurement at 20.5 "C and 23 "C compared with measurement at 18.5 "C (curing at 20.5 "C). L= low-alkali, N = normal-alkali, S = 5% silica fume, 32= w/c (%).

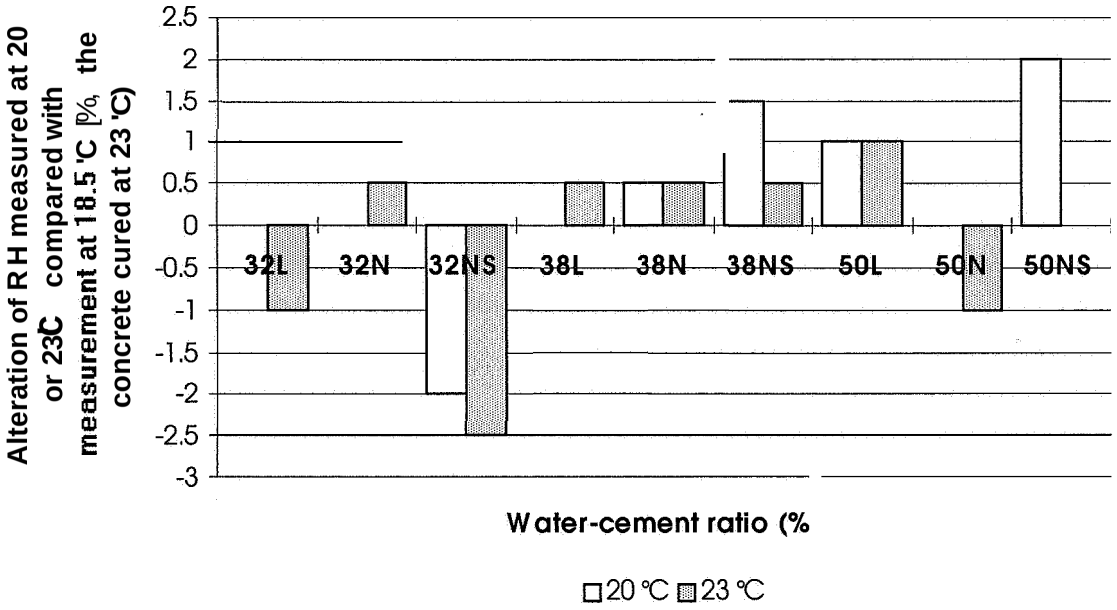

Fig. 9. Alteration of RH with measurement at 20.5 °C and 23 °C compared with measurement at 18.5 °C (curing performed at 23 °C). L= low-alkali, N = normal-alkali, S = 5% silica fume, 32= w/c (%).

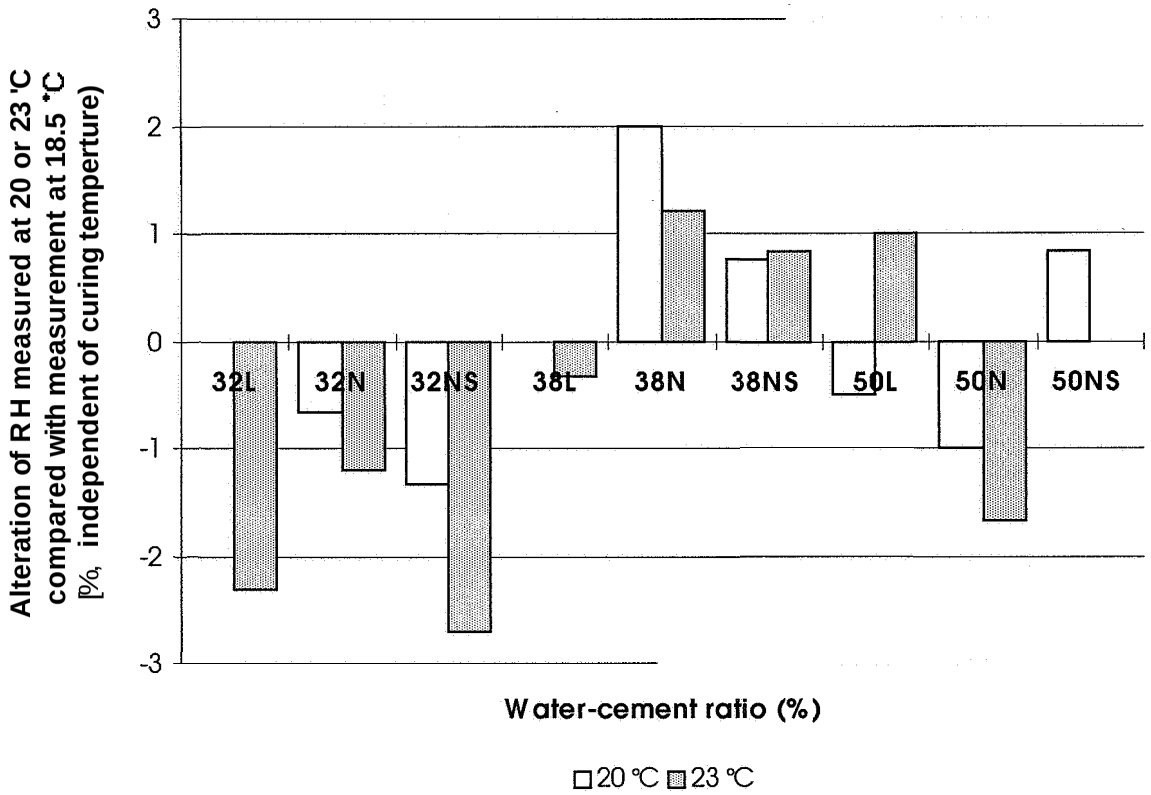

Fig. 10. Alteration of RH with measurement at 20.5 °C and 23 °C compared with measurement at 18.5 °C (independent of temperature of curing). L= low-alkali, N = normal-alkali, S = 5% silica fume, 32= w/c (%).

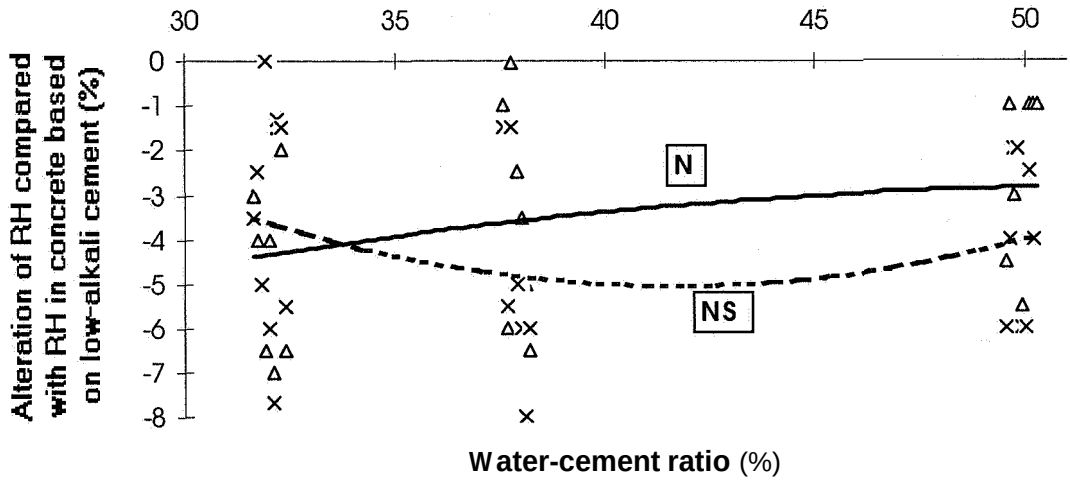

a N = Normal-alkali cement × NS = Normal-alkali cement + 5% silica fume

Fig. 11. Influence of cement type and silica fume on RH versus w/c compared with RH in concrete based on low-alkali cement.

35 Influence of cement type and silica fume on RH when it was held constant

Figure 12 shows the influence of cement type and silica fume on RH compared with RH in concrete based on low-alkali cement when RH was held constant, i.e. Figure 12 shows the decline of RH. The influence of cement type and silica fume on RH varied between -2 and -9%.

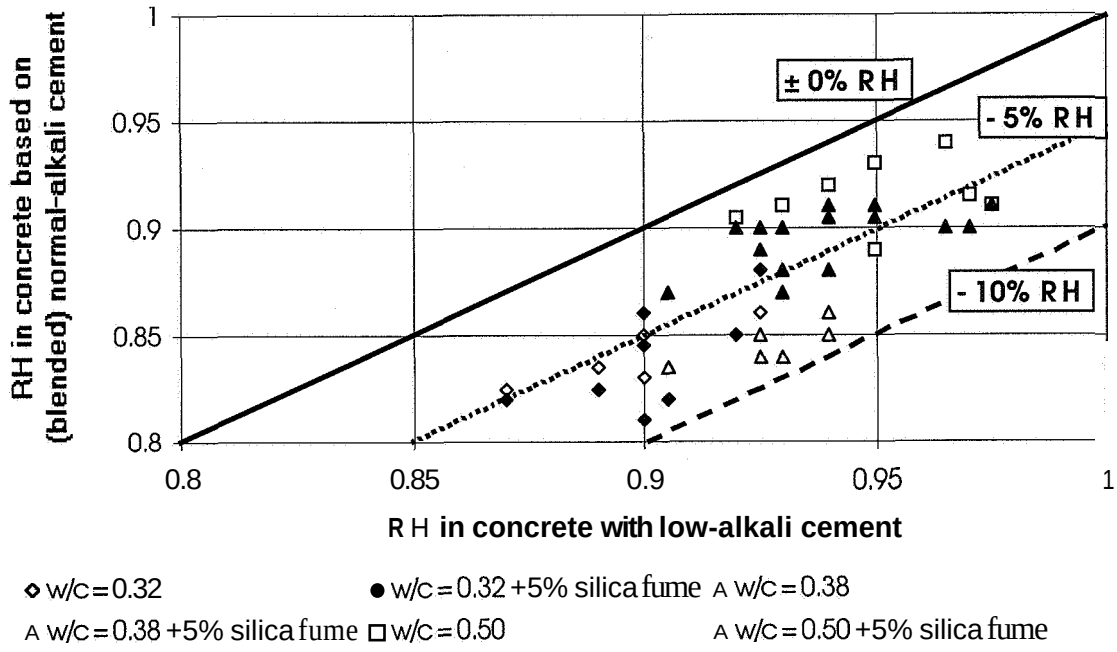

Fig. 12. Influence of cement type and silica fume on RH versus RH compared with RH in concrete based on low-alkali cement.

4 Correctness

4.1 The w/c-variations in concrete due to the moisture content in the sand

The sand was planned to have a moisture content varying between 3% and 4%. This variation in the moisture content would have produced concrete with ± 0.01 in variation of w/c. However, recalculations of w/c on the basis of the measured moisture content in the sand of each batch of concrete showed larger variation of the moisture content. The moisture varied between 3% and 4.8%, which produced a concrete with −0.01, +0.025 in variation of w/c.

4.2 Effect of handling and curing of the cylinders on moisture losses at curing

The specimens were cast in steel moulds and then, after demoulding, quickly placed in the 3-mm thick plastic pipe. Moisture-proof plugs tightened the ends of the pipe. Figure 13 shows the moisture losses through different kinds of moisture insulation:

1. Butyl rubber clothing
2. Aluminium foil
3. 3-mm plastic pipe

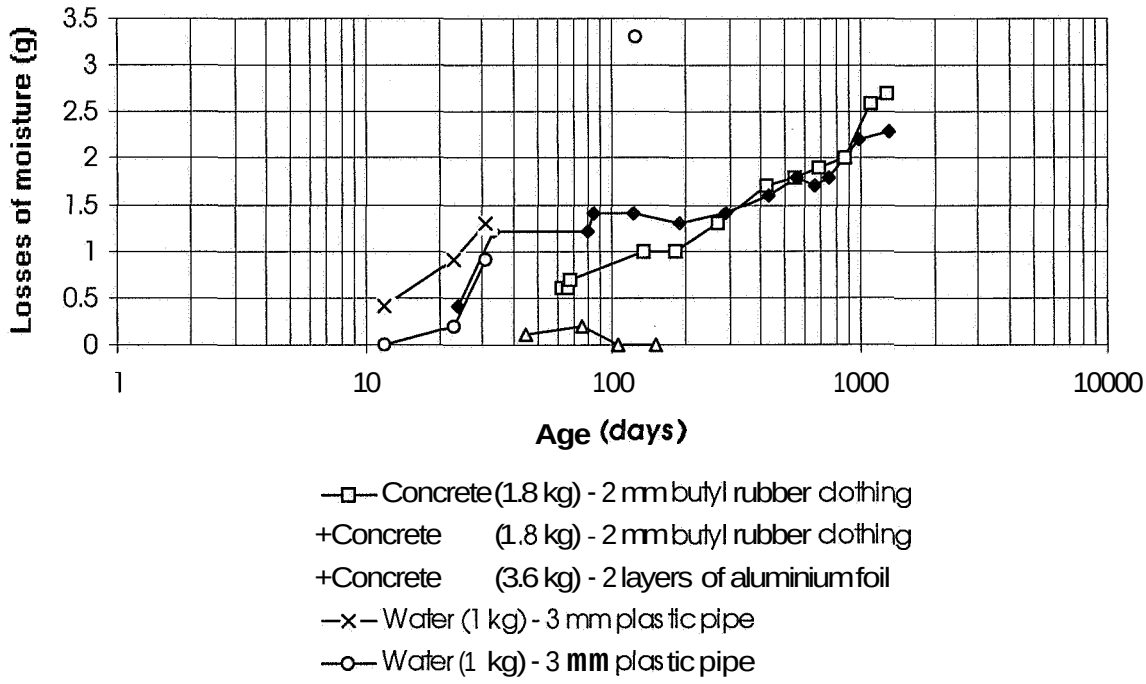

Fig. 13. Moisture losses through different kinds of moisture insulation: butyl rubber clothing, aluminium foil or 3-mm plastic pipe.

Aluminium foil showed no loss of moisture at all but required a certain time for application. The moisture losses during the time of application were much larger than the losses observed with rubber clothing or plastic pipes. Table 6 shows the measured net moisture losses from the specimens during the 28-day curing time. Moisture uptake (+) was observed in some cases, probably due to measurement faults or/and adsorption of moisture in the plastic pipe.

Table 6. Measured moisture losses from specimens during the 28-day curing time (%).

Concrete	32L	32N	32NS	38L	38N	38NS	50L	50N	50NS
18 "C	-0.05	-0.03	-0.05	-0.03	-0.08	-0.04	-0.09	+0.06	+0.07
20.5 °C	-0.08	+0.03	-0.06	-0.03	+0.01	-0.04	-0.10	-0.04	-0.04
23 "C	-0.03	-0.05	-0.03	-0.10	-0.01	-0.06	-0.12	-0.05	+0.05

Notations: L= low-alkali, N = normal-alkali, S = 5% silica fume, 32= w/c (%).

As observed in Table 6, the moisture losses were small, hardly detectable, and may not have affected RH in the specimens. (Compared with the cement content in the concrete, c, the observed moisture losses, w_e, were less than $w_e/c < 0.006$ kg/kg.)

4.3 Calibration of the hydraulic press device and the dew-point meters

The hydraulic press device was calibrated 1 year before the measurement of strength was performed. The calibration showed index +13 kN, i.e. the strength given in Figure 2 is generally to be increased by 2 MPa. It was essential to set the time of measurement of the dew-point meters sufficiently long. It was found that 14 h was required to obtain stability of moisture between the pores in the concrete and the probe of the dew-point meter [3]. The time of measurement thus was set at 22 h. It was also essential to limit the number of measurements to two on the same sample. Otherwise systematic faults may occur [20].

The results in Figure 10 show that a negative temperature dependence existed (about 0.6% lower RH at 5 "C higher temperature), which was in contrast to other results [21-22]. Before the measurement of RH in the concretes took place a standard calibration with a humidity generator was performed at 20 "C. Calibration of the dew-point meters was performed afterwards according to the saturated salt method ASTM E 104-85 [18]. RH produced by the saturated salt was adjusted to the current temperature of measurement according to Table 7.

Table 7. RH in saturated salts.

Type of salt	18.5 "C	20.5 "C	23 "C
NaCl	75.53	75.46	75.37
KCl	85.35	85.03	84.65
KNO_3	94.89	94.53	94.03
K_2SO_4	97.69	97.57	97.42

During calibration of the salts the solution was placed in a glass tube insulated from variations in the ambient temperature with heat insulation. The solution of the salt was separated from the RH-probe by a partial permeable membrane. The temperature of the salt was stabilised at the specific temperature for 3 days before the calibration took place. The calibration was performed for 22 h.

Figure 14 shows that the two calibration methods coincided reasonably well at 18.5 "C. However, at 20.5 °C and 23 "C a difference of about 2% RH existed. Calibration with [18] showed about 2% higher RH than calibration with the humidity generator, Figures 15 and 16. It was concluded that relevant RH-analyses can be performed after salt-calibration only [18].

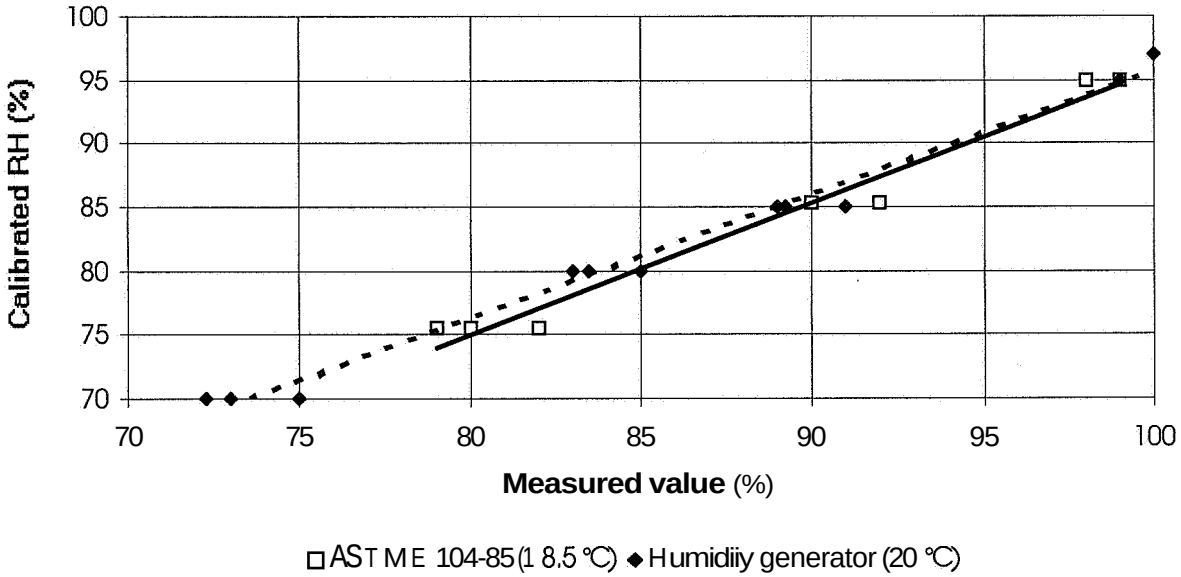

Fig. 14. RH calibrated according to ASTM E 104-85 (18.5 "C), [18], and according to humidity generator (20 "C).

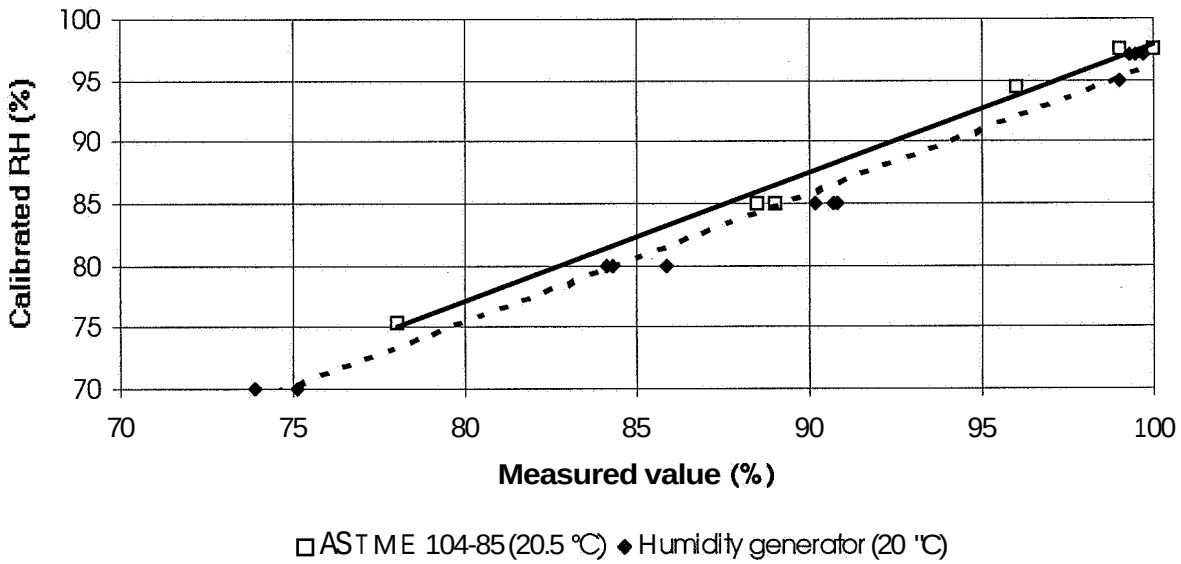

Fig. 15. RH calibrated according to ASTM E 104-85 (20.5 "C), [18], and according to humidity generator (20 "C).

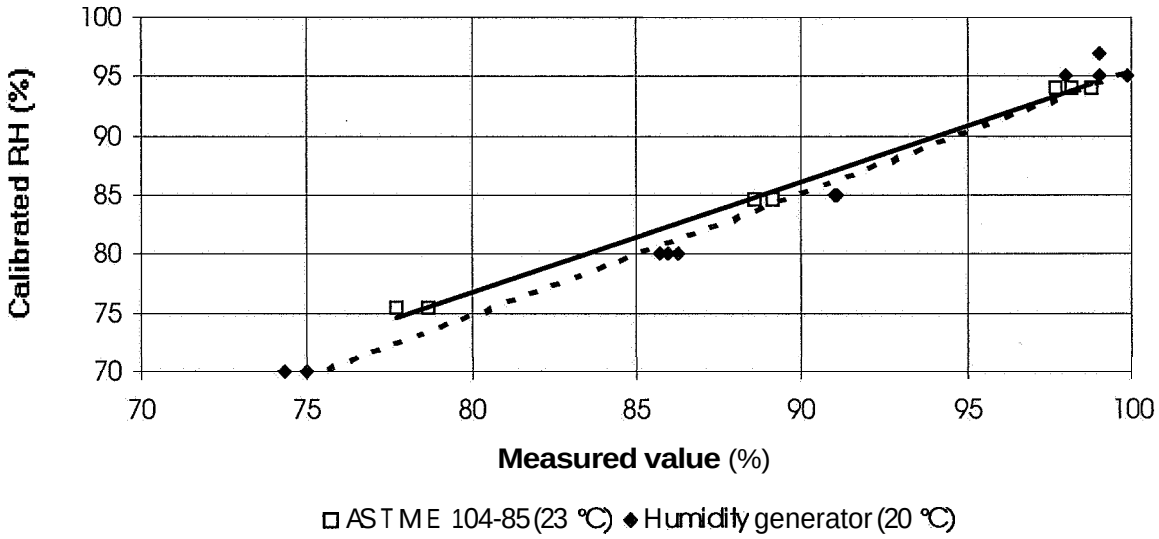

Figure 16. RH calibrated according to ASTM E 104-85 (23 "C), [18], and according to humidity generator (20 "C).

5 Self-desiccationat 6 months' age

5.1 Influence of cement type and silica fume on self-desiccation when w/c was held constant

Figure 17 shows the influence of cement type and silica fume on RH compared with RH in concrete based on low-alkali cement when w/c was held constant, i.e. Figure 17 shows the decline of RH. Part of the decline in RH due to the cement type (which varied between 4 and 8% at 28 days' age) was dependent on the so-called alkali-effect [19]. However, when silica fume was added to the concrete the pozzolanic reaction slightly reduced the alkali-effect. Perhaps variations in RH versus w/c were due to the available amount of pore solution for the probe to react properly.

5.2 Influence of cement type and silica fume on self-desiccation when RH was held constant

Figure 18 shows the influence of cement type and silica fume on RH compared with RH in concrete based on low-alkali cement when RH was held constant, i.e. Figure 18 shows the decline of RH. The influence of cement type and silica fume on RH varied between -2 and -9%.

6 Analyses on self-desiccation

6.1 Influence of age, w/c, cement type and/or silica fume on RH (Q))

Figures 19-22 give data on RH (Ø) versus w/c and $(w/c)_{eff} = w/(c+2\cdot s)$ for the studied concretes (1 and 6 months' age). From Figures 19 and 20 the following equation was calculated:

$$Ø = [A\cdot\ln(t) + B]\cdot(w/c) + C\cdot\ln(t) + D \quad (1)$$

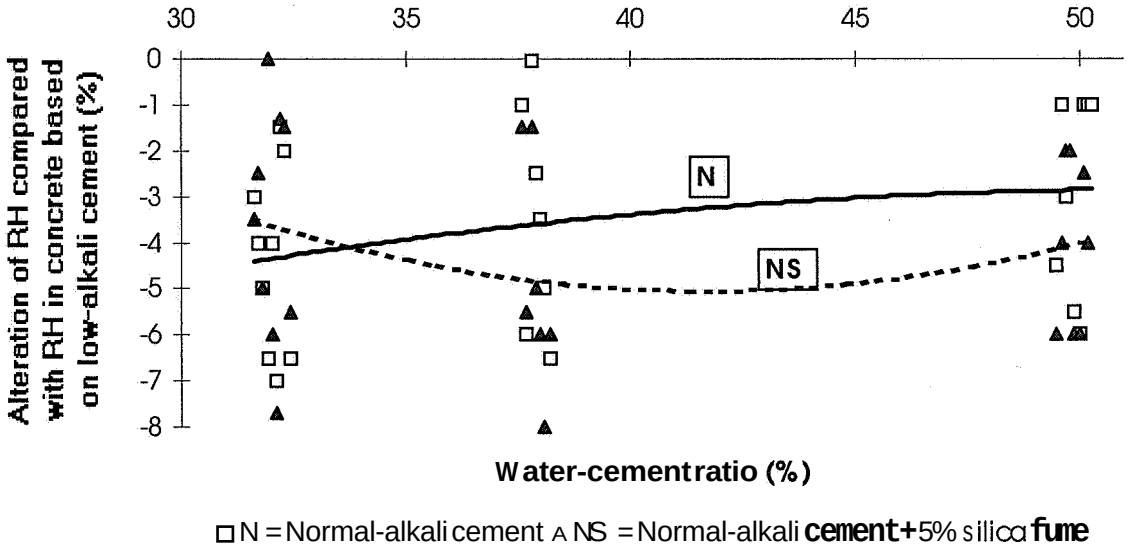

Fig. 17. Influence of cement type and silica fume on RH versus w/c compared with RH in concrete based on low-alkali cement.

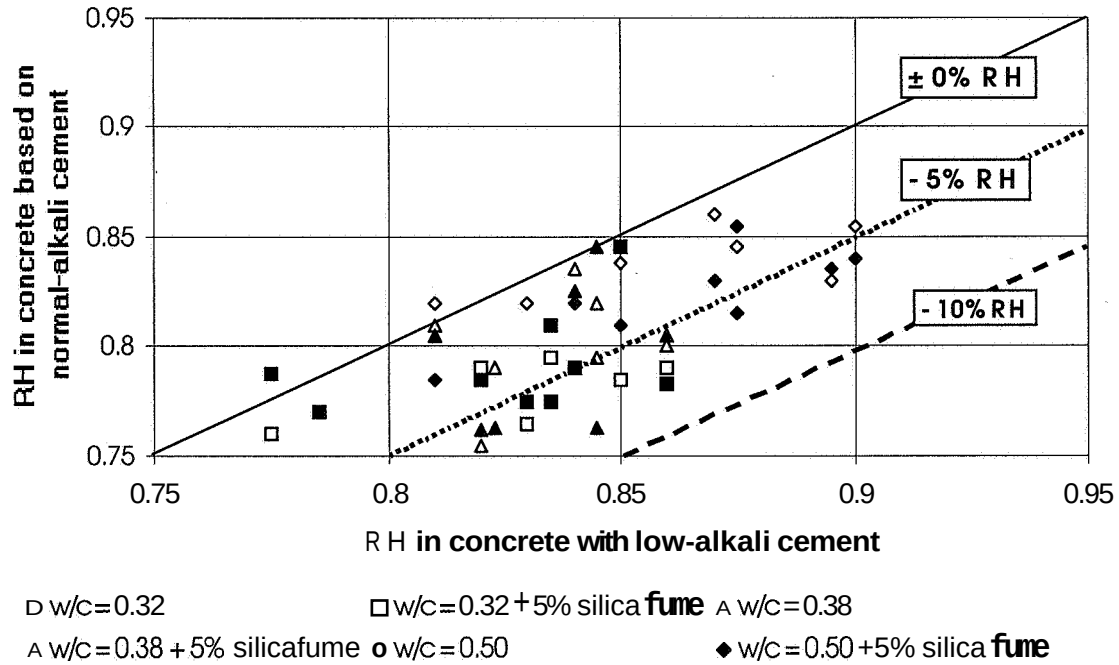

Fig. 18. Influence of cement type and silica fume on RH versus RH compared with RH in concrete based on low-alkali cement. Six months' age.

ln(t)	denotes the natural logarithm of the concrete age, t, in months
A, B, C, D	denotes constants given in Table 8
	denotes an accuracy parameter given below
Y_i	denotes the measured value
Y_m	denotes the average measured value

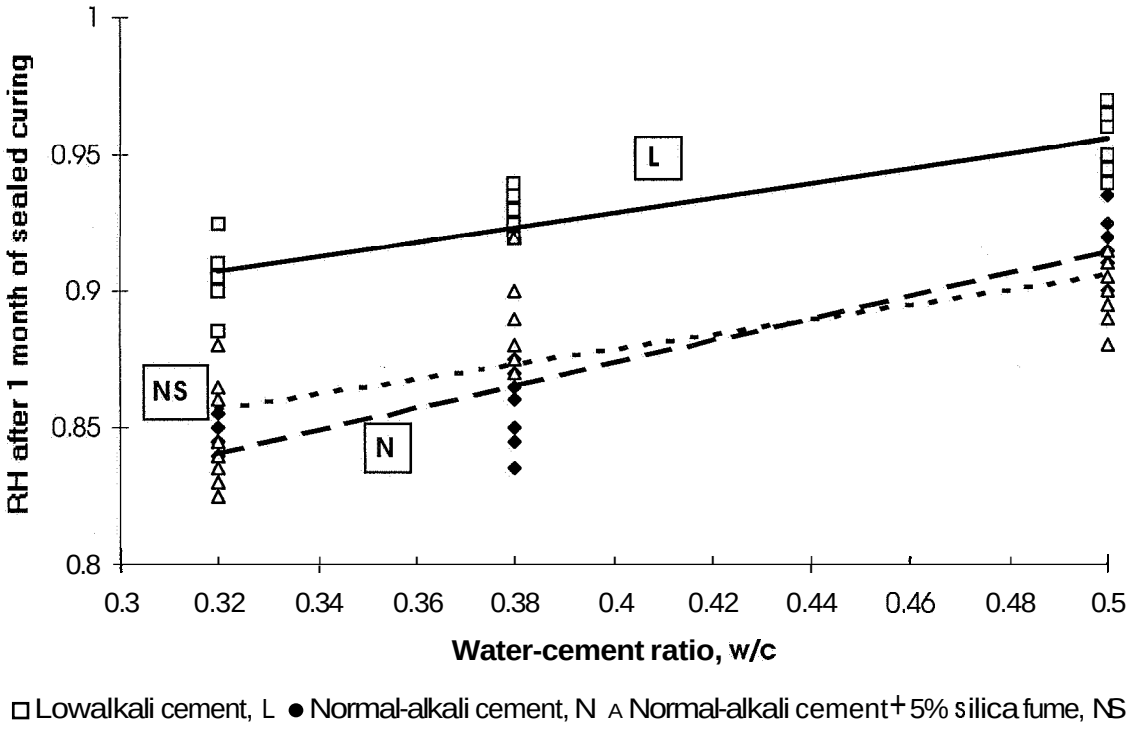

Fig. 19. RH versus w/c, 1 month's age. L= low-alkali, N = normal-alkali, S = 5% silica fume, 32= w/c (%).

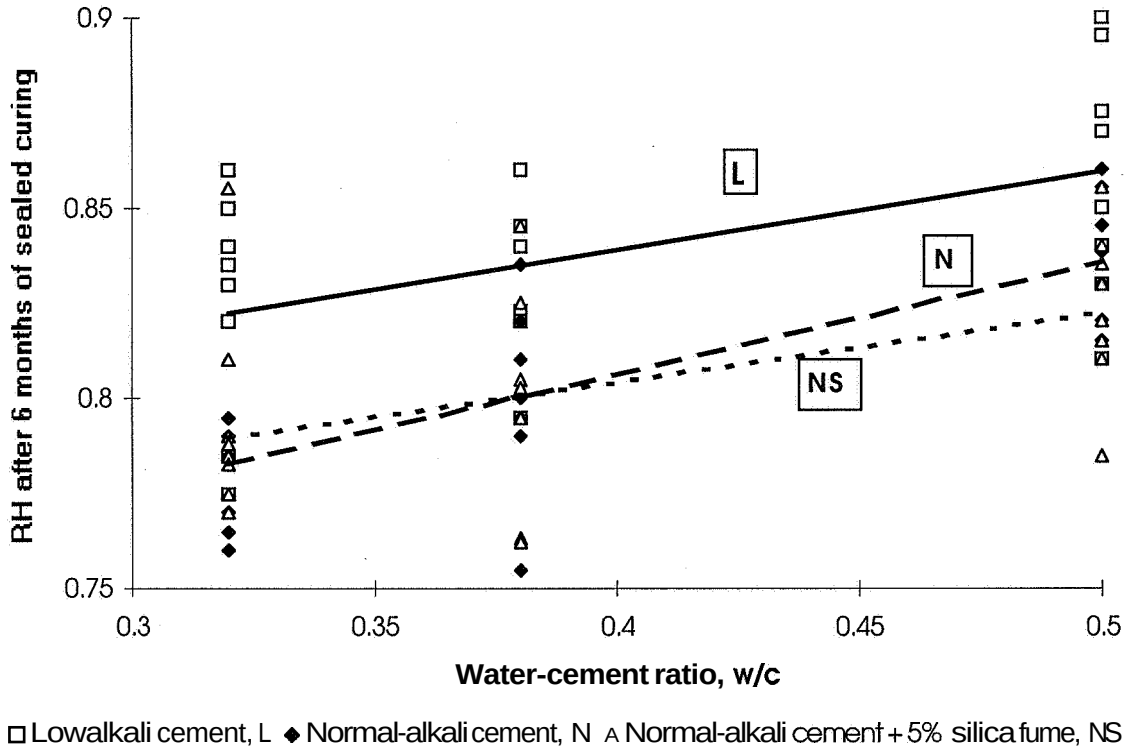

Fig. 20. RH versus w/c, 6 months' age. L= low-alkali, N = normal-alkali, S = 5% silica fume, 32= w/c (%).

Table 8. Constants in equation (1)

Cement type, silica fume	A	B	C	D	R^2
Low-alkali (L)	0.0378	0.185	-0.042	0.83	0.63
Normal-alkali (N)	0.0588	0.219	-0.059	0.79	0.75
Normal-alkali + 5% silica fume (NS)	0.0351	0.223	-0.051	0.78	0.49

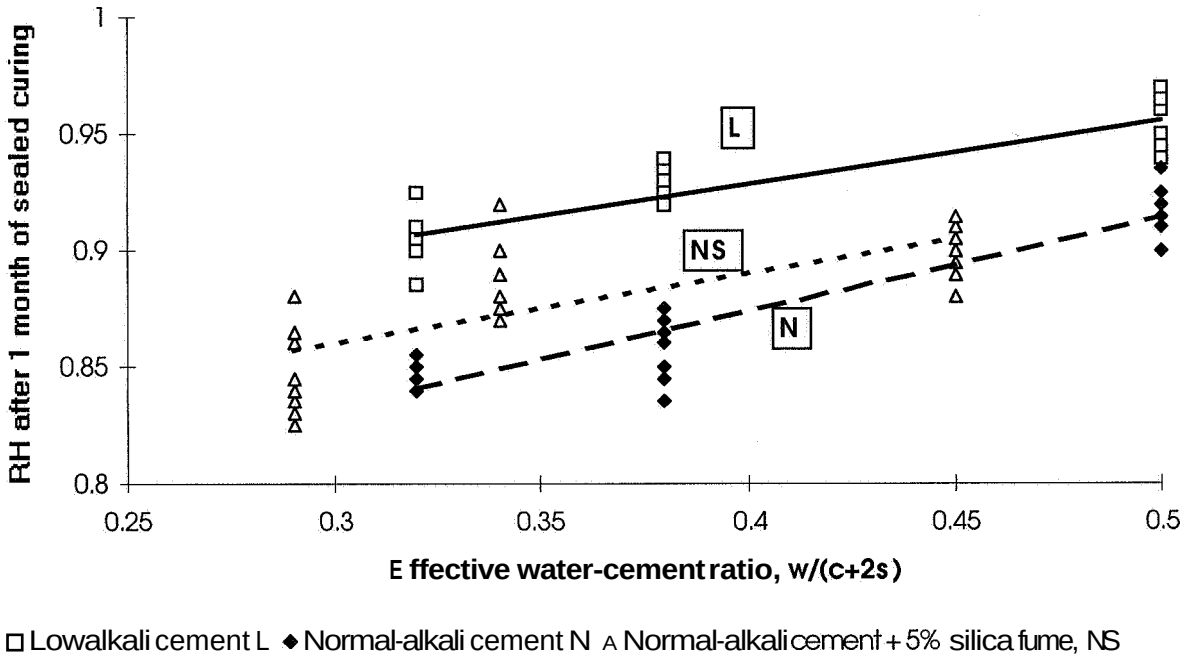

Fig. 21. RH versus $(w/c)_{eff}$, 1 month' age. L= low-alkali, N = normal-alkali, S = 5% silica fume, 32= w/c (%).

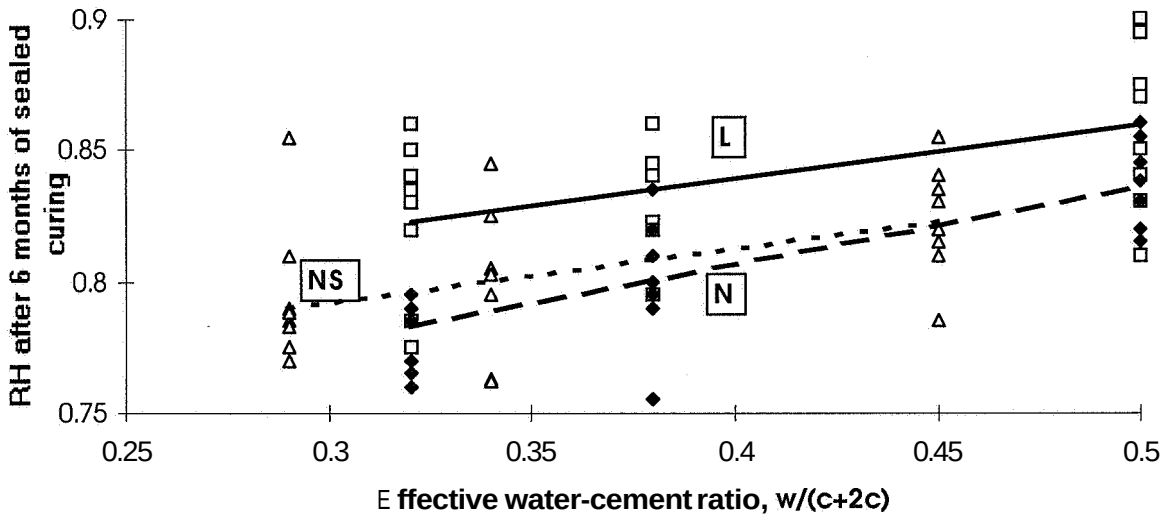

Fig. 22. RH versus $(w/c)_{eff}$, 6 months' age. L= low-alkali, N = normal-alkali, S = 5% silica fume, 32= w/c (%).

$$R^2 = 1 - \frac{\sum (Y_i - Y_m)^2}{(\sum Y_i^2) - \frac{(\sum Y_i)^2}{n}} \qquad (2)$$

Figures 19 and 20 confirm the results that concrete based on normal-alkali cement with or without 5% silica fume exhibits about 5% RH-decline compared with low-alkali cement based concrete. At low w/c the influence of silica fume was less than the influence of normal-alkali cement, Figures 19-20. Normal-alkali cement exhibited about 5% lower RH after self-desiccation than low-alkali cement. The so-called alkali-effect [19] and probably also the chemical composition of the cement affected the degree of self-desiccation, RH. The component of Alite, C_3S, was the same in both the cements, Table 1. However, the remaining clinker components, Belite, C_2S, Aluminate, C_3A, and Ferrite, C_4AF, varied quite a lot between the cements studied. The content of alkalis, K_2O and Na_2O, most probably also affected RH in the concrete.

6.2 Comparison with other research

The present results were compared with studies on 8 concretes made of the same type of cement [23]. The w/c varied between 0.22 and 0.58. The concretes were made in large elements, 250 kg each. Half of the concretes contained 10% silica fume as calculated on the basis of the cement content. More than 230 RH-measurements were done in plastic pipes in the concrete elements at ages varying between 1 and 15 months. Some measurements were performed at 90 months' age [23]. RH in the concrete, Ø, cured at 20 °C was correlated to age and w/c:

$$Ø_S(t,w/c) = 1.13\cdot[1-0.065\cdot\ln(t)]\cdot(w/c)^{0.24\cdot[1-0.1\cdot\ln(t)]} \quad \{1<t<15 \text{ m}; 0.2<w/c<0.6\} \qquad (3)$$

$$Ø(t,w/c) = 1.09\cdot(w/c)^{0.17\cdot(1+0.0451\cdot t)} \quad \{1<t<15 \text{ months}; 0.2<w/c<0.6\} \qquad (4)$$

ln(t) denotes the natural logarithm of age, t, in months (m)
w/c denotes the water-cement ratio
S denotes 10% silica fume

The following equations were obtained for 1 month's age and/or 5% silica fume:

$$Ø_{S5}(1,w/c) = 0.55\cdot[(w/c)^{0.18} + (w/c)^{0.24}] \qquad (5)$$

$$Ø(1,w/c) = 1.09\cdot(w/c)^{0.18} \qquad (6)$$

S5 denotes 5% silica fume

Table 9 provides a comparison between RH measured in the concretes of this project and RH estimated according to equations (5) and (6).

Table 9. Measured RH at 1 month's age and RH estimated according to equations (5) and (6).

w/c	Low-alkali cement	Estimation equation (6)	Difference in RH	Normal-alkali cement with 5% silica fume	Estimation by eq. (5)	Influence of type of cement, ΔØ
0.32	0.903	0.890	0.013	0.855	0.875	-0.02
0.38	0.923	0.917	0.006	0.874	0.906	-0.032
0.50	0.954	0.964	-0.01	0.906	0.960	-0.054

The estimation of RH according to equation (6) coincided reasonably well with the measured RH. Concrete based on normal-alkali cement and 5% silica fume exhibited significantly larger differences between measured and estimated RH due to the influence of components of the cement. Autogenous shrinkage occurs when RH in sealed concrete decreases due to chemical shrinkage of the water [5,24]. A relationship between RH and shrinkage was linear, Figure 4 [25]. Recently it was shown that a significant relationship exists between, on one hand, the amount of the chemical components C_3A and C_4F in cement paste and, on the other hand, autogenous shrinkage [26]. The influence of these components was ten times as large as that of the components C_2S and C_3S. Based on estimations of **A 0** given in Table 6 and provided the degree of hydration shown in Table 10, [27-30], it was feasible to conceive the following equation:

$$\Delta Ø = 6 \cdot \Delta(C_3A) \cdot \alpha_{C3A} + 8.6 \cdot \Delta(C_4AF) \cdot \alpha_{C4AF} - k \cdot \Delta(K_2O) \qquad (7)$$

A denotes difference in a property between low-alkali cement and normal-alkali cement (by weight)

a denotes degree of hydration

Table 10. Adopted 28-day degree of hydration in the estimation of equation (6) [27-29].

w/c	α_{C3A}	α_{C4AF}	k
0.32	0.67	0.45	-5
0.38	0.74	0.53	-4.7
0.50	0.83	0.62	-6.6
0.65	0.93	0.74	-9

7 Concluding remarks

The article presents an experimental and numerical study on self-desiccation and strength of 9 concretes at 28 days' age. Furthermore the self-desiccation was studied at 6 months' age. In all 81 concrete cylinders were studied. The following conclusions were drawn:

- Self-desiccation of concrete was mainly dependent on w/c and age of the concrete.
- RH at self-desiccation was fairly independent of moderate variations in curing temperature.

- Small variations of temperature at the time of measurement (± 0.5 "C) did not affect the measured RH, provided that the dew-point meter was calibrated at the same temperature.
- The maximum standard deviation of the measurements was 1.5% RH given a small shift of temperature during the time of measurement (± 0.5 "C).
- The average standard deviation was 0.7% RH under the same assumption, i.e. small shift in temperature during the time of measurement (± 0.5 "C).
- The calibration of dew-point meters was preferably performed at the temperature of measurement (± 0.5 "C).
- Two "C differences in temperature during the measurements of RH caused a systematic fault of ≈ ± 1.5 %RH, which normally means that the measurement is regarded as inaccurate.
- The recommendation is to maintain ± 2 "C during the curing time of the concrete but ± 0.5 "C during the time of measurement of RH (22h) and also during the time of calibration of dew-point meters (22h). The same requirements probably apply for other types of probes.
- The strength was reduced when the curing temperature was increased from 18 "C to 23 "C.
- Concrete with normal-alkali cement obtained 5% lower RH than with low-alkali cement.
- RH in concrete with normal-alkali cement was not significantly affect by 5% silica fume.
- The chemical composition of the cement had a substantial influence on the measured self-desiccation mainly due to the so-called alkali-effect.

8 Acknowledgement

Cementa Ltd, NORDTEST and the Swedish Union of Concrete Manufactures financed the research, which hereby is gratefully acknowledged. I am also most grateful to Professor Göran Fagerlund for his comments and his critical reviews of this article.

References

1. T. C. Powers, T. L. Brownyard (1947). *Studies of Physical Properties of Hardened Portland Cement Paste.* Research Laboratories of the Portland Cement Association. Bulletin 22. Journal of the ACI. Michigan. USA. Oct. 1946-April 1947. Vol. 43,984-987.
2. B. Persson (1997). *Chemical Shrinkage and Self-desiccation in High Performance Concrete.* Proc. Int. Seminar on Self-desiccation and Its Importance in Concrete Technology. Ed.: .B. Persson, G. Fagerlund. TVBM-3075. Lund Institute of Techn. Lund, 116-132.
3. B. Persson (1997). *Moisture in Concrete Subjected to Different Kinds of Curing.* Materials and Structure. RILEM, 30, 533-544.

4. O.M. Jensen, P.F. Hansen (1995). *Autogenous Relative Humidity Change in Silica Fume-Modified Cement Paste.* Advances in Cement Research. 7, No. 25, 33-38.
5. B. Persson (1997). *Self-desiccation and Its Importance in Concrete Technology.* Materials and Structures. RILEM, 30,293-305
6. B. Persson (1996). *Hydration and Strength of High-Performance Concrete.* Advanced Cement Based Materials. Elsevier. New York, 3, 107-123.
7. K. Tuutti (1982). *Corrosion of Steel in Concrete.* The Cement and Concrete Research Institute. Report Fo 4:82. CBI. Stockholm. Sweden, 277-286,302-303.
8. G. Fagerlund (1976). *The Critical Degree of Saturation Method - a General Method of Estimating the Frost Resistance of Materials and Structures.* Report Fo 12:76. The Cement and Concrete Research Institute. Stockholm. Sweden.
9. G. Fagerlund (1994). *Influence of Environmental Factors on the Frost Resistance of Concrete.* TVBM-3059. Lund Institute of Techn. Lund. Sweden, 19-22.
10. G. Fagerlund (1997). *Effect of Self-desiccation on the Internal Frost Resistance of Concrete.* Proc. Int. Seminar on Self-desiccation and Its Importance in Concrete Technology. Ed.: B. Persson, G. Fagerlund. TVBM-3075. Lund Institute of Techn. Lund, 227-238.
11. L.-0. Nilsson (1980). *Moisture Problems at Concrete Floors.* TVBM-3002. Lund Institute of Technology. Division Building Materials. Lund. Sweden, 36-51.
12. K. Norling Mjörnell (1994). *Self-desiccation in Concrete.* Report P-94:2. Division of Building Materials. Chalmers University of Technology. Gothenburg. Sweden, 21-28.
13. B. Persson (1993). *Self-desiccating High-Strength Concrete Slabs.* Proceedings at the 3rd International Symposium of High-Strength Concrete. Norway. 1993. Ed.: Holand, Sellevold, 882-889.
14. S. Sandberg (1997). *Composition of the Cements.* Private communication. Scancem Research Ltd. Slite.
15. M. Hassanzadeh (1994). *Fracture Mechanical Properties of High-Performance Concrete.* Report M4:05. Consortium HIGH-PERFORMANCE CONCRETE. Division of Building Materials. Lund Institute of Technology. University of Lund. Lund, 9-15.
16. B. Persson (1996). *"Ideal partikelfördelning i färsk betong" Ideal Grading of Particles in Fresh Concrete.* Betong 3/95, Bygg & Bo Media, Stockholm 6-8 *(In Swedish).*
17. B. Persson (1997). *Long-term Effect of Silica Fume on the Principal Properties of Low-temperature-cured Ceramics.* CCR, 27, 1667-1680.
18. ASTM E 104-85 (1985). *Standard Practice for Maintaining Constant Relative Humidity by Means of Aqueous Solutions.* The ASTM. Philadelphia, 33-34,637.
19. G. Hedenblad; M Janz (1994). *Effect of Alkali on the Measured Internal Relative Humidity in the Concrete.* Report TVBM-3057. Lund Institute of Technology, Lund, 5-12.
20. G. Hedenblad (1997). *Measurement of Moisture in High Performance Concrete.* Proc. Int. Seminar on Self-desiccation and Its Importance in Concrete Technology. Ed.: B. Persson, G. Fagerlund. TVBM-3075. Lund Institute of Techn. Lund, 31-45.

21. K. Mjornell Norling (1997). *Moisture in High-Performance Concrete.* Doctoral Thesis. Report P-97: 6. Chalmers University of Technology. Gothenburg, 5-24.
22. L. O. Nilsson (1987). *Temperature Effects in Relative Humidity Measurements on Concrete* - Some Preliminary Studies. The Moisture Research Group informs. Report 1987:1. The Swedish Council of Building Research. Stockholm, 84.
23. B. Persson (1998). *Pozzolanic Interaction between Portland Cement and Silica Fume in Concrete.* Sixth CANMET/ACI International Conference on Fly Ash, Silica Fume, Slag and Natural Pozzolans in Concrete. Tokushima, Japan, 631-660.
24. B. Persson (1996). *(Early) Basic Creep of High Performance Concrete.* 4th International Symposium on the Utilisation of High Performance Concrete. Paris, 405-414.
25. V. Baroghel-Bouny (1997). *Experimental Investigation of Self-Desiccation in High Performance Materials - Comparison with Drying Behaviour.* Proc. Int. Seminar on Self-desiccation and Its Importance in Concrete Technology. Ed.: B. Persson, G. Fagerlund. TVBM-3075. Lund Institute of Techn. Lund, 72-87.
26. E. Tazawa, S. Miyazawa (1997). *Effect of Cement Composition on Autogenous Shrinkage in Concrete.* Proc. of the 10th Int. Congr. on the Chemistry of Cement. Gothenburg, 2ii072.
27. H.F.W. Taylor (1987). *Cement Chemistry.* Academic Press. London, 205.
28. L.E. Copeland, R.H. Bragg (1955). *Measurement of Self-desiccation in Portland Cement Paste.* ASTM Bulletin no 204.
29. B. Persson (1992). *"Hogpresterande betongs hydratation, struktur och hållfasthet." Hydration, structure and strength of High Performance Concrete.* Report TVBM-1009. Div. Building Materials. Lund Institute of Technology. Lund, 211.
30. B. Persson (1999). *Effect of Cement Type, Silica Fume, Water-cement Ratio, Age and Moderate Shift in Temperature on Self-desiccation in Concrete.* 111999. Edited by the Nordic Concrete Federation. Oslo, 97-116.

Linear vs. volumetric autogenous shrinkage measurement : Material behaviour or experimental artefact ?

BARCELO L., BOIVIN S., RIGAUD S., ACKER P., CLAVAUD B.
Lafarge, Laboratoire Central de Recherche, Lyon, France

BOULAY C.
Laboratoire Central des Ponts et Chaussées, Paris, France

Abstract :
The general trend characterising the evolution of concrete technology is an increase of compactness of the material. Consequently, the important quantities of binders, the use of powerful water reducing admixtures, the increase of the range of particle size distribution through the use of silica fume lead to a decrease of water to binder ratio. For this type of concrete (mostly high performance concrete), it is nowadays well known and acknowledged that, among all types of shrinkage, autogenous shrinkage caused by hydration of the paste becomes predominant regarding cracking sensitivity. Thus, the characterisation of autogenous shrinkage of cement paste by a proper measurement technique is an important issue. Two types of tests are possible, i.e. volumetric and linear tests. This article focuses on the differences between those two types of measurement and on the problem of interpretation of results drawn by such differences. It finally raises the question of the validity of isotropy of deformations generally accepted in the hardened state.
Keywords :
Autogenous shrinkage, test method, volumetric measurement, linear measurement, isotropy.

1 Introduction and purpose of the study

Autogenous shrinkage of concrete is caused by self-desiccation which occurs due to hydration. Water is combined with anhydrous cement to create hydrates in such a way that the total absolute volume decreases. This phenomenon, called chemical shrinkage, was first described by Le Chatelier [1]. This volume reduction can be measured by two methods which are discussed in ref. [2]. In the plastic state, the absolute volume changes correspond to the external volume changes because concrete has a very poor rigidity. Furthermore, deformations are not isotropic; they favour the vertical direction. For this reason, it is important to differentiate the measurements done horizontally or vertically [3]. In the hardened state, the absolute volume reduction caused by the

hydration reactions still exists but the material is then quite stiff. The volume reduction is taken in the core of the material and a liquid-vapour interface appears : it is the self-desiccation. Hua [4] demonstrated that capillary pressure created by water menisci could quantitatively explain autogenous shrinkage in the hardened state. This mechanism accounts for the fact that autogenous shrinkage of concrete mainly depends on the total amount of chemical shrinkage as well as on the distribution of porous network.

Several improvements of concrete performances lead to an increasingly compact matrix with high amounts of binder. To comply with this, mix designers increased the range of particle size distribution by adding silica fume, and used powerful water reducing admixture... This trend of concrete technology increases the importance of autogenous shrinkage towards cracking sensitivity, and raises the problem of its measurement. Aïtcin [5] emphasised the point that drying shrinkage measurements on ordinary concrete are done under reliable conditions, which are well established in standards and test methods. Nevertheless, he concluded that those methods were not appropriate for autogenous shrinkage measurement on high performance concrete.

Two types of autogenous shrinkage measurements on cement paste can be found in the literature, i.e. linear and volumetric. Each method presents advantages and drawbacks: linear tests are generally easier to manage and used in a lot of laboratories, but, contrary to volumetric tests, they do not allow to monitor the plastic state of the material. For this reason, it is necessary to understand and compare the results of the two types of measurements to be able to coordinate the two sets of results and obtain complementary data. It is the objective of this article.

After a brief review of the principle of each type of test, linear measurements and volumetric measurements are compared in this study, from the time of casting up to 48 hours of hydration. Differences in the results are then emphasised and discussed.

2 Autogenous shrinkage measurement

2.1 Volumetric test methods

One of the first volumetric measurement was performed by Del Campo in 1959 [6]. The cement paste (about 200g) is cast inside a latex membrane. The membrane is put in a vessel filled with mercury. The vessel is closed and topped by a capillary tube. The deformations are directly read with the motion of the mercury surface in the tube. Since Del Campo, other authors used similar experiments (Edmeades 1966, Haas 1975) [7].

Three main artefacts can be identified for this kind of measurement technique [6, 8, 9]:

1. A non accurate temperature control can turn the device into a thermometer (!),
2. The pressure exerted on the sample by the membrane and the surrounding liquid may break the growing crystals,
3. The presence of bleeding water may lead to an overestimation of autogenous shrinkage (the measure is then closer to a measure of chemical shrinkage than of autogenous shrinkage).

Setter et al. [7] assessed the influence of bleeding water on the measurement but were not able to control this parameter.

A new method was proposed by Sellevold et al. [10] through Verboven and Van Gemert experiments [11]. After pouring the cement paste into a latex membrane, the sample is then rotated to avoid bleeding. The measurement of autogenous shrinkage is done discontinuously by hydrostatic weighing. The rotation seems to avoid bleeding quite well, even for cement pastes having a W/C of 0.5 [12]. With those experiments, it was then possible to assess that in the plastic state, autogenous shrinkage and chemical shrinkage did coincide [14].

2.2 Linear test methods

Most of the linear test methods for shrinkage measurement are based on the same principle: the samples are cast in prismatic molds and length changes are monitored by LVDT or other displacement transducers.

When the measure is performed vertically, samples are usually demolded, sealed with aluminium sheets to prevent moisture evaporation [14] and stored at constant temperature. The length of the sample is measured discontinuously and the measurements generally starts 24 hours after casting. Standard ASTM C490 [15] gives a good overview of this type of tests.

When the measure is performed horizontally, the measurement of length changes is directly done in the molds. The measurements generally start earlier than previously. An example of this type of measurement is given by Tazawa et al. [16].

One of the major drawbacks of linear measurements is that the measurement does not start at the beginning of hydration but later, when :

- the material is set, demolded and protected against evaporation if the test is run vertically,
- the material is rigid enough to overcome the friction between the shrinking paste and the mold if the test is run horizontally.

Jensen et al. [17] proposed an apparatus called dilatometer to measure linear autogenous shrinkage from the time of casting. To obtain this, corrugated plastic molds are used.

3 Test methods used in the present study

3.1 Linear autogenous shrinkage measurement

3.1.1 Linear type 1: measurement in the hardened state

3.1.1.1 Measurement on cylinders

This method is derived from KHEIRBEK [18] and LE ROY [19].

The molds that are used have a cylindrical shape (diameter : 2cm, length : 16 cm). They are made with PTFE ("TEFLON"), which is a good barrier against water vapour. The two ends of the molds are metallic cylindrical heads 1cm thick. Cramping with the paste is done through a screw (cf. Fig. 1). On the centre of the top face of the head (the hidden face in Fig. 1), a track allows the precise positioning of a transducer.

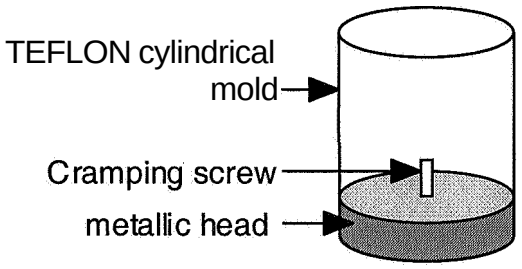

Fig. 1. Testing equipment for linear vertical measurement.

Samples are cast vertically under vibration (amplitude 0.25 mm). From the time of casting up to the time of setting, they are rotated upside down with a constant speed. When the cement paste is rigid enough, samples are demolded from the TEFLON envelope and sealed with auto-adhesive aluminium sheets. The change in length is then continuously recorded with a LVDT, whose precision is 1 μm (the measure is done vertically)

To be sure that autogenous conditions are met during the test, the weight of the samples is monitored after casting, before demolding, after sealing and at the end of the measurement. No weight loss was measured during the experiments. Measurement of densities of different sections of the samples were performed to ensure that no bleeding occurred during rotation.

3.1.1.2 Measurement on prisms

An alternative method has been used in this article. Samples are 4x4x16 cm prisms, cast horizontally under vibration (amplitude 0.25 mm) in molds equipped with screws (similar to the molds recommended in ASTM C490 [15]). A glass plate is set on the top of the mold and glued with silicon to prevent from moisture exchanges. When the paste is rigid enough, samples are demolded and sealed with auto-adhesive aluminium sheets. Measurement is done as in § 3.1.1.1.

3.1.2 Linear type 2: measurement from the time of setting

This method is quite similar to the one described by Tazawa et al. In ref. [16]. Contrary to this author, the mold is metallic to allow a good temperature regulation. 4x4x16 cm samples are used. After mixing, the paste is cast under vibration (amplitude 0.25 mm) in the mold equipped with cramping screws. Just after casting, a glass plate is set on the top of the mold and glued with silicon to prevent from moisture exchanges. The measurement starts just after those operations.

3.2 Volumetric autogenous shrinkage measurement

The volumetric test method used in this study is a new method developed in LAFARGE laboratories. It allows continuous measurement of autogenous deformations of cement paste, from the time of casting of the material. This apparatus is briefly described in ref. [20]. For a great part, it was inspired of [11], and combines the rotation of the samples with a continuous measure.

The measurement of shrinkage begins after 30 minutes of hydration (beginning of hydration is set at contact of cement and water during mixing). The accuracy of the measurement is approximately 0.3 mm^3 for a total deformation above 1 cm^3.

The following table summarises the different methods used in this study:

Table 1. Test methods used in the study

	Geometry of sample	Preparation of sample	Measure
Linear type 1	cylinders 0 2 – H16 cm	• cast vertically under vibration, • rotated up to setting, demolded after setting, • sealed with auto-adhesive aluminium sheets.	performed vertically after 16 hours of hydration.
	prisms 4x4x16 cm	cast horizontally under vibration, • no rotation, demolded after setting, • sealed with auto-adhesive aluminium sheets.	
Linear type 2	prisms 4x4x16 cm	cast horizontally under vibration.	performed horizontally, in the mold, from the time of casting.
Volumetric	about 60 cm^3	• poured into a latex membrane, • rotated during the measure.	performed from the time of casting, with rotation of the sample.

4 Materials and mixing procedure

The cement used for this study is a CEM I 52.5 CP2. The chemical composition, Bogue composition and fineness are given in the following tables.

Table 2. Chemical composition (%)

CaO (C)	SiO_2 (S)	Fe_2O_3 (F)	Al_2O_3 (A)	SO, (S)	MgO (M)	Alcalis		L.O.I.
						K_2O	Na_2O	
64,85	20,31	2,91	4,93	2,98	0,9	0,64	0,17	1,5

Table 3. Bogue Composition (%)

C_3S	C_2S	C_3A	C_4AF
55,7	14,5	8,1	8,9

Fineness: 3330 cm^2/g.

Water demand: 28,3 %

The cement paste used in this study has a W/C of 0.26 and is prepared with a Kenwood mixer, with a 3.5 minutes long mixing procedure. The beginning of mixing is taken as the zero point on the time scale.

5 Results

To allow comparison of results between linear and volumetric data, hypothesis of isotropic behaviour is made. Conversion of volumetric shrinkage into equivalent linear shrinkage is then done by equation :

$$\frac{\Delta V}{V} = 3 \cdot \frac{\Delta l}{l} \qquad (1)$$

Fig. 2 presents the results obtained on 5 samples for the volumetric test and **2** samples for the linear one. It appears from that figure that the two sets of data corresponding to linear and volumetric measurements are quite different. To analyse those differences, the results will be compared on different time scales : 0 to 6 hours, 5 to 24 hours and **24** to **48** hours. At the beginning of each time scale, the values of deformations are set to 0.

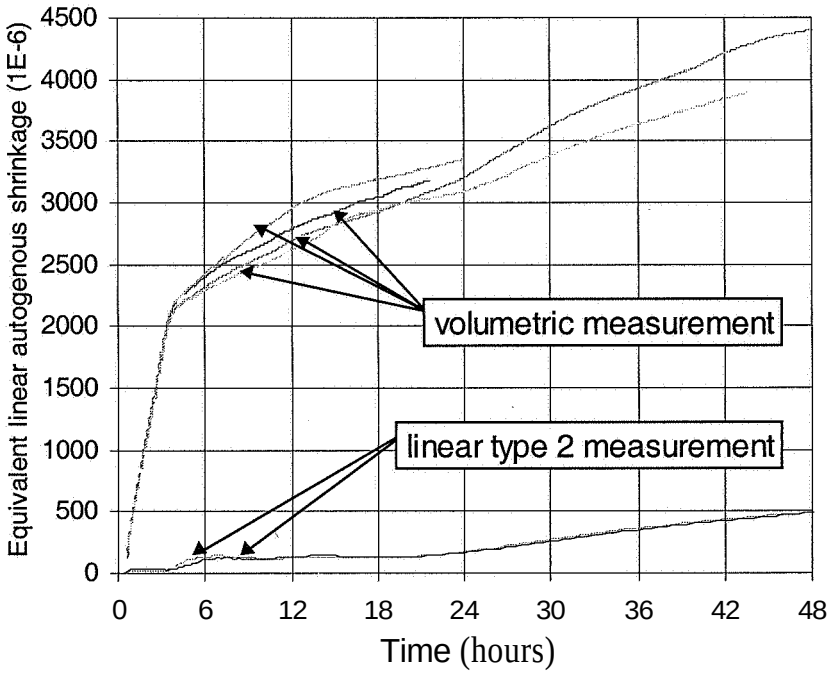

Fig. 2. Comparison of volumetric and linear results.

5.1 Comparison between 0 and 6 hours

Fig. *3* presents the comparison of results between 0 and 6 hours. The main observation is that no shrinkage is seen before 3.5 hours with the type 2 linear measurement (i.e. in the horizontal direction), while a significant amount of shnnkage is recorded with the volumetric measurement up to that point.

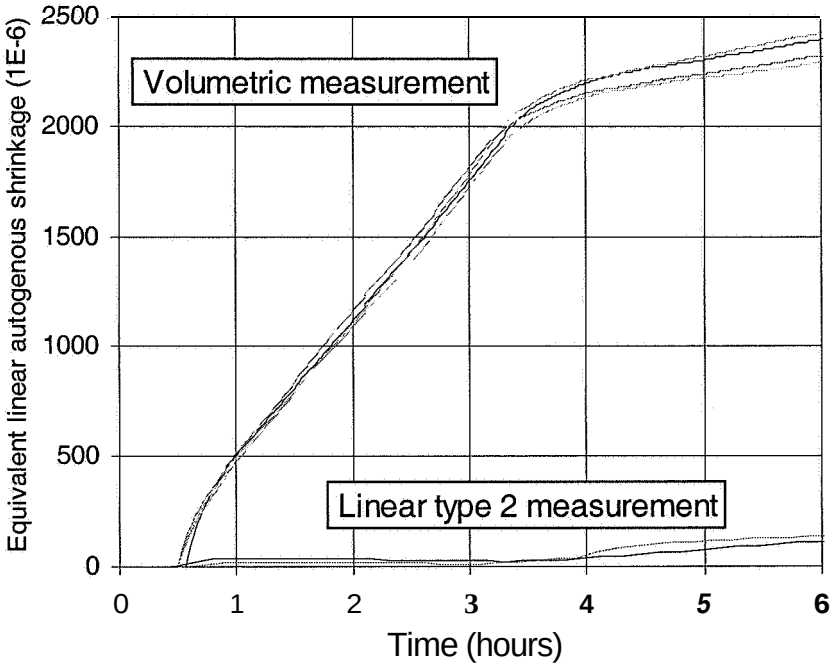

Fig. 3. Comparison of volumetric and linear results between 0 and 6 hours.

Fig. 4 illustrates the fact that the volumetric measurement of autogenous shrinkage perfectly corresponds to chemical shrinkage[i] from 0 to 2.5 hours. After that time, the autogenous shrinkage curve diverges from the chemical shrinkage curve till a quite pronounced knee point (3.5 hours) we call *stifening threshold.* In ref. [2], this point was related to an elastic modulus of the paste of about 2 GPa.

Concerning the linear measurement, no noticeable deformation is seen before 3.5 hours. This corresponds quite well to the *stifening threshold* defined on the volumetric shrinkage curve.

Based on those results, it is possible to conclude that before the stiffening threshold, all the deformations recorded in the volumetric experiment correspond to vertical deformations, which are not accessible with the linear measure performed in the horizontal direction. This is consistent with observations made by Radocea [21] (cf. Fig. 5).

It appears from the comparison of Fig. 3 and Fig. 5 that the value of 2200 - 2300 μm/m measured in this study at 5 hours for volumetric autogenous shrinkage corresponds quite well to the value of 2.5 mm/m of vertical deformation measured by Radocea at 5 hours.

Volumetric method allows to define very precisely the stiffening threshold that corresponds to the transition of mechanical behaviour from a dense suspension of solid particles to a porous solid.

[1] Chemical shrinkage is measured according to the weighing method described in [2].

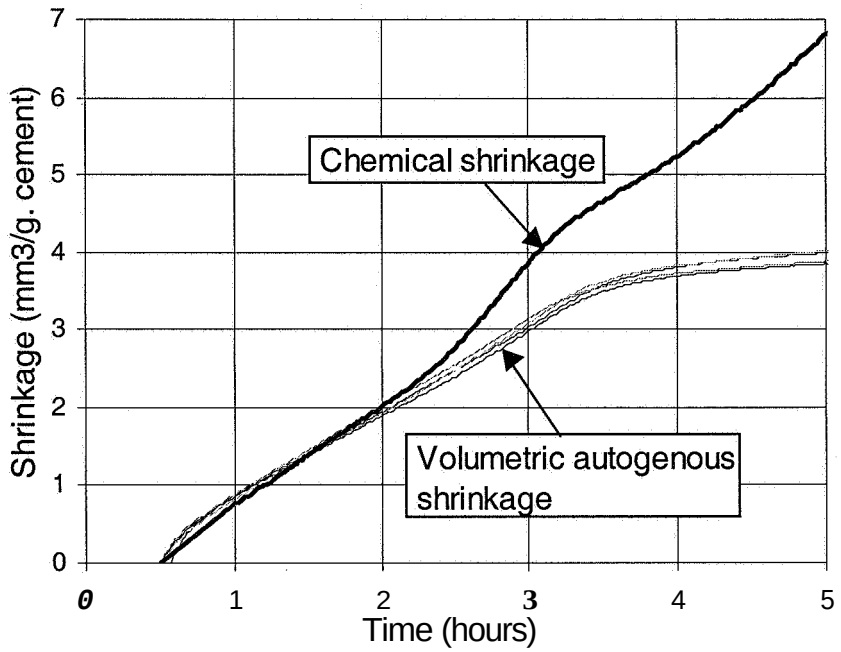

Fig. 4. Volumetric autogenous shrinkage vs chemical shrinkage.

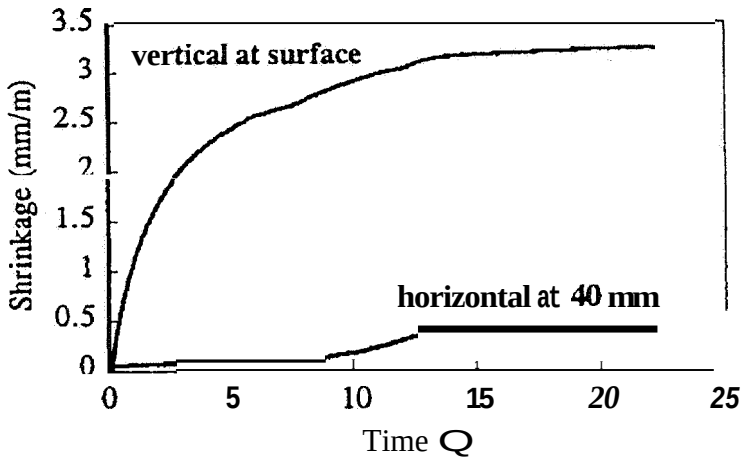

Fig. 5. Vertical and horizontal deformations for a W/C=0,3 cement paste [21].

5.2 Comparison between 5 and 24 hours

Fig. 6 presents the comparison between volumetric shrinkage and linear shrinkage (type 2 measurement) from 5 to 24 hours of hydration. Results from the two families of experiments are very different. In particular, linear shrinkage remains very low.

As seen in the literature, the origin of this problem may be the friction at the interface between the paste and the mold in the linear type 2 measurement. To check this assumption, linear type 1 measurements were carried out on 1) cylindrical samples and 2) samples having the same geometry (4x4x16 cm) and history (no rotation) than those used for the linear type 2 measurement (cf. § 3.1.1). The measurement only starts at 16 hours, time at which the samples have been demolded and sealed with aluminium sheets (the results presented are the average results based on 3 samples).

The results (Cf. Fig. 7) show that linear shrinkage obtained with the type 1 measurement (i.e. vertically, on demolded samples) is not of the same order of magnitude than linear shrinkage obtained with the type **2** measurement (i.e. horizontally, in the mold). Even after setting, friction seems to be high enough to restrain deformations in the type 2 configuration.

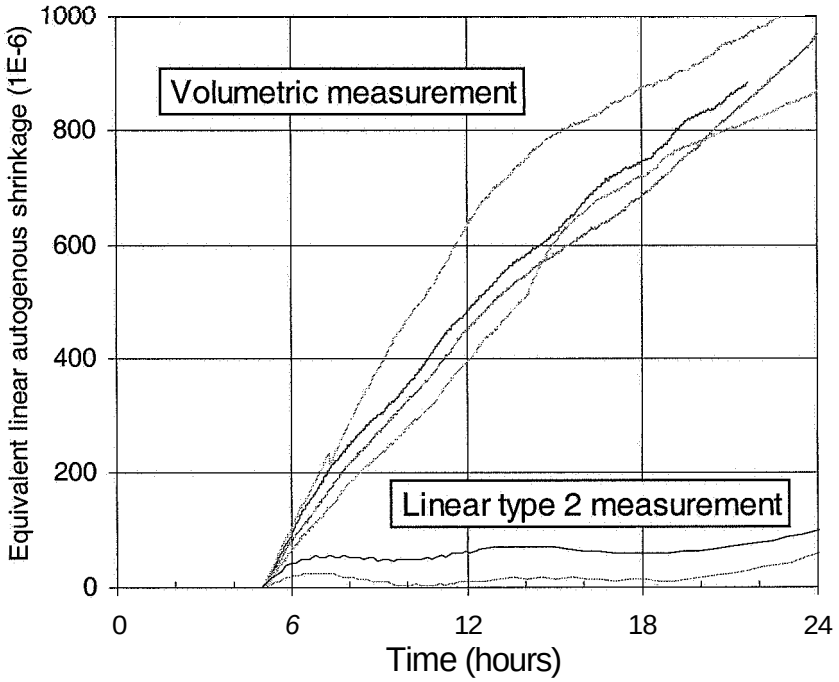

Fig. *6*. Comparison of volumetric and linear results between 5 and **24** hours.

Despite the quite high dispersion of the volumetric measurement, the rate of shrinkage seems to be of the same order of magnitude (a little higher) than results obtained for linear type 1 measurement.

5.3 Comparison between 24 and 48 hours

As seen in Fig. **8,** from **24** hours up to **48** hours, the two types of linear measurements are in very good agreement. The rigidity of the cement paste is then high enough to overcome friction in the type **2** configuration. However, results obtained with volumetric measurements fully diverge from others (the lower curve did not diverge up to **24** hours). Values obtained with volumetric measurement are *3* times as large as those obtained with linear measurement at *36* hours.

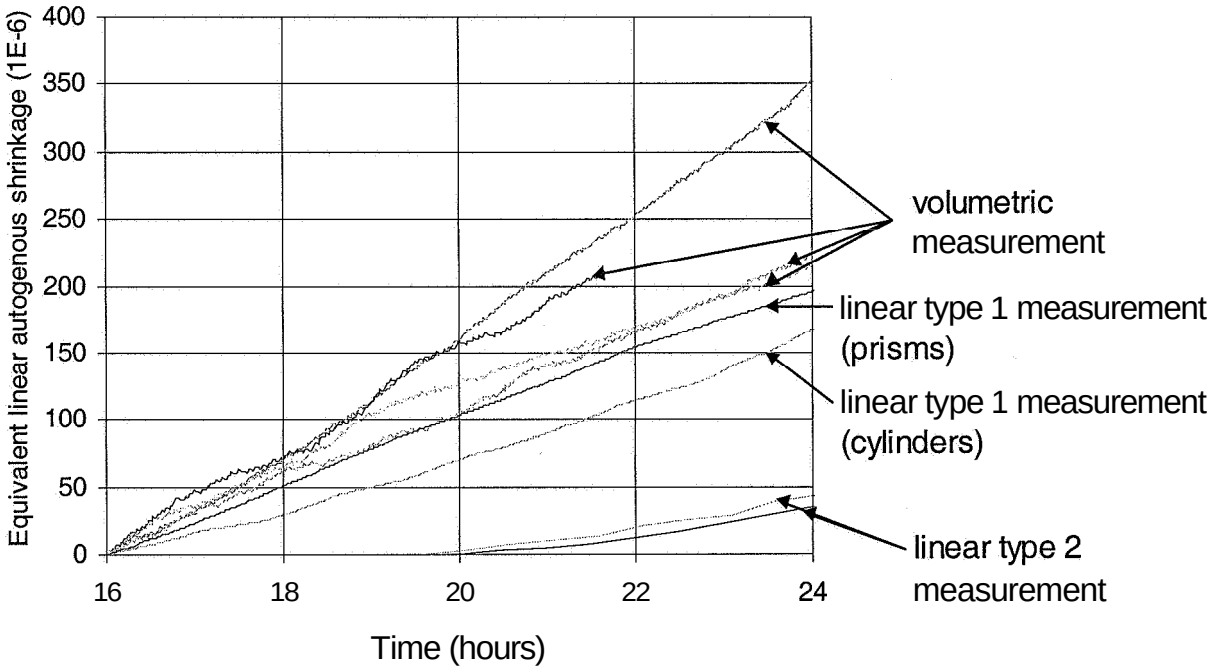

Fig. 7. Comparison of volumetric and linear results between 16 and 24 hours

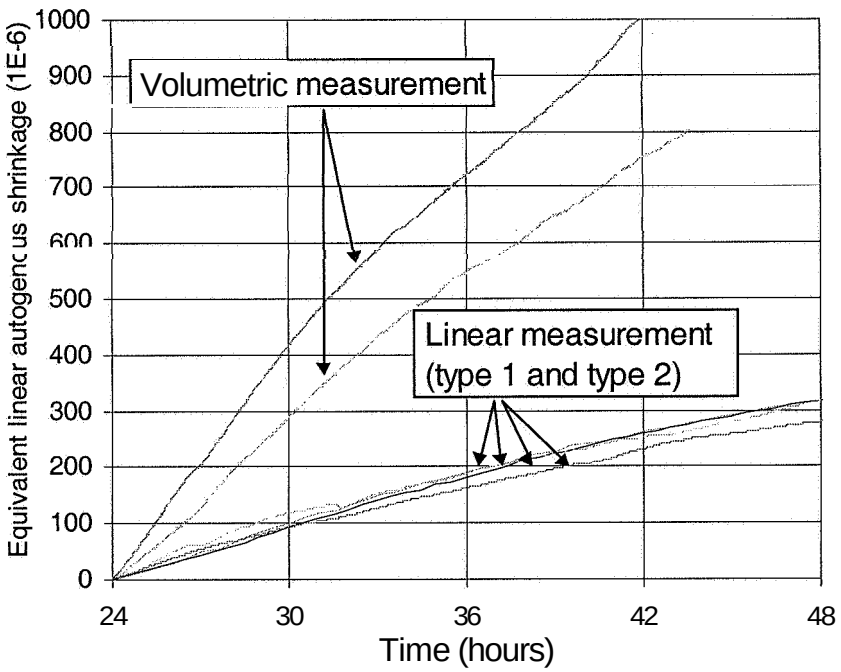

Fig. 8. Comparison of volumetric and linear results between 24 and 48 hours.

6 Discussion

The problem of non equivalence between volumetric and linear test methods has to be considered over different time scales:

- From the time of casting up to the time of setting, deformations are not isotropic. The results obtained in this study confirm that, before setting, volumetric shrinkage corresponds very well to chemical shrinkage, and that no linear shrinkage is observed in the horizontal direction. Chemical shrinkage is then entirely transformed into vertical deformations.
- The difference between the two types of linear measurements tends to prove that the problem of friction at the interface paste / mold at early age can be a source of error. In particular, type 2 method cannot be used to determine the initial rate of autogenous shrinkage.
- In the hardened state, the problem of non equivalence between linear and volumetric measurements is more surprising. Since linear measures with different set-ups and sample geometries give identical results, it is possible to consider this type of measurement as a reliable one. Regarding the volumetric test method, it is necessary to further evaluate the possible artefacts of the measure. This will be the objective of this discussion.

Three types of potential artefacts are frequently presented in the literature for volumetric test methods. Those artefacts (cf. **92.1)** are **1)** a non accurate control of temperature, 2) the influence of the membrane pressure and 3) the presence of bleeding water on the surface of the sample. With regards to the test method used in this study, the following remarks can be done:

- Fig. 9 is an example of evolution of temperature of the water which is very close to the sample in the volumetric test. Control of temperature appears to be quite efficient, and is probably not the source of an overestimation of the volumetric deformations. Fig. 9. Example of evolution of temperature in the surrounding water of the sample in the volumetric test.

- Bleeding is probably not the origin of the differences, because:

    1. during the volumetric experiment, the sample is rotated,
    2. W/C of cement paste is very low, lower than water demand,
    3. considering the rate of chemical shrinkage, all the bleeding water would have been re-absorbed at 24 hours in case of bleeding.

- Finally, the pressure of the membrane can be a possible artefact, not in the liquid state, because the liquid suspension is incompressible, but just after, at the beginning of building up of the porous network. The pressure of the membrane may be high enough to break the first mineral network. Nevertheless, if pressure is the artefact, one can wonder what is the behaviour of cement paste in quite massive structures, when proper weight is important. Moreover, it is possible to assume that, even if the pressure of the membrane is responsible for some differences at early age, this effect would drastically decrease as the rigidity of the material increases. As was seen previously, this is not the case.

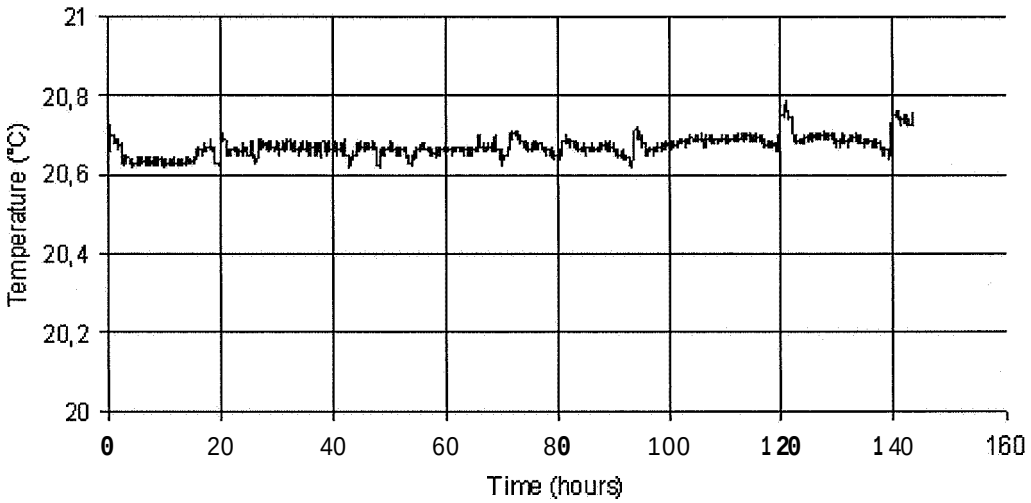

Fig. 10. Example of evolution of temperature in the surrounding water of the sample in the volumetric test.

An other type of artefact, which is not mentioned in the literature, has to be considered. In a real structure, as self-desiccation appears, menisci of water create capillary pressure dependant on the radius of those menisci. This capillary pressure is the difference between pressure in the gas constituting one part of the porous network, and the pressure in the water constituting the other part of the porous network. In a structure, capillary porosity is connected to the surface of concrete and as soon as gas has percolated in the porous network, atmospheric pressure is imposed in the gas. At a given moment, the capillary pressure is then the difference between atmospheric pressure and the pressure in water. In the case of the volumetric test, the sample is sealed in a membrane. When gas percolates in the porous network, the atmospheric pressure is not imposed in this gas. This pressure is lower than the atmospheric pressure and decreases as the volume of gas increases in the sample. In absolute value, capillary pressure is then more important. This difference can create an increase in autogenous shrinkage.

To quantify the importance of this difference (which is purely caused by the testing method), the pressure in water caused by capillary pressure has been calculated as a function of relative humidity in two ways. The pressure in gas in the porous network has been taken equal (1) to the atmospheric pressure and (2) to the partial pressure of vapour at the equilibrium with the meniscus for the given Relative Humidity. Fig. 11 presents the relative error between those two values as a function of Relative Humidity.

When Relative Humidity is lower than 0.95, the relative error done becomes inferior to 1%. It is caused by the fact that in absolute value, below this Relative Humidity, the capillary pressure is very important facing atmospheric pressure. But, just at the beginning of creation of menisci (Relative Humidity close to 100%), the error is very high (about 1400%) and can create differences in the autogenous shrinkage.

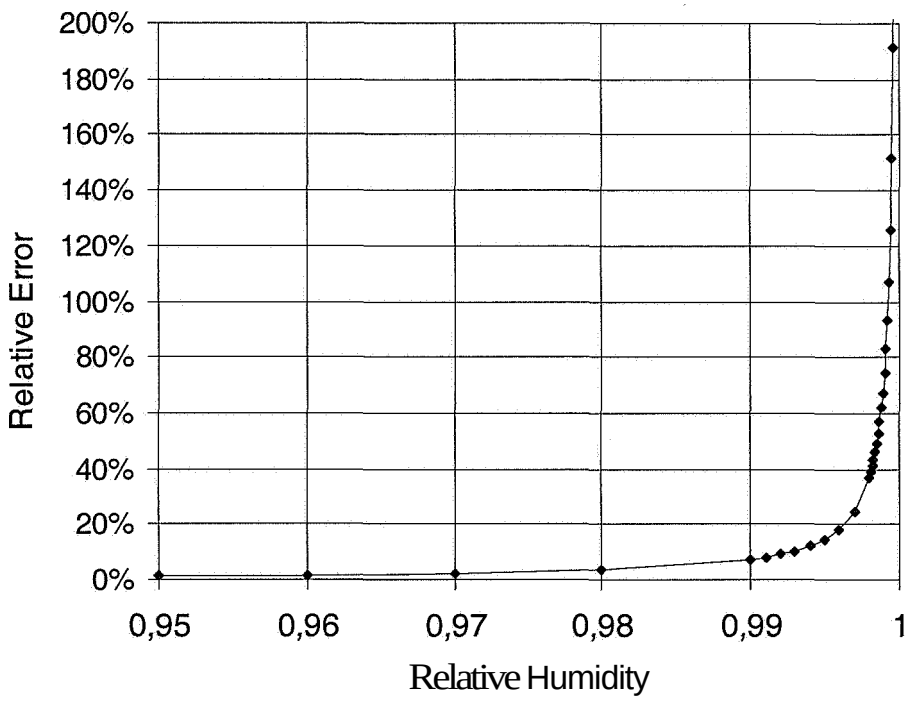

Fig. 11. Relative error done on the value of pressure in water assuming atmospheric pressure or partial pressure of vapour in the gas of the porous network.

Fig. 12 plots the evolution of Relative Humidity with time for the cement paste used. The period corresponding to 95-100% of relative humidity is between 35 and 55 hours. This period is consistent with the time scale where differences between volumetric and linear methods were observable (24 – 48 hours). According to this analysis, one can assume that the differences between the two measurements would decrease after about 60 hours of hydration (i.e. for HR<0.95). Fig. 13 presents the comparison of linear and volumetric results after 48 hours. Even on this time scale, the differences between the two sets of experiments still remains. This means that, even if the difference in gas pressure can be a source of error in the volumetric measurement, it does not entirely explain the observed differences in autogenous shrinkage.

One last explanation concerning the observed differences between linear and volumetric experiments could be a non-isotropy of deformations. New experiments have to be carried out to further check this point. A first surprising result is described in ref. [22] and [23], where axial and lateral strains were measured on concrete specimens (samples are cylinders having a diameter of 16 cm and a length of 100 cm; the concrete has a W/C of 0,5). Fig. 14 presents the preliminary results, where the measured lateral strain appears to be 1.6 times the axial strain. This apparent anisotropy has been attributed at that point to a non-homogeneous aggregate distribution caused by the use of non-cored cylinder specimens.

Regarding this last hypothesis, measure of deformations in lateral and axial directions should be performed on cement pastes and on cored concrete specimens to assess if deformations are isotropic or not in the linear test configuration, and if this could explain the observed differences between linear and volumetric experiments.

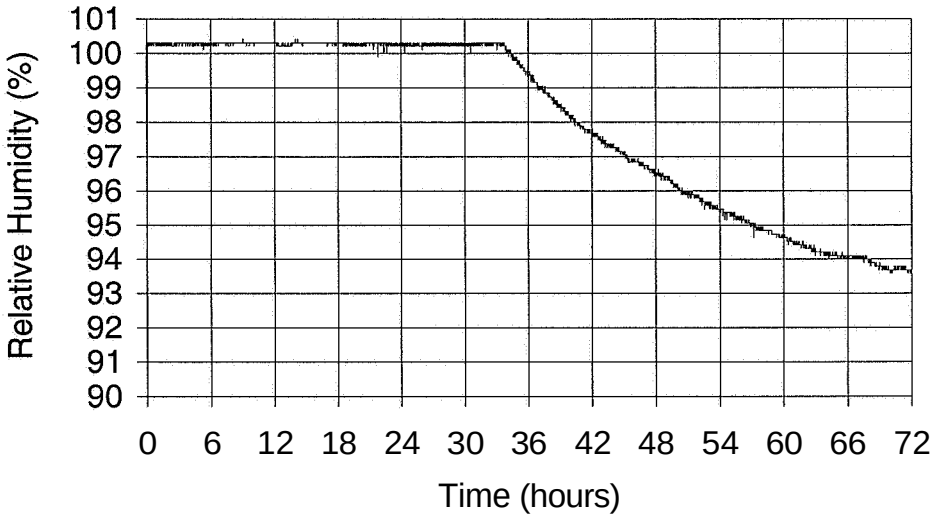

Fig. 12. Evolution of Relative Humidity with time.

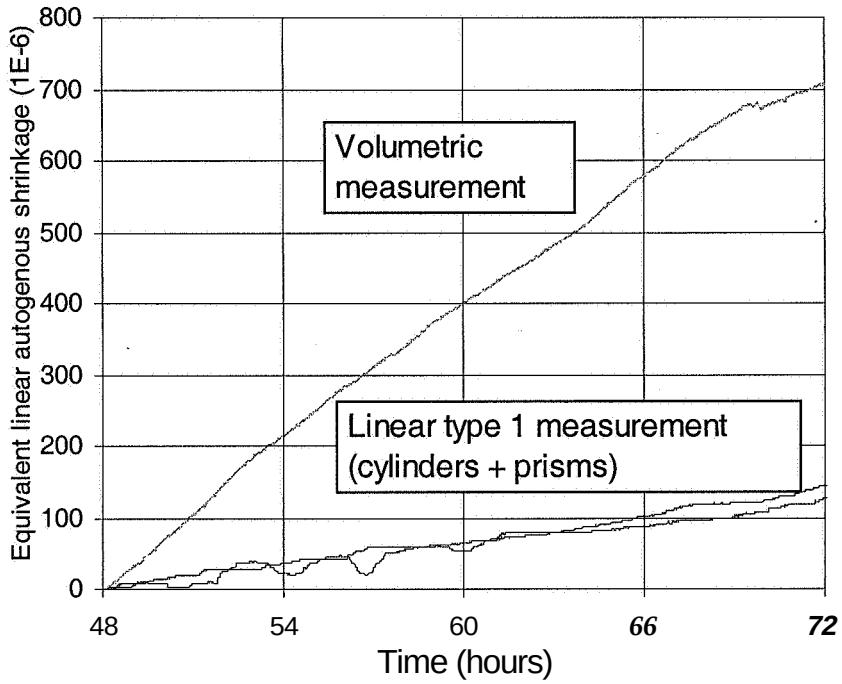

Fig. 13. Comparison of volumetric and linear results after 48 hours.

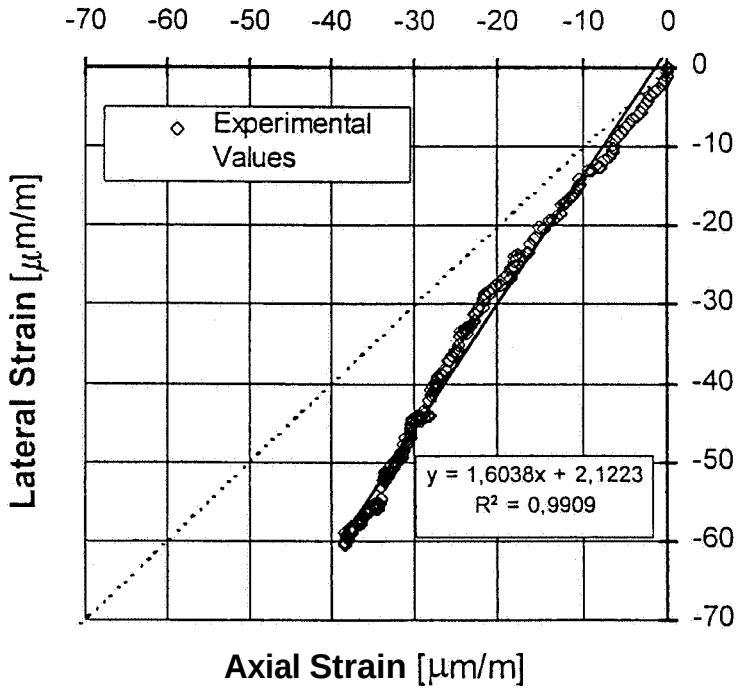

Fig. 14. Lateral strain versus axial strain in shrinkage test on concrete specimens (preliminary results from [22]).

7 Conclusions

Based on the experiments performed in this study, the following conclusions can be drawn:

- Before setting, autogenous shrinkage corresponds quite well to chemical shrinkage but no linear shrinkage is observed in the horizontal direction. Chemical shrinkage is then entirely transformed into vertical deformations.
- The continuous volumetric method allows to define precisely the stiffening threshold, which marks the transition from a dense suspension of solid particles to a porous solid.
- Several hours after setting, friction at the interface between the paste and the mold restrains deformations in the type 2 linear measurement. This test method is not able to give the initial rate of autogenous shrinkage.
- Later after setting, type 1 and type 2 linear measurements coincide. Results given by volumetric method diverge and give results about 3 times as large. No explanation for this phenomenon has been found at this point. Assumptions regarding the effect of the difference of gas pressure in the volumetric experiments or the possibility of a non isotropic behaviour have been made. Further research is needed to confirm these hypothesis.

8 References

1. LE CHATELIER H., *Sur les changements de volume qui accompagnent le durcissement des ciments.* Bulletin de la Société pour l'Encouragement de l'Industrie Nationale, 1900. 5ème série(tome 5): p. 54-57.
2. BOIVIN S., ACKER P., RIGAUD S., CLAVAUD B., *Experimental assessment of chemical shrinkage of hydrating cement paste.* in *AUTOSHRINK'98 - International Workshop on Autogenous Shrinkage of Concrete.* 1998. Hiroshima.
3. Japan Concrete Institute. *JCI Committee report of technical committee on Autogenous Shrinkage of Concrete.* in *International Workshop on Autogenous Shrinkage of Concrete : Autoshrink'98.* 1998. Hiroshima (Japan).
4. HUA C., ACKER P., EHRLACHER A., *Analyses and models of the autogenous shrinkage of hardening cement paste. I: Modelling at macroscopic scale.* Cement and Concrete Research, 1995. 25(7): p. 1457-1468.
5. AITCIN P.C. *Autogenous shrinkage measurement.* in *International Workshop on Autogenous Shrinkage of Concrete : Autoshrink'98.* 1998. Hiroshima (Japan).
6. BUIL M., *Contribution à l'étude du retrait de la pâte de ciment durcissante,* 1979, Ecole Nationale des Ponts et Chaussées: Paris. p. 67.
7. SETTER N., ROY D.M., *Mechanical features of chemical shrinkage of cement paste.* Cement and Concrete Research, 1978. 8: p. 623-624.
8. BOULAY C., PATIES C., *Mesure des déformations du be'ton au jeune âge.* Materials and Structures, 1993. 26: p. 307-311.
9. HAMMER T.A. *Test methods for linear measurement of autogenous shrinkage before setting.* in *AUTOSHRINK'98 - International Workshop on Autogenous Shrinkage of Concrete.* 1998. Hiroshima (Japan).
10. SELLEVOLD E.J, BJONTEGAARD O., JUSTNES H., DAHL PA., *High performance concrete : Early volume change and cracking tendency.* in *Thermal Cracking in Concrete at Early Ages.* 1994: E&FN Spon.
11. VERBOVEN F., VAN GEMERT A., *Chemical shrinkage of cement pastes,* 1994, Katholieke Universiteit Leuven: Leuven.
12. JUSTNES H., VAN GEMERT A., VERBOVEN F., SELLEVOLD E.J., *Total and external chemical shrinkage of low w/c ratio cement pastes.* Advances in Cement Research, 1996. 8(31).
13. JUSTNES H., VAN GEMERT A., VERBOVEN F., SELLEVOLD E., VAN GEMERT D.,. *Influence of measuring method on bleeding and chemical shrinkage values of cement pastes.* in *10th International Congress the Chemistry of Cement.* 1997. Goteborg.
14. TOUTLEMONDE F., LE MAOU F., *Protection des éprouvettes de be'ton vis-2-vis de la dessiccation. Le point sur quelques techniques de laboratoire.* Bulletin des laboratoires de Ponts et Chaussées, 1996. 203(Mai-Juin 1996): p. 105-119.
15. ASTM C490-93a, *Standard Practice for Use of Apparatus for the Determination of Length Change of Hardened Cement Paste, Mortar, and Concrete,* Annual Book of ASTM Standards, Vol 04.01.
16. TAZAWA E., MIYAZAWA S. *Autogenous shrinkage caused by self-desiccation in cementitious materials.* in *9th International Congress on the Chemistry of Cement.* 1992. New Delhi.
17. JENSEN O.M., HANSEN P.F., *A dilatometer for measuring autogenous deformation in hardening portland cement paste.* Materials and Structures, 1995. 28: p. 406-409.

18. DUVAL A., KHEIRBEK A., BAROGHEL-BOUNY V., *Influence de la fumée de silice sur le retrait endogène de la pâte de ciment.* in *Science des Matériaux et Propriétés des Be'tons, 1ères Rencontres Internationales de Toulouse.* 1998. Toulouse.
19. LE ROY R., *Déformations instantanées et différées des be'tons h hautes performance,* . 1995, Ecole Nationale des Ponts et Chaussées: Paris. p. 376.
20. HU C., BARCELO L., *Investigation on the shrinkage of Self Compacting Concrete for building construction.* in *International Workshop on Self Compacting Concrete.* 1998. Koshi.
21. RADOCEA A., *Autogenous volume change of concrete at very early age - Model and experimental data,* in *Self-Dessiccation and its importance in Concrete Technology - International Research Seminar in Lund.* 1997.
22. ULM *F.J.,* LE MAOU *F.,* BOULAY C., *Creep and shrinkage coupling : New review of some evidence. Revue française de génie civil - Numéro spécial vol 3, n 2-3, to be published in may* 1999.
23. LE MAOU *F.,* ROSSI P., *Mesure de la de'formation transversale différée d'un be'ton lors d'un essai de retrait et d'un essai de fluage*, to be published in Bulletin des Laboratoires des Ponts et Chaussées.

EFFECTS OF CEMENT PSD ON POROSITY PERCOLATION AND SELF-DESICCATION

Cement PSD and self-desiccation

D.P. BENTZ
National Institute of Standards and Technology, Gaithersburg, MD USA

Abstract

The degree of self-desiccation in field concrete depends on the availability of external water to replace that consumed due to the chemical shrinkage that occurs during cement hydration. As the cement hydrates, the capillary porosity depercolates, drastically slowing down this rate of external water ingress. In this paper, computer simulations are used to investigate the effects of cement particle size distribution (PSD) on capillary porosity percolation and the empty porosity created by chemical shrinkage. In addition, simulations are conducted with a single aggregate in the model microstructure to investigate the effects of cement PSD on interfacial transition zone (ITZ) microstructure at this aggregate interface. Because the largest pores empty first during self-desiccation, the ITZ region in systems containing aggregates is characterized by the presence of a large volume fraction of empty porosity relative to that found in the bulk paste. The cement PSD influences both the volume and size distribution of empty pores, which will in turn control the internal relative humidity reduction and autogeneous shrinkage for these materials. Thus, cement PSD is one material parameter available for engineering the self-desiccation and autogeneous shrinkage behavior of low water-to-cement ratio concretes.

Keywords: Chemical shrinkage, hydration, interfacial transition zone, microstructure, particle size distribution, percolation, self-desiccation, simulation.

1 Introduction

In 1935, Powers [1] reported that during cement hydration, external water is absorbed by the hydrating cement paste to replace that consumed by chemical shrinkage (the hydration products occupying a smaller volume than the reactants). When external water is not present or not readily available to the hydrating system, self-desiccation occurs and empty pores are created within the microstructure. Based on the Kelvin-Laplace equation, these empty pores will cause a reduction in the internal relative humidity (RH) [2], in turn inducing capillary stresses within the remaining capillary water. These stresses will cause a measurable deformation, referred to as the autogeneous shrinkage of the mortar or concrete specimen.

The magnitude of autogeneous shrinkage in conventional concrete mixtures is very small, but increases dramatically as the water-to-cement (w/c) ratio decreases to the values used in high-performance concretes.

The reduction in internal RH is mainly dependent on two factors: the volume of empty pore space created and the pore size distribution of the cement paste [3]. Similar to a mercury intrusion experiment where the largest connected pores first fill with mercury, during self-desiccation, the largest pores will empty first. Thus, the moisture content vs. relative humidity tends to follow the measured desorption isotherm of the material [4]. When attempting to engineer the autogeneous shrinkage and internal RH of a concrete for field use, one can attempt to regulate either the amount of empty pore space, its size distribution, or both.

One material parameter that influences both of these properties is the particle size distribution (PSD) of the cement. Naturally, the size distribution of the cement particles has a large influence on the initial and hydrated pore size distribution of the cement paste. While the volume of chemical shrinkage is proportional to hydration [1]and would be expected to be independent of cement PSD at equal degrees of hydration, the availability of external water does depend on the cement PSD in the following manner. In measuring the chemical shrinkage of a variety of cement pastes, Geiker [5] has shown that for a given w/c ratio, there exists a critical degree of hydration beyond which the rate of water ingress is unable to keep up with that needed to maintain saturation. This point corresponds to the depercolation of the capillary pore space [6, 7]. Once the capillary porosity becomes disconnected, water must penetrate via the much smaller pores in the C–S–H gel, so that the penetration rate slows by one order of magnitude or more. Recently, simulation studies have indicated that this depercolation of the capillary porosity is dependent on the cement PSD [8], with coarser cements requiring a larger degree of hydration to achieve depercolation. Thus, under proper curing conditions, a coarser cement may result in a reduction in both the empty porosity created by chemical shrinkage and the autogeneous shrinkage of the specimen. In this paper, computer simulations are applied to studying the influence of cement PSD on capillary porosity percolation, empty porosity created by chemical shrinkage, and interfacial transition zone (ITZ) microstructure.

2 Computer Modelling Techniques

All simulations presented in the results section were conducted using the NIST 3-D cement hydration and microstructural development model, which has been described previously [9]. The PSDs used were measured on actual cements [8] and bracket the PSDs currently produced by cement manufacturers. The fine cement had a median particle diameter of about 5 pm and a Blaine surface area of 640 m^2/kg, while the coarse cement had a median particle diameter of about 30 pm and a Blaine surface area of 210 m^2/kg. The composition of the cement determined by quantitative microscopy was 59 % C_3S, 25.9 % C_2S, 0.6 % C_3A, and 14.2 % C_4AF, with hemihydrate added at a mass percentage of 4.6 % [8]. Recently, a number of properties of these two model cements have been studied in detail [10]. Both cement paste and concrete (w/c=0.3) microstructures were simulated. In the latter case, the presence of an aggregate is simulated by placing a 2-pixel wide sheet of aggregate through the middle of the 3-D microstructure. For the 30 pm cement, simulations were also conducted with a 10 % silica fume replacement of cement (mass basis). The silica fume, modelled as 0.5 pm particles, reacts with the calcium hydroxide produced during hydration and also results in a reduction in the overall Ca/Si ratio of the C–S–H gel [11, 12]. The cements

were modelled as either $100 \times 100 \times 100$ ($1\ \mu m$/pixel) or $200 \times 200 \times 200$ ($0.5\ \mu m$/pixel) 3-D microstructures.

The hydration simulations were executed under two different curing conditions. In one case, the hydration was executed under totally sealed conditions, so that no additional water was available to replace that consumed due to chemical shrinkage. In this case, empty porosity is created within the microstructure to account for the water "volume" lost due to chemical shrinkage [9]. In the second case, referred to as saturated/sealed curing, the hydration was executed under saturated conditions until the capillary porosity became depercolated, at which point all subsequent hydration was performed under sealed conditions. Under saturated conditions, no empty porosity is created within the microstructure during hydration, as it is assumed that all needed water is readily available from the external environment to replace that "lost" via chemical shrinkage. Previously, Powers has suggested the moist curing of field concrete only to the point where the capillary porosity depercolates [13], as subsequent curing beyond this may be of little value.

3 Results

3.1 Percolation and chemical shrinkage in cement pastes

At equivalent w/c ratios, the initial average interparticle spacing will be greater for a coarser cement system as can be seen in Fig. 2, subsequently presented in section 3.2. This will result in a greater degree of hydration being required to disconnect the capillary pore network. A quantitative comparison of depercolation of capillary porosity for the systems examined in this study is provided in Fig. 1. While the 5 pm system depercolates at a capillary porosity of about 0.21, the 30 pm system capillary pore network remains percolated down to a porosity of about 0.15. The addition of 10 % (replacement for cement on a mass basis) silica fume particles, much finer than the 30 pm cement, slightly shifts the percolation threshold to a higher porosity of about 0.16. Since water is easily imbibed into the cement paste before depercolation of the capillary porosity, the coarser cements would be expected to provide an enhanced "curability", as they will continue to imbibe water after the finer cements' pore networks have depercolated [8].

This shift in porosity percolation threshold will also influence the empty porosity created by chemical shrinkage and the resultant autogeneous shrinkage occurring in water-cured cement pastes. Table 1 summarizes the empty and water-filled porosity present after executing 5000 cycles (about 25,000 hours or 1040 days) of the hydration model for both saturated/sealed and sealed curing conditions. The empty porosity due to chemical shrinkage for the finer cement is greater than that for the coarser cement for two reasons. First, the increased hydration of the finer cement results in an increase in chemical shrinkage, particularly evident in the systems hydrated under sealed conditions. Second, because the finer cement switches from saturated to sealed curing (when the capillary porosity depercolates) at a higher capillary porosity, it produces a greater amount of empty porosity during the "sealed" hydration stage. At a degree of hydration of 0.59, equivalent to that ultimately achieved by the 30 pm cement, the empty porosity volume fraction of the 5 pm cement is 0.024, 60 % higher than that observed for the coarser cement.

In Table 1, the presence of 10 % silica fume is seen to result in a slight increase in the volume of empty porosity for both curing conditions, in agreement with previous simulation results [14]. While not directly addressed by the simulations, the cement PSD and inclusion of silica fume will also affect the pore size distribution of the hydrated cement paste. In two systems with equivalent total porosities and equivalent amounts of chemical shrinkage, the

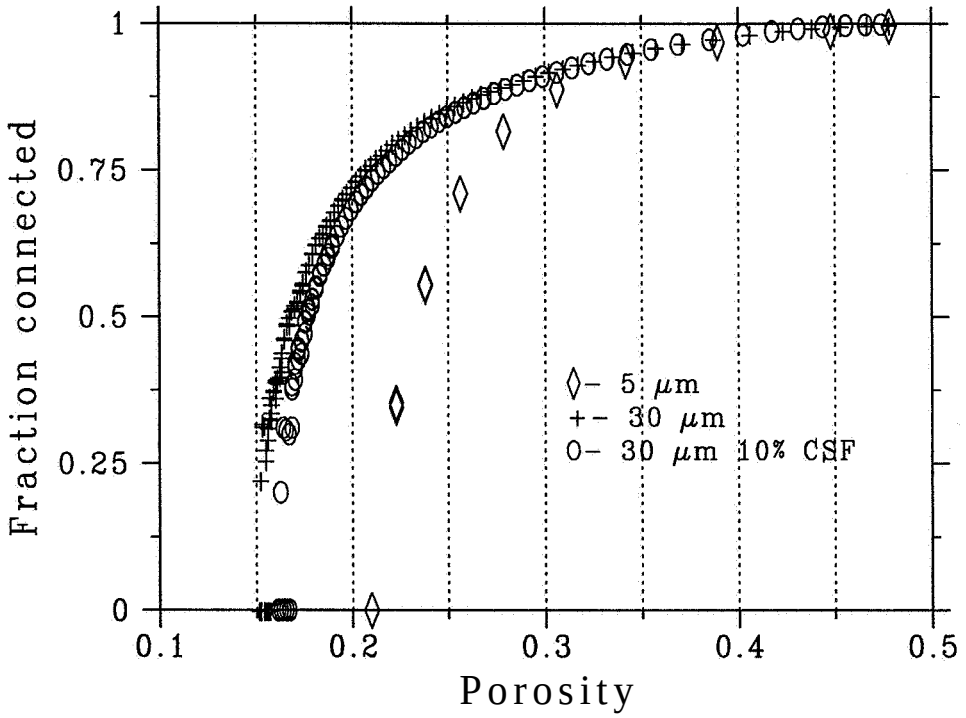

Fig. 1: Fraction connected porosity vs. total porosity for w/c=0.3 cement pastes of varying cement PSD and silica fume content. System size is 200 × 200 × 200 (0.5 μm/pixel).

system with finer pores will exhibit a greater reduction in internal RH and a greater amount of autogeneous shrinkage [15]. In general, a reduction in empty porosity (due to chemical shrinkage) and resultant autogeneous deformation should be observed when using a more coarsely ground cement [10].

3.2 Interfacial transition zone (ITZ) microstructure

In addition to affecting the overall percolation of the capillary porosity and the amount of empty porosity, the cement PSD also has a significant effect on the local microstructure of the ITZ. It has been previously illustrated using computer modelling that the thickness of the ITZ region will be on the order of the median diameter of the cement PSD [16]. Thus, the use of a coarser cement will increase the thickness of the ITZ region and also result in the presence of larger "pores" in this region. Since the largest pores empty first during self-desiccation, a large fraction of empty porosity may be created within the ITZ region

Table 1. Porosity of cement pastes after 5000 cycles of hydration (w/c=0.3)

PSD	Silica fume (%)	Empty porosity fraction	Water-filled porosity fraction	Degree of hydration
5	0	0.031	0.012	0.71
5[a]	0	0.077	0.009	0.64
30	0	0.015	0.083	0.59
30[a]	0	0.070	0.043	0.57
30	10	0.021	0.066	0.57
30[a]	10	0.074	0.048	0.52

[a] totally sealed hydration

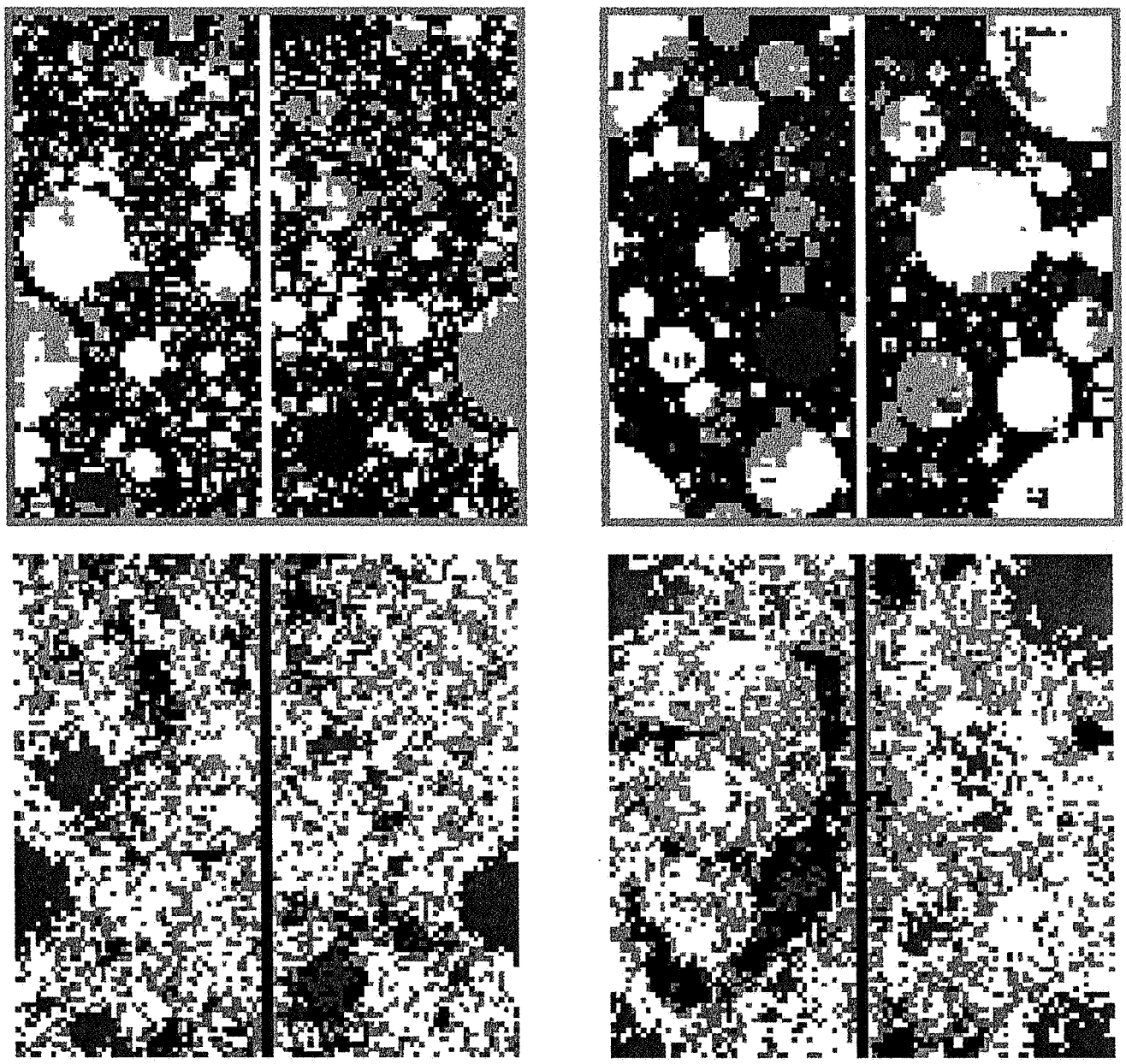

Fig. 2: Original and final 100×100 2-D microstructure images for upper left: original w/c=0.3 PSD=5 pm, upper right: original w/c=0.3 PSD=30 pm, lower left: final w/c=0.3 PSD=5 pm, and lower right: final w/c=0.5 PSD=30 pm. Final images are for hydration under totally sealed conditions. In the original images, phases from brightest to darkest are: C_3S, C_2S, C_3A, C_4AF, hemihydrate, and porosity. In the final images, phases from brightest to darkest are: C–S–H gel, other hydration products, unhydrated cement, and empty porosity. Central bar extending across the microstructure is the flat plate aggregate.

[10]. This is illustrated in Fig. 2 which shows 2-D plane sections from the initial and final microstructures (from the 3-D model) for the two different cement PSDs. One can clearly observe the larger pore sizes present with the coarser cement, particularly in the ITZ region. The final images show that often these larger pores empty during hydration, creating an ITZ microstructure that is significantly different from that of the bulk cement paste. While these large pores are likely detrimental from a strength viewpoint, they may actually reduce the autogeneous shrinkage in these systems, as for the same amount of chemical shrinkage, the emptying of larger pores will result in less of a decrease in internal RH and thus, less measurable autogeneous shrinkage [15].

A quantitative analysis of this phenomena is provided in Fig. 3, which provides plots of the water-filled and empty capillary porosity as a function of distance from the aggregate surface for the initial and final microstructures. The appearance of a local maxima at a distance of about 5 pixels in the final empty porosity curves, particularly prominent for the systems cured under totally sealed conditions, corresponds to the large empty pores observed in the final microstructural images provided in Fig. 2. The peak is seen to be much higher for the coarser cement, due to the inefficient packing of the cement particles in the vicinity of the aggregate surface and the larger average pore size. For the water-filled porosity, the profile increases basically in a monotonic fashion as the aggregate is approached, due both to the initial cement particle packing and the one-sided growth effect [17]. For the empty porosity, however, the value actually decreases very near to the aggregate surface, as the pores a finite distance from the aggregate are first emptied during self-desiccation and a "thin (several pixel) water film" remains on the aggregate surface to be filled in by subsequent hydration.

4 Conclusions

The effects of cement particle size distribution on self-desiccation in cement pastes have been examined using computer simulations. Coarser cements influence self-desiccation in these systems by:

1. increasing the hydration needed to depercolate the capillary pore network,
2. increasing the average pore size due to particle spacing considerations, and
3. modifying the interfacial transition zone microstructure by introducing more and larger pores which may remain as empty pores following hydration.

All of these effects should result in a reduction in the measured autogeneous shrinkage of cement pastes and concretes produced using a coarser cement, in agreement with the experimental results of Jensen [18].

5 References

1. Powers, T.C. (1935) Absorption of water by portland cement paste during the hardening process. *Industrial and Engineering Chemistry,* Vol. 27. pp. 790-4.
2. Gause, G.R., and Tucker Jr., J. (1940) Method for determining the moisture condition in hardened concrete. *Journal of Research of the National Bureau of Standards,* Vol. 25. pp. 403-16.
3. Hua, C., Acker, P., and Erlacher, A. (1995) Analyses and models of the autogenous shrinkage of hardening cement paste: I. Modelling at macroscopic scale. *Cement and Concrete Research,* Vol. 25, No. 7. pp. 1457-68.
4. Nilsson, L.O. (1994) private communication.

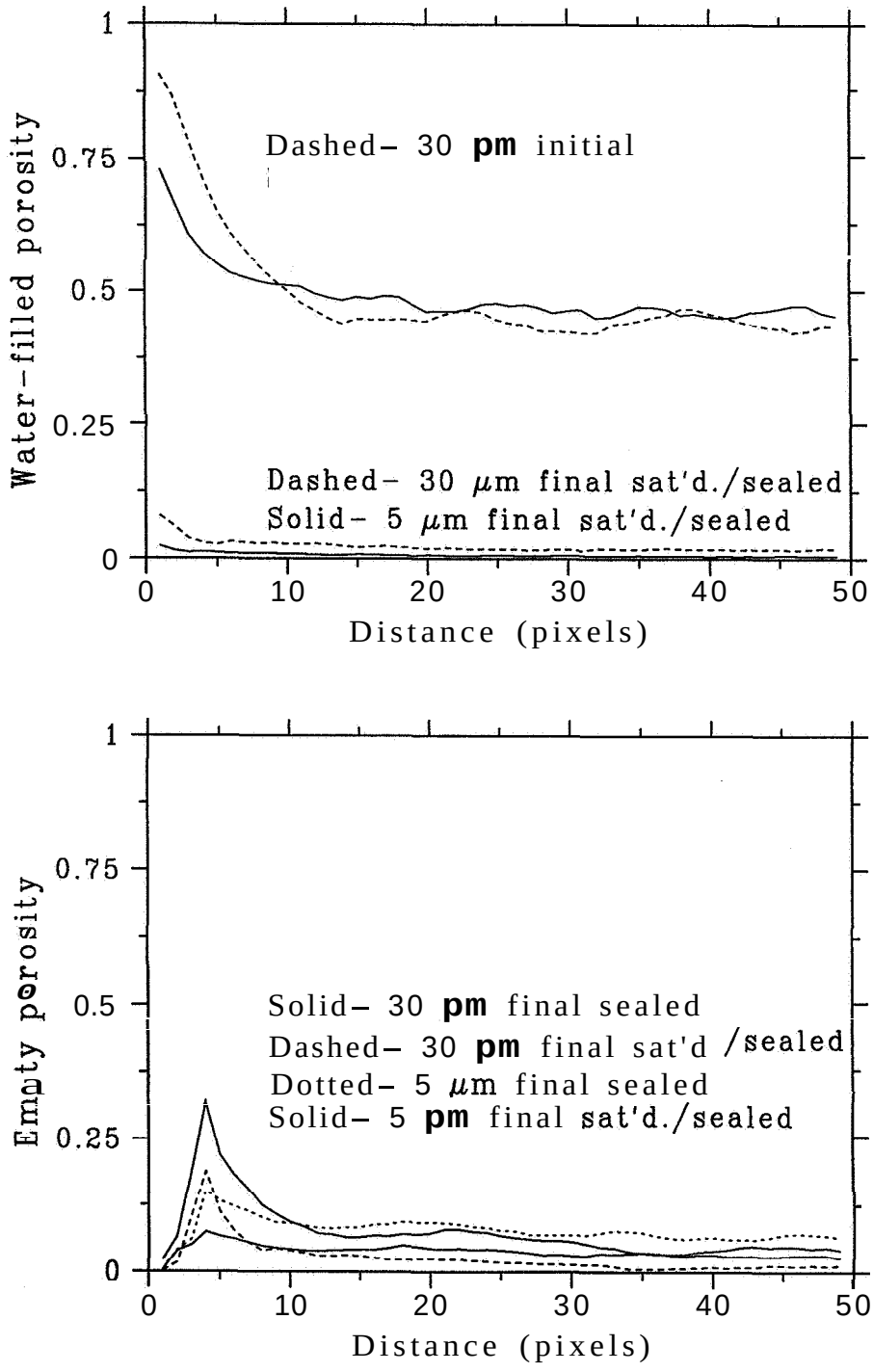

Fig. 3: Water-filled (upper) and empty (lower) porosity volume fractions vs. distance from aggregate, w/c=0.3. Final curves for empty porosity are for hydration under sealed or saturated/sealed curing conditions.

5. Geiker, M. (1983) Studies of portland cement hydration: Measurements of chemical shrinkage and a systematic evaluation of hydration curves by means of the dispersion model, Ph. D. Thesis, Technical University of Denmark.
6. Powers, T.C. (1959) Capillary continuity or discontinuity in cement pastes. PCA Bulletin, No. 10. pp. 2-12.
7. Bentz, D.P., and Garboczi, E.J. (1991) Percolation of phases in a three-dimensional cement paste microstructural model. Cement and Concrete Research, Vol. 21. pp. 324-44.
8. Bentz, D.P., and Haecker, C.J. (1999) An argument for using coarse cements in high performance concrete. to appear in Cement and Concrete Research, Vol. 29.
9. Bentz, D.P. (1997) Three-dimensional computer simulation of portland cement hydration and microstructure development. Journal of the American Ceramic Society, Vol. 80, No. 1. pp. 3-21.
10. Bentz, D.P., Garboczi, E.J., Haecker, C.J., and Jensen, O.M. (1999) Effects of cement particle size distribution on performance properties of cement-based materials, submitted to Cement and Concrete Research.
11. Bentz, D.P., Waller, V., and DeLarrard, F. (1998) Prediction of adiabatic temperature rise in conventional and high-performance concretes using a 3-D microstructural model. Cement and Concrete Research, Vol. 28, No. 2. pp. 285-97.
12. Lu, P., Sun, G.K., and Young, J.F. (1993) Phase composition of hydrated DSP cement pastes. Journal of the American Ceramic Society, Vol. 76. pp. 1003-7.
13. Powers, T.C. (1947) A discussion of cement hydration in relation to the curing of concrete. Proc. *of* the Highway Research Board, Vol. 27. pp. 178-88.
14. Bentz, D.P., Snyder, K.A., and Stutzman, P.E. (1997) Microstructural modelling of self-desiccation during hydration, in Self-Desiccation and Its Importance in Concrete *Technology* (eds. B. Persson and G. Fagerlund), Lund University, Lund, Sweden, pp. 132-40.
15. Jensen, O.M., and Hansen, P.F. (1996) Autogeneous deformation and change of the relative humidity in silica fume-modified cement paste. ACI Materials Journal, Vol. 93, No. 6. pp. 539-43.
16. Bentz, D.P., Schlangen, E., and Garboczi, E.J. (1995) Computer simulation of interfacial zone microstructure and its effect on the properties of cement-based composites, in *Materials* Science of Concrete *IV* (eds. J.P. Skalny and S. Mindess), The American Ceramic Society, Westerville, OH, pp. 155-99.
17. Garboczi, E.J., and Bentz, D.P. (1991) Digital simulation of the aggregate-cement paste interfacial zone in concrete. Journal of Materials Research, Vol. 6, No. 1. pp. 196-201.
18. Jensen, O.M. (1995) Influence of cement type upon autogeneous deformation and change of the relative humidity. Technical Note, University of Aberdeen.

EVALUATION OF UNDER-PRESSURE IN THE PORE WATER OF SEALED HIGH PERFORMANCE CONCRETE, HPC

B. PERSSON
Division of Building Materials, Lund University, Box 118, 221 00 Lund, Sweden

Abstract
This article outlines an experimental and numerical study on the estimation of under-pressure in the pore water of HPC. For this purpose 96 sealed cylinders made of 8 HPCs with w/c varying between 0.25 and 0.38, based on low-alkali Portland Cement, were manufactured. Five or ten per cent silica fume was used in the HPCs as calculated on the basis of the cement content. Basic creep was studied on two thirds of the cylinders and autogenous shrinkage on the rest. The measurement was done from 0.01 s until 3 years' age. Parallel studies of hydration, strength and internal relative humidity were performed on 450 cubes manufactured from the same batches that were used for the cylinders. The results indicated high influence of w/c, age and silica fume on the under-pressure in the pore water of HPC. The work was performed at Division of Building Materials, Lund Institute of Technology, Sweden 1992-1995.
Keywords: Autogenous shrinkage, Basic creep, Concrete, High Performance Concrete, Hydration, Relative Humidity, Self-desiccation, Silica fume, Strength.

1 Introduction, objective and general layout of the study

1.1 Introduction

Self-desiccation of HPC causes a phenomenon called autogenous shrinkage, an unfavourable property of HPC. Autogenous shrinkage and consequently also self-desiccation occurs even under wet conditions due to the low permeability of HPC. The self-desiccation of HPC is more pronounced with decreased water content of the HPC [1]. The smaller the water-cement ratio, the larger is also the autogenous shrinkage due to self-desiccation. A method for calculating the autogenous shrinkage based on the internal relative humidity was proposed [2].

1.2 Objective

It was the objective of the work to estimate a relationship between the under-pressure in pore water of HPC, RH, basic creep and shrinkage. The influence of the HPC mix design on the pore under-pressure was to be studied, i.e. effect of silica fume and w/c.

1.3 General layout of the study

Table 1 shows the time schedule for the work [3].

Table 1. Time-schedule for the work

Year	1992				1993				1994				95
Quarter* of *year	***1***	***2***	***3***	***4***	***1***	***2***	***3***	***4***	***1***	***2***	***3***	***4***	***1***
Autogenous shrinkage	-	---	---	---	---	---	---	---	---	---	---	---	---
Compressive strength	-	---	---	---	---	---	---	---	---	-	---	---	---
Hydration	-	---	---	---	---	---	---	---	---	-	---	---	---
Internal relative humidity	-	---	---	---	---	---	---	---	---	-	---	---	---
Long-term loading	-	---	---	---	---	---	---	---	---	---	---	---	---
Quasi-instantaneous load	-	---	---	---	---	-							
Short-term creep	-	---	---	---	---	-							

A new method of rapid loading and simultaneous registration of measurements was developed. The age of the HPC was 1, 2 or 28 days at the commencement of testing. At 1 and 2 days' age a stresslstrength ratio of 0.6 applied; at 2 and 28 days 0.3. The loading, as much as 100 kN, was applied very rapidly within 0.01 s. The quasi-instantaneous loading gave the possibility of estimating the initial strain (true modulus of elasticity) and very early creep [4]. This was of great interest for prestressed structures when the loading from the strands is transferred to the HPC at early ages. The rapid loading method also separated the elastic strain of the HPC from the viscous elastic and the plastic part. The early creep rate seems to be constant at a certain age of the HPC. It was then fairly independent of the water content. The initial strain at rapid load was dependent on w/c. It also was fairly linear related to the square-root strength which coincided well with the properties of normal HPC.

After the quasi-instantaneous loading of the cylinders, the deformations were continuously studied over a period of 66 hours. The results showed astonishing parallelism to the compliance for different types of mature HPCs. The compliance could be expressed by similar functions that were fairly independent of wlc. The differences in compliance due to the maturity of the HPC were remarkably large, The creep of a young HPC was more than twice as much as that of an old HPC at the same stresslstrength ratio. At the same age, 2 days, there also was some influence of the stresslstrength ratio on the size of the creep.

The long-term compliance has been studied for at least 1200 days for 3 of the HPCs (12 cylinders). Twenty HPC cylinders of 8 HPCs studied in the spring-loading devices were unloaded after at least 1 year of creep deformation. The elastic recovery strain after unloading was more or less identical to the same property after the short-term tests, i.e. the modulus of elasticity was more or less linear related to the square-root strength. It was possible to distinguish the plastic creep from the elastic and the viscous elastic after the long-term creep period as the same HPC batch was used to cast cylinders for the short-term and the long-term tests [3]. When the elastic strain exceeded 0.5 per mil, the increased strain seemed to be only of the plastic, i.e. remaining type. The creep rate was smaller at 10% silica fume in the HPC than at 5% silica fume of the cement content. The rate of creep was larger, even after long time, for HPCs that were loaded at early ages than for mature HPCs.

2 Experimental

2.1 Material

Aggregates of crushed quartzite and natural sand of gneiss apply for six recipes. In the studies only the low-alkali Portland cement was used. The air-entrainment varied between 1 and 7 % calculated on the total volume of the HPC. Superplasticiser based on melamine formaldehyde applies for all recipes. In two recipes silica fume slurry applies together with crushed granite and natural sand based on granite. Table 2 shows the main characteristics of the aggregate [5], Table 3 in turn shows the composition of the cement [6] and Table 4, finally shows the mix design of the HPCs in the study [3].

Table 2 Main characteristics of the aggregates [5].

Material/ characteristics	Young's modulus	Compressive strength	Split strength	Ignition losses
Granite, Norrkoping	61.2 GPa	153 MPa	9.6 MPa	1.67%
Natural sand, Bålsta	59.1 GPa	234 MPa	14 MPa	1.95 %
Natural sand, Åstorp				0.79 %
Pea gravel, Toresta				1.62 %
Quartzite sandstone, Hardeberga	60.2 GPa	332 MPa	15 MPa	0.28 %

Table 3. Chemical composition of cement resolved by X-ray fluorescence analysis.

X-ray fluorescence analysis:	
CaO	64.9 %
SiO_2	22.2 %
Al_2O_3	3.36 %
Fe_2O_3	4.78 %
MgO	0.91 %
ICP-analysis:	
K_2O	0.56 %
Na_2O	0.04 %
LECO aperture:	
Ignition losses at 950 °C	0.63 %
SO_3	2.00 %
Physical properties:	
Specific surface according to Blaine	302 m^2/kg
Density	3220 kg/m^3
Setting time:	
Vicat	135 min.
Water	26.0 %
Standard test (prisms 40x40x160 mm):	
1 day	11.0 MPa
2 days	20.2 MPa
7 days	35.8 MPa
28 days	52.6 MPa

Table 4. HPC mix composition, etc (kg/m^3 dry material, etc.; R= silica fume slurry)

Material/Mix	50	90	90L	90R	110	130	130R	150
Air-entraining agent, Cementa 88L (vinsole resin)	0.06		0.04					
Cement, Degerhamn Anläggning Standard	440	445	450	450	500	525	480	540
Granite, Norrkoping 12-16							1065	
Natural sand, Bålsta 0-8				780			770	
Natural sand, Åstorp 0-8	840	850	790		765	765		750
Pea gravel, Toresta 8-16				1075				
Quartzite sandstone, Hardeberga 8-12	470							
Quartzite sandstone, Hardeberga 12-16	470	965	930		1020	1005		1060
Silica fume, granulated	22	45	45		50	53		54
Silica fume slurry				23			48	
Superplasticiser, Cementa Flyt 92 (melamine formaldehyde)	3.3	5.5	4.3	5.3	4.8	6.4	7.8	9.6
Water-cement ratio	0.38	0.37	0.37	0.33	0.31	0.30	0.30	0.25
Air-content (volume-%	7.0	0.9	4.5	0.9	0.9	0.9	0.9	1.0
Density (kg/m^3)	2250	2475	2380	2480	2500	2510	2520	2540
Slump (mm)	140	160	170	145	200	230	45	45
28-day strength (MPa)	60	110	92	101	127	137	122	143
1-year strength (MPa)	69	124	108	115	139	144	135	162
2-year strength (MPa)		127	121	115	145	149	131	162

2.2 Specimen

The circular moulds had an inner diameter of 55.5 mm and a length of 300 mm. Six cast-in items were placed 25 mm from the ends of the mould and 2 items on opposite sides at the middle of the mould. Three-mm bolts through the steel fixed the items. The cast-in items had a diameter of 8 mm and a depth of 16 mm. They were provided with flanges and edged to avoid movement in the HPC. The cube moulds were also made of steel. Thermo couples were cast in one cylinder and one cube out of each batch. After measuring air-entrainment and density, the moulds were filled up under vibration. The cylinders were levelled off at the upper end. A 10-mm steel plate was fixed and vibrated to the end of the cylinder horizontal (lying down). The ends of the cylinder were very smooth and no grinding was necessary. All specimens were placed in a rubber container to avoid losses of moisture. After casting and placing in the rubber container the specimens were stored in a 20-"C climate chamber. The endothermic period of about 7 h appeared, followed by the exothermic one.

2.3 Procedure of manufacturing the specimens

After 16 hours the bolts were loosened from the cast-in items and the moulds removed. The specimens (both cylinders and cubes) were then insulated by a 2-mm vulcanised butyl rubber cloth. Butyl rubber cloths were placed at the ends of the cylinder and removed in some cases right before testing. Clamp hoses were placed at the end of the cylinders for avoiding moisture losses. The specimens were stored in a 20-"C climate chamber. Some temperature movements took place in the HPC due to the heat of hydration. The maximum temperature was 24" C about 20 h after casting.

2.4 Compressive strength, RH and hydration

After demoulding the butyl-rubber cloth, the cube was measured and tested for compressive strength. The ultimate stress was applied at a rate of 1 MPa/s in a Seidner testing machine. Directly after the compressive strength tests were performed, fragments of the HPC (minimum 5 mm in size) were collected in 100-ml glass test tubes in order to measure RH. The tubes were filled up to 213. Then rubber plugs tightened them. The tubes with the fragments were kept in a 20-"C room. A Protimeter dew point meter was used to measure the internal relative humidity, RH. The probe of the dew point meter was entered into the test tube and rubber-tightened to the glass. Since HPC contains very little moisture the required period of measurement to obtain a stable value (equilibrium between the moisture in the air in the pores of the HPC and the air around the sensor of the dew point meter) of RH was at least 22 hours. The minimum period was thus set at 24 hours. Calibration of the dew point meters took place [7].

The specimen for measurement of hydration consisted of an eighth of a 100-mm cube. Right after testing the compressive strength, the bottom eighth of the cube (0.3 kg) was further crushed, divided into two parts and placed in small containers. A fan in a 105-"C oven then immediately dried the HPC fragments. The fragments were less than 5 mm in size. After at least one week of intensive drying the fragments were ignited at 1050 °C for 16 hours. Before any weighing the material was cooled in an exsiccator. By compensating for losses during the ignition of the different materials according to the degree of hydration, w_n/c, was established [8].

2.5 Quasi-instantaneous, short-term and long-term basic creep and shrinkage

As mentioned above, it is of great interest to study the quasi-instantaneous deformations of HPC [4]. Applying the loading very rapidly would be very useful for research on creep of HPC. However, for mature HPC no differences seem to exist depending on whether the loading is rapidly applied or not [9]. At early age and at a high stresslstrength ratio plastic deformations probably dominate the deformation. Figure 1 shows the specimen used in the experiment with quasi-instantaneous deformations. The measurement was carried out in an MTS machine on four points outside the specimen by Schlumberger displacement and gauging transducers.

The quasi-instantaneous loading was immediately followed by studies of the basic creep during 66 h. The research was carried out in an MTS machine. The same conditions applied as in Figure 1. The testing room was air-conditioned to avoid displacements due to temperature movements. Figure 2 shows the specimen that was used in long-term creep studies performed in spring-loading devices. Measurements were taken on 3 + 3 points by Huggenberger or Proceq mechanical devices.

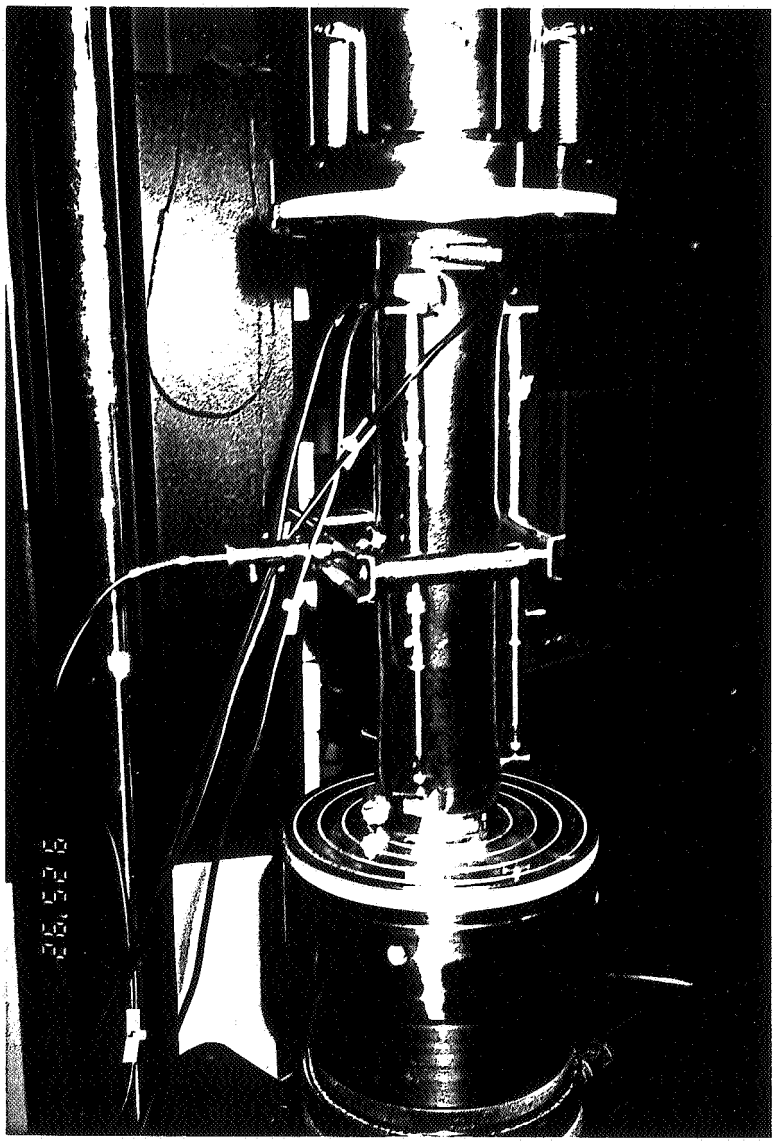

Figure 1. Specimen used in the quasi-instantaneous and short-term creep studies [3].

Parallel to the commencement of the quasi-instantaneous loading in the MTS machine an identical specimen was placed in the spring-loading device, Figure 2. The weight of the specimen was taken before it was placed. The measuring points were stiffly connected to the steel cast-in items in the specimen by pin bolts of 3-mm diameter. The length between the longitudinal measuring points was 250 mm. The steel plates of the device were adjusted horizontal and parallel before the location of the specimen. The position of the cylinder was adjusted to avoid eccentricities in the device. The moisture stability in the specimen was secured by sealing compounds between the butyl-rubber clothing of the specimen and the steel plate of the device. A total of 32 specimens cast of 8 different HPCs were used in parallel studies on autogenous shrinkage. The identical same batches of HPC were used as in the experiments on quasi-instantaneous loading.

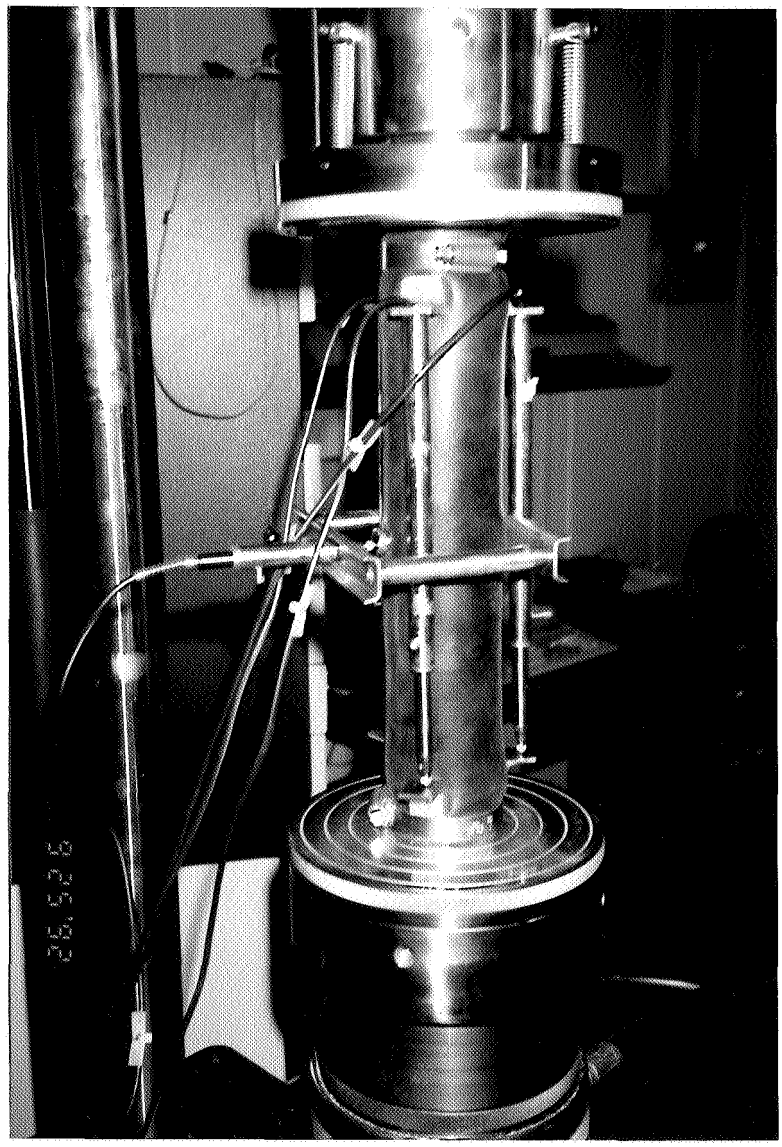

Figure 1. Specimen used in the quasi-instantaneous and short-term creep studies [3].

Parallel to the commencement of the quasi-instantaneous loading in the MTS machine an identical specimen was placed in the spring-loading device, Figure 2. The weight of the specimen was taken before it was placed. The measuring points were stiffly connected to the steel cast-in items in the specimen by pin bolts of 3-mm diameter. The length between the longitudinal measuring points was 250 mm. The steel plates of the device were adjusted horizontal and parallel before the location of the specimen. The position of the cylinder was adjusted to avoid eccentricities in the device. The moisture stability in the specimen was secured by sealing compounds between the butyl-rubber clothing of the specimen and the steel plate of the device. A total of 32 specimens cast of 8 different HPCs were used in parallel studies on autogenous shrinkage. The identical same batches of HPC were used as in the experiments on quasi-instantaneous loading.

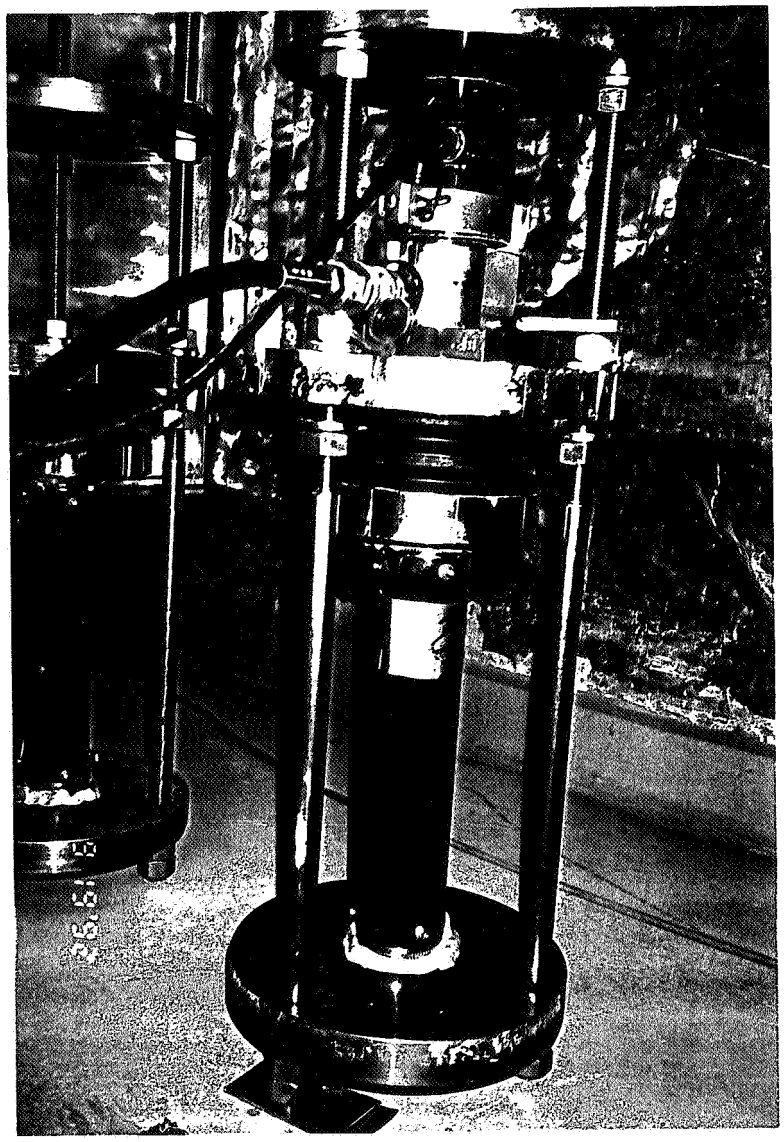

Figure 2. Specimen and equipment used in the long-term experiments.

After demoulding and insulation by butyl rubber clothing, 6 stainless steel screws were fixed into cast-in items in the cylinder. Measurements were taken on three sides of the cylinder on a length of 250 mm within 1 h from demoulding [10]. Later, after cooling, the specimen was placed in a 20-"C climate chamber. A Huggenberger or/and a Proceq mechanical device was used. Gloves were used for avoiding temperature effects on the devices. Figure **3** shows details of the measure point of the specimen. In spite of all the careful precautions some faults existed, causing unforeseen water losses. The specimens were continuously weighed to detect this loss. Possible absorption of water in the butyl rubber insulation would affect the total weight of the specimen. Temperature movements had a small effect on the measurements of the autogenous shrinkage. Effects of hydration heat were avoided by obtaining the measurements at 20 °C. A thermo couple was cast in the specimen and the temperature was followed as the first measurement was performed.

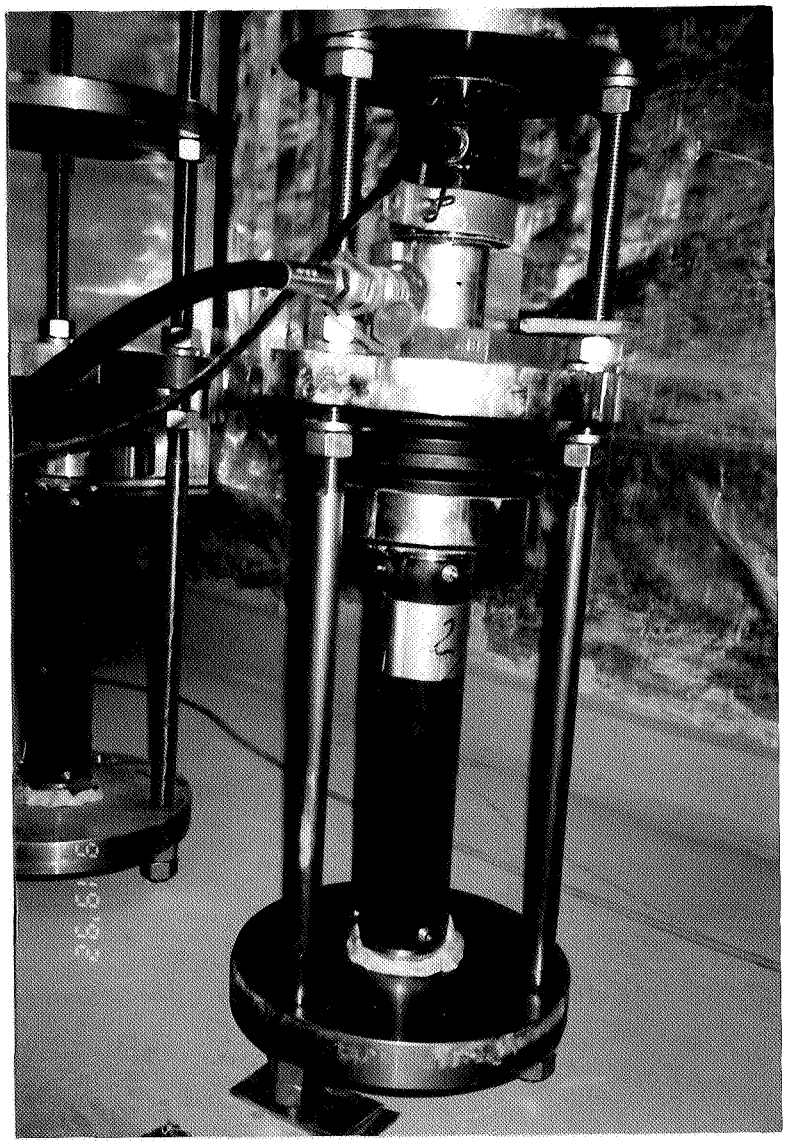

Figure 2. Specimen and equipment used in the long-term experiments.

After demoulding and insulation by butyl rubber clothing, 6 stainless steel screws were fixed into cast-in items in the cylinder. Measurements were taken on three sides of the cylinder on a length of 250 mm within 1 h from demoulding [10]. Later, after cooling, the specimen was placed in a 20-"C climate chamber. A Huggenberger or/and a Proceq mechanical device was used. Gloves were used for avoiding temperature effects on the devices. Figure 3 shows details of the measure point of the specimen. In spite of all the careful precautions some faults existed, causing unforeseen water losses. The specimens were continuously weighed to detect this loss. Possible absorption of water in the butyl rubber insulation would affect the total weight of the specimen. Temperature movements had a small effect on the measurements of the autogenous shrinkage. Effects of hydration heat were avoided by obtaining the measurements at 20 °C. A therrno couple was cast in the specimen and the temperature was followed as the first measurement was performed.

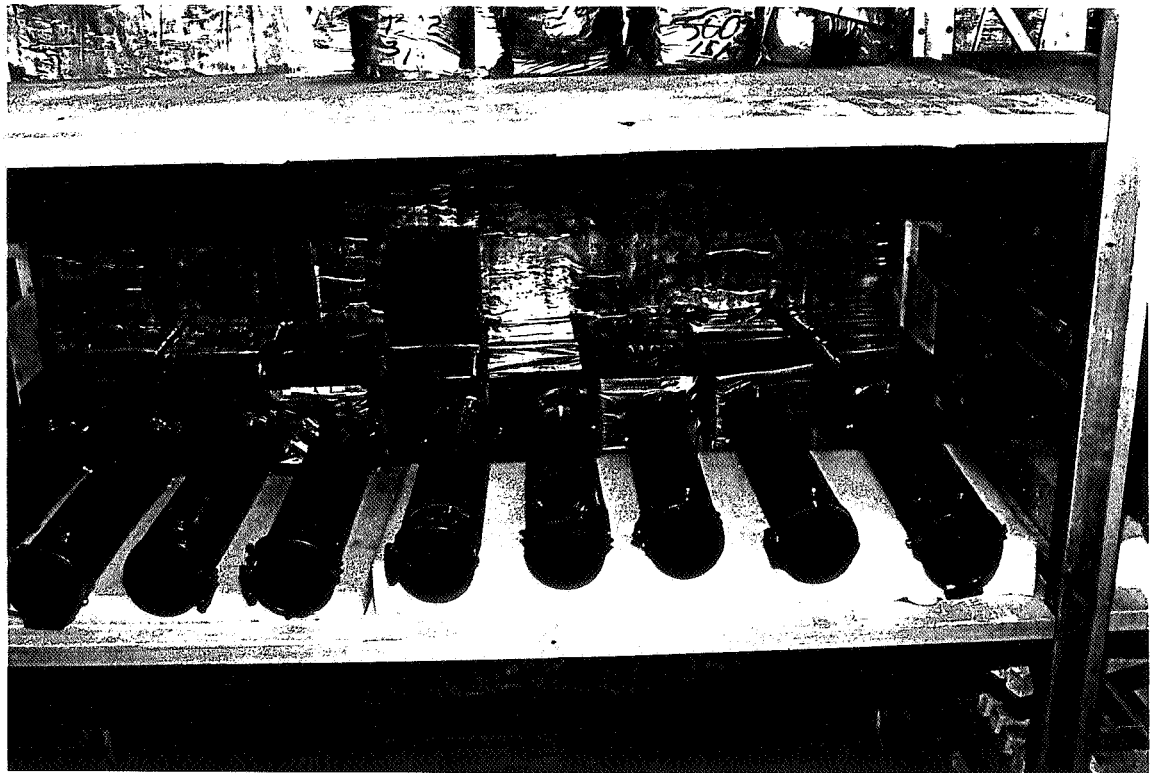

Figure 3. Specimens for studies of autogenous shrinkage. Cubes for strength tests.

3 Results

3.1 Compressive strength

Figure **4** shows the development of strength in the HPCs.

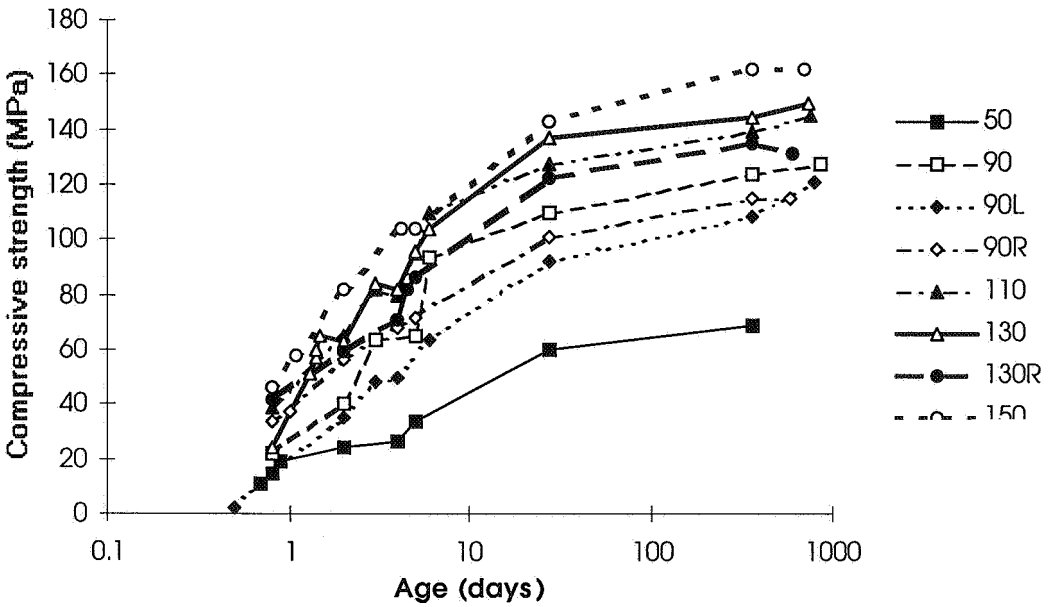

Figure 4. Developments of strength in the HPCs. Notations are given in Table 4 [3].

Figure 3. Specimens for studies of autogenous shrinkage. Cubes for strength tests.

3 Results

3.1 Compressive strength

Figure 4 shows the development of strength in the HPCs.

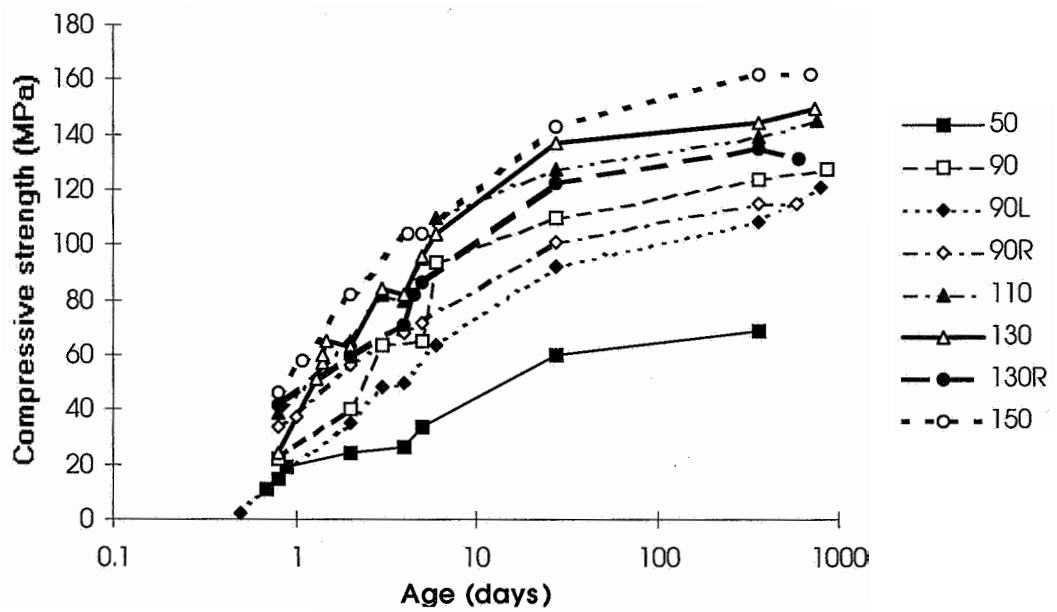

Figure 4. Developments of strength in the HPCs. Notations are given in Table 4 [3].

3.2 RH

Figure 5 shows the development of RH in the HPCs.

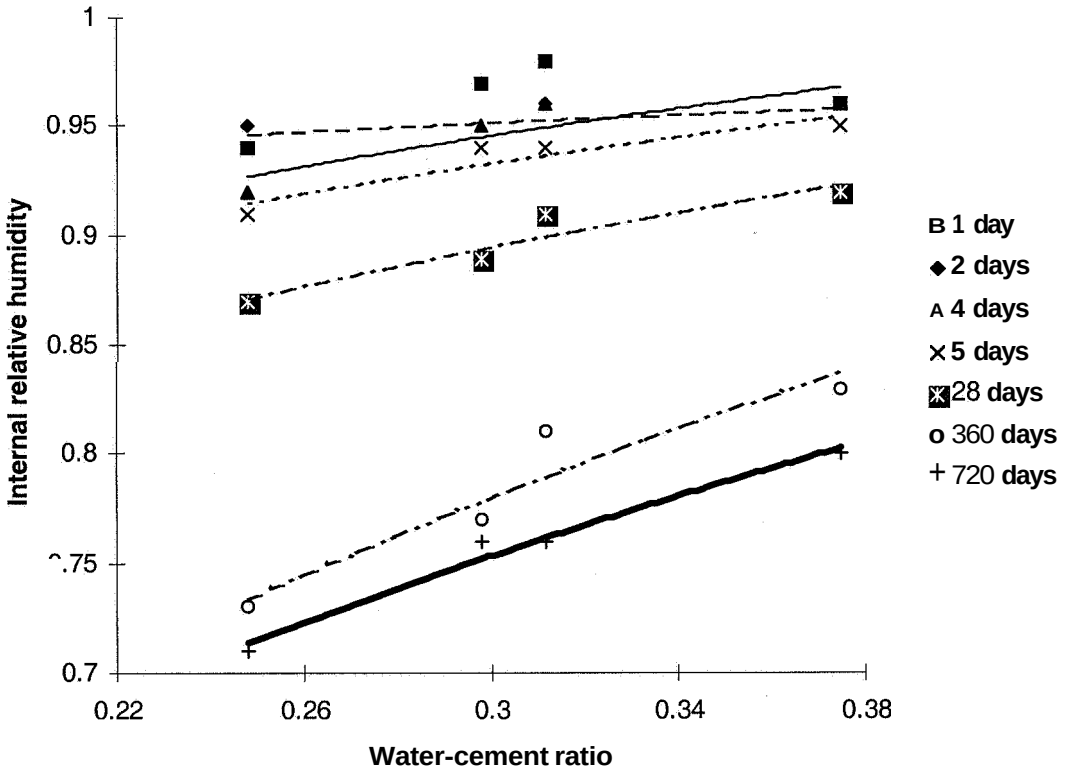

Figure 5. Developments of RH in the HPCs. Notations are given in Table 4 [3].

Assuming an average RH decrease of 18% between 5 days and 2 years of age, the following expression applies for the self-desiccation (at an age less than about ½ year, a correction, A@for the recipes 90R and 130R with silica fume slurry applied):

$$\phi = 0.38\cdot[w/(c+2\cdot s) + 2.4 - 0.1\cdot \ln t] - \Delta\phi \qquad (1)$$

c denotes the cement content (kg/m^3)
s denotes the content of silica fume (kg/m^3)
t denotes the age of the HPC (days)
w denotes the water content (kg/m^3)
$\Delta\phi$ = - 0.03 for the recipe 90R at an age less than about ½ year
$\Delta\phi$ = - 0.04 for the recipe 130R at an age less than about ½ year

The rate of self-desiccating was expressed by the following equation (day^{-1}):

$$d\phi/dt = 0.038/t \qquad (2)$$

3.3 Hydration

Figure 6 shows the degree of hydration versus age for the HPCs in study [3].

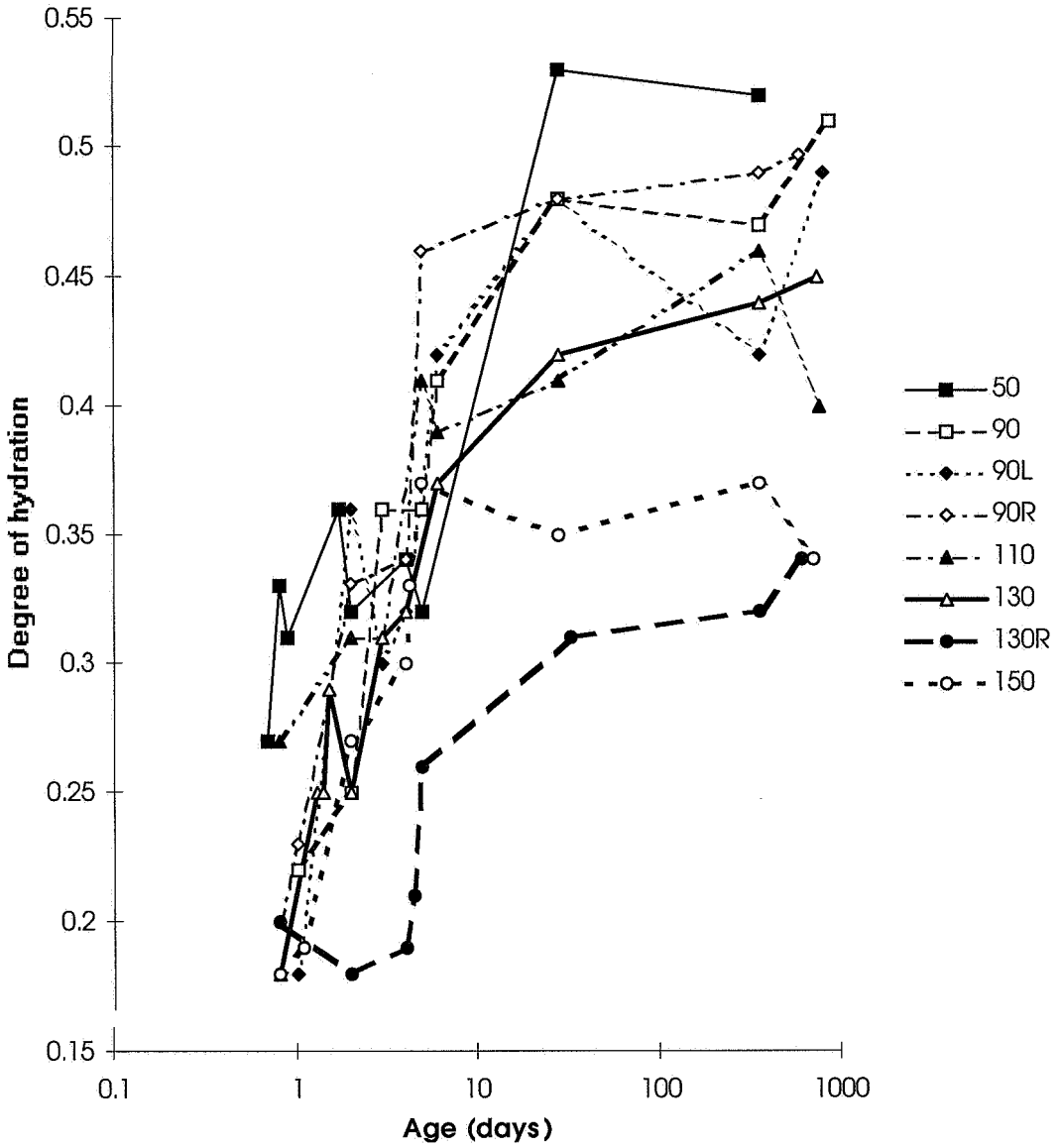

Figure 6. Degree of hydration versus age for the HPCs in study [3], Table 4.

The following expression applied for the 28-day relative hydration, w_n/w_{28}:

$$w_n/w_{,28} = k_w \cdot 0.17 \cdot [2.25 - w/(c+2 \cdot s)] \qquad (3)$$

k_w = 0.75 for the recipe 90R
k_w = 1.09 for the recipe 130R

The resisting symbols in equation (3) are given above.

3.4 Quasi-instantaneous basic creep

Figure 7 shows the quasi-instantaneous creep versus time of loading for the HPCs [3]. Similar results were also obtained for all the HPCs at early ages [3].

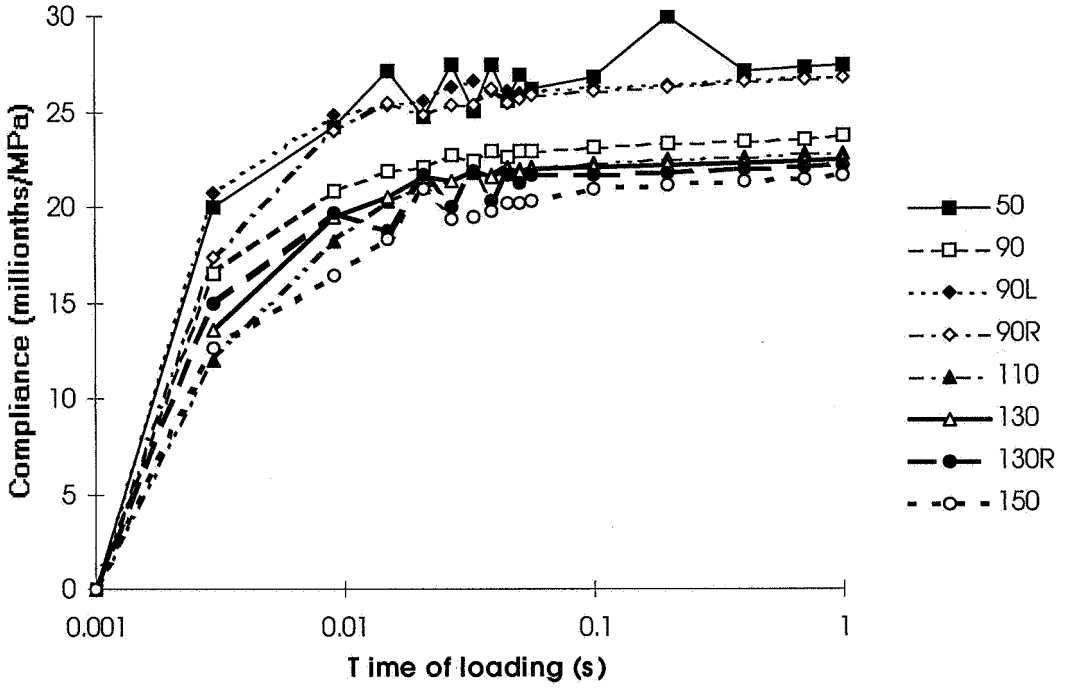

Figure 7. Quasi-instantaneous creep versus time of loading for the HPCs, Table 4.

3.5 Short-term basic creep

Figure 8 shows the short-term creep versus time of loading for the HPCs [3]. Results of short-term creep were also obtained for the HPCs at early ages [3].

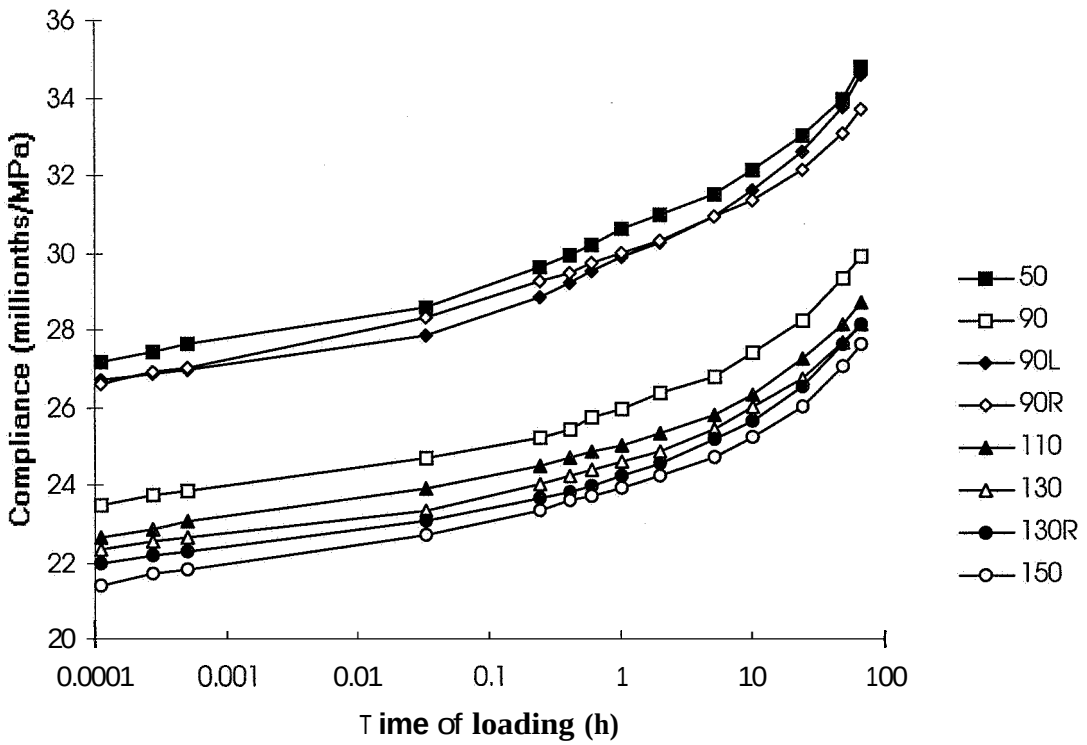

Figure 8. Short-term creep versus time of loading for the HPCs, Table 4.

3.6 Long-term basic creep

Figure **9** shows the long-term creep versus time of loading for the HPCs [3]. Results of long-term creep were also obtained for HPCs that were loaded at early ages [3].

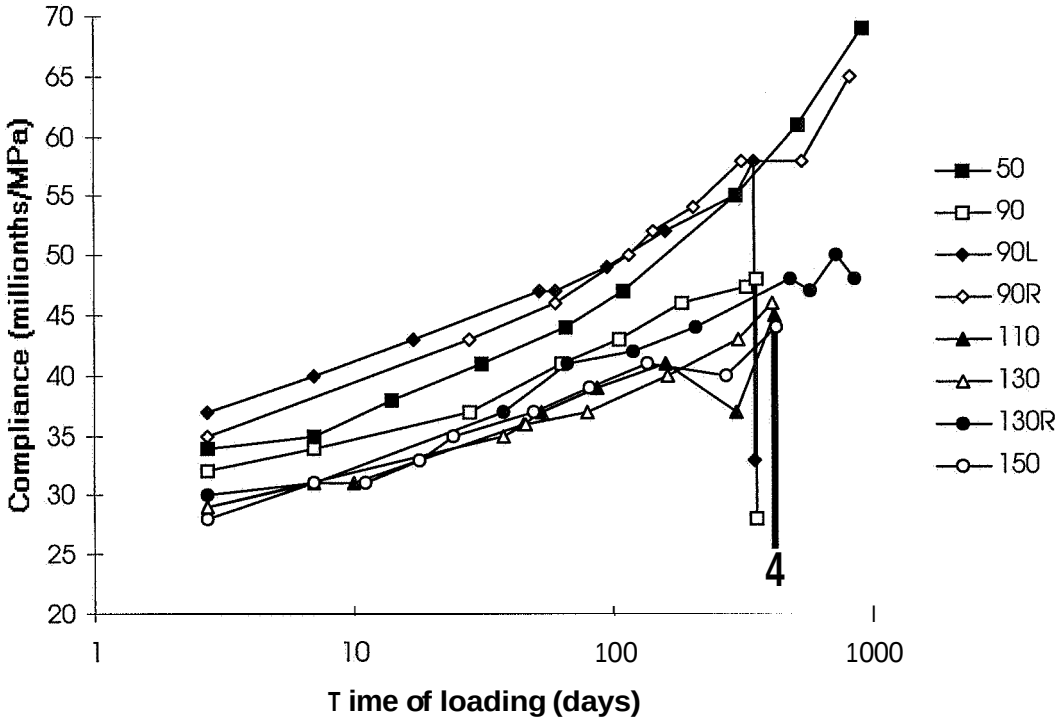

Figure 9. Long-term creep versus time of loading for the HPCs, Table 4.

3.7 Autogenous shrinkage

Figure **10** shows the autogenous shrinkage versus RH for the HPCs [3].

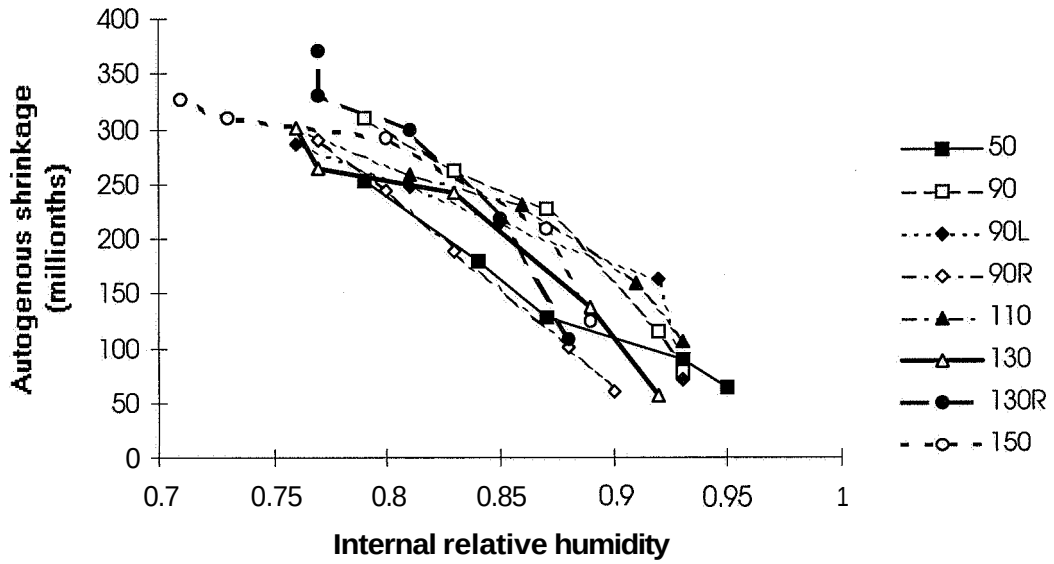

Figure 10. Autogenous shrinkage versus RH for the HPCs [3], Table 4.

4 Analysis

4.1 General

The interaction between autogenous shrinkage and compliance, J, was estimated, i.e. the effect of compliance on autogenous shrinkage. At basic creep with no external loading the forces are balanced within the HPC. The interaction between the autogenous shrinkage and the compliance may be written (millionths/MPa):

$$J = \varepsilon_{aut}/\sigma \qquad (4)$$

J_{aut} denotes compliance (millionths/MPa)
ε_{aut} denotes the autogenous shrinkage strain (millionths)
σ denotes the stress in the HPC caused by autogenous shrinkage (MPa)

Two of the parameters, compliance, J, and deformation due to autogenous shrinkage, ε_{aut}, were measured. The third parameter, the internal loading causing an internal stress in the HPC pores due to the decrease of relative humidity, RH, had its origin in the self-desiccation of the HPC, Chapter 3.2. The self-desiccation, ϕ, in turn, was dependent on w/c, the content of silica fume, initially also the type of silica fume (granulated silica fume or silica fume slurry) and the time as shown in Chapter 3.2 above. The time of self-desiccation was replaced with the degree of hydration, α, as known from Chapter 3.3 above. The self-desiccation, Q was caused by the air-filled pore volume created as the product of the degree of hydration, a, and the cement content of the HPC, c, Figure 11, [11]:

$$\delta w_n \approx 0.063 \cdot \alpha \cdot c \qquad (5)$$

c denotes the cement content of the HPC (Mg/m^3)
α denotes the degree of hydration
δw_n denotes the air-filled pore volume caused by the chemical shrinkage

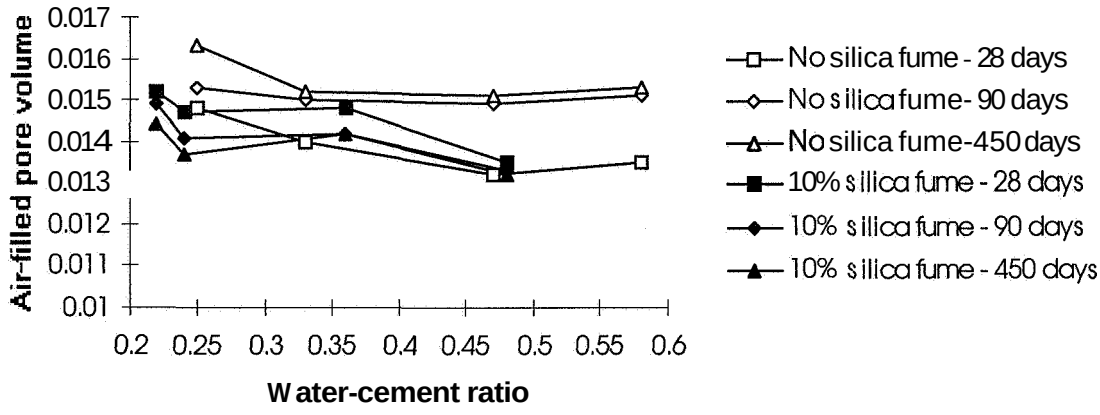

Figure 11. Self-desiccation, Q, was caused by the air-filled pore volume created as the product of the degree of hydration, a, and the cement content of the HET, c [11].

4.2 Internal forces from the pore water

Since the air-filled pore volume most probably initially was a sphere, it was transferred into a specific area to obtain the effect of the decrease of the internal relative humidity on the autogenous shrinkage [12]:

$$A_{\delta wn} = 4\cdot\pi\cdot[(0.063\cdot\alpha\cdot c)/(4\cdot\pi)]^{2/3} \approx (\alpha\cdot c)^{2/3}/140 \quad (6)$$

c denotes the cement content of the HPC (Mg/m^3)
$A_{\delta w_n}$ denotes the specific area of the pore volume caused by the chemical shrinkage
a denotes the degree of hydration

The internal force in the HPC caused by the decrease of the relative humidity in the HPC was expressed with the following equation:

$$F_{\delta w_n} = - A_{\delta w_n} \cdot p(\phi) \quad (7)$$

$p(\phi)$ denotes the under-pressure in the pores at self-desiccation, ϕ
$A_{\delta w_n}$ denotes the specific area of the air-filled pore volume according to eq. (6)
$F_{\delta w_n}$ denotes the internal force caused by the decrease of the relative humidity

4.3 Internal forces from the HPC

At each age the internal stress of the HPC was expressed by the compliance, J. The compliance also covered the deformation of the aggregate, the cement paste, while also taking into account the continuous creep of the HPC caused by the autogenous shrinkage. According to equation (4) the internal specific force in the HPC due to the decrease of the internal relative humidity was obtained:

$$Fc = (1- A_{\delta wn})\cdot \varepsilon_{au}/J \quad (8)$$

$A_{\delta wn}$ denotes the specific area of the air-filled pore volume according to equation (5)
F_c denotes the internal specific force in the HPC due to the decrease of the relative humidity with self-desiccation, ϕ
J denotes the compliance of the HPC
ε_{au} denotes the autogenous shrinkage of the HPC

4.4 Equilibrium of internal forces

For static reasons the internal forces the internal forces were balanced, i.e. the forces from the under-pressure in the pore water, $F_{\delta w_n}$, were compensated for by compressive forces in the HPC, F_c:

$$F_c = F_{\delta w_n} \quad (9)$$

Taking into account that $A_{\delta wn}$ was very small, i.e.:

$$(1 - A_{\delta w_n}) \approx 1 \quad (10)$$

the following expression for the under-pressure was obtained from equations (4) - (9):

$$p(\phi) = (140 \cdot \varepsilon_{aut}) / [J \cdot (\alpha \cdot c)^{2/3}] \quad (11)$$

c denotes the cement content of the HPC (N.B.: Mg/m^3)
$p(\phi)$ denotes a function of the internal relative humidity of the HPC (MPa)
J denotes the compliance of the HPC (millionths/MPa)
a denotes the degree of hydration
ε_{aut} denotes the autogenous shrinkage of the HPC (millionths)
ϕ denotes the internal relative humidity of the HPC with self-desiccation

4.5 Evaluation of internal forces

The following parameters of equation (11) were obtained simultaneously for all the HPCs studied throughout whole the experiment (the parameters were studied from the same batch of HPC or each occasion, Table 4):

1. Autogenous shrinkage, ε_{au}, Chapter 3.7 above
2. Compliance, J, Chapters 3.4 - 3.6 above
3. Hydration, a, Chapter 3.3 above
4. Internal relative humidity, ϕ, Chapter 3.2 above
5. The cement content, c, of the HPC was known, Table 4.

Figure 12 gives the under-pressure in the pores of the HPCs as a function of the internal relative humidity of the HPC. The type of HPC is indicated, Table 4.

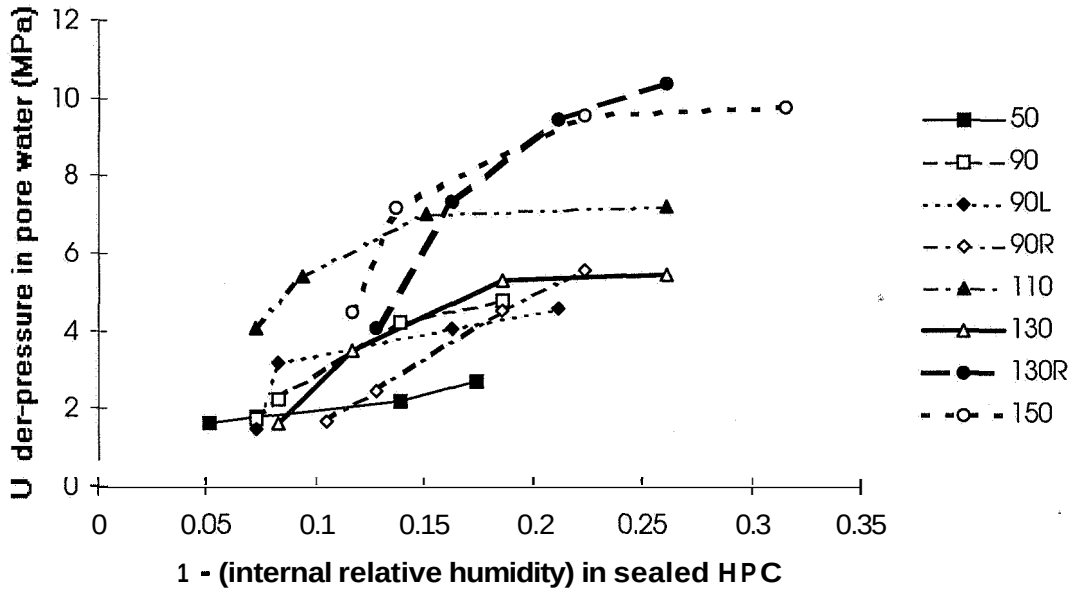

Figure 12 The under-pressure in the pores of the HPCs as a function of the internal relative humidity of the HPC. The type of HPC is indicated, Table 4.

From Figure 12 the following equation was obtained for the under-pressure in the pores of the HPCs (MPa) [2]:

$$p(\phi,w/c) = 10 \cdot k_S \cdot \{2.55 - 1.9 \cdot w/C \cdot [2 + \ln(1-\phi)] + \ln(1-\phi)\} \quad (12)$$

C	denotes the cement content of the HPC (kg/m^3)
k_S	=0.5 for HPCs with 5% granulated silica fume, k_S =1 for HPCs with 10% silica fume, k_S =1 for HPCs with 5% silica fume slurry and k_S =2 for HPCs with 10% silica fume slurry (as calculated on the basis of the cement content)
$p(\phi,w/c)$	denotes the under-pressure in the pores of the HPC (MPa)
w	denotes the mixing water of the HPC (kg/m^3)
ϕ	denotes the internal relative humidity of the HPC

The evaluated under-pressure was dependent on the type of HPC, mainly the water-cement ratio, the content of silica fume and, finally, the type of silica fume (granulated or slurry) as indicated in Figure 12. The HPC which contained 5% silica fume, type 50 and 90R, exhibited lower under-pressure than remaining HPCs with 10% silica fume based on the cement content of the HPC. Generally the evaluated under-pressure was lower than the under-pressure calculated by others, for example [13], who estimated 45 MPa at the internal relative humidity, RH = 0.75. Those differences may be due to the creep in the HPC during autogenous shrinkage (relaxation). The creep in the HPC was compensated for by use of equation (1) but not in the studies presented by [13]. The risk of cracking, for example, were diminished if the creep during autogenous shrinkage in the HPC was accounted for.

5 Summary and conclusions

An study of creep and shrinkage in HPC was performed leading to an expression for the evaluation of under-pressure in the pore water of High Performance Concrete, HPC. The following parameters were required for the evaluation of under-pressure:

1. Autogenous shrinkage
2. Compliance
3. Hydration
4. Internal relative humidity
5. The cement content

The following conclusions were drawn:

1. The evaluated under-pressure was dependent on the type of HPC, mainly the water-cement ratio, the content of silica fume and the type of silica fume
2. The calculated under-pressure was lower than the under-pressure calculated by others, perhaps due to the creep in the HPC during autogenous shrinkage
3. The risk of cracking, for example, may be diminished when the creep due to autogenous shrinkage in the HPC is accounted for.

6 Acknowledgement

Financial support by the Swedish-Norwegian Consortium of High Performance HPC (BFR, Cementa, Elkem, Euroc Beton, NCC Bygg, NUTEK, SKANSKA and Strangbetong) is gratefully acknowledged. I am also grateful to Professor Göran Fagerlund at Division of Building Materials, Lund Institute of Technology, for his review.

References

1. T. C. Powers, T. L. Brownyard (1947). *Studies of Physical Properties of Hardened Portland Cement Paste.* Research Laboratories of the Portland Cement Association. Bulletin 22. ACI Journal. USA. Vol. 43, 984-987
2. B. Persson (1996). *(Early) Basic Creep of High-Performance HPC.* 4th International Symposium on the Utilisation of High-Performance HPC. Paris. France. LCPC. Paris. Ed. by F de Larrard and R Lacroix., 405-414.
3. B. Persson (1995). *Basic Creep of HPC.* Report M6:14. Lund Institute of Technology. Division Building Materials. Lund, 292 pp.
4. P Acker (1993). *Creep and shrinkage of HPC.* Proceedings of the Fifth International RILEM Symposium in Barcelona. E&FN Spon. London, 7-14.
5. M Hassanzadeh (1994). *Fracture Mechanical Properties of HPC.* Report M4:05. Lund Institute of Technology. Division of Building Materials. 1994, 8-13
6. B Persson (1992). *"Hogpresterande betongs hydratation, struktur och hållfasthet". Hydration, Structure and Strength of HPC.* Report TVBM-1009. Lund Inst. of Techn. Div. Building Materials. Lund, 75-97; 99-123. *(In Swedish.)*
7. ASTM *E* 104-85 (1985). *Standard Practice for Maintaining Constant Relative Humidity by Means of Aqueous Solutions.* ASTM. Philadelphia, 33,637.
8. J Byfors (1980). *Plain HPC at Early Ages.* Report FO 3:80. The Swedish Cement and HPC Research Institute, CBI. Stockholm. 1980, 40-43
9. Z P Bazant (1993). *Creep and Shrinkage Prediction Model for Analysis and Design of HPC Structures - Model B_3.* Guidelines for Formulation of Creep and Shrinkage. RILEM TC107. Material and Structures E & FN Spon, 357-365.
10. Z P Bazant; I Carol (1993). *Preliminary Guidelines and Recommendations for Characterising Creep and Shrinkage in Structural Design Codes.* Proceedings of the Fifth International RILEM Symposium in Barcelona. E&FN Spon. London, 805-829.
11. B Persson (1993). *Self-desiccating High-Strength HPC Slabs.* Proceedings of the 3rd Symposium of High-Strength HPC in Lillehammer. 1993. Ed. by I Holand and E Sellevold, 882-889.
12. E.-I. Tazawa (1997). *Effect of Self Stress on Flexural Strength of Gypsum Polymer Composite.* Proceedings of an International Seminar on Self-desiccation and Its Importance in HPC Technology. Ed.: B. Persson and G. Fagerlund. TVBM-3075. Lund Institute of Technology Lund, 15-26.
13. J Brooks; J P Hynes (1993). *Creep and Shrinkage of Ultra High-Strength Silica Fume HPC.* Proceedings of the Fifth International RILEM Symposium in Barcelona. E&FN Spon. London. Pp. 493-498.

A MODEL OF SELF-DESICCATION IN CONCRETE

ADRIAN RADOCEA
Department of Engineering Sciences, Physics and Mathematics
Karlstad University
651 88 Karlstad, Sweden

Abstract
A model that describes self-desiccation as a function of the degree of hydration, cement content and initial water content has been developed. The change in relative humidity in three concrete compositions has been compared with the model and an acceptable agreement has been found. The physical approach of the model brings out several interesting aspects of self-desiccation, for example the influence of hydration products on the geometry of capillary pores. An important conclusion is that the model together with experimental investigations could enlarge our understanding of the development of the pore structure of cement paste.

Notation

C	cement content	kg/m^3
g	gravitational constant	m/s^2
h	capillary rise	m
k1	coefficient	
M	molar mass of water	18 kg/kmole
p_s	partial water pressure at saturation	Pa
P	porosity	m^3/m
P_w	water pressure	Pa
P_a	air pressure	Pa
r	capillary radius or mean radius of curvature	m
R	universal gas constant	8314 J/kmole K
s	specific surface	m^2/kg
T	absolute temperature	K

W	initial water content	kg/m^3
We	evaporable water	kg/m^3
Wn	chemically bound water	kg/m^3
W/C	water/cement ratio	
α	degree of hydration	
Φ	relative humidity	
ρ	density of water	1000 kg/m^3
σ	surface tension of water	N/m
θ	angle of contact between water and the walls of the capillary	

1. Model formulation

Self-desiccation is the decrease of the relative humidity in concrete when water movement from or to the cement paste is prevented. Self-desiccation is caused by cement reactions, that both decrease the total porosity and the amount of evaporable water. Furthermore, contraction of the system cement + water results in development of pores filled with air and water vapour.

The degree of saturation of cement paste We/P can be calculated by using equation (1) and (2).

$$We = W - 0.25\alpha C \tag{1}$$

$$P = W - 0.1875\alpha C \tag{2}$$

$$\frac{We}{P} = \frac{W - 0.25\alpha C}{W - 0.1875\alpha C} = \frac{\frac{W}{C} - 0.25\alpha}{\frac{W}{C} - 0.1875\alpha} \tag{3}$$

The diagram in Fig. 1 shows that the decrease of the degree of saturation is larger at lower W/C-ratios, which is also an explanation of a higher self-desiccation in these cases [3]. Another way to show the influence of the proportion between total porosity and evaporable water content on relative humidity is to use a part of a sorption isoterm, see Fig. 2. The contraction of the system cement + water makes the volume of evaporable water to be lower than the total volume of the pores, but only the largest pores are empty.

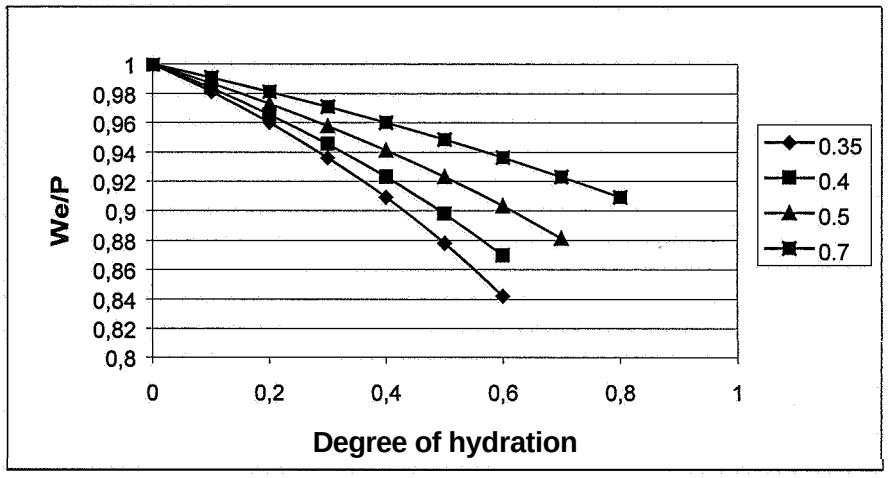

Fig. 1. The degree of saturation at different W/C-ratios.

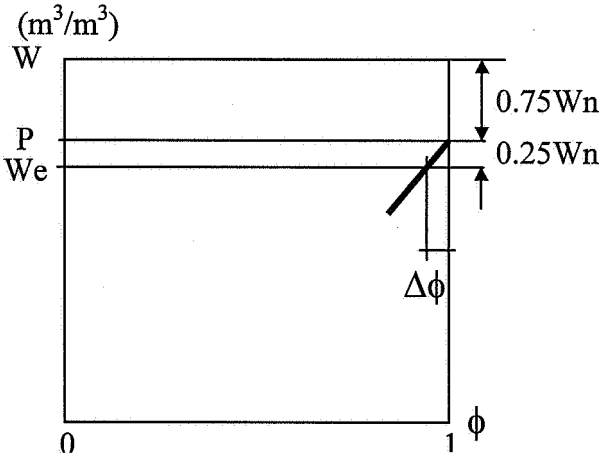

Fig. 2. Decrease in relative humidity caused by contraction.

According to equation (3), the degree of saturation depends only on W/C-ratio and the degree of hydration. The question is if it possible to express relative humidity as function of the same parameters.

By combining Kelvin and Laplacé equations, equation (4) and (5), a relationship between relative humidity and the mean radius of curvature of a water meniscus can be obtained, see equation (6).

$$Pw = ps - \frac{RT\rho}{M} \ln \Phi \tag{4}$$

$$Pa - Pw = \frac{2\sigma}{r} \tag{5}$$

$$\frac{2\sigma}{r} = p_a - \frac{RT\rho}{M} \ln \Phi \tag{6}$$

The problem is now to express the mean radius of curvature as a function of the initial water content, cement content and degree of hydration.

Carman [4] proposed equation (7) to express the capillary rise in find sand beds.

$$h = \frac{\sigma s(1-P)}{\rho g P} \tag{7}$$

For a cylindrical pore the capillary rise is described by equation (8).

$$h = \frac{20\cos\theta}{\rho g r} \tag{8}$$

Equation (7) and (8), together with the assumption that the angle of contact between water and the walls of the capillary is zero, gives:

$$r = \frac{2P}{s(1-P)} \tag{9}$$

The surface of the gel pores should be proportional to the amount of chemically bound water [2]:

$$Vm = 0.26Wn \tag{10}$$

where Vm is the amount of absorbed water corresponding to a layer of water molecules.

Considering that a water molecule has the dimension of 3.5Å, the specific surface of the gel pores can be calculated by the following equation:

$$s = \frac{0.26Wn}{3.5 \cdot 10^{-10} \rho} \tag{11}$$

Equation (2), (9) and (11) give:

$$r = \frac{2(W - 0.1875\alpha C)}{\frac{0.26 \cdot 0.25\alpha C}{3.5 \cdot 10^{-10}\rho}\left(1 - \frac{W + 0.1875\alpha C}{\rho}\right)} \tag{12}$$

The mean radius of the equivalent pore, see equation (12), is plotted in Fig. 3.

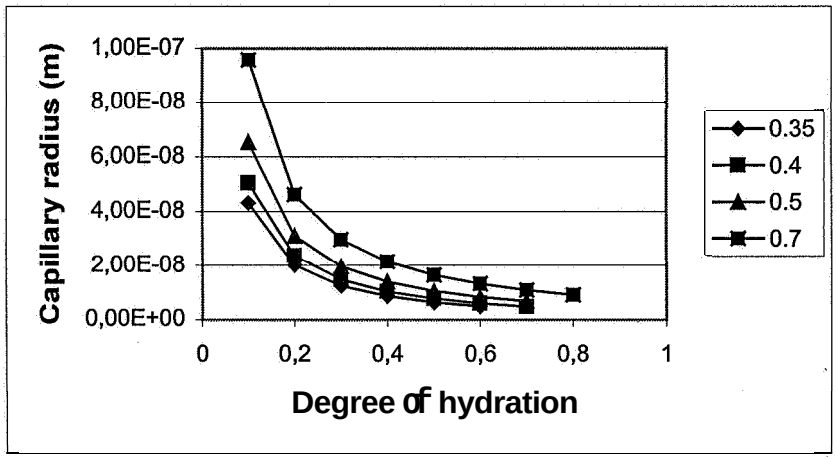

Fig. 3. Mean radius of the equivalent pore as function of degree of hydration and W/C-ratio.

When all constants in equation (6) are replaced by values, the relative humidity becomes a function of the mean pore radius, which in its turn depends on the degree of hydration and W/C-ratio. Equation (13) is plotted in Fig. 4.

$$\Phi = \exp\left(\frac{101325 - 0.146r}{1.345 \cdot 10^{8}}\right) \tag{13}$$

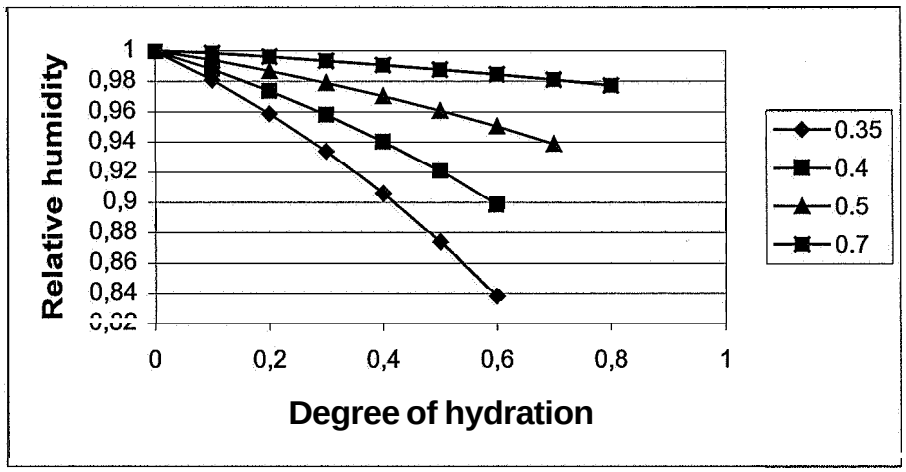

Fig. 4. Self-desiccation at different W/C-ratio.

2. Discussion and conclusions

It is may be too optimistic to think that Carman equation applied on a cylindrical pore could describe the complex structure of the pore system of cement paste, but let us try it and see what happens.

The diagram in Fig. 5 shows the difference between calculated and measured development of self-desiccation in concrete with 0.4 W/C-ratio. The time dependence of the degree of hydration corresponds to Swedish Std-Portland cement. The proposed model gives higher self-desiccation, which can be explained by the fact that not all the reaction products affect the capillary pores, i.e. the specific surface in equation (12) is too large. Our purpose is to find out the radius of an equivalent pore. This pore corresponds to the mean radius of curvature of the empty pores at a given degree of hydration.

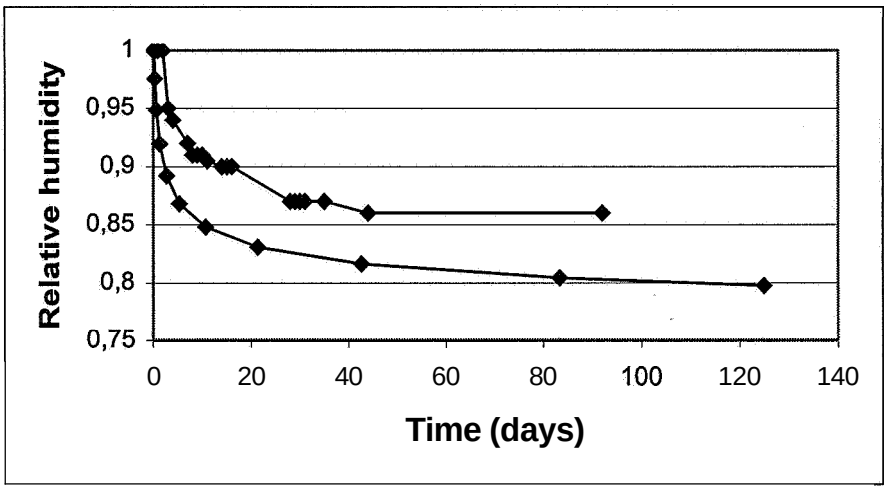

Fig. 5. Calculated and measured development of relative humidity.

In order to obtain a better agreement between the two curves, a coefficient k1, see equation (14) and Fig. 5 can be used to increase the mean radius of curvature.

$$r = \frac{2(W - 0.1875\alpha C)}{k1 \cdot \frac{0.26 \cdot 0.25\alpha C}{3.5 \cdot 10^{-10}\rho}\left(1 - \frac{W + 0.1875\alpha C}{\rho}\right)} \qquad (14)$$

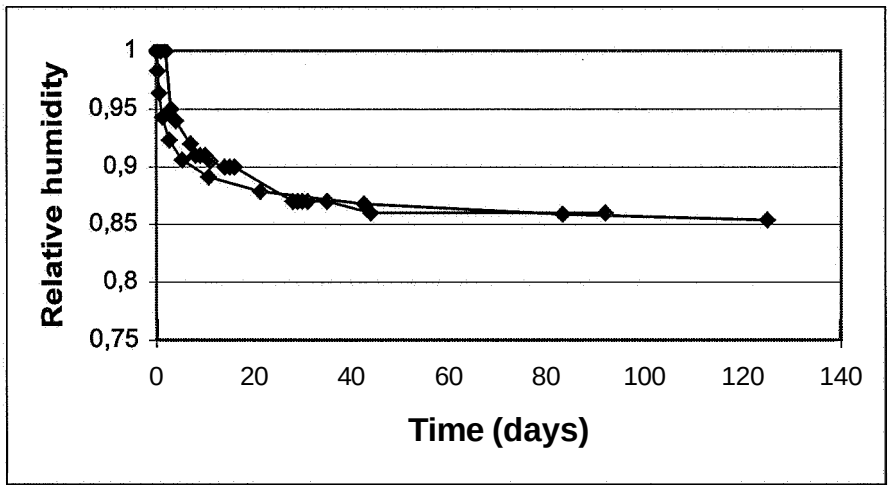

Fig. 6. Calculated and measured development of relative humidity (k1=0.7).

It can be noticed that the most important difference between the two curves in Fig. 6 is the displacement of the measured curve caused by fact that the relative humidity during the first three days was found to be 100%. This cannot really be true since measurements of capillary pressure indicate that the concrete becomes unsaturated after approximately four hours after placing. It is sooner a problem caused by the difficulty to measure relative humidity near 100 %. The diagram in Fig. 7 shows self-desiccation in two other concrete compositions.

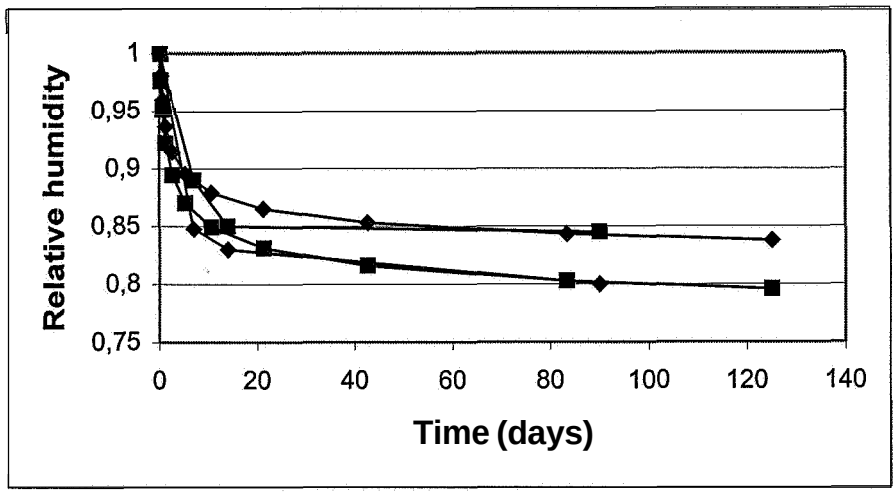

Fig. 7. Measured and calculated development of relative humidity in concrete with 0.35 and 0.4 W/C-ratio. The coefficient k1 is 0.87 and 0.83.

The influence of the reaction products, and consequently their specific surface, on the change of the pore radii of the capillaries has to be higher at lower W/C-ratio. At high W/C-ratio (see Fig. 8) only the outer surface of the reaction products really affect the distance between the cement grains. This surface is larger than the surface of the cement grain, but much lower than the surface of the reaction products. Thus the coefficient k1 must describe these conditions. It is probable that the coefficient k1 is not only dependent on W/C-ratio but also on the specific surface of the cement and the type of cement.

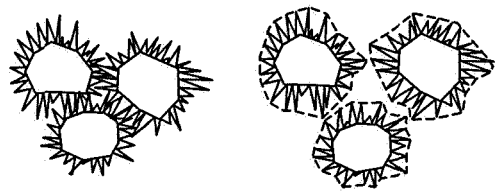

Fig. 8. Cement grains and reaction products at low and high W/C-ratio

The examples shown in Fig. 6 and Fig. 7 indicate that the proposed model can be used to estimate the development of self-desiccation in concrete. In order to improve the accuracy of the model, the coefficient k1 has to be determined by using one or two measurements of relative humidity in sealed samples.

Experimental investigations are necessary to answer several important questions: does the model describe the development of the capillary radii in cement paste, is the coefficient k1 a constant or it also depends on the degree of hydration, is the coefficient k1 proportional to the W/C-ratio, i. e. the initial distance between cement grains, do additives and admixtures affect k1?

Equation (13) and (14) enable us to express the relative humidity as a function of well-known physical parameters. Thus the proposed model together with experimental investigations could be used to investigate the change in the geometry of capillary pores and consequently enlarge our understanding of the development of the pore structure of cement paste. The model could be verified by studying the influence of W/C-ratio and type of cement on the change of the sorption isoterm at different degree of hydration. An example is shown in Fig. 9 and Fig. 10.

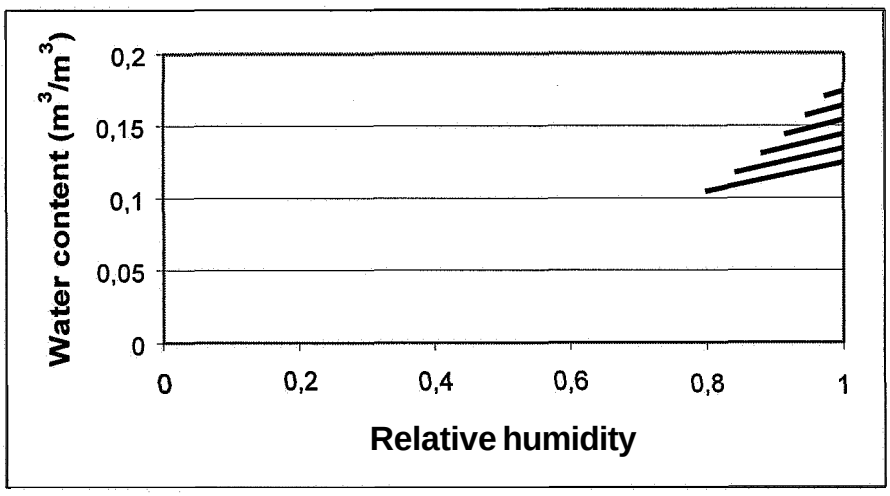

Fig. 9. Calculated decrease of relative humidity at degree of hydration between 0.1-0.6 (W/C=0.35).

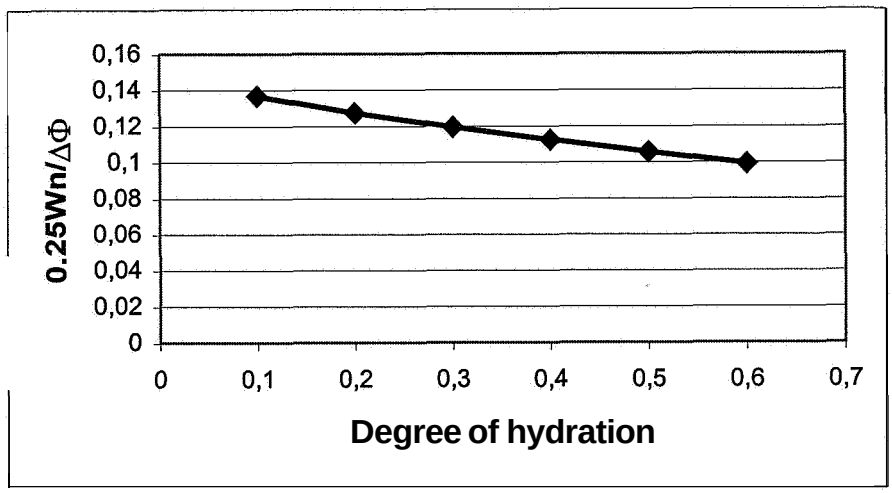

Fig. 10. Change in slope of the curves in Fig. 9.

3. References

1. Atlassi E, Norling K and Radocea A. (1991) Fuktfri betong – en fråga om rätt materialkombination(in Swedish), Betong, September.
2. Berntsson L. (1992) Concrete technology (in Swedish), CTH.
3. Betonghandbok – material. (1994) Page 291, AB Svensk Byggtjänst (in Swedish).
4. Carman P C. (1941) Capillary rise and capillary movement of moisture in fine sands, Soil Science, 52.
5. Mjörnell-Norling K. (1997) Moisture conditions in high performance concrete – mathematical modelling and measurements.

EXPERIMENTAL STUDIES ON REDUCTION OF AUTOGENOUS SHRINKAGE AND ITS INDUCED STRESS IN HIGH-STRENGTH CONCRETE

R. SATO
Faculty of Engineering, Hiroshima University, Hiroshima, Japan
S. TANAKA
Central Research Laboratory, Taiheiyo Cement Corporation, Chiba, Japan
T. HAYAKAWA
Department of Civil Engineering, Utsunomiya University, Utsunomiya, Japan
M. TANIMURA
Central Research Laboratory, Taiheiyo Cement Corporation, Chiba, Japan

Abstract

The benefits of reducing autogenous shrinkage of concrete on restrained stress in reinforced concrete members made with high-strength concrete were experimentally investigated. In case of conventional high-strength concrete, extreme fiber tensile stresses of about *2.5* to *3.5* N/mm^2 were observed. On the other hand, in case of high-strength concrete made with low heat Portland cement used in combination with shrinkage reducing agent and expansive additives to reduce autogenous shrinkage greatly, extreme fiber tensile stress was ten times lower than that measured on conventional high-strength concrete. These tendencies can be evaluated by 2D-FEM analysis based on the principle of superposition and taking into account the time dependency of creep.

Keywords: high-strength concrete, autogenous shrinkage, stress, low heat Portland cement, shrinkage reducing agent, expansive admixture, creep.

1 Introduction

When investigating cracking of high-strength concrete (HSC) made with low water-to-binder (W/B) ratio, restrained stress due to autogenous shrinkage cannot be ignored [1]. For example, in rigid-frame RC structures with an important *[2]*external restraint, it is pointed out that HSC develops cracking, and the reduction of autogenous shrinkage can be of great importance. In order to reduce autogenous shrinkage of HSC, the use of low heat Portland cement (Belite-rich cement), shrinkage reducing agent and expansive admixture as well as their combination was investigated [3-6]. However, in almost studies published in literature, material properties are the main concern, thus the benefit of reducing autogenous shrinkage of concrete on restrained stress in reinforced concrete (RC) members made with HSC is not sufficiently investigated. The objectives of this study are as follows:

1. To determine the effect of a ternary combination of low heat Portland cement, shrinkage reducing agent and expansive admixture on autogenous shrinkage of HSC.
2. To evaluate the restrained stress of beams cast with HSC made with 23% W/B, low heat Portland cement used in combination with shrinkage reducing and expansive admixtures.
3. To simulate the restrained stress by two-dimensional finite element method (2D-FEM) based on the principle of superposition and taking into account the time dependency of creep.

2 Experimental program

2.1 Materials and mixture proportions

Materials and mixture proportions of the concrete mixtures used are summarized in Table 1. Both concrete mixtures were prepared with same WE3 of 23% and containing 10% silica fume replacement. Conventional HSC (AS) was made with ordinary Portland cement while the second mixture refereed to as New-developed HSC (LAS) was prepared using low heat Portland cement combined with shrinkage reducing agent and expansive admixture.

Table 1. Mixture proportions of concrete (kg/m^3)

Symbol	Type of cement	W/B (%)	SF/B (%)	s/a (% volume)	W	C	SF	EX	S	G	SRA	SP
AS	NC	23	10	41	161	630	70	0	629	912	0	14
LAS	LC	23	10	41	161	600	70	30	630	914	6	15.4

Symbols in Table 1:

G: coarse aggregate, fineness modules (6.78), specific gravity under saturated surface-dry
NC: ordinary Portland cement, specific surface area (3.500cm^2/g), and specific gravity (3.15)
LC: low-heat Portland cement, specific surface area (3.500cm^2/g), specific gravity (3.22)
SF: silica fume, specific surface area (200.000cm^2/g), and specific gravity (2.2)
S: fine aggregate, fineness modules (2.80), specific gravity under saturated surface-dry (2.61) (2.63), maximum size of coarse aggregate (20mm)
EX: expansive admixture
SRA: shrinkage reducing agent
SP: high-range water reducing agent

2.2 Test methods

2.2.1 Compressive strength and elastic modulus

The compressive strength and elastic modulus of concrete were measured according to JIS A 1108 and JSCE-G502 (Draft) specifications, respectively. Measurements of compressive strength and elastic modulus were performed immediately after final setting. The variation of elastic modulus of concrete with age was determined according to Eq. (1).

$$E(t) = E_{28} \exp(s_E[1-((28a_E)/(t-a_E))^{0.5}]) \quad (1)$$

$E(t)$ Elastic modulus at an age of t days

E_{28} Elastic modulus obtained after 28 days of age and 20 water curing

s_E, a_E Coefficients related to type of cement and setting time, respectively

t Effective age of concrete (days) adjusted according to Eq. (2)

$$t = \sum_{i=1}^{n} \Delta t_i \exp\left[13.65 - \frac{4000}{273 + T(\Delta t_i)/T_0}\right] \quad (2)$$

Δt_i denotes the number of days when a temperature T prevails

2.2.2 Autogenous shrinkage strain

For each concrete mixture shown in Table 1, three 153050 prismatic specimens without restriction were prepared to measure the autogenous shrinkage strain. At the center of each specimen, a strain gauge with an elastic modulus of 49 N/mm^2 and a thermocouple were embedded. The gauge can allow measurement of 100-mm length in the longitudinal direction. The autogenous shrinkage strain was obtained by using the measured strain and temperatures and taking into consideration compensation due to temperature change. The concrete thermal expansion coefficient was assumed to be equals to $10 \cdot 10^{-6}$ [7].

2.2.3 Autogenous shrinkage stress in beam specimens

The dimensions of beam specimens and configuration of steel bars are shown in Fig. 1. The reinforcement ratios are summarized in Table 2. In order to measure autogenous shrinkage stress in the beam specimens, both tension and compression reinforcements in the specimens were equipped with strain gauges. For each mixture, two beam specimens were prepared and sealed with aluminum foil and polyester sheet after demoulding to prevent evaporation or absorption of water. The temperature inside the concrete specimens was measured using thermocouples. The extreme fiber tensile stress due to autogenous shrinkage was determined by considering equilibrium force according to Eq. (3).

$$\sigma \cdot y = \frac{Ps + Ps'}{Ac} + \frac{M}{Ie} \cdot \frac{h}{2} \quad (3)$$

$$Ps = As \cdot Es \cdot \varepsilon \cdot s \quad (4)$$

$$Ps' = As' \cdot Es' \cdot \varepsilon \cdot s' \quad (5)$$

$$M = P_s \cdot e_s + P_{s} \cdot e'_s \quad (6)$$

$\sigma \cdot y$ Extreme fiber stress on tension

A_s, E_s, ε_s	Cross-sectional area, elastic modulus, and strain of tension reinforcement
A_s, E_s', ε_s'	Cross-sectional area, elastic modulus and strain of compressive reinforcement
A_c	Cross-sectional area of concrete
ε_s, ε_s'	Distance from center of beam height to tension and compression reinforcement
Z_e	Equivalent geometrical moment of inertia
h	Height of beam

2.3 Numerical analysis method

In order to analyze the restrained stress due to autogenous shrinkage, newly developed 2D-FEM analysis based on the principle of superposition enables one to evaluate the stress with reinforcement restraint [2]. The basic data required for analysis are autogenous shrinkage strain, elastic modulus, and creep coefficient, and for autogenous shrinkage strain and elastic modulus, measured and calculated value according to Eq.1 were used. As for creep coefficient, the modified CEB-FIP MODEL CODE 1990 (MC90) [8] equation was adopted to evaluate creep behavior at very early age (less than one day).

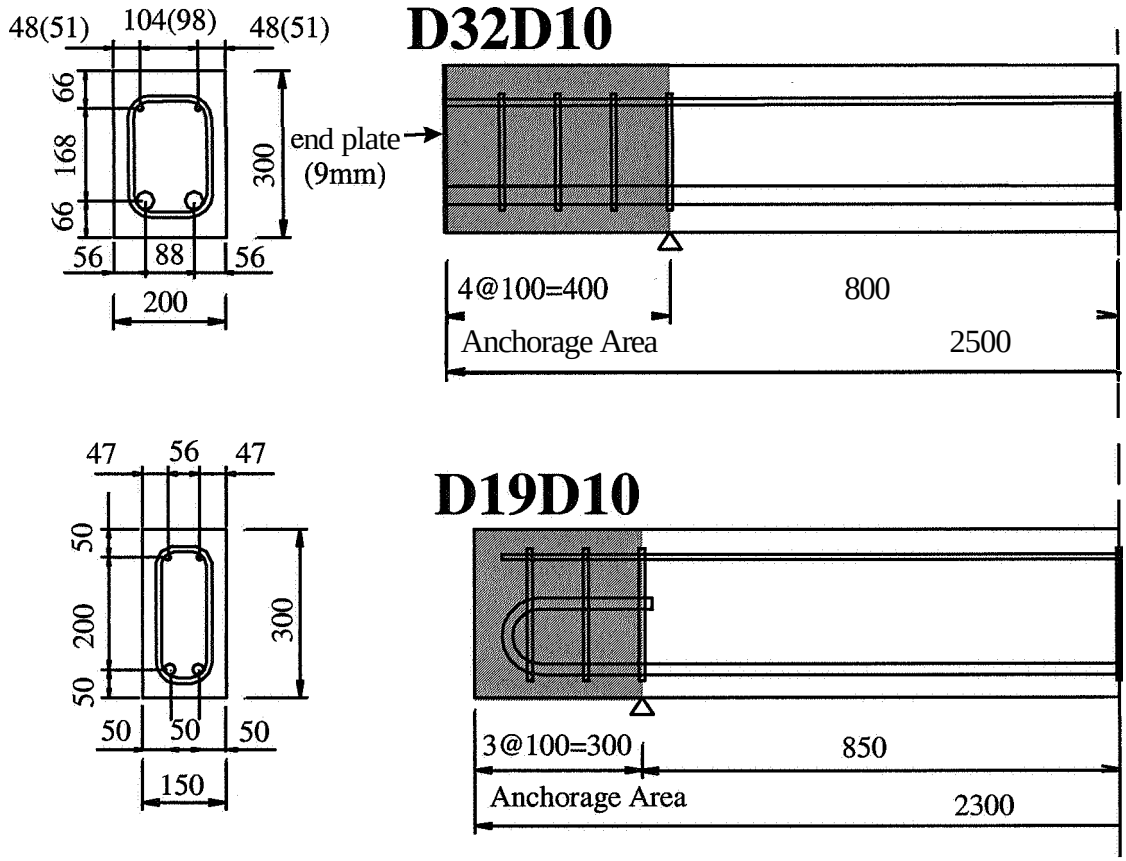

Fig. 1. Dimensions and configuration of steel bars of beam specimen.

Table 2. Reinforcement ratio

Symbol	Tension reinforcement		Compression reinforcement	
	Configuration	Ratio(%)	Configuration	Ratio(%)
D32D19	2@D32	3.4	2@D19	0.3
D19D10	2@D19	1.4	2@D10	0.4

$$\phi\left(t_{i+1/2}, t_j\right) = \phi_0 \times \left\{ \frac{\left(t_{i+1/2} - t_j\right)/t_1}{\beta_H + \left(t_{i+1/2} - t_j\right)/t_1} \right\}^{0.3} \quad (7)$$

ϕ_0 Notional creep coefficient: $\phi_0 = \phi_1 \times [(a-1)/(a - t_j^b)]$

t_i Effective age of concrete (day) adjusted according to Eq (2)

β_H Coefficient for the effect of environmental condition on rate of creep

t_1 1day

$$\beta_H = c \times t_j - d$$

In this analysis, the constants a, b and d necessary to calculate $_0$ and $_H$ are as follows:

Concerning the conventional high-strength concrete (AS) made with ordinary Portland cement, the constants obtained from using compression creep test data determined on high-early strength Portland cement were provisionally adopted. These values are:

$$\phi_1 = 1.68, a = 2.03, b = -1.03, c = 4.52, d = 1.45$$

Concerning the high-strength concrete (LAS) made with low heat Portland cement, shrinkage reducing agent and expansive admixture, the constants obtained from compression creep test data determined on only low heat Portland cement were provisionally adopted. These values are:

$$\phi_1 = 5.29, a = 1.37, b = -1.70, c = 9.30, d = 7.69$$

Furthermore, $_0$ and $_H$ are modified according to Eq. (7) to allow analysis even for very early age (less than 1 day) [9].

3 Results and discussions

3.1 Compressive strength and elastic modulus

The measured compressive strength and elastic modulus as a function of effective age are shown in Figs. 2 and 3, respectively. In Fig. **3,** the regression equation according to Eq. (1) is drawn. Compared to AS concrete, the development of strength of LSA mixture is lower, which may be due to the type of cement, which is a low heat Portland cement. For the elastic modulus, almost similar tendency to that obtained with compressive strength was observed. At the age of 28 days, the observed compressive strength of both concrete mixtures gains about 100 N/mm^2.

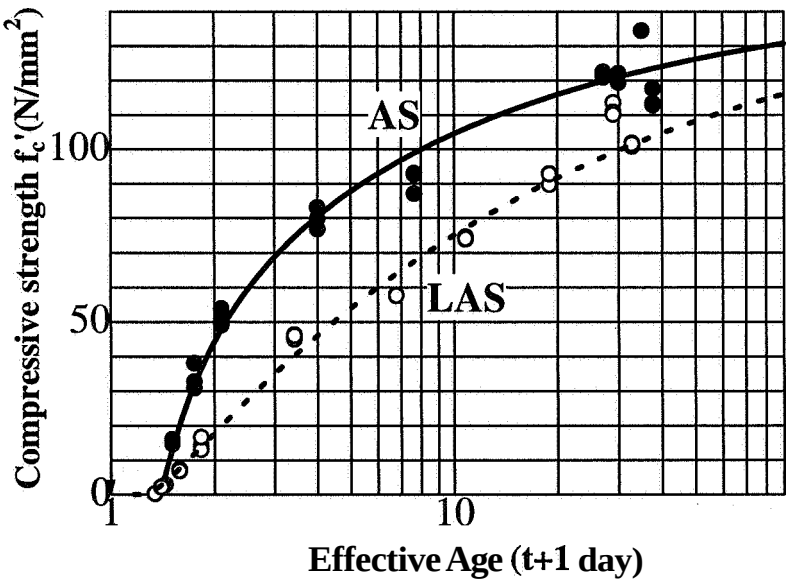

Fig. 2. Development of compressive strength.

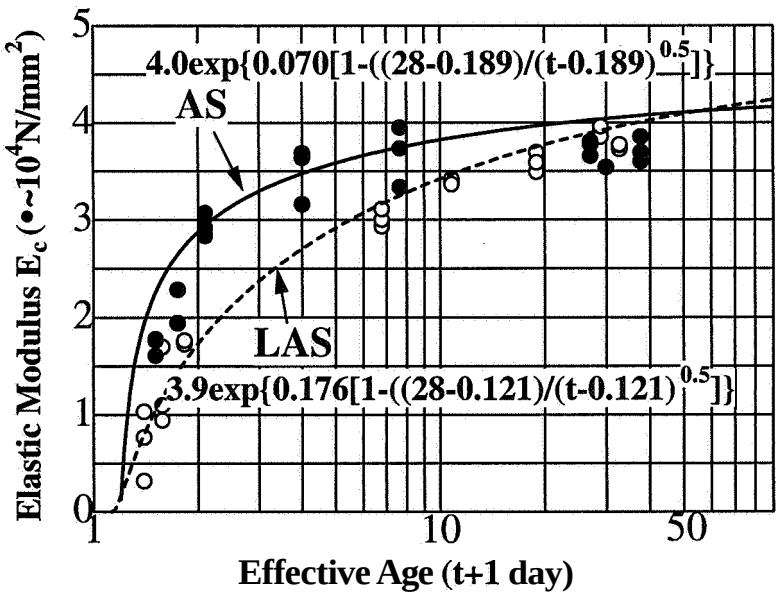

Fig. **3.** Development of elastic modulus.

3.2 Autogenous shrinkage strain

The variation of autogenous shrinkage strains with age is shown in Fig. 4. In the case of **AS** concrete, autogenous shrinkage strain of about $70 \cdot 10^{-6}$ was observed after a long period corresponding to 80 days. For **LAS** mixture the autogenous shrinkage strain was almost constant after one day of age, and was $25 \cdot 10^{-6}$ after the long period of 80 days, such a value which represents one third of that obtained with **AS** mixture, thus confirming the benefit of using a ternary combination of low heat Portland cement, shrinkage reducing agent and expansive admixture.

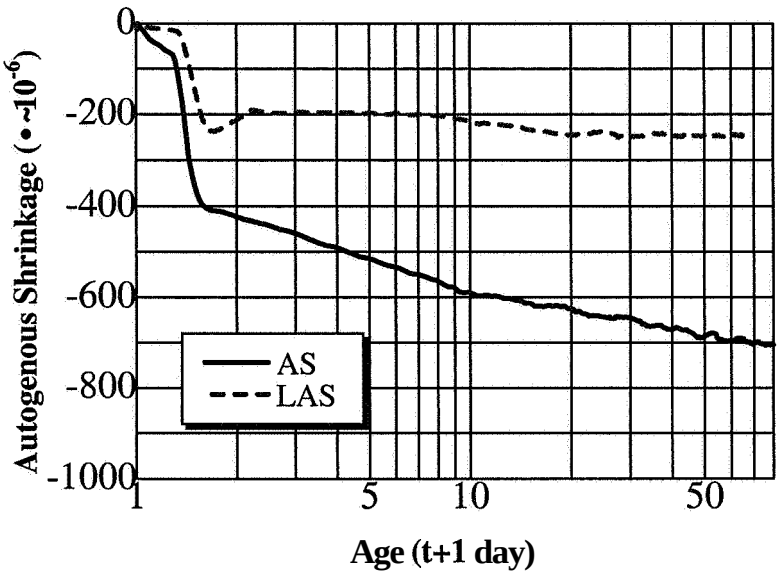

Fig. 4. Time-dependent change of autogenous shrinkage

3.3 Autogenous shrinkage stress in beam specimens

Figs. 5 and 6 show the variation of extreme fiber tensile stresses with the age for 1.4 and 3.4% reinforcement ratios, respectively. In the case of AS concrete, a large stress was observed at early age. After a long period corresponding to 58 days, extreme fiber tensile stresses of about 3.5 and 2.5 N/mm^2 were observed for 3.4% (D32 D10) and 1.4% (D19 D10) tension reinforcement ratios, respectively. Compared with AS mixtures, the stress of 0.2-0.3 N/mm^2 obtained in the case of LAS concrete was much smaller regardless of the reinforcement ratio, which was approximately ten times smaller than that used with AS concrete beam.

Based on these results, it can be confirmed that LSA mixture may therefore provide considerable contribution in reducing retrained stress in RC members. The extreme fiber tensile stress values obtained from 2D-FEM analysis are shown in Figs. 5 and 6 for D32D10 and D19D10 configurations, respectively. It was observed that the analytical and measured values are in approximate agreement with measured values. As mentioned above, referred values are used for creep coefficient in this analysis. We believe that the difference between analytical and experimental values may be reduced by considering the real values. As can be seen in Figs. 5 and 6, the extreme fiber tensile stress measured on LAS beams is approximately two times lower than that measured on AS beams. The same tendency is also observed with predicted values. Therefore, the 2D-FEM analysis adopted in this study can provide evaluation of restrained stress in RC members due to autogenous shrinkage.

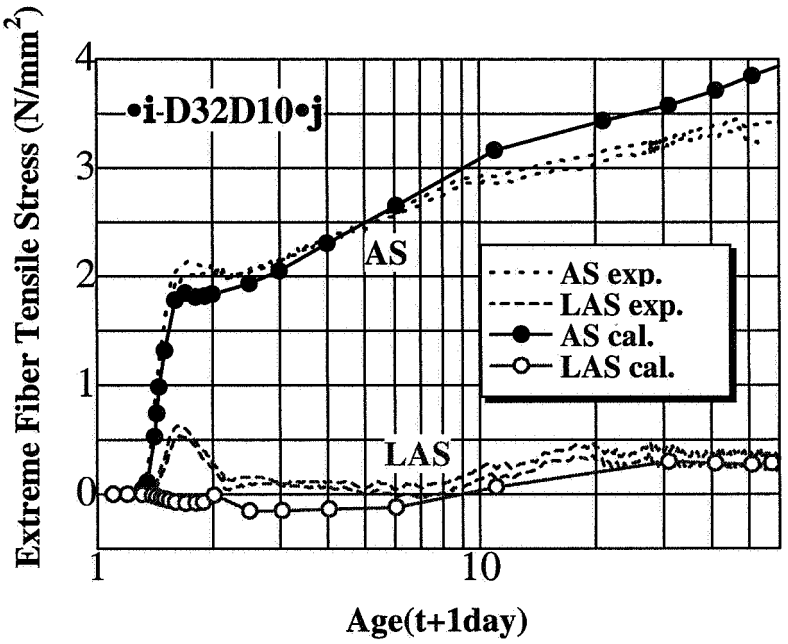

Fig. 5. Time-dependent change of extreme fiber tensile stress (D32D10)

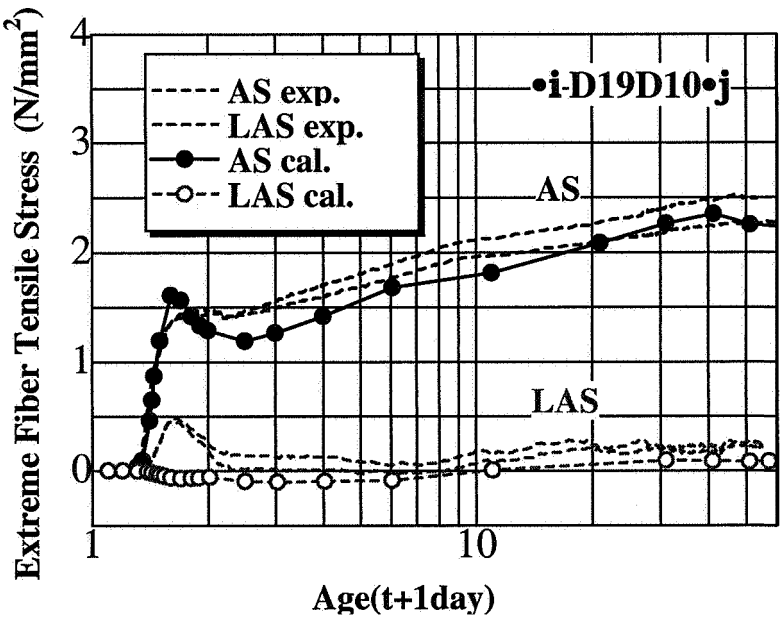

Fig. 6. Time-dependent change of extreme fiber tensile stress (D19D10)

4. Conclusions

Based on results presented in this paper, the following conclusions can be warranted.

(1) Autogenous shrinkage strain of HSC made with 23% W/B and low heat Portland cement used in combination with shrinkage reducing agent and expansive admixture (LAS) is about one-third (113) to that of conventional HSC made with same W/B and an ordinary Portland cement (AS). On the other hand, both LSA and AS concrete develop comparable compressive strength and elastic modulus values after 28 days of age.

(2) Regardless of the reinforcement ratio, extreme fiber tensile stress of beams cast with LAS concrete is ten times lower than that measured on AS concrete. Thus, it can be confirmed that LSA concrete may contribute a great deal to reducing retrained stress in RC members.

(3) Restrained stress may have an important effect on mechanical properties of RC members, such as craclung development, shearing behavior, deflection, etc., so more investigations should be carried out to clarify such influence.

(4) It is confirmed that the analytical value obtained from 2D-FEM analysis based on the principle of superposition and taking into account the time dependency of creep can allow accurate evaluation of the restrained stress due to autogenous shrinkage in RC beams. The difference between analytical and experimental values can be reduced by considering actual constants determined from experiment involved in the analysis.

References

[1] E. Tazawa, Y. Matsuoka, S. Miyazawa, S. Okamoto: *Effect of Autogenous Shrinkage on Self Stress in Hardening Concrete, Thermal Cracking in Concrete at Early Age*, pp. 221-228, 1994 (in Japanese)

[2] T. Hayakawa, M. Xu, R. Sato, K. Imamoto: *A two Dimensional FEM Analysis on Autogenous Shrinkage of RC Indeterminate Structure made of High Strength Concrete*, Proceeding of the JCI, Vol. 20, No.2, pp. 1027-1032, 1998 (in Japanese)

[3] S. Tanaka, A. Sugiyama, A. Ogawa, R. Omita: *Properties of High Fluidity Concrete of Super Workable Concrete, Proceedings of the JCI*, Vol. 17, No.1, pp. 157-162, 1995 (in Japanese)

[4] A. Ogawa, K. Sakata, S. Tanaka: A Study on Reducing Shrinkage of Highly-Flowable Concrete, Advanced in Concrete Technology, Proceedings, CANMETIACI, pp. 55-72, 1995

[5] M. Takeuchi, S. Tanaka, T. Okamoto, *Stress Caused by Autogenous Shrinkage Stress and Crack Resistance of High Strength Concrete with Belite Rich Cement*, Summaries of Technical Papers of Annual Meeting Architectural Institute of Japan, A-l Materials and Construction, pp. 807-808, 1996 (in Japanese)

[6] R. Chikamatsu, N. Takeda, N. Miura, S. Sogo, *Study on Lower Shrinkage of High Strength, High Fluidity Concrete*, Proceedings of the JCI, Vol. 19, No. 1, pp. 169-174, 1998 (in Japanese)

[7] JCI COMMITTEE REPORT: Technical Committee on Autogenous Shrinkage of Concrete JCI, 1996.11 (in Japanese)

[8] CEB-FIP MODEL CODE. 1990

[9] Y. Yang, R. Sato, K. Imamoto, M. Xu: *Estimation of Stresses of High-Strength Concrete Due to Autogenous Shrinkage*, Proceedings of the JCI, Vol. 19, No.1, pp. 757-762, 1997 (in Japanese)